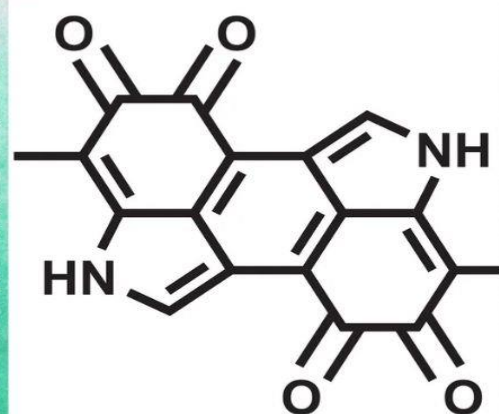
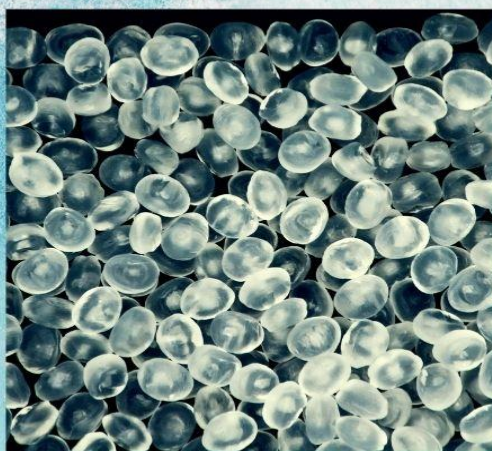
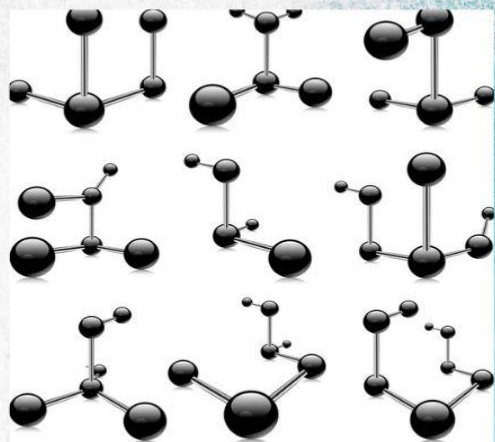




**UniKL**  
UNIVERSITI  
KUALA LUMPUR



**UPM**  
UNIVERSITI PUTRA MALAYSIA  
BERILMU BERBAKTI



# PROCEEDINGS OF THE INTERNATIONAL SYMPOSIUM ON POLYMERIC MATERIALS 2022 (ISPM2022)

14-15th June 2022

Organized by:

Advanced Engineering Materials and Composite  
Research Centre (AEMC), Department of Mechanical  
and Manufacturing Engineering,  
Universiti Putra Malaysia, Malaysia

Supported by:

Universiti Kuala Lumpur Malaysian Institute of  
Chemical and Bioengineering Technology  
(UniKL MICET), Malaysia  
The Plastics & Rubber Institute Malaysia (PRIM), Malaysia

Editors:

S. M. Sapuan  
R. A. Ilyas  
M. Y. M. Zuhri  
E. S. Zainudin  
M. Jawaid  
Z. Leman  
A. N. A. Yahaya  
M. A. Azman  
M. Zulkifli  
N. A. Khalil  
N. Z. M. Zuhudi  
C.N. Aiza Jaafar  
M. N. M. Azlin  
K. Z. Hazrati  
M. M. Harussani  
M. F. Banjar  
R. M. O Syafiq  
A. Nazrin  
A. F. Lajulliadi  
J Tarique

*ISPM2022*

*The International Symposium on Polymeric Materials 2022*

# **THE INTERNATIONAL SYMPOSIUM ON POLYMERIC MATERIALS 2022 (ISPM2022)**

**14<sup>th</sup> - 15<sup>th</sup> JUNE 2022**

Advanced Engineering Materials and Composite  
Research Centre (AEMC)

Mechanical and Manufacturing Engineering,

Faculty of Engineering

Universiti Putra Malaysia (UPM)

© **Proceedings of the International Symposium on Polymeric Materials 2022 (ISPM2022)**

All right reserved

No part of this publication may be reproduced, stored in retrieval system in a retrieval system of transmitted, in any form of by any means, electronics, mechanical, photocopying, recording of otherwise, without the prior permission of the copyright owner.

Published by:

Advanced Engineering Materials and Composites Research Centre (AEMC),  
Department of Mechanical and Manufacturing Engineering,  
Faculty of Engineering, 43400 UPM Serdang,  
Selangor Darul Ehsan,  
Malaysia

Editors:

S. M. Sapuan  
R. A. Ilyas  
M. Y. M. Zuhri  
E. S. Zainudin  
M. Jawaid  
Z. Leman  
A. N. A. Yahaya  
M. A. Azman  
M. Zulkifli  
N. A. Khalil  
N. Z. M. Zuhudi  
C. N. Aiza Jaafar  
M. N. M. Azlin  
K. Z. Hazrati  
M. M. Harussani  
M. F. Banjar  
R. M. O. Syafiq  
A. Nazrin  
A. F. Lajulliadi  
J. Tarique

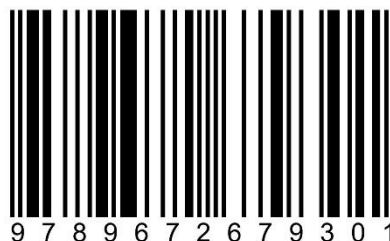
ISBN: 978-967-26793-0-1

Printed by:

Syarikat Perniagaan Weng Sing  
Lot 452A, Jalan Susur 1, Taman Sri Serdang  
43300 Seri Kembangan,  
Selangor Darul Ehsan.  
Tel.: 03-8948 7244  
Email: weng\_sing@yahoo.com

Fax: 03-8945 5168

ISBN 978-967-26793-0-1



*ISPM2022*

*The International Symposium on Polymeric Materials 2022*

**ORGANIZER**



**SUPPORTED BY**



## TABLE OF CONTENT

CONTENTS	PAGES
PREFACE	ix
Foreword from Chairman of ISPM2022	xi
Foreword from President of PRIM	xii
Foreword from Dean, Faculty of Engineering, UPM	xiv
Plenary Speaker 1 Potential and Limitations of Polymers for the New Millenium <b>Prof. Dr. Vijay Kumar Thakur</b>	xvi
Keynote Speaker 1 Modelling of Surface Roughness and Delamination in Drilling PB Panels with Coated Carbide Spade Drills – RSM Approach <b>Prof. Dr. S. Prakash</b>	xvii
Keynote Speaker 2 Malaysian Glove Industry Post-Covid – Prospects and Strategies to Stay Ahead <b>Mr. Pong Kai See</b>	xviii
Keynote Speaker 3 Natural Hydroxyapatite from Fish Scales as Potential Fillers in Polymer Composite for Biomedical Applications <b>Prof. Ts. Dr. Ismail Zainol</b>	xix
Keynote Speaker 4 Consistency of Natural Rubber - Effect of Coagulant on Processing Properties <b>Dr. Wirach Taweepreda</b>	xxi
Keynote Speaker 5 Effect of Dispersion Time for Nanoparticles in DGEBA Shape Memory Polymer Composite Manufacturing <b>Assoc. Prof. Dr. Mainul Islam</b>	xxii
Tentative Program	xxiii
International Advisory Scientific Committee	xxv
Organizing Committee	xxvi
Full Paper	xxvii
<b>NON-LINEAR FINITE ELEMENT ANALYSIS OF OIL PALM FIBER COMPOSITES FOR FUSED DEPOSITION MODELING (FDM)</b> M. N. Ahmad, M. R. Ishak, M. M. Taha, F. Mustapha, Z. Leman	1
<b>THE EFFECT OF PE-g-MA ON THE PROPERTIES OF LOW DENSITY POLYETHYLENE (LDPE)/THERMOPLSTICS BANANA PEEL STARCH (TBPS) FILMS</b> F. Hashim, N. H. C. Ismail, N. A. M. Zaini, S. N. Din, Z. A. S. A. Salim	5
	iv

<b>ANTIMICROBIAL CAPABILITY OF INORGANIC MATERIAL AS FILLER FOR THERMOPLASTIC ELASTOMER – A STATE OF THE ART REVIEW</b> F. N. J. Abedin, A. N. A. Yahaya, N. A. Khalil, M. Zulkifli	9
<b>MECHANICAL PROPERTIES AND CONDUCTIVITY OF POLYANILINE-CELLULOSE-LATEX HYBRID</b> M. F. Banjar, A. N. A. Yahaya, N. A. Khalil, A. A. Al-Dulaimi, M. Singh, M. Zulkifli	13
<b>SUCCESSFUL COMMERCIALIZATION OF NATURAL FIBRE REINFORCED COMPOSITES</b> S.F.K. Sherwani, S. M. Sapuan, E.S. Zainudin, Z. Ieman, A. Khalina	16
<b>A COMPOSITE HYDROGEL BEADS BIO-SORBENT FOR REMOVAL COPPER: EFFECT OF pH OF COPPER SOLUTION</b> A.S.A. Rahman, N.A. Khalil, M.S. Hossain, A.N.A. Yahaya, M. Zulkifli	19
<b>POLYMER MATRIX MATERIAL SELECTION FOR SUSTAINABLE TWO-STROKE MARINE DIESEL ENGINE CROSSHEAD BEARING DESIGN USING TOPSIS METHOD</b> R. V. Yiow, M.R. Mansor	23
<b>A COMPARATIVE REVIEW OF THE EFFECTS OF DIFFERENT FIBRE CONCENTRATIONS ON ARROWROOT FIBRE AND OTHER FIBRE-REINFORCED COMPOSITE FILMS</b> J. Tarique, S.M. Sapuan, E.S. Zainudin, K.Z. Hazrati, A. Khalina, R.A. Ilyas, I. Aliyu	26
<b>GREEN FIBRES AS SUSTAINABLE AND RENEWABLE RESOURCE FOR DEVELOPMENT OF BIONANOCOMPOSITE: A REVIEW</b> R.M.O. Syafiq, S.M. Sapuan, M.Y.M. Zuhri, S.H. Othman, R.A. Ilyas, K.Z. Hazrati, A. Nazrin, S.F.K. Sherwani, J. Tarique, M.M. Harussani, M.D. Hazrol	30
<b>ELECTROMAGNETIC WAVE REDUCTION OF MULTIWALLED CARBON NANOTUBES MIXED NANOMETER <math>CoFe_2O_4</math> AT HIGHER FREQUENCY RANGE</b> F. M. Idris, H. Kaco, S. M. Mohd, N. M. Jan, M. S. E. Shafie, F. Esa, Z. M. Idris	33
<b>APPLICATIONS OF NANOCELLULOSE AND ITS COMPOSITES IN BIO PACKAGING-BASED STARCH</b> M. Mahardika, D. Amelia, Azril, E. Syafri	36
<b>STUDY OF INPUT PARAMETER CHANGES TOWARD LOW DENSITY POLYETHYLENE'S PRODUCT PROPERTIES</b> N. L. Bekri, I. Idris, A. M. Som, M. N. Murat, F. S. Rohman, R. A. Ilyas, A. Azmi	40
<b>CUTTING FORCE MEASUREMENT OF OIL PAM EMPTY FRUIT BUNCH FIBER REINFORCED POLYMER MATRIX COMPOSITES</b> M. K. Wahid, R. Jumaidin, M. H. Osman, A. Rahman, M. H	43
<b>TENSILE PROPERTIES OF A HYBRID KENAF-GLASS FIBRE REINFORCED UNSATURATED POLYESTER COMPOSITE SHAFT</b> N. A. Zakaria, M. R. Ishak, F. Mustapha, N. Yidris	46
<b>THE EFFECT OF DIFFERENT PULPING TIME ON DEGRADATION OF LIGNIN IN KAPOK FIBER (<i>CEIBA PENTANDRA, L.</i>)</b>	48

F. A. Rezekinta, A. Kasim, E. Syafri, I. Chaniago, F. Ridwan

<b>EXPERIMENTAL ANALYSIS OF KERF TAPER ANGLE IN CUTTING PROCESS OF SUGAR PALM FIBER REINFORCED UNSATURATED POLYESTER COMPOSITES WITH ABRASIVE WATER JET CUTTING TECHNOLOGY</b>	50
F. Masoud, S. M. Sapuan, M. K. A. M. Ariffin, Y. Nukman, E. Bayraktar	

<b>CONCEPTUAL DESIGN OF THE CAR GEAR CONSOLE PANEL MADE BY GLASS/NATURAL FIBER REINFORCED HYBRID POLYMER COMPOSITE</b>	53
J. Yusuf, Z. Leman, S.M. Sapuan	

<b>NATURAL FIBER REINFORCED POLYMER COMPOSITES: OPPORTUNITIES, CHALLENGES, AND ITS APPLICATIONS</b>	56
N.A. Maidin, S.M. Sapuan, M.T. Mastura, M.Y.M. Zuhri	

<b>TEMPORARY SOUND BARRIER SYSTEM FROM RICE HUSK POLYMERIC COMPOSITE</b>	61
H. M. Ariff, D. W. Jung, T. H. Rafin, Z. Leman, K. A. M. Rezali, R. Calin	

<b>BIODEGRADABLE SYNTHETIC POLYMER IN ORTHOPAEDIC APPLICATION: A REVIEW</b>	64
F. D. Al-shalawi, M. A. A. Hanim, M. K. A. Ariffin, C. L. S. Kim, D. Brabazon, R. Calin, M. O. Alosaimi	

<b>RECENT ADVANCES IN POLYMER AND PEROVSKITE BASED THIRD-GENERATION SOLAR CELL DEVICES</b>	67
T. F. Alhamada, M. A. A. Hanim, A. A. Nuraini, W. Z. Wan Hasan, D. W. Jung	

<b>FABRICATION OF HALOCHROMIC POLYLACTIC ACID (PLA) FILAMENT FOR 3D PRINTING</b>	70
Q. H. Chan, M. Z. Zamri, A. Rusli, Z. A. A. Hamid, M. K. Abdullah, M. D. Syafiq, K. I. Ku Marsilla	

<b>ISOLATION AND CHARACTERIZATION OF NANOCRYSTALLINE CELLULOSE FROM BIOFUEL WASTE BY ORGANIC ACID HYDROLYSIS</b>	73
H. Holilah, D. V. Ramadhani, N. Jadid, T. P. Oetami, A. Asranudin, R. Ediati, D. Prasetyoko	

<b>FABRICATION OF PES/POM-TiO<sub>2</sub> MIXED MATRIX MEMBRANE WITH PHOTOCATALYTIC ACTIVITY FOR METHYLENE BLUE REMOVAL</b>	76
S. Zhafiri, T. Gunawan, N. Widiastuti	

<b>TENSILE PROPERTIES OF SEA APPLE LEAF (SALF) FILLER REINFORCED POLYESTER COMPOSITE</b>	79
A.E. Hadi, J.P. Siregar, T. Cionita, A.P. Irawan, D.F. Fitriyana, R. Junid	

<b>UTILIZATION OF POLYETHYLENE TEREPHTHALATE (PET) PLASTIC BOTTLE WASTE AS A MEMBRANE WITH SEVERAL MODIFICATIONS FOR THE REMOVAL OF CHROMIUM IONS IN WASTEWATER</b>	85
B. T. I. Ali, N. Widiastuti, Y. Kusumawati, J. Jaafar	

<b>LATEX DIPPING FILM OF CREAMED SKIM NATURAL RUBBER LATEX</b>	88
P. Ramchan, W. Taweepreda, D. Veerasamy	

<b>MODIFICATION OF CHITOSAN-BASED MEMBRANE WITH EPOXIDIZED</b>	91
--	----

**NATURAL RUBBER**

A. Wichianchom, W. Taweepreda, Q. Ali, M. Zulkifli

**THE EFFECT OF CHEMICAL TREATMENT TOWARDS PHYSICAL DIMENSIONS OF SUGAR PALM FIBER/PLA COMPOSITE FILAMENT FOR FDM**

M. H. M. Nasir, M. M. Taha, Nadlene R

95

**STARCH-BASED PLASTICS: A BIBLIOMETRIC ANALYSIS (1990-2021)**

A.H. Nordin, R.A. Ilyas, N. Ngadi

98

**COMPRESSION PROPERTIES OF SQUARE CORE SANDWICH STRUCTURE MADE OF KENAF/PLA COMPOSITE**

M.A.H.M. Yusri, M.Y.M. Zuhri, M.R. Ishak, M.A. Azman

101

**PHYSICO-CHEMICAL PROPERTIES OF PVC RESIN MEMBRANE BLENDING WITH PEG**

S. Seansukato, W. Taweepreda, S. Lamlong, A. Gangasalam

103

**DEVELOPMENT OF 3D PRINTED HUMAN BRAIN MODELS USING THERMOPLASTIC POLYURETHANE/RUBBER BLENDS FOR ANATOMY TEACHING PROMOTING KINAESTHETIC LEARNING PURPOSES**

S. H. A. Hisham, I. F. Ismail, S. A. Shamsuddin, S. N. H. Hadie, Z. Mohd Ismail, F. Kasim, N.A. Sapiai, N. A. Mat Zin, K. I. Ku Marsilla

106

**MAGNETIC CHITOSAN HYDROGEL BEADS AS ADSORBENT FOR COPPER REMOVAL FROM AQUEOUS SOLUTION**

N.A. Khalil, A.M.A. Huraira, S.N.D. Janurin, A.N.S. Fizal, N. Ahmad, M. Zulkifli, M.S. Hossain, A.N.A. Yahaya

110

**EFFECT OF PARAMETERS MANIPULATION ON CELLULOSE EXTRACTION PROCESS USING ECO-FRIENDLY SOLVENT AND PRODUCTION OF CELLULOSE TRANSPARENT FILM FROM OIL PALM FROND**

A. F. Lajulliadi, N. A. Khalil, A. N. A. Yahaya, M. Zulkifli

114

**INTERFACIAL SHEAR PROPERTIES OF TREATED KENAF/POLYPROPYLENE WITH SILANE PVA/ UREA**

N. I. S. Anuar, S. Zakaria, Q. Zuo, C. Wan

117

**INFLUENCE OF AMMONIUM POLYPHOSPHATE (APP) AND SODIUM HYDROXIDE (NaOH) SURFACE TREATMENTS ON KENAF FIBRES THERMAL PROPERTIES**

W. N. W. Jusoh S.A.S. Abdullah, A. H. A. Hamzah, R. Z. Abidin, T. T. Harun, Nurafiqah N.K., Z. Sahwee, S. Ahmad, N. L. M. Kamal, S. A. Hamid, N. Norhashim

121

**EFFECT OF WOVEN FABRIC GEOMETRICAL PARAMETERS ON THE PERMEABILITY BEHAVIOUR OF WOVEN FLAX FABRICS**

W. M. I. W. Zaludin, N. Z. M. Zuhudi, K. D. M. Aris

124

**CONVERGENCE OF FINITE ELEMENT MODEL FOR TRANSIENT THERMAL SIMULATION OF COMPOSITE LAMINATE**

E. E. S. M. Noor, N. Z. M. Zuhudi, A. N. A. Yahaya, M. Zulkifli

127

**RECYCLING OF THE BAMBOO FIBRE COMPOSITES AND THEIR HYBRIDS**

N.Z.M. Zuhudi, K. Jayaraman, R. J. T. Lin

131

vii



<b>UV-SHIELDING BIODEGRADABLE FILMS BASED ON CARBOXYMETHYL CELLULOSE FILLED WITH HENNA EXTRACTS</b> N. Danmatam, D. Pattavarakorn	134
<b>WATER ABSORPTION BEHAVIOUR OF BAMBOO-GLASS HYBRID POLYPROPYLENE COMPOSITES</b> N.Z.M. Zuhudi, K. Jayaraman, R. J.T. Lin	137
<b>A REVIEW: RMS – RAPID MOTION SCANNER TECHNIQUE ON MEASURING MATERIAL VELOCITY AND THICKNESS OF FLAX FIBER PREPREG</b> S. N. Fatin, K. D. M. Aris, M. N. Ismail	140
<b>POLYMERIC MATERIALS USED FOR IMMOBILIZATION OF MICROALGAE FOR THE BIOREMEDIATION OF PALM OIL MILL EFFLUENT</b> M.E. Azni, M. Suhaini, R. Noorain, S.H.S. Mariam, M.N. Azra, Y.Y Yeong, M. Rozyanti	143
<b>VARIATION AND KINETICS OF POLY(3-HYDROXYBUTYRATE) DEPOLYMERIZATION BEHAVIOR IN STEAM-ASSISTED HYDROLYSIS</b> E. N. Othman, H. Ariffin, N. Haruo, A. Yoshito, M. Ahmad, M. Z. W. Yunus, M. A. Hassan	146
<b>NANOFILLER-CONTENT RUBBER COMPOSITES</b> A. S. Norfarhana, R.A. Ilyas, N. Ngadi, A.H. Nordin, Nur Hafizah Ab Hamid	149
<b>INFLUENCE OF FILAMENT FABRICATION PARAMETER ON TENSILE PROPERTIES OF 3D PRINTING PLA FILAMENT</b> S. Hamat, M.R. Ishak, S.M. Sapuan, N. Yidris	152
<b>EXPERIMENTAL ANALYSIS OF COMPRESSION PROPERTIES IN 3D PRINTING PLA FILAMENT</b> S. Hamat, M.R. Ishak, S.M. Sapuan, N. Yidris	156
<b>EFFECT OF FILAMENT FABRICATION PARAMETER ON FLEXURAL PROPERTIES OF 3D PRINTING PLA FILAMENT</b> S. Hamat, M.R. Ishak, S.M. Sapuan, N. Yidris	160
<b>NORMALIZATION OF IMPACT ENERGY BY DIFFERENT LAYER ARRANGEMENT FOR KENAF-GLASS HYBRID COMPOSITE LAMINATES</b> S. Yunus, Z. Salleh, N. R. N. M. Masdek, A. Jumahat, S. Kushairi, F. A. Ghazali, Z. Halim	163
<b>CONDUCTIVITY AUGMENTATION OF POLYANILINE (PANI)-PEDOT: PSS HYBRID INDUCED COTTON FABRIC</b> M. S. Parvez, M. M. Rahman	164
Acknowledgements	165

**PREFACE**

**S.M. Sapuan**

Advanced Engineering Materials and Composites Research Centre (AEMC), Department of Mechanical and Manufacturing Engineering, Universiti Putra Malaysia, 43400 UPM Serdang, Selangor, Malaysia

**R.A. Ilyas**

School of Chemical and Energy Engineering, Faculty of Engineering, Universiti Teknologi Malaysia, 81310 UTM Johor Bahru, Johor, Malaysia

Centre for Advanced Composite Materials (CACM), Universiti Teknologi Malaysia, 81310 UTM Johor Bahru, Johor, Malaysia

Institute of Tropical Forestry and Forest Products (INTROP), Universiti Putra Malaysia, 43400 UPM Serdang, Selangor, Malaysia

**M.Y.M. Zuhri**

Advanced Engineering Materials and Composites Research Centre (AEMC), Department of Mechanical and Manufacturing Engineering, Universiti Putra Malaysia, 43400 UPM Serdang, Selangor, Malaysia

**E.S. Zainudin**

Advanced Engineering Materials and Composites Research Centre (AEMC), Department of Mechanical and Manufacturing Engineering, Universiti Putra Malaysia, 43400 UPM Serdang, Selangor, Malaysia

**M. Jawaid**

Laboratory of Biocomposite Technology, Institute of Tropical Forestry and Forest Products (INTROP), Universiti Putra Malaysia, 43400 UPM Serdang, Selangor, Malaysia

**Z. Leman**

Department of Mechanical and Manufacturing Engineering, Faculty of Engineering, Universiti Putra Malaysia, 43400, UPM, Serdang, Selangor, Malaysia

Advanced Engineering Materials and Composites Research Centre (AEMC), Department of Mechanical and Manufacturing Engineering, Universiti Putra Malaysia, 43400 UPM Serdang, Selangor, Malaysia

**A.N.A. Yahaya**

Universiti Kuala Lumpur, Branch Campus Malaysian Institute of Chemical and Bioengineering Technology, 78000 Alor Gajah, Melaka, Malaysia

**M.A. Azman**

Advanced Engineering Materials and Composites Research Centre (AEMC), Department of Mechanical and Manufacturing Engineering, Universiti Putra Malaysia, 43400 UPM Serdang, Selangor, Malaysia

**M. Zulkifli**

Green Chemistry and Sustainability Cluster, Universiti Kuala Lumpur, Branch Campus Malaysian Institute of Chemical and Bioengineering Technology, Taboh Naning, 78000 Alor Gajah, Melaka, Malaysia

## *ISPM2022*

### *The International Symposium on Polymeric Materials 2022*

#### **N.A. Khalil**

Universiti Kuala Lumpur, Branch Campus Malaysian Institute of Chemical and BioEngineering Technology, 78000 Alor Gajah, Melaka, Malaysia

#### **N.Z.M. Zuhudi**

Aero Composite Cluster, Universiti Kuala Lumpur Malaysian Institute of Aviation Technology (UNIKL MIAT), Lot 2891, Jalan Jenderam Hulu, 43800 Dengkil, Selangor, Malaysia

#### **C.N. Aiza Jaafar**

Advanced Engineering Materials and Composites Research Centre (AEMC), Department of Mechanical and Manufacturing Engineering, Universiti Putra Malaysia, 43400 UPM Serdang, Selangor, Malaysia

#### **M.N.M. Azlin**

Laboratory of Biocomposite Technology, Institute of Tropical Forestry and Forest Products (INTROP), Universiti Putra Malaysia, 43400 UPM Serdang, Selangor, Malaysia

#### **K.Z. Hazrati**

Advanced Engineering Materials and Composites Research Centre (AEMC), Department of Mechanical and Manufacturing Engineering, Universiti Putra Malaysia, 43400 UPM Serdang, Selangor, Malaysia

German Malaysian Institute, Jalan Ilmiah, Taman Universiti, 43000, Kajang, Selangor, Malaysia

#### **M.M. Harussani**

Department of Transdisciplinary Science and Engineering, Tokyo Institute of Technology, Meguro, Tokyo 152-8552, Japan

#### **M. F. Banjar**

Universiti Kuala Lumpur, Branch Campus Malaysian Institute of Chemical and BioEngineering Technology, 78000 Alor Gajah, Melaka, Malaysia

#### **R.M.O. Syafiq**

Laboratory of Biocomposite Technology, Institute of Tropical Forestry and Forest Products (INTROP), Universiti Putra Malaysia, 43400 UPM Serdang, Selangor, Malaysia

#### **A. Nazrin**

Laboratory of Biocomposite Technology, Institute of Tropical Forestry and Forest Products (INTROP), Universiti Putra Malaysia, 43400 UPM Serdang, Selangor, Malaysia

#### **A.F. Lajulliadi**

Universiti Kuala Lumpur, Branch Campus Malaysian Institute of Chemical and BioEngineering Technology, 78000 Alor Gajah, Melaka, Malaysia

#### **J. Tarique**

Advanced Engineering Materials and Composites Research Centre (AEMC), Department of Mechanical and Manufacturing Engineering, Universiti Putra Malaysia, 43400 UPM Serdang, Selangor, Malaysia



# Foreword

**Chairman**

**Prof. Ir. Dr. Mohd Sapuan Salit**

**International Symposium on Polymeric  
Materials 2022**

Assalamualaikum and good day.

I would like to welcome all plenary and keynote speakers, all the VIPs, and other international and local participants of International Symposium of Polymeric Materials 2022 (ISPM 2022) comprising judges, session chairs, sponsors, international advisory committee, technical committee, emcee, editors of proceedings, paper presenters and others. ISPM 2022 is organized by Advanced Engineering Materials and Composites Research Centre (AEMC), Department of Mechanical and Manufacturing Engineering, Universiti Putra Malaysia and supported by Universiti Kuala Lumpur and Plastics and Rubber Institute Malaysia (PRIM).

This is the first International Symposium of Polymeric Materials organized as an upgrade from a series of National Symposia of Polymeric Materials anchored by PRIM since early 2000 and as a founding Head of AEMC, I am honoured to be invited to jointly chair this inaugural event.

Polymer, plastics, rubbers and polymer composites, the topics that are mainly discussed in this symposium are indeed very important materials and they have served the mankind for long time and we are continuing to derive benefits from these materials. Nowadays these materials are used in different industries such as energy, biomedical, packaging, automotive, agriculture, aerospace and building and construction.

I am happy to declare that a total of 59 papers are presented with participants are mainly from Malaysia and there are also guests from Jordan, Pakistan, Thailand, India, Australia, Indonesia, and Scotland, joining this symposium. We also made effort to publish all the papers in proceedings and this book is distributed to all participants during the early part of the symposium. After the symposium, all paper presenters will be invited to submit full papers for journal publications. During this symposium, we are giving away six awards in two major categories; the Best Paper Awards and The Best Oral Presenter Awards in the forms of certificates, plaques, cash money and books.

Finally, I thank the sponsors, i.e., Springer Singapore, PRIM and UniKL for their contribution. I hope you enjoy participating this symposium

Regards

Prof. Ir. Dr. Mohd Sapuan Salit

Chairman of International Symposium of Polymeric Materials 2022 (ISPM2022)



# Foreword

**President**

**Mr. Chan Pak Kuen**

**The Plastics & Rubber Institute  
Malaysia**

Greetings, I am delighted to present the Opening address for the International Symposium of Polymeric Materials or ISPM 2022 held on online platform.

On behalf of the PRIM Management Committee, I wish to take this opportunity to congratulate the Advanced Engineering Materials and Composite Research Centre, Department of Mechanical & Manufacturing Engineering of Universiti Putra Malaysia for initiative and commitment in organizing ISPM 2022. It is indeed commendable as we all have gone through over 2 years of hiatus of Covid pandemic. Although Malaysia has now transitioned from pandemic to endemic, we are aware the importance of continuing to be vigilant and safe. Therefore, the postponed ISPM 2022 held virtually is most appropriate and timely in order to encourage and attract participants from both local and overseas. I was informed there will be deliberation of 59 papers which include 6 plenary and keynotes as well as 25 % overseas participants during the 2-day session. I also understand the symposium will feature different themes, such as Polymer Technology and Biopolymer, Natural Fibre Composite and Rubber-based Composites, Nanocomposite and Advanced Manufacturing.

I recall the last edition which was the National Symposium of Polymeric Materials hosted by UniKL was held in conjunction with the International Rubber Conference 2018 organised by PRIM at KLCC. The overwhelming response led to the decision of upgrading from NSPM to ISPM. Prof. Ir. Dr. Mohd Sapuan bin Salit who was in attendance readily accepted our invitation to host the inaugural event. Many thanks to Prof. Ir. Dr. Mohd Sapuan bin Salit and the joint Chairman, Assoc. Prof. Dr. Zulkiflle bin Leman. The concern about utilization of synthetic fibre and its effects on environmental health has brought researchers from various backgrounds working on solving the issue. Thus, green technology and renewable energy based on natural fibres have paved new and innovative ways for a sustainable future. In conclusion, it is my aspiration that this conference will be a foundation for the growth of new ideas related to sugar palm and allied fibre products towards a better tomorrow.

PRIM takes pride in supporting the staging of this Symposium because it is in line with our mission in promoting the practice and development of polymer science and technology through education/training and conference like this to fulfil the needs of both individuals and the industry.

It is well recognized that Malaysian economy could no longer depend on the cheap labour. To remain competitive in the global market, future economy will be driven with increasing emphasis on knowledge, productivity and education. It is only knowledge that will add value

## *ISPM2022*

### *The International Symposium on Polymeric Materials 2022*

to our industry and enhance our global competitiveness. Therefore, the partnership and collaboration between PRIM and local Universities in enhancing technical knowledge will have a complementing role to play in meeting national objectives

Polymeric materials have become an essential and ubiquitous part of our lives. There is not a day we can live without using any of the polymeric materials. We sleep on it, drive on it, sit on it, walk on, sail on it, play with it and so on. Therefore, such widespread use confirms the success and the immense benefits of the polymeric materials. However, this carries with it the dire need to continually focus on research and development effort in order to fulfil increasing stringent future requirements.

Henceforth, I am sure the technical and research papers which will be presented at this symposium will generate stimulating discussion and certainly enrich our knowledge on polymeric materials development. It is our wish that all the research findings, if not already economically exploited, will lead to full commercialization one day thus driving us to have competitive edge in research and technology in global market.

On that note, I wish to congratulate once again the organizing committee for the initiative and splendid effort in organising this inaugural Symposium.

P K Chan

President 2021-2023

The Plastics & Rubber Institute Malaysia



# Foreword

Dean

**Prof. Ir. Dr. Mohd Khairol Anuar b.  
Mohd Ariffin**

**Faculty of Engineering, UPM**

Assalamualaikum Warahmatullahi Wabarakatuh.

I wish to extend my deepest gratitude to all the esteemed delegates and guests for attending the International Symposium on Polymeric Materials 2022 (ISPM 2022) virtually. Although we are doing it fully online, this virtual gathering is considered as one of the most significant and memorable forms of gathering too. The sharing of best practices in this event offers new insights that can ensure a sustainable research and publication through interesting discoveries

It is grateful for me to be here today at this event, it is indeed a meaningful occasion. It has to come to my attention the International Symposium on Polymeric Materials 2022 (ISPM 2022) is a public private partnership event organised by the Advanced Engineering Materials and Composites (AEMC) from Faculty of Engineering, Universiti Putra Malaysia in collaboration with Universiti Teknologi Malaysia, Universiti Kuala Lumpur Malaysian Institute of Chemical and Bio-Engineering Technology (UniKL MICET), as well The Plastics & Rubber Institute Malaysia (PRIM). It takes great effort to bring all professionals around the globe together to share experiences, knowledge and evidence-based practices in the special knowledge field in Malaysia. By having this platform can open up more opportunities to reflect and improve the different approaches in special knowledge.

The ISPM 2022 is an upgrade of a series of National Symposium on Polymeric Materials (NSPM) jointly organized by The Plastics Rubber Institute Malaysia (PRIM) and some local universities since early 2000. It all started as an idea from the Universiti Putra Malaysia, Universiti Kuala Lumpur Malaysian and The Plastics & Rubber Institute Malaysia (PRIM) to provide a medium to bring together researchers, scientists, and engineers from academia, research institutions and industry to exchange information, experiences and expertise in the field of polymer material, hence to foster research relations between the universities and the industries.

It is known that for academicians and researchers, conducting research is important for us to provide new knowledge in helping the society in solving various problems. Additionally, it is vital to contribute to betterment of society particularly in this digital era. We all understand that the purpose of conducting research is to inform action, prove theories, and contribute to developing knowledge and innovation in a field or study. The study should seek to contextualize its findings within the larger body of the research. Thus, it should always be of high quality of research work to provide and produce good knowledge that can be applied outside of the research setting.

## *ISPM2022*

### *The International Symposium on Polymeric Materials 2022*

In order to make this international symposium success, the ISPM 2022, indeed, needs a lot of hard works and commitment from the organizing committees. Therefore, I would like to express my utmost appreciation towards the organizing committees of ISPM 2022, honorable speakers, participants and guests for the support and contribution. I hope everyone will obtain invaluable insights and knowledge from other researchers during this event. I believe that this international symposium will be beneficial to all and wish all the best for all participants.

Thank you and best wishes.

**PROF. IR. DR MOHD KHAIROL ANUAR MOHD ARIFFIN**



**PLENARY SPEAKER 1**



**Vijay Kumar Thakur**

Professor and Founding Head of the Biorefining and Advanced Materials Research Centre, SRUC, Edinburgh, UK

**PROFILE**

**Prof. Dr. V. K. Thakur** is a Full Professor and Founding Head of the Biorefining and Advanced Materials Research Centre at SRUC, UK and also holds an Adjunct Professor position in the Research School of Polymeric Materials, Jiangsu University, China; Riga Technical University; UPES; Shiv Nadar University and Visiting Professor at Cranfield University, UK. He did his post-doctoral study in Materials Science & Engineering at Iowa State University and received a PhD in Polymers Science (2009). His expertise includes the synthesis and processing of sustainable and functional polymer materials. He has been a PI/ Co-PI on several projects sponsored by BAE Systems; EPSRC (EP/T024607/1); Royal Academy of Engineering (IAPP-33- 24/01/2017; IAPP18-19\295); RESAS; UIF (SFC); UKIERI (DST/INT/UK/P164/2017); Innovate UK; and others. He has published over 350 SCI journal articles, 2 patents, 52 books & 40 book chapters on polymers and materials science (H-index 84, >22,500 citations). He sits on the editorial board of several SCI journals as Associate Editor/ Editor/ Editorial Advisory Board Member. He has been named among World's Top 2 % Scientists in 2021 with a Global Rank of #122nd in the Polymers category and #133rd in the Nanoscience and Nanotechnology category (Scopus/ Stanford University List) and is also among Highly Cited Researchers (Clarivate Web of Science) list since 2020

**ABSTRACT**

**POTENTIAL AND LIMITATIONS OF POLYMERS FOR THE NEW MILLENNIUM**

Polymer nanocomposites are rapidly emerging as novel materials for a number of advanced engineering applications. Especially polymer nanocomposites have drawn greater attention globally due to their applications in various fields such as biomedical, remediation, pulsed power systems, optoelectronics, temperature, defence, vapour/liquid sensing, and energy harvesting, transistors, and inverters. Polymers have been found to exhibit several advantages such as flexibility, easy processing and manufacturing, high breakdown strength along with high energy density (in the case of dielectric materials), while the fillers provide other requisite characteristics needed for specific applications. The combination of both the polymers and fillers provides enhanced properties depending on the type and nature of polymer matrices as well as fillers. So, in this lecture, I will be mainly talking about our work on the synthesis and processing of polymer-based materials for advanced applications.

**KEYNOTE SPEAKER 1**



**S. Prakash**

Professor & Dean-Mechanical, School of Mechanical Engineering, Sathyabama Institute of Science and Technology, Chennai, India

**PROFILE**

**Prof. Dr. S. Prakash**, M.E., PhD, has over 28 years of teaching experience and 15 years of research and administration experience with a demonstrated history of working in the higher education field. Skilled in Curriculum Development, Artificial Intelligence (AI), Research, and Teaching. Strong education professional graduated from Sathyabama University. He joined Sathyabama Institute of Science and Technology as a Senior lecturer in July 1998. He has completed his PhD in 2011 from Sathyabama Institute of Science and Technology. His research areas include Composites Machining, Optimization and Modelling self-healing etc. and more specially in machining composites. He has so far published more than 100 technical papers in indexed and peer reviewed journals and conference of international repute. He has obtained funded research project from different government agencies and currently he is the Principal Investigator of AICTE funded project under AICTE-MODRAB scheme. He has published seven patents so far. He is a recipient of prestigious National and International awards including ASDF, IARA and Venus awards for his innovative work in Engineering and Technology in the years 2018 and 2019 respectively. He is a Fellow of IPE, senior member in IMQE and member of different professional bodies. Dr. Prakash is a recognized editor and reviewer of various reputed journals under Science direct, Springer, Taylor and Francis, Inderscience etc. He has co-authored five different technical books. Considering his expertise in teaching and contributions to the institution he was awarded the Best Teacher Award for the years 1999-2000, 2006-2007, 2006-2007, 2008-2009 and 2011-2012.

**ABSTRACT**

**STRUCTURAL AND MECHANICAL PROPERTIES OF BIOPLASTICS HYBRID BASED FIBBER BETWEEN PALM SUGAR FIBER (PSF)/PINEAPPLE LEAF FIBER (PLF) MODEL**

The effects of the delamination in the critical buckling load failure of E-Glass /epoxy composite laminates are analysed. The buckling load of rectangular composite plates is determined by carrying out the experimental work for different aspect ratios of range 2 to 3. The specimens are made with unidirectional fibres of orientation (90°/45°/-45°/0°) s. The width of long 100 mm and 50 mm at the centre of the plate, a single substantial delamination is made at the mid layer produced by Teflon film using hand lay-up technique. The buckling loads of plates were found by using simply supported boundary condition and kept the other side edges free. The experimental buckling loads were found from the graph drawn for vertical displacement vs load. By drawing the graph for the vertical displacement Vs Load, the experimental buckling load can be calculated. Using finite element software of ANSYS the experimental results were validated.

**KEYNOTE SPEAKER 2**



**Pong Kai See**

FPRI, FPRIM, MSc (Techno-economics), BSc (Hons) CNAALondon

**PROFILE**

**Pong Kai See** One of Sekhar’s “rubber babies”, a select group of high achieving students sent overseas to study rubber science and technology, tasked with transforming Malaysia from exporter of commodity natural rubber to world player in finished rubber products. He was a member of the international team of rubber experts that charted Malaysia’s “rubber industrialization” strategy in 1972, and later pioneered Malaysian exam glove manufacturing in 1980s. He was M.D. of Handee Engineering, first company to be granted pioneer status by MIDA to make glove dipping machines. At age 75 he is still active in sharing his knowledge and experience and is a regular lecturer in PGRT/GPRIM, DPRIM and SCLT and other rubber courses. He writes regularly on rubber techno-economic issues.

**ABSTRACT**

**MALAYSIAN GLOVE INDUSTRY POST-COVID - PROSPECTS AND STRATEGIES TO STAY AHEAD**

Rosy market forecasts in the early days of COVID prompted a lot more investment than prudent in new glove capacity, by major players in Malaysia, Thailand and China as well as new players outside the glove industry. When demand of gloves returned to normal after the boom, a lot of new capacity will become stranded. What is going to happen? Will there be a price war? Or will these factories simply close shop and disappear? China were the first country to control COVID and came out of lockdown in April 2020. China had early mover advantage and were able to capture the market of new glove demand when capacity became available ahead of competitors. China is now the #2 glove producer and is snapping at the heels of Malaysia, the #1 producer. In this talk I shall speculate on possible scenarios and suggest strategies Malaysian glove makers can adopt to stay ahead.

KEYNOTE SPEAKER 3



**Ismail Zainol**

Professor, Chemistry Department, Universiti Pendidikan Sultan Idris (UPSI)

**PROFILE**

**Prof Ts. Dr Ismail Zainol** received his PhD from UMIST, Manchester, United Kingdom in 2001 and he was a senior researcher at SIRIM Berhad for 15 years before joining Chemistry Department, Universiti Pendidikan Sultan Idris (UPSI). His main research interests are polymer composites and biomaterials. Currently, he explores the usage of fish scales in Biomaterials application with collagen as wound dressing and hydroxyapatite as fillers in biocomposite. With over 28 years experiences, Prof. Ts. Dr Ismail has been recognized for his outstanding contributions in polymer composite materials as well as biomaterials in various applications. Nowadays, he has contributed more than 60 papers in peer-reviewed journals, more than 20 papers in conferences, some chapters in books, four patents and referees for 20 journal papers. He also successfully graduated 8 PhD students and 6 MSc students and now one PhD and two MSc are still working towards completion. His leadership is reflected through the election as President of Malaysian Biomaterials Society (MBS) and appointed as MOHE grant evaluator. Prof. Ts Dr. Ismail Zainol's research has been widely recognized nationally and internationally. Among of them, he is the recipient of three prestigious awards from UPSI namely Staff Excellence Award for the year 2013, 2014 and 2015 for achievement in product commercialization and research grant. His research has won 15 Gold Awards in various exhibitions at national and international levels such as WIPO Award 2012, Intellectual Property Award 2012, Menteri Besar Perak Award 2013, Grand Prize from Romania 2013, Anugerah Malam Citra Inovasi KPT, 2013 and Malaysian Innovative Product Awards 2015. The biggest achievement in his career was the winner of overall awards (Grand Award, Best Award and Gold Award) in PECIPTA 2015 for his innovation in fish scales hydroxyapatite in water filter applications. Two of his research products have been successfully commercialized such as collagen extraction technology from fish scales and applications of natural hydroxyapatite for water filter applications.

**ABSTRACT**

**NATURAL HYDROXYAPATITE FROM FISH SCALES AS POTENTIAL FILLERS IN POLYMER COMPOSITE FOR POTENTIAL BIOMATERIAL APPLICATIONS**

A natural hydroxyapatite (HA) material which is extracted from natural sources has become the main alternative to chemically synthesized HA since they are similar in structure but relatively cheap with excellent biological properties. Currently, HA is gaining prominence for applications as fillers in polymer composite for orthopedic implants and dental materials. This study focuses on the extraction of HA ( $\text{Ca}_{10}(\text{PO}_4)_6(\text{OH})_2$ ) from fish scales (FsHA) using thermo-degradation technique, mechanically treated into irregular shape of particles morphology and applied them as biocompatible fillers in thermoplastic and thermoset polymers. The extracted FsHA was analyzed using FTIR, XRD and SEM-EDX techniques. Meanwhile, the particles size was analyzed using particles size analyzer. The cytotoxicity of the FsHA polymer composites was evaluated using Alamar blue assay. The SEM analysis revealed that the irregular shape of FsHA particles has the size of around 10  $\mu\text{m}$  and the EDX result indicated the Ca/P ratio of the FsHA materials was about 1.83. The FTIR and XRD analyses results confirmed the highly crystalline materials with secondary phase of beta tricalcium phosphate ( $\beta$ -TCP) was produced from FsHA after sintering at 1200 °C. The highly crystalline natural FsHA particle which was obtained

from this research holds a promising feature as reinforcement fillers in polymer composite. They have increased the mechanical properties of high density polyethylene (HDPE) with the results of tensile strength, Young's modulus and flexural modulus of 28.3 MPa, 1272 MPa and 796 MPa, respectively. Similarly, FSHA has become excellent fillers in epoxy resin with improvement in mechanical properties and the biocompatibility of the composites. With the addition of liquid natural rubber (LNR) in the composite, the fracture toughness of the epoxy composite was increased up to 24 fold (16.2 MPa m<sup>1/2</sup>). In vitro cytotoxicity analysis verified that the developed FSHA polymer composites were non-toxic and it has a great potential to be used for biomedical applications.

**KEYNOTE SPEAKER 4**



**Wirach Taweepreda**

Assistant Professor, Division of Physical Science, Faculty of Science, Prince of Songkla University

**PROFILE**

**Dr. Wirach Taweepreda** graduated as a Chemist in Prince of Songkla University (PSU), Thailand. He completed his master degree in polymer science and technology at Mahidol University, Thailand and completed his PhD thesis in School of Chemistry at University of Bristol, U.K. His research interest involves the polymer applications for Bio-Circular and Green Economy. Since 2005, he was appointed Lecturer at the Polymer Science Program, Department of Materials Science and Technology, Faculty of Science, PSU, initially teaching courses in Fundamental of Elastomer, Polymer Physics, and Polymeric Membrane. From 2012 onwards, he is working as Assistant Professor in the same department. He coordinating as principal investigator for many projects which is funded by Thailand Research Funding (TRF), National Science and Technology Development Agency (NSTDA), and Ministry of Higher Education, Science, Research and Innovation (MHESI) for solving industrial problems and develop new products. Current research involves the polymeric materials for industrial waste treatment and recovery for Greener Eco-Environment process. He collaborated with Universiti Kuala Lumpur on project research study and supervision in postgraduate education. He was supervisor to post-graduated students in M.Sc. (15) and Ph.D. (9) levels and published 51 original articles in peer review international journal, 2 Patents (PCT), 21 Thai Patents, and 2 book chapters

**ABSTRACT**

**CONSISTENCY OF NATURAL RUBBER – EFFECT ON PROCESSING PROPERTIES**

The present works proposed to find out quantitative effects of method and condition of preparation of STR20 on its processing properties (mastication and mixing properties) including those of their filled compounds. The results obtained revealed that type and amount of acid used to coagulate the latex and also the drying temperature of the coagulum had influential effect on rheological properties of the raw rubber and also on the value of PRI. Furthermore, variation in rheological and thermal oxidative properties of the prepared NR were confirmed to have only small effect on processing properties of NR, or at least not to the extent that was previously believed. However, the properties of the rubber compounds obtained were still varied depending on the initial rheological properties of raw NR. Therefore, consistency in rheological properties of NR compound could only be obtained if the initial properties of NR were consistent. Results of the present study must be further verified by industrial-scale study before a definite conclusion could be made.

KEYNOTE SPEAKER 5



**Mainul Islam**

Associate Professor, Mechanical Engineering, School of Mechanical and Electrical Engineering of Faculty of Health, Engineering and Sciences and Centre for Future Materials in the University of Southern Queensland, Australia.

**PROFILE**

**Associate Professor Dr Mainul Islam** is an academic in Mechanical Engineering with specialisation in Composite Materials in the School of Mechanical and Electrical Engineering at the University of Southern Queensland (USQ), Australia. He also belongs to the Centre for Future Materials at USQ for conducting research. He completed his PhD in Mechanical Engineering at the University of Newcastle, Australia. He is a graduate and also former Assistant Professor in Mechanical Engineering of Khulna University of Engineering & Technology (KUET), Bangladesh. He got Master degree in Structural Engineering from Kyushu University, Japan. He has been with USQ since 2008 just after completing PhD. His current research interests are in the areas of smart and sustainable composites and shape memory polymeric materials especially for infrastructure and biomedical applications. He has over 150 research publications based on his research outcomes. He has been able to secure a total of over \$1.5M research funding jointly and individually during his academic career so far. He has supervised over 15 PhD students to their completion. He serves as Editorial Board member for several renowned journals and Technical Committee member for several international conferences. He is a Fellow (FIEAust) and Chartered Professional Engineer (CPEng) of Engineers Australia.

**ABSTRACT**

**EFFECT OF DISPERSION TIME FOR NANOPARTICLES IN DGEBA SHAPE MEMORY POLYMER COMPOSITE FABRICATION**

Shape-memory polymers (SMPs) are smart materials that can change shape upon an external stimulus. This phenomenon is called the shape memory effect (SME), which is caused by entropy change due to rapid molecular motion in the polymer segments. Due to the inherently weak thermomechanical properties, use of SMPs are limited in many engineering applications. Therefore, SMPs are often reinforced with fibres and nanoparticles (NPs). NPs offered greater flexibility due to their superior physical, chemical, electrical, mechanical, and thermal properties. However, the homogeneous distribution of NPs is crucial for composition's stability and enhancement of the base material's properties. Among the different techniques used for dispersing NPs, ultrasonic irradiation has shown excellent emulsifying and crushing performance. The sonication process is essential for mitigating agglomerates; however, prolonged sonication time probably increases epoxy temperature, micro-bubbles, cavitation, breaking apart molecules and finally degrading the epoxy resin performances. This paper provides critical insight of nanoparticle dispersion into diglycidyl ether of bisphenol A epoxies (DGEBA). DGEBA epoxy resin was added to TiO<sub>2</sub> NPs and sonicated for 60 minutes with 5 minutes intervals while the temperature of epoxy was maintained below 60°C by using a water cooling throughout the sonication process. The process parameters such as amplitude, mode, epoxy volume and the weight percentage of NPs were kept constant. After each sonication step, Fourier-transform infrared spectroscopy (FTIR) was performed using Thermo Scientific™ and analysed through OMNIC™ Professional quantitation software. In accordance with FTIR results, until 30 minutes of the sonication, DGEBA resin was not degraded. In order to confirm the performances and the reinforcing effect of NPs, thermo-mechanical and shape memory properties were compared with the neat specimen. The outcomes of this research have suggested quick guidance to find optimum NP dispersion time for DGEBA resins, which has been hardly studied before.

## INTERNATIONAL SYMPOSIUM ON POLYMERIC MATERIALS 2022

14 – 15 JUNE 2022

Day 1: 14 June 2022 (Tuesday)

Time	Event Day-1		
0800 – 0830	Session Login & Preparation		
0830 – 0900	(Session MC) Fatin Najwa Joynal Abedin	Opening Ceremony	
0900 – 0905		Lagu Negaraku and Putra Gemilang	
0905 – 0910		1. Dua recitation by <b>Dr. Faisal Sherwani</b>	
0910 – 0915		2. Welcoming speech by Chairman of ISPM2022 <b>Prof. Ir. Dr. Mohd Sapuan Salit</b>	
0915 – 0920		3. Welcoming speech by President of PRIM <b>Mr. Chan Pak Kuen</b>	
0920 – 0930	4. Opening speech by Dean, Faculty of Engineering, UPM <b>Prof. Ir. Dr. Mohd Khairol Anuar b. Mohd Ariffin</b>		
0920 – 0930	4. Photo session		
0930 – 1000	Break		
0930 – 1000	(Chair) Dr. Mohammad Jawaid	Plenary Speaker 1: <b>Prof. Vijay Kumar Thakur</b>	
1000 – 1030		Title: Potential and Limitations of Polymers for the New Millenium	
1000 – 1030	(Chair) Dr. Mohammad Jawaid	Keynote Speaker 1: <b>Prof. Dr. S. Prakash</b>	
1030		Title: Modelling of Surface Roughness and Delamination in Drilling PB Panels with Coated Carbide Spade Drills – RSM Approach	
1030	Session Login & Preparation		
Track	Polymer Technology and Biopolymer		Natural Fibre Composites and Rubber-based Composites
	Room 1		Room 2
1030 – 1050	Chair: <b>Dr. Siti Hajar Sheikh Md Fadzullah</b>		Chair: <b>Assoc. Prof. Ts. Dr. Che Nor Aiza Jaafar</b>
	PR-01 ( <b>Mohd Nazri Ahmad, Mohamad Ridwan Ishak, Mastura Mohammad Taha, Faizal Mustapha and Zulkiflle Leman</b> ) Non Linear Finite Element Analysis of Oil Palm Fiber Composites for Fused Deposition Modeling (FDM)		PR-03 ( <b>F. N. J. Abedin, A. N. A. Yahaya, N. A. Khalil, M. Zulkifli</b> ) Antimicrobial Capability of Inorganic Material as Filler for Thermoplastic Elastomer - A State of The Art Review
1050 – 1105	PR-02 ( <b>Faiezah Hashim</b> ) The effect of PE-g-MA on the properties of Low Density Polyethylene (LDPE)/ Thermoplastic Banana Peel Starch (TBPS) Films		PR-04 ( <b>M. F. Banjar, A. N. A. Yahaya, N. A. Khalil, M. Singh, M. Zulkifli</b> ) Mechanical Properties and Conductivity of Polyaniline-Cellulose-Latex Hybrid
1105 – 1120	PR-07 ( <b>R.V. Yiow and M.R. Mansor</b> ) Polymer Matrix Material Selection for Sustainable Two-Stroke Marine Diesel Engine Crosshead Bearing Design Using Topsis Method		PR-08 ( <b>J. Tarique, S.M. Sapuan, E.S. Zainudin, A. Khalina and R.A. Ilyas</b> ) A Comparative Review of The Effects of Different Fibre Concentrations on Arrowroot Fibre and Other Fibre-Reinforced Composite Films
1120 – 1135	PR-13 ( <b>Nur Liyana Bekri, Iylia Idris, Ayub Md Som, Fakhrony Sholahudin Rohman, Muhamad Nazri Murat, Dinie Muhammad, Ahmad Ilyas Rushdan and Ashraf Azmi</b> ) Study of Input Parameter Changes Toward Low Density Polyethylene's Product Properties		PR-58 ( <b>S. Hamat, M.R. Ishak, S.M. Sapuan, N. Yidris</b> ) Experimental Analysis of Compression Properties in 3D Printing PLA Filament
1135 – 1150	PR-22 ( <b>Azmah Hanim Mohamed Ariff, D. W. Jung, Tahrim Hossain Rafin, Zulkiflle Leman, Khairil Anas Md Rezali, and Recep Calin</b> ) Temporary Sound Barrier System from Natural Fibre Polymeric Composite		PR-16 ( <b>MK Wahid, R Jumaidin, MH Osman and Ab Rahman M. H</b> ) Cutting Force Measurement of Oil Palm Empty Fruit Bunch Fiber Reinforced Polymer Matrix Composites
1150 – 1350	Break		
1350 – 1420	(Chair) Ts. Dr. Muzafar Zulkifli	Keynote Speaker 2: <b>Mr. Pong Kai See</b>	
1420	Title: Malaysian Glove Industry Post-Covid – Prospects and Strategies to Stay Ahead		
1420	Session Login & Preparation		
Track	Polymer technology and Biopolymer		Natural fibre composites and Rubber-based composites
	Room 1		Room 2
1420 – 1435	Chair: <b>Dr. Ridwan Yahaya</b>		Chair: <b>Ts. Azrena Abdul Karim</b>
	PR-23 ( <b>Faisal Dakhelallah Alshalawi, Azmah Hanim binti Mohamed Ariff, Mohd Khairol Anuar bin Mohd Ariffin, Collin Looi Seng Kim, Dermot Brabazon, Recep Calin</b> ) Biodegradable Synthetic Polymer in Orthopaedic Application: A Review		PR-17 ( <b>Nur Afifah Zakaria, Mohamad Ridwan Ishak, Faizal Mustapha, Noorfaizal Yidris</b> ) Tensile Properties of a Hybrid Kenaf-Glass Fiber Reinforced Unsaturated Polyester Composite Shaft
1435 – 1450	PR-24 ( <b>T. F. Alhamada, M. A. Azmah Hanim, A. A. Nuraini, W. Z. Wan Hasan, D. W. Jung</b> ) An Overview of Recent Advances in Polymer Solar Cell and Perovskite Solar Cell: Materials, Fabrication Methods, and Energy Conversion Efficiency		PR-18 ( <b>Fransiska angelina rezekinta, Anwar kasim, Edi syafri, Irawati, Firman ridwan</b> ) The effect of different pulping time on degradation of lignin in kapok fiber ( <i>Ceiba pentandra, L.</i> )
1450 – 1505	PR-29 ( <b>Syahman Zhafiri, Triyanda Gunawan, Nurul Widiastuti</b> ) Fabrication of PES/POM-TiO <sub>2</sub> Mixed Matrix Membrane with Photocatalytic Activity for Methylene Blue Removal		PR-32 ( <b>P. Ramchan, W. Taweepreda, D. Veerasamy</b> ) Latex Dipping Film of Creamed Skim Natural Rubber Latex
1505 – 1520	PR-31 ( <b>Badrut Tamam Ibnu Ali, Nurul Widiastuti, Yuly Kusumawati, Juhana Jaafar</b> ) Utilization Of Polyethylene Terephthalate (PET) Plastic Bottle Waste as a Membrane with Several Modifications for The Removal of Chromium Ions in Wastewater		PR-14 ( <b>S. Yunus, Z. Salleh, N. R. N. M. Masdek, A. Jumahat, F. A. Ghazali, Z. Halim</b> ) Normalization of Impact Energy by Different Layer Arrangement for Kenaf-Glass Hybrid Composite Laminates
1520 – 1535	PR-57 ( <b>S. Hamat, M.R. Ishak, S.M. Sapuan, N. Yidris</b> ) Influence of Filament Fabrication Parameter on Tensile Properties of 3D Printing PLA Filament		
End			



INTERNATIONAL SYMPOSIUM ON POLYMERIC MATERIALS 2022

14 – 15 JUNE 2022

Day 2: 15 June 2022 (Wednesday)

Time		Event Day-2		
0830 – 0900		Session Login & Preparation		
0900 – 0930		<b>(Chair)</b> <b>Assoc. Prof. Dr. Edi Syams Zainudin</b>	<b>Keynote Speaker 1: Prof. Ts. Dr. Ismail bin Zainol</b>	
			Title: Natural Hydroxyapatite from Fish Scales as Potential Fillers in Polymer Composite for Biomedical Applications	
0930 – 1000			<b>Keynote Speaker 2: Assoc. Prof. Dr. Mainul Islam</b>	
			Title: Effect of Dispersion Time for Nanoparticles in DGEBA Shape Memory Polymer Composite Manufacturing	
1000		Session Login & Preparation		
Track		<b>Polymer technology and Biopolymer</b>	<b>Natural fibre composites and Rubber-based composites</b>	<b>Nanocomposite and Advanced manufacturing of composite</b>
		<b>Room 1</b>	<b>Room 2</b>	<b>Room 3</b>
		<b>Chair: Dr. Aisyah Humaira Alias</b>	<b>Chair: Assoc. Prof. Ts. Dr. Muhd Ridzuan Mansor</b>	<b>Chair: Ts. Dr. Mohd Adrinata Shahraruzaman</b>
1000 – 1015		PR-34 (M. S. Parvez, M. M. Rahman) Conductivity Augmentation of Polyaniline (PANI)-PEDOT: PSS Hybrid Induced Cotton Fabric	PR-35 (A. Wichianchom, W. Taweeprada, Q. Ali) Modification of Chitosan-Based Membrane with Epoxidized Natural Rubber	PR-36 (Mohd Hakim M.N., Mastura M.T., Nadlene R.) The Effect of Chemical Treatment Towards Physical Dimensions of Sugar Palm Fiber/PLA Composite Filament for FDM
1015 – 1030		PR-37 (A.H. Nordin, R.A. Ilyas, N. Ngadi) Starch-Based Plastics: A Bibliometric Analysis (1990-2021)	PR-41 (S. H. A. Hisham, S. A. Shamsuddin, S. N. H. Hadie, Z. Mohd Ismail, F. Kasim, A. Rusli, Z. A. A. Hamid, and K. I. Ku Marsilla) Development of 3D Printed Human Brain Models using Thermoplastic Polyurethane/Rubber Blends for Anatomy Teaching Promoting Kinaesthetic Learning Purposes	PR-38 (M.A.H.M. Yusri, M.Y.M. Zuhri, M.R. Ishak and M.A. Azman) Compression Properties of Sandwich Structures Made of Kenaf/PLA Composite
1030 – 1045	<b>Session 3</b>	PR-40 (Sirisak Seansukato, Wirach Taweeprada, Chanaphan Lamlong, and Arthanareeswaran Gangasalam) Physico-Chemical Properties of PVC Resin Membrane Blending with PEO	PR-46 (Wan Muhammad Izzat Wan Zaludin, Nurul Zuhairah Mahmud Zuhudi, Khairul Dahri Mohd Aris) Effect of the Fabric Geometrical Parameters on the Permeability Behaviour of Woven Flax Fabrics	PR-47 (Ezriq El Sufri Mohd Noor, Nurul Zuhairah Mahmud Zuhudi, Ahmad Naim Ahmad Yahaya, Muzafar Zukifli) Convergence of Finite Element Model for Transient Thermal Simulation of Composite Laminate
1045 – 1100		PR-43 (A. F. Lajulladi, N. A. Khalil, A. N. A. Yahaya, M. Zulkifli) Effect of Parameters Manipulation on Cellulose Extraction Process Using Eco-Friendly Solvent and Production of Cellulose Transparent Film from Oil Palm Frond	PR-50 (N.Z.M. Zuhudi, K. Jayaraman, R. J.T. Lin) Water Absorption Behaviour of Bamboo-Glass Hybrid Polypropylene Composites	PR-42 (N.A. Khalil, A.M. Abu Huraira, S.N.D. Janurin, A.N.S. Fizat, N. Ahmad, M. Zulkifli, M.S. Hossain, A.N. Ahmad Yahaya) Magnetic Chitosan Hydrogel Beads as Adsorbent for Copper Removal from Aqueous Solution
1100 – 1115		PR-25 (N.M. Nurazzi, N. Abdullah, S.Z.N. Demon, N.A. Halim and I.S. Mohamad) Non-Covalent Functionalisation Poly (3-Hexylthiophene-2,5-Diy) Wrapped Hydroxylated Multi-Walled Nanocomposites: Effect of Reaction Time	PR-52 (S A S Abdullah, N Z M Zuhudi, K D Mohd Aris, M D Isa) The Effect of Alkali Treatment Under Various Condition on Physical and Tensile Properties of Kenaf Fiber	PR-59 (S. Hamat, M.R. Ishak, S.M. Sapuan, N. Yidris) Effect of Filament Fabrication Parameter on Flexural Properties of 3D Printing PLA Filament
1115 – 1130			PR-30 (A.E. Hadi, J.P. Siregar, T. Cionita, A.P. Irawan, D.F. Fitriyana, R. Junid) Tensile Properties of Sea Apple Leaf (SALF) Filler Reinforced Polyester Composite	
1130 – 1200	<b>(Chair)</b> <b>Prof. Dr. Arthanareeswaran Gangasalam</b>	<b>Keynote Speaker 3: Dr. Wirach Taweeprada</b>		
		Title: Consistency of Natural Rubber - Effect of Coagulant on Processing Properties		
1200 – 1400	Break			
1400	Session Login & Preparation			
Track		<b>Polymer technology and Biopolymer</b>	<b>Natural fibre composites and Rubber-based composites</b>	<b>Nanocomposite and Advanced manufacturing of composite</b>
		<b>Room 1</b>	<b>Room 2</b>	<b>Room 3</b>
		<b>Chair: Dr. Siti Hasnah Kamaruddin</b>	<b>Chair: Dr. Nadlene Razali</b>	<b>Chair: Dr. Muhamad Amin Azman</b>
1400 – 1415		PR-44 (Noor Intan Saffinaz Anuar, Chao Lu, Sarani Zakaria, Sinyee Gan, Qi Zuo & Chunhong Wang) Interfacial Bonding Properties of Treated Kenaf/Polypropylene with Silane PVA/ Urea	PR-53 (M.E. Azni, M. Suhaini, R. Noorain, S.H.S. Mariam, M.N. Azra, Y.Y. Yeong, M. Rozyanti) Polymeric Materials Used for Immobilization of Microalgae for The Bioremediation of Palm Oil Mill Effluent	PR-51 (Sharifah Nor Fatin 1, Khairul Dahri bin Mohd Aris2, Muhammand Najib bin Ismail) A Review: RMS - Rapid Motion Scanner Technique on Measuring Material Velocity and Thickness of Flax Fiber Prepreg
1415 – 1430	<b>Session 4</b>	PR-45 (Wan Nursheila Wan Jusoh, S.A.S. Abdullah, A.H. Ahmad Hamzah, R. Zainal Abidin, T. Tengku Harun, Nurafiqah N.K, Z. Sahwee, Shahrul Ahmad, N. L. Mohd Kamal, S. Abdul Hamid, N. Norhashim) Influence of Ammonium Polyphosphate (APP) and Sodium Hydroxide (NaOH) Surface Treatments on Kenaf Fibres Thermal Properties	PR-48 (Nurul Zuhairah Mahmud Zuhudi, Krishnan Jayaraman, Richard TJ Lin) Recycling of The Natural Fibre Composites and Their Hybrids: A Preliminary Study	PR-54 (Othman Elmy-Nahida, Hidayah Ariffin, Haruo Nishida, Yoshito Andou, Mansor Ahmad, Wan Md Zin Wan Yunus, Mohd Ali Hassan) Variation and Kinetics of Poly(3-Hydroxybutyrate) Depolymerization Behavior in Steam-Assisted Hydrolysis
1430 – 1445		PR-49 (N. Danmatam and D. Pattavarakorn) UV-Shielding Biodegradable Films Based on Carboxymethyl Cellulose Filled with Henna Extracts	PR-21 (N.A. Maidin, S.M. Sapuan, M.T. Mastura, M.Y.M. Zuhri) Natural Fiber Reinforced Polymer Composites: Opportunities, Challenges and Its Applications	PR-56 (A. S. Norfarhana, R.A. Ilyas, N. Ngadi, A.H. Nordin, Nur Hafizah Ab Hamid) Nanofiller-Content Rubber Composites
1445 – 1500	Break			
1500	<b>(Session MC)</b> <b>Fatin Najwa Joynal Abedin</b>	<b>Closing ceremony</b>		
		1. Award ceremony 2. Hand-over ceremony and Closing speech <b>Assoc. Prof. Dr. Zulkiflle Leman</b>		
<b>End</b>				

**INTERNATIONAL ADVISORY SCIENTIFIC COMMITTEE**

1. **PROF. DR. EMIN BAYRAKTAR**  
Supmeca, FRANCE.
2. **PROF. DR. HAIRUL ABRAL**  
Unand, INDONESIA.
3. **PROF. DR. ARTHANAREESWARAN GANGASALAM**  
NIT, Trichy, INDIA.
4. **PROF. DR. WESLEY CANTWELL**  
Khalifah University of Science Technology and Research, Abu Dhabi, UAE.
5. **PROF. DR. SALEEM HASHMI**  
DCU, REPUBLIC OF IRELAND.
7. **PROF. DR. ISMAIL ZAINOL**  
UPSI, MALAYSIA
8. **ASSOC. PROF. DR. SEONGSU KIM**  
KAIST, KOREA
9. **ASSOC. PROF. DR. YASIR NAWAB**  
National Textile University, PAKISTAN
10. **ASSOC. PROF. DR. TAWEECHAI AMORNSAKCHAI**  
Mahidol University, THAILAND
11. **DR. MAINUL ISLAM**  
University of Southern Queensland, AUSTRALIA
12. **DR. AGUNG EFRIYO HADI**  
Universitas Abulyatama, Aceh, INDONESIA
13. **DR. EDI SYAFRI**  
Politeknik Payakumbuh, INDONESIA
14. **DR. MANROSHAN SINGH**  
Malaysian Rubber Board (MRB), MALAYSIA
15. **DR. RIZA WIRAWAN**  
ITB, INDONESIA
16. **PROF. DR. D. S. PRAKASH**  
Sathyabama Institute of Science & Technology, Chennai, INDIA
17. **MR. CHAN PAK KUEN**  
The Plastics & Rubber Institute Malaysia (PRIM), MALAYSIA

**ISPM2022 ORGANIZING COMMITTEE**

<b>Chairman:</b>	Prof. Ir. Dr. Mohd Sapuan Salit
<b>Joint-Chairman:</b>	Assoc. Prof. Dr. Zulkiflle Leman
<b>Secretary I:</b>	Ts. Nor Afifah binti Khalil
<b>Secretary II:</b>	Dr. Mohd Zuhri bin Mohamed Yusoff
<b>Secretary III:</b>	Dr. Ahmad Ilyas bin Rushdan
<b>Secretary IV:</b>	Ms. Aida Syafiqah Abdul Rahman
<b>Secretary V:</b>	Ms. Fatin Najwa Joynal Abedin
<b>Treasurer I:</b>	Assoc. Prof. Dr. Edi Syams bin Zainudin
<b>Treasurer II:</b>	Assoc. Prof. Dr. Che Nor Aiza binti Jaafar
<b>Treasurer III:</b>	Mr. Azhareensyah Bin Aman
<b>Unit of Technical and Publication:</b>	Prof. Ir. Dr. Mohd Sapuan Salit (Head) Assoc. Prof. Dr. Mohammad Jawaid Assoc. Prof. Ts. Dr. Ahmad Naim bin Ahmad Yahaya Dr. Ahmad Ilyas bin Rushdan Dr. Muhammad Amin Azman Mr. Muhammad Harussani Moklis Mr. Mohd Faizar Banjar Mr. Ahmad Fiqhri Lajulliadi
<b>Unit of Publicity, Registration and Communication:</b>	Ts. Dr. Muzafar bin Zulkifli (Head) Dr. Ahmad Ilyas bin Rushdan Ts. Dr. Zatil Hazrati binti Kamaruddin Dr. Nazrin Nurarief Mardi bin Asmawi Mr. Mohd Azlin bin Mohd Nor
<b>Unit of Logistic and Protocol:</b>	Dr. Mohd Zuhri Mohamed Yusoff (Head) Dr. Mohamad Omar Syafiq bin Razali Mr. Ahmad Nor Syimir Fizal
<b>Unit of Sponsorship:</b>	Assoc. Prof. Dr. Nur Ismarrubie binti Zahari (Head) Assoc. Prof. Dr. Mohamad Ridhwan bin Ishak Mr. Faisal Al-Shalawi Mr. Alhamada Thaer Mr. Tarique Jamal
<b>Unit of Award and Merchandise:</b>	Assoc. Prof. Dr. Mohamad Ridwan bin Ishak

*ISPM2022*

*The International Symposium on Polymeric Materials 2022*

# **FULL PAPERS**

## **NON-LINEAR FINITE ELEMENT ANALYSIS OF OIL PALM FIBER COMPOSITES FOR FUSED DEPOSITION MODELING (FDM)**

M. N. Ahmad<sup>1,4,7\*</sup>, M. R. Ishak<sup>1,2,3\*</sup>, M. M. Taha<sup>4</sup>, F. Mustapha<sup>1</sup> and Z. Leman<sup>5,6</sup>

<sup>1</sup>Department of Aerospace Engineering, Faculty of Engineering, Universiti Putra Malaysia, Serdang 43400, Selangor, Malaysia

<sup>2</sup>Aerospace Malaysia Research Centre (AMRC), Universiti Putra Malaysia, Serdang 43400, Selangor, Malaysia

<sup>3</sup>Laboratory of Biocomposite Technology, Institute of Tropical Forestry and Forest Products (INTROP), Universiti Putra Malaysia, Serdang 43400, Selangor, Malaysia

<sup>4</sup>Faculty of Mechanical and Manufacturing Engineering Technology, Universiti Teknikal Malaysia Melaka, Hang Tuah Jaya, 76100 Durian Tunggal, Melaka, Malaysia

<sup>5</sup>Department of Mechanical and Manufacturing Engineering, Faculty of Engineering, Universiti Putra Malaysia, Serdang 43400, Selangor, Malaysia

<sup>6</sup>Advanced Engineering Materials and Composites Research Centre, Faculty of Engineering, Universiti Putra Malaysia, Serdang 43400, Selangor, Malaysia

<sup>7</sup>Centre of Smart System and Innovative Design, Universiti Teknikal Malaysia Melaka Hang Tuah Jaya, 76100 Durian Tunggal, Melaka, Malaysia

---

### **ABSTRACT**

Engineers and manufacturers can benefit from finite element analysis (FEA) data of mechanical properties of 3D-printed products to enhance the quality and performance. Fused deposition modelling (FDM) is a filament-based rapid prototyping technology that enables the introduction of novel composite materials as long as they can be produced as feedstock filaments. In prior research, a novel material, oil palm fiber composites filament, was produced for FDM. Then, the tensile and flexural test were conducted according to ASTM 638 and ASTM 730 using universal testing machine. In this paper, the uniaxial tensile test, flexural test, and the construction of a material model for the prediction of the stress-strain response were simulated using nonlinear FEA. The plots of von Mises stress, resulting displacement, and strain were created. In addition, the derived von Mises plasticity material model and boundary conditions accurately represented the behavior of the specimen under uniaxial tension load, with only minimal differences between actual and theoretical results. The tensile and flexural strengths of oil palm fiber composite (3wt%) were 33.14 and 33.81 MPa, respectively, according to the results of the FEA simulation. The difference between simulation and experimental error was minor, ranging from 5.4 to 15.2 percent. The aim of this research was to apply non-linear FEA to validate experimental results from tensile and flexural tests of oil palm fiber composites filament, which would be used as a raw material for FDM.

*Keywords:* FEA, FDM, oil palm fiber composite, tensile, flexural.

---

### **INTRODUCTION**

Additive manufacturing (AM), also known as three-dimensional (3D) printing, has gradually gained traction in the manufacturing industry [1-3]. The technology of printing object layer upon layer by additive manufacturing (AM) has been largely used in the recent decades [4-8]. FDM was invented in 1989 (Stratasys Inc., Eden Prairie, MN, USA), and it has been widely used for manufacturing plastic materials [9]. Previously, there were some researches on development of new composite material using natural fiber for FDM include wood/PLA [10], powder/nylon [11], fiberglass/ABS [12] and carbon fibers/ABS [13]. Ahmad et al. [14] discovered the material properties for 3, 5, and 7 wt% of oil palm fiber composites were shear thinning behavior where the flow index,  $n$ , was less than 1, and the trend of apparent viscosity was decreased with the increment in the shear rate value.

Finite element analysis (FEA) is a powerful and prevalent numerical technique that has been developed into an indispensable modern tool for the modelling and simulation of various engineering processes, particularly in food packaging industries [15]. Provaggi et al. recently employed FEA to predict mechanical properties of 3D printed polymers under compression and concluded that inputs provided by FEA could be potentially useful for reducing product design and development time [16]. Their work, which was focused on the linear elastic region, suggested that in 3D printed PLA specimen with 100% infill density, maximum von Mises stresses was considerably higher than the compressive yield strength.

---

#### *Article history:*

Received: 10 March 2022

Accepted: 7 June 2022

Published: 14 June 2022

---

#### *E-mail addresses:*

mohdnazri.ahmad@utem.edu.my (M.N. Ahmad)

mohdridzwan@upm.edu.my (M.R. Ishak)

\*Corresponding Author

Pastor-Artigues et al., on the other hand, conducted FEA studies on 3D printed under tension, compression as well as bending condition [17]. Rodriguez et al. [18] studied the mechanical behavior of FDM ABS materials. They found that the reduction of strength was 22%–57% when ABS monofilament turned to FDM ABS materials. Sood et al. [19] researched the influence of process parameters including layer thickness, orientation, raster angle, raster width and air gap on tensile strength, flexural strength and impact strength of FDM material. Zhao et al. [20] has carried out the study on mechanical behavior of polylactic acid manufactured parts under tensile conditions by experimentally and numerically, and the effects of printing pattern and infill density on ultimate tensile strength (UTS)-weight ratio and the modulus of elasticity. The result showed the modulus of elasticity of FDM manufactured polylactic acid with three infill patterns and any infill density with an average prediction error of 14.80%. Lakshman et al. [21] used Polyester as matrix and banana fibers as reinforcements to produce the composites. The mechanical properties such as tensile strength, impact strength and flexural strength were determined by appropriate test procedures and are validated using FEA software. However, none of previous studies conducting the validation process using FEA for oil palm fiber composite for FDM. Therefore, the aim of this research is to perform FEA simulation to validate experimental results of tensile and flexural tests, which could be used as a reference for future study.

**MATERIALS AND METHODS**

*Materials*

Fig. 1 shows the specimens of ABS- oil palm fiber composite (3wt%) fabricated by FDM, Flash Forge model. The printing parameters were set to fine speed, 0.2mm layer thickness, 0 degree of orientation and solid infill. The tensile and flexural specimens were printed according to ASTM 638 and ASTM 730. The experimental data include yield, tensile and flexural strength of fiber composite as shown in TABLE 1. It is useful in FEA analysis to insert the input of material properties to be analyzed.



Fig. 1: Printed specimens ABS- oil palm fiber composite (3wt%)

TABLE 1 Mechanical properties values of ABS-oil palm fiber composite (3wt%)

Properties	3wt%
<b>Yield strength</b>	14.9 MPa
<b>Tensile strength</b>	35.3 MPa
<b>Elastic modulus</b>	1.88 GPa
<b>Flexural strength</b>	31.98 MPa

*Methods*

Although experimental approaches could accurately characterize the tensile behavior of parts manufactured by FDM, both fabrication and testing are costly and time consuming. Therefore, finite element analysis (FEA) emerges as a substitute for modelling and estimating tensile strength and the effective modulus of plasticity of the actual products. In this study, three-dimensional finite element models were constructed and simulate in the Dassult Systeme Solidworks Simulation software. The accuracy of the simulation model was validated by comparing the tensile and flexural strength from the experimental. The method of FEA comprises of 3 main sections are pre-processing, analysis and post-processing as in Fig. 2.

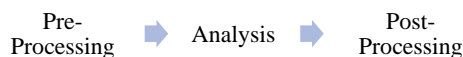


Fig. 2: Steps of performing FEA

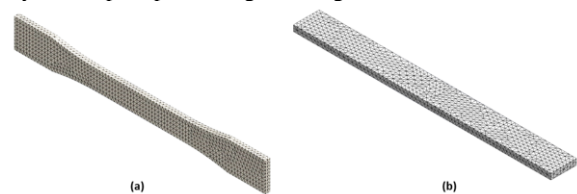


Fig. 3: Mesh (a) ASTM 638 for tensile specimen and (b) ASTM 730 for flexural specimen

The first step in FEA was pre-processing by creating the 3D model of the samples. Then, for analysis step, the mesh model was assigned with appropriate loads and boundary conditions. The mesh model for tensile and flexural samples as in Fig. 3. In addition, the mesh parameters were set to 2 mm for element size and 0.1 mm tolerance. The final step is post-processing was used to assess the response of a structure under various loads such as static, impact, thermal, fatigue, and torque, and the FEA results were displayed in the form of tables, graphs, charts, deflected shapes of structures, and animation.

**RESULTS AND DISCUSSION**

FEA simulation shows the derived von mises plasticity material model and boundary conditions accurately represented the behavior of the specimen under uniaxial tension load, with only minimal differences between actual and theoretical results. Fig. 4(a) shows the result of n mises stress distribution for tensile test and Fig. 4(b) illustrates the resultant displacement of flexural sample. Refer to TABLE 2, tensile and flexural strengths of oil palm fiber composite (3wt%) were 33.14 and 33.81 MPa, respectively, according to the results of the FEA simulation. For 0wt% oil palm fiber composite, the tensile and flexural test were 24.70 and 62.83 MPa. The tensile result shows the value of 3wt% fiber loading was higher than 0wt%. Thus, it shows the significance impact by adding 3% of oil palm fiber could be improved the mechanical strength of the printed part

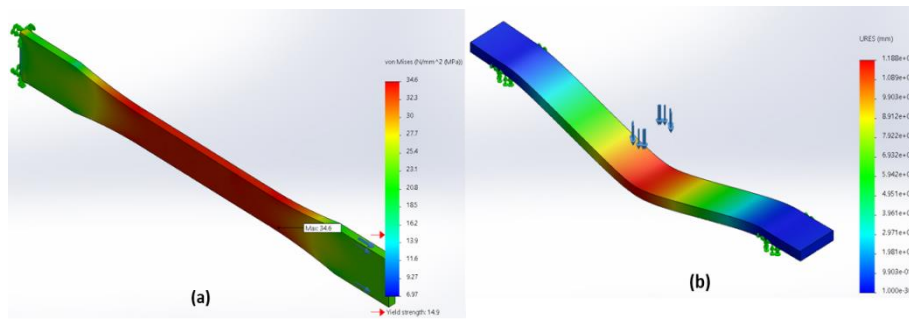


Fig. 4: Result of (a) von mises stress distribution test and (b) resultant displacement

TABLE 2 Comparison of simulation and experimental data

Mechanical Properties	Simulation		Experiment		Error (%)	
	0wt%	3wt%	0wt%	3wt%	0wt%	3wt%
Ultimate tensile strength (MPa)	24.70	33.14	29.14	35.30	15.24	6.47
Flexural strength (MPa)	62.83	33.81	69.35	31.98	9.40	5.41

Fig. 5 shows the stress vs strain curve of simulation and experiment data for 0 and 3wt% of oil palm fiber composite. The difference between simulation and experimental error was minor, ranging from 5.4 to 15.2%. This deviation could be due to the slight variation in the input values like density, applied force, boundary conditions and other selection of input parameters during modelling and test analysis. The smallest error 5.41% of simulation and experiment data was found at 3wt% of oil palm fiber composite. The result was similar to Balasubramanian et al. [22], he discovered that the experimental and analytical results of tensile and flexural test differ by about 2%–6%.

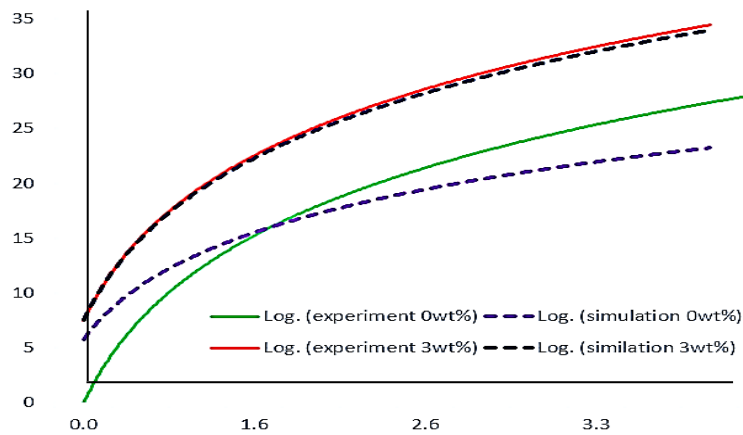


Fig. 5: Stress vs strain curve of simulation and experiment data

**CONCLUSIONS**

Non-linear FEA was used to validate tensile and flexural tests of oil palm fiber composites. The experimental and analytical results are found to be in good agreement, with a margin of error of roughly 5%–15%. This simulation model could be utilized to forecast the uniaxial tensile and flexural behavior of 3D printed oil palm fiber composites parts that cover the nonlinear region prior to failure.

**ACKNOWLEDGEMENTS**

The authors appreciate the financial support provided by Universiti Putra Malaysia and the Ministry of Higher Education (Malaysia) through the Fundamental Research Grant Scheme (FRGS), grant no. FRGS/1/2019/TK05/UPM/02/11 (5540205). The authors would also like to express their gratitude to the Centre of Research and Innovation Management, Universiti Teknikal Malaysia Melaka for providing financial assistance through the Journal Publication Incentive Grant (JURNAL/2020/FTKMP/Q00061)

**REFERENCES**

- [1] Gardan, J. Additive manufacturing technologies: State of the art and trends. *Int. J. Prod. Res.* 2016, 54, 3118–3132.
- [2] Berman, B. 3-D printing: The new industrial revolution. *Bus. Horiz.* 2012, 55, 155–162.
- [3] Guo, N.; Leu, M.C. Additive manufacturing: Technology, applications, and research needs. *Front. Mech. Eng.* 2013, 8, 215–243. [Google Scholar] [CrossRef]
- [4] X. Wang, M. Jiang, Z. Zhou, J. Gou, D. Hui, 3D printing of polymer matrix composites: a review and prospective, *Compos. Part B* 110 (2017) 442–458.
- [5] B. N. Turner, R. Strong, S. A. Gold, A review of melt extrusion additive manufacturing processes: I. Process design

- and modeling, *Rapid Prototyp. J.* 20 (3) (2014) 192–204.
- [6] B. Utela, D. Storti, R. Anderson, M. Ganter, A review of process development steps for new material systems in three dimensional printing (3DP), *J. Manuf. Process.* 10 (2) (2008) 96–104.
- [7] M. Vaezi, H. Seitz, S. Yang, A review on 3D micro-additive manufacturing technologies, *Int. J. Adv. Manuf. Technol.* 67 (5–8) (2013) 1721–1754.
- [8] P. Parandoush, D. Lin, A review on additive manufacturing of polymer-fiber composites, *Compos. Struct.* 182 (2017) 36–53.
- [9] Dudek P (2013) FDM 3D printing technology in manufacturing composite elements. *Arch Metall Mater* 58(4):1415–1418
- [10] Tao Y, Wang H, Li Z et al (2017) Development and application of wood flour-filled polylactic acid composite filament for 3D printing. *Material* 10(4):339. <https://doi.org/10.3390/ma/0040339>
- [11] Masood SH, Song WQ (2004) Development of new metal/polymer materials for rapid tooling using fused deposition modelling. *Mater Des* 25(7):587–594
- [12] Zhong W, Li F, Zhang Z et al (2001) Short fiber reinforced composites for fused deposition modeling. *Mater Sci Eng A* 301(2):125–130
- [13] Ning F, Cong W, Qiu J et al (2015) Additive manufacturing of carbon fiber reinforced thermoplastic composites using fused deposition modeling. *Compos Part B Eng* 80:369–378
- [14] Ahmad, M. N., Ishak, M. R., Taha, M. M., Mustapha, F., & Leman, Z. (2021). Rheological and Morphological Properties of Oil Palm Fiber-Reinforced Thermoplastic Composites for Fused Deposition Modeling (FDM). *Polymers*, 13(21), 3739.
- [15] Fadiji, T., Coetzee, C. J., Berry, T. M., Ambaw, A., & Opara, U. L. (2018). The efficacy of finite element analysis (FEA) as a design tool for food packaging: A review. *Biosystems Engineering*, 174, 20–40.
- [16] Provaggi E, Capelli C, Rahmani B, Burriesci G, Kalaskar DM. 3D printing assisted finite element analysis for optimising the manufacturing parameters of a lumbar fusion cage. *Mater Des.* 2019;163:107540.
- [17] Pastor-Artigues M-M, Roure-Fernández F, Ayneto-Gubert X, Bonada-Bo J, Pérez-Guindal E, Buj-Corral I. Elastic Asymmetry of PLA Material in FDM-Printed Parts: Considerations Concerning Experimental Characterisation for Use in Numerical Simulations. *Materials.* 2020;13(1):15.
- [18] J.F. Rodríguez, J.P. Thomas, J.E. Renaud, Mechanical behavior of acrylonitrile butadiene styrene (ABS) fused deposition materials. Experimental investigation, *Rapid Prototyp. J.* 7 (3) (2001) 148–158.
- [19] A.K. Sood, R.K. Ohdar, S.S. Mahapatra, Parametric appraisal of mechanical property of fused deposition modelling processed parts, *Mater. Des.* 31 (1) (2010) 287–295.
- [20] Zhou, X., Hsieh, S. J., & Ting, C. C. (2018). Modelling and estimation of tensile behaviour of polylactic acid parts manufactured by fused deposition modelling using finite element analysis and knowledge-based library. *Virtual and Physical Prototyping*, 13(3), 177-190
- [21] C. Lakshman et al., Mechanical performance and analysis of banana fibre reinforced epoxy composites, *Int. J. Sci. Res. Eng. Technol.* 6 (5) (2017) 440–444
- [22] Balasubramanian, K., Rajeswari, N., & Vaidheeswaran, K. (2020). Analysis of mechanical properties of natural fibre composites by experimental with FEA. *Materials Today: Proceedings*, 28, 1149-1153.



## **THE EFFECT OF PE-g-MA ON THE PROPERTIES OF LOW DENSITY POLYETHYLENE (LDPE)/THERMOPLASTICS BANANA PEEL STARCH (TBPS) FILMS**

F. Hashim<sup>1\*</sup>, N. H. C. Ismail<sup>1</sup>, N. A. M. Zaini<sup>1</sup>, S. N. Din<sup>1</sup>, Z. A. S. A. Salim<sup>2</sup>

<sup>1</sup> *Fakulti Sains Gunaan, Universiti Teknologi MARA Cawangan Perlis, 02600 Arau, Perlis, Malaysia.*

<sup>2</sup> *Fakulti Sains Gunaan, University Teknologi MARA, 40450 Shah Alam, Selangor Darul Ehsan, Malaysia*

---

### **ABSTRACT**

The environmental issues caused by the disposal of plastic waste have sparked interest in the production of environmentally friendly polymers. Low density of polyethylene (LDPE) is increasingly being used for food packaging and non-food packaging due to outstanding properties, ease of processing and higher ultraviolet (UV) resistance. However, the inability of LDPE to decompose in nature is opposed to disintegration and degradation, which is a genuine environmental issue. The introduction of banana peel starch (BPS), which is natural, abundant, organic and biodegradable is a potential way to increase the susceptibility of LDPE to environmental degradation. Banana peels are a waste product ideal for producing bioplastics accounting for 18.5% of starch sources. The effects of PE-g-MA as compatibilizer and various amount of banana peel starch towards the properties of LDPE/BPS were determined using fourier transform infra-red (FTIR), tensile testing and differential scanning calorimetry (DSC). As confirmed by FTIR analysis, there was interaction between PE-g-MA with the matrix, thus enhanced the tensile and thermal properties of the films. Hence, it was suggested that development of sustainable plastic material based on banana peel starch and LDPE was ideal for the replacement of single-use, petroleum based and persistent packaging

*Keywords:* bioplastics, banana peel, LDPE, food packaging.

---

### **INTRODUCTION**

Universal demand for plastics led using petroleum-based plastic materials has increased and added stress to the existing waste management [1]. Plastic waste produced will accumulate as a landfill and slowly producing dangerous chemicals and threatening the environment, flora and fauna. The environmental issues caused by the plastic waste disposal have sparked interest in the production of environmentally degradable or environmentally friendly polymers. Low-density polyethylene (LDPE) is a type of thermoplastic polymer used most commonly in various applications including the development of bottles, toys, cover for laboratory equipment, plastic bags, packaging materials, trash bins, floor tiles and shipping envelopes [2]. Banana peels are a waste product that accounts for around 18% to 33% of the total amount of banana fruit [3]. Banana peels have many benefits such as biodegradable, cost-effective, environmentally friendly and sustainable. Due to the large amount of banana peel waste, it can be utilized to make thermoplastic starch (TBPS). The major drawback of LDPE/starch composites is the incompatibility of highly polar starch and nonpolar LDPE, which results in a reduction in mechanical properties. This incompatibility prevents the formation of strong interfacial hydrogen bonds between starch and LDPE phases. The addition of compatibilizers is a traditional and industrial method for improving the compatibility and poor interfacial bonding between the two phases of immiscible polymer blends. Among commercially available compatibilizers, polyethylene grafted maleic anhydride (PE-g-MAH) is the most common and useful for LDPE/starch composites. Thus, this study aims are to prepare a series of LDPE/TBPS films with the presence of PE-g MA as a compatibilizer and to investigate their mechanical performance and thermal properties.

---

#### *Article history:*

Received: 10 March 2022

Accepted: 7 June 2022

Published: 14 June 2022

---

#### *E-mail addresses:*

faiezahashim@uitm.edu.my (F. Hashim)

hafizah477@uitm.edu.my (N. H. C. Ismail)

nurulaizan@uitm.edu.my (N. A. M. Zaini)

sitiner432@uitm.edu.my (S. N. Din)

\*Corresponding Author

MATERIALS AND METHODS

Materials

Banana peel waste used in this study was obtained in Arau (Perlis, Malaysia). LDPE commercial (LDF 260GG) of density 0.921 g/cm<sup>3</sup> was supplied with of 2 g/10 min of melt flow rate and a moisture content of 8.3%, glycerol and acetic acid.

Methods

Extraction of starch

Banana peels were peeled and chopped into little pieces after being separated from the flesh. For 45 minutes, banana peels were dipped in a 0.2 M sodium metabisulphite solution. The peels were then heated for 30 minutes in a beaker containing 800 mL of distilled water. The banana peels were then blended in a blender and then the blended product was allowed to settle, yielding the starch.

Preparation of LDPE/TBPS film

The blends were prepared by melt blending of LDPE/TBPS films in an internal mixer equipped with roller rotors. The mixing was conducted at a temperature of 150 °C and the speed of the rotor was fixed for 10 minutes at 55 rpm. The compositions of materials used in the preparation of films are given in TABLE 1. After the mixing completed, the compounds were compression molded under pressure for 10 minutes.

TABLE 1: Composition of prepared LDPE/TBPS film

Sample (%)	LDPE (%)	TBPS (%)	Glycerol (%)	Compatibilizer (%)
0	90	0	5	5
5	85	5	5	5
10	80	10	5	5
15	75	15	5	5
20	70	20	5	5

RESULTS AND DISCUSSION

Fourier Transforms Infrared (FTIR) Analysis

FTIR analysis was used to assess the effect of the compatibilizers on the LDPE/TBPS films. Fig. 1 depicts the FTIR spectrum of the films with and without the compatibilizer. The bands in the 2850–2900 cm<sup>-1</sup> region of the FTIR spectrum were attributed to LDPE CH<sub>2</sub> stretching vibrations [4]. With the presence of PE-g-MAH, it should be an obvious band at 1738 cm<sup>-1</sup> that related to ester group due to reaction between anhydride group and hydroxyl group. Peaks in TBPS can be found at 1150 and 1078 wavenumbers, which were attributed to C-OH stretching vibration. With the addition of compatibilizers, the shape and intensity of these peaks changed [5]. Increases in PE-g-MAH intensity were observed at this peak. Peak intensity decreased at 1150 and 1078 wavenumbers when PE-g-MAH was used as the compatibilizer. The better compatibility of the polymer blend meant the correlative peaks shifted and the peak shapes altered owing to the mechanism of compatibility. The FTIR spectra revealed that PE-g-MAH successfully interacted with TBPS and the FTIR spectra were confirmed by the increased in tensile strength and thermal properties.

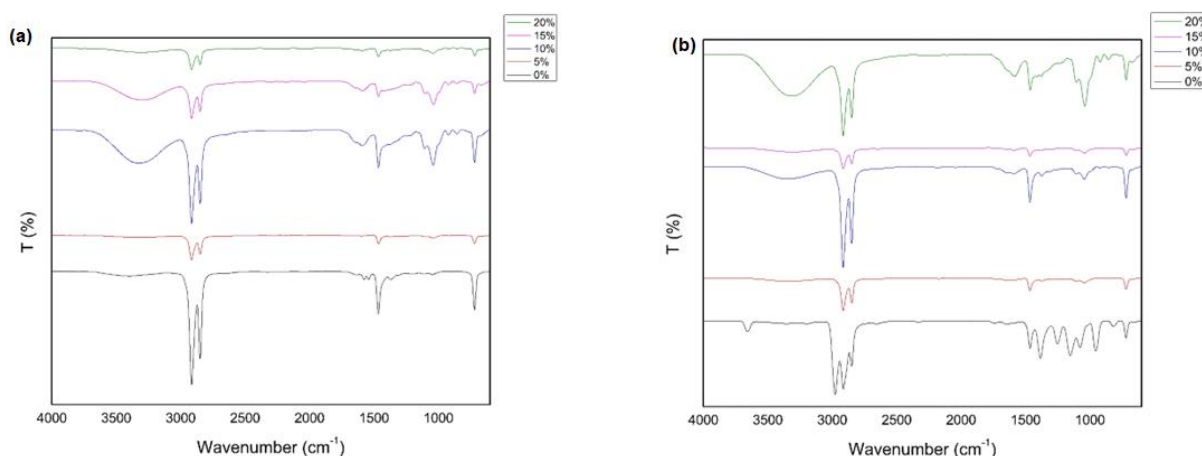


Fig. 1: FTIR spectrum of LDPE/TBPS film (a) without compatibilizer and (b) with compatibilizer

Tensile strength

The tensile properties of the composites can be strongly influenced by the adhesion between the matrix and the filler. Fig. 2 shows the effect of compatibilization technique and filler loading on the tensile strength of LDPE/TBPS films. It can be observed that the tensile strength for both compounds had decreased with increasing of filler loadings. This might be due to the poor adhesion of banana peel starch in LDPE matrices. The nature of starch is hydrophilic and reduced the interfacial

adhesion. Thus, lead to lack of compatibility between the hydrophilic starch and hydrophobic LDPE. It is happened due to the difficulties to achieve homogeneous dispersion of filler at higher filler loading [6]. However, at similar filler loading, LDPE/TBPS film with compatibilizer, exhibited higher tensile strength compared with uncompatibilizer films. The corporation of PE-g-MAH into the composites improved the filler-matrix bonding due to the interaction and chemical bonds between the maleic anhydride and the hydroxyl groups in the filler. LDPE/TBPS film with compatibilizer exhibit higher Young's modulus than LDPE/TBPS film without compatibilizer at any filler loading. This is probably due to the good interfacial adhesion among filler and matrix with the presence of PE-g-MAH.

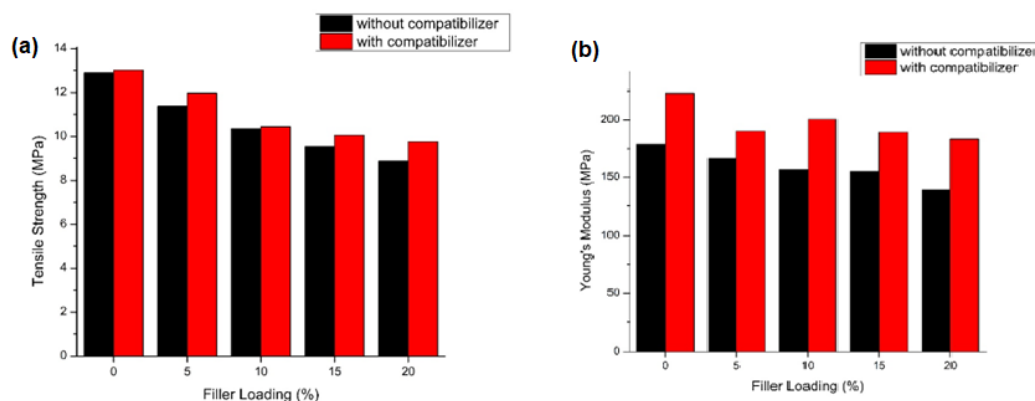


Fig. 2: Tensile strength for LDPE/TBPS film with compatibilizer and LDPE/TBPS film without compatibilizer at different filler loadings; a) tensile strength b) Young Modulus

#### Thermal Properties

Differential scanning calorimetry (DSC) was used to determine the melting temperature ( $T_m$ ) and degree of crystallinity ( $X_c$ ). TABLE 2 compares the thermal properties of LDPE/TBPS films with and without a compatibilizer. According to the TABLE 2, increasing TBS loadings reduced  $T_m$  and  $X_c$ . These were attribute by the TBS's lower thermal stability.  $T_m$  and  $X_c$  of LDPE/TBPS films with compatibilizer are higher than LDPE/TBPS films without compatibilizer when Pe-g-MA is present.

TABLE 2: Thermal properties of LDPE/TBPS film

Sample	Without compatibilizer			With compatibilizer		
	Melting Temperature ( $T_m$ )	$\Delta H$ (J/g)	% Crystallinity ( $X_c$ )	Melting Temperature ( $T_m$ )	$\Delta H$ (J/g)	% Crystallinity ( $X_c$ )
0%	107.4	42.48	14.65	107.7	51.132	17.63
5%	106.5	41.225	14.96	107.3	44.036	15.98
10%	106.3	35.554	13.62	107.2	39.02	14.95
15%	105.5	31.868	12.93	107	37.05	15.03
20%	105	17.997	7.76	106.5	29.638	12.78

#### CONCLUSIONS

In conclusion, a LDPE/TBPS films have been successfully prepared. The addition of PE-g-MA as compatibilizer has enhanced the tensile and thermal properties of the films.

#### ACKNOWLEDGEMENTS

The authors would like to thank Universiti Teknologi MARA Cawangan Perlis for the financial support through the Geran Dana Pembudayaan Penyelidikan Dalamam (DPPD) scholarship. 600-TNCPI 5/3/DDN (09) (015/2020).

**REFERENCES**

- [1] A. Rahman, and C.D. Miller, “ Microalgae as a Source of Bioplastics. In *Algal Green Chemistry: Recent Progress in Biotechnology*”, 2017, doi.org/10.1016/B978-0-444-63784-0.00006-0
- [2] V.O. Bulatovic, L. Mandic, L. A. Turkovic, D.K. Grgic, A. Jozinovic, R. Zovko, and E.G. Bajsic, “Environmentally friendly packaging materials based on thermoplastic starch,” *Chemical and Biochemical Engineering, Quarterly*, 33(3), pp. 347–361, 2019, doi: Hamzah.org/10.15255/CABEQ.2018.1548.
- [3] S.A. Abdul Shukor , N.Z. Noriman, S. Omar, N.A. Dahham, Faris, S, D. Saad and J. Haliza, “UV-visible performance of urea beads coated with banana peels bioplastic and epoxidized, natural rubber, pp. ?, 2020. *AIP Conference Proceeding*.
- [4] S. Yuvaraj, and N. Rajeswari, “Preparation of low-density polyethylene (LDPE)/modified banana epidermis starch (MBES) based biodegradable films and their study for its suitability in food packaging applications”. *Materials Research Express*, 6(12). 2019, doi.org/10.1088/2053-1591/ab549b
- [5] A.R.H. Fatimah, A.G. Supri, and Z. Firuz, “The effect of polyethylene-grafted-maleic anhydride as compatibilizer on properties of of Recycled High-Density Polyethylene/Ethylene Vinyl Acetate/Taro Powder (*Colocasia esculenta*) composites,” *Journal of Advanced Research in Materials Science*, 10(1), pp. 26–39. 2015,
- [6] N.A. Azieyanti, A. Amirul, S.Z. Othman and H. Misran, “Mechanical and Morphology Studies of Bioplastic-Based Banana Peels,” *Journal of Physics: Conference Series*, 1529(3), 2020, doi: org/10.1088/1742-6596/1529/3/032091

## ANTIMICROBIAL CAPABILITY OF INORGANIC MATERIAL AS FILLER FOR THERMOPLASTIC ELASTOMER – A STATE OF THE ART REVIEW.

F. N. J. Abedin<sup>1</sup>, A. N. A. Yahaya<sup>1</sup>, N. A. Khalil<sup>1</sup>, M. Zulkifli<sup>2\*</sup>

<sup>1</sup>Universiti Kuala Lumpur, Branch Campus Malaysian Institute of Chemical and BioEngineering Technology, 78000 Alor Gajah, Melaka, Malaysia

<sup>2</sup>Green Chemistry and Sustainability Cluster, Universiti Kuala Lumpur, Branch Campus Malaysian Institute of Chemical and Bioengineering

---

### ABSTRACT

Increasing morbidity and mortality rate around the world due to antimicrobial resistance had attracted numerous research interest, particularly on producing polymeric materials with antimicrobial properties. Those researchers aim to overcome and minimizing the major infection problems caused by antimicrobial resistance. These antimicrobial polymeric materials are the alternative to conventional biocide. The aim of such articles are to minimize the transmission of microbes to the human after in contact with contaminated surfaces. In this paper, we aim to provide an overview of inorganic material with antimicrobial properties as filler for thermoplastic elastomer. The antimicrobial mechanism against pathogen is discussed. This paper also shares several techniques used to produce polymeric materials with antimicrobial properties. We hope to advance knowledge in the field and encourage more research into the production of antimicrobial material based on polymers.

*Keywords:* thermoplastic elastomer, antimicrobial polymers, nanoparticles.

---

### INTRODUCTION

According to a World Health Organizations (WHO) report, disease caused by antimicrobial resistance (AMR) could kill 10 million people per year by 2050, causing massive economic damage, and up to 24 million people will be impoverished by 2030 as a result of antimicrobial resistance [1,2]. The rapid growth of health-threatening germs through contamination on touched surfaces is a global concern, particularly in healthcare facilities where antimicrobial resistant bacteria lead to the emergence of healthcare-associated infections (HAIs) associated with medical devices. Generally, antibiotics are administered to the patients in order to overcome the infection caused by bacteria, but overuse of the antibiotics has resulted to development of multidrug resistant bacteria, necessitating more complicated and stronger formulations to combat the disease efficiently. Consequently, the alternative to prevent contaminations from the microorganisms are by ceasing the production of the bacteria on various substrates surfaces that human are exposed everyday by inhibiting the growth and development or by preventing the adhesions of the bacteria [3].

The evolution of bacteria species such as *Escherichia coli* (*E. coli*), *Staphylococcus aureus* (*S. aureus*), and *Pseudomonas aeruginosa* (*P. aeruginosa*) increase the interest in studies of antimicrobial materials. This is due to traditional biocides which are natural and have low molecular weight chemicals led to accumulation of dead bacteria on the antibacterial surface that have antibiotics agents. Thus, the antibacterial functional groups blocked by the dead bacteria and form biofilm which will cause harm to human body. In addition, formation of biofilm is more resistant than planktonic bacteria by 100-1000 times, limits the activity of antibiotics efficacy only at the top layer and shields the bottom layer, resulting in antimicrobial resistance. Thus, the development of antimicrobial material had become an interest academically and commercially as the alternative to traditional antibiotics.

Currently, most researchers are focusing in producing antimicrobial coatings based in polymers and nanocomposites. This is due to polymer composites are widely used in for production of surfaces and objects. Antimicrobial polymeric materials can be applied in various industries including tissue engineering, prosthetics material, textiles, electronics, automotive, food packaging and household appliances [3]. So, a developed antimicrobial polymer composites should be able to inhibit any bacteria instantly without have harmful effects for the consumers and environment as well as mechanically strong for intended applications. Therefore, the incorporation of inorganic materials such as silver nanoparticles, graphene and its derivatives, zinc oxide and aluminium oxide as the fillers and antimicrobial agent, into polymer can be promising approach to developed new

antimicrobial polymeric material by promoting excellent antimicrobial efficacy compared to conventional biocides [4]–[6].

---

#### Article history:

Received: 10 March 2022

Accepted: 7 June 2022

Published: 14 June 2022

---

#### E-mail addresses:

Fatinnajwa.joyal@outlook.com (F.N.J. Abedin)

ahmadnaim@unikl.edu.my; (A. N. A. Yahaya)

afifah.khalil@s.unikl.edu.my; (N. A. Khalil)

muzafar@unikl.edu.my; (M. Zulkifli)

\*Corresponding Author

In literature, there are various techniques were applied to improve the antimicrobial properties of thermoplastics elastomer (TPE). Some of the methods are based on the reinforcement antimicrobial agents into the polymer matrix such as blending, coating or embedding that affecting the molecular contact between the agents and polymer surface. The molecular contact can influence the biocide action towards the bacteria. Furthermore, by depending on the application, the materials need to have certain mechanical, thermal, rheological, chemical resistance and stability under

harsh processing situations. Usually, the method used to provide biocide properties to polymers is by incorporating the antimicrobial agents into TPE during extrusion process by melt compounding method.

**ANTIMICROBIAL CAPABILITY OF POLYMERIC MATERIALS**

Antimicrobial materials have become essential but not limited to industries such as healthcare and biomedicine. Furthermore, WHO has listed some of most critical and high priority pathogens that have high resistance towards antibiotics and common antibacterial treatment. The most common bacteria are ESKAPE pathogens (“*Enterococcus faecium*, *Staphylococcus aureus*, *Klebsiella pneumoniae*, *Acinetobacter baumannii*, *Pseudomonas aeruginosa*, and *Enterobacter spp.*”) [2]. These pathogens may cause serious illness and infections that may led to high mortality rate.

Device related infections (DRI) are common in healthcare industry where the medical devices and implants are infected with bacteria. Bacteria growth on the surface of the devices such as urinary catheter and orthopedic implants are most frequent infections at hospitals [3]. Other than that, the infections that are commonly seen as devices-related are contact lenses, pacemakers, vascular graft and prosthetic joints [3]. This is caused by the contamination of pathogens or bacteria that leads to the formation of mature biofilms on the surface of the devices that increase the probability of developing secondary blood stream infection. For instance, the most frequent bacteria found on the medical device-related infections are *S. aureus* and *E. coli*. Usually, prescription of antibiotics is seen to have benefits in inhibiting formation of biofilm and reduce the risks of infections and lower the mortality rate. Unfortunately, as mention in reports by Olmos and colleagues, will cause systemic toxicity and multidrug resistant bacteria [3]. The death toll caused by drug resistant infections is increasing in past two decades around the world as the resistance rate of bactericidal increasing up to 23,000 strains of bacteria including *E. coli*, *Klebsiella sp.*, *Enterobacter sp.*, *P. aeruginosa*, *Acinetobacter sp.*, vancomycin-resistant *Enterococcus faecium*, and methicillin-resistant *Staphylococcus aureus* (MRSA) in Mexico only [8]. From the references mentioned, the most used strains in the studies are *E. coli*, *S. aureus* and *S. epidermidis* as these strains are commonly found in medical-devices related infections to analyses the antibacterial properties of thermoplastics, as shown in TABLE 1.

TABLE 1 Summarized antibacterial activity of thermoplastics from several studies.

Composite	Strains	Conclusion	Reference
Titanium alloys- Chitosan/Polyethylene Oxide (PEO)/Bioactive Glass Nanofibre	<i>S. epidermidis</i> <i>E. coli</i>	The fillers improve antibacterial and osteoconductive properties	[9]
ABS-Polymeric quaternary phophonium salts (PBrMAP-n)	<i>E. coli</i> <i>S. aureus</i>	High concentration of PBrMAP-n (10 wt%) is needed to exhibit antibacterial activity	[10]
ABS- AgNPs	<i>E. coli</i> <i>C. albicans</i> <i>A. baumannii</i> <i>P. aeruginosa</i> <i>S. aureus</i>	Gram-positive strains are more resistant towards AgNPs compared to Gram-Negative strains	[11]
Cellulose Acetate- Aluminium Nitride	<i>S. epidermidis</i> <i>E. coli</i>	High condensation of antibacterial agent (>10wt%) shows better antibacterial activity	[6]

Therefore, apart from using antibiotics as treatment, the use of antimicrobial coatings has seen to be other way to address the problem. Cobos and co-workers studied the possibilities of GO-AgNPs hybrid as the antibacterial agent for PVA as wound dressing. Cobos et al. [4] examined the effect of hybrid content loading (0.5,1.0,2.0,5.0 wt%) to enhance the mechanical, thermal and physical properties of PVA and concluded that all formulation of PVA filled with the hybrid exhibit antibacterial properties. The authors concluded that antibacterial properties exhibits by PVA/GO-AgNPs is due to AgNPs in the hybrid. Previous study by Cobos et al. [12] studied the effect of antibacterial properties of PVA/GO synthesized by one-step process with L-ascorbic acid as reducing agent in aqueous solutions where there was no activity against bacteria strains over the GO loading range. Furthermore, antibacterial activity of GO depends on lateral-dimensions and method of GO synthesized. It is explained that larger sheet of GO have higher antibacterial activity against bacteria if synthesized in suspension. On the other hand, smaller GO sheets exhibit stronger antibacterial activity when GO composite is produced by surface coating [12]. Moreover, it is also determined that the antibacterial activity of GO based polymer composite depends on the graphene concentration. In terms of mechanical properties Cobos et al. [12] reported that 2.0 wt% of GO enhanced the tensile strength and modulus up to 28% and 13% respectively. This study supported by the study made by F.N Joynal Abedin et al. [13] on the effect of GO loading content (0.5 to 2.0 phr), the study showed marginal enhancement for mechanical and thermal properties of ABS/GO/SEBS-g-MAH composite. Cobos et al. [4] concluded that the fillers effectively inhibits the development of bacteria and *S. aureus* shows higher susceptibility towards the films compared to *E. coli* [4]. This statement is also supported by Lee et al [7] where the killing efficiency of 5 wt% modified clay against Gram-negative *E. coli* and Gram-positive *S. aureus* is 98.5 % and 99.9% respectively. The authors explained that the difference in resistant is due to the difference in type of cell wall. It is reported that the thick cell wall of Gram-positive bacteria contains many peptidoglycan layers while the Gram-negative bacteria’s cell wall consists of two membranes. Inner part of the membrane is a cytoplasmic cell membrane, the outer layer consists of lipopolysaccharide (LPS) that act as protective barrier and in between the membranes, there is thin peptidoglycan layer. Thus, it is proved that the *E. coli* is more resistant than that of *S. aureus*.

Some reports are contradicted with the studies by Mahendra et al [14] and Pittol et al [5], where the authors reported that the killing efficiency towards Gram-negative is higher compared to Gram-positive bacteria. Mahendra et al [14] studied the effects

of different loading of GO on the antimicrobial properties of PC against *E. coli* and *S. aureus*. Mahendra et al. [14] reported that the inhibition zone for *E. coli* is significantly higher than *S. aureus* that indicates the killing efficacy of antibacterial agent, GO is higher towards *E. coli*. In other study made by Liu et al [15] shows an evidences that GO is have highest killing efficiency towards *E. coli* compared to other graphene derivatives (graphite, graphite oxide, reduced graphene oxide). But the study only focused only on one type of bacteria which is *E. coli*. Thus, the study can only prove that GO have the capability to act as antibacterial agent without the knowledge on percentage of killing efficiency towards other bacteria.

Furthermore, the mechanism of antibacterial activity of GO still do not have conclusive evidence and need further investigation. In contrast with the knowledge of silver nanoparticle's (AgNPs) antibacterial activity. Most of the researcher have studied the mechanism of the nanoparticles as it is a well-known antibacterial agent for polymeric materials. Generally, positively charged silver ions get into contact with negatively charged bacterial wall that cause changes in membrane morphology and led to higher permeability that allows the nanoparticles to penetrate into the cell membranes and disrupts the cell [16].

## CONCLUSION

Thermoplastics elastomer (TPE) with antimicrobial properties are excellent alternative for traditional biocide and one of the solutions to the antimicrobial resistance (AMR) problem. However, the composite itself need further investigation and analysis to determine the effectiveness of antimicrobial activity towards the bacteria strains. Aspect that can be discovered are mechanisms of reaction and also mechanisms of antibacterial activity. The improvement of mechanical, thermal and physical properties of composite also can be studied.

## ACKNOWLEDGEMENTS

The authors would like to thank Universiti Kuala Lumpur for the financial support through the UniKL Excellent Research Grant Scheme (UERGS).

## REFERENCES

- [1] WHO, "New report calls for urgent action to avert antimicrobial resistance crisis," *World Health Organization*, 2019. <https://www.who.int/news/item/29-04-2019-new-report-calls-for-urgent-action-to-avert-antimicrobial-resistance-crisis> (accessed Jul. 14, 2021).
- [2] N. F. Kamaruzzaman *et al.*, "Antimicrobial polymers: The potential replacement of existing antibiotics?," *Int. J. Mol. Sci.*, vol. 20, no. 11, 2019, doi: 10.3390/ijms20112747.
- [3] D. Olmos and J. González-benito, "Polymeric materials with antibacterial activity: A review," *Polymers (Basel)*, vol. 13, no. 4, pp. 1–30, 2021, doi: 10.3390/polym13040613.
- [4] M. Cobos, I. De-La-Pinta, G. Quindós, M. J. Fernández, and M. D. Fernández, "Synthesis, Physical, Mechanical and Antibacterial Properties of Nanocomposites Based on Poly(vinyl alcohol)/Graphene Oxide-Silver Nanoparticles," *Polymers (Basel)*, vol. 12, no. 723, pp. 1–18, 2020.
- [5] M. Pittol, D. Tomacheski, D. N. Simões, V. F. Ribeiro, and R. M. C. Santana, "Antimicrobial performance of thermoplastic elastomers containing zinc pyrithione and silver nanoparticles," *Mater. Res.*, vol. 20, no. 5, pp. 1266–1273, 2017, doi: 10.1590/1980-5373-MR-2017-0137.
- [6] T. P. M. Sunthar *et al.*, "Antibacterial property of cellulose acetate composite materials reinforced with aluminum nitride," *Antibiotics*, vol. 10, no. 11, 2021, doi: 10.3390/antibiotics10111292.
- [7] M. Lee, D. Kim, J. H. Kim, J. K. Oh, H. Castaneda, and J. H. Kim, "Antimicrobial Activities of Thermoplastic Polyurethane/Clay Nanocomposites against Pathogenic Bacteria," *ACS Appl. Bio Mater.*, vol. 3, no. 10, pp. 6672–6679, Oct. 2020, doi: 10.1021/acsabm.0c00452.
- [8] E. Garza-González *et al.*, "A snapshot of antimicrobial resistance in Mexico. Results from 47 centers from 20 states during a six-month period," *PLoS One*, vol. 14, no. 3, p. e0209865, Mar. 2019, doi: 10.1371/JOURNAL.PONE.0209865.
- [9] F. Boschetto *et al.*, "Antibacterial and osteoconductive effects of chitosan/polyethylene oxide (PEO)/bioactive glass nanofibers for orthopedic applications," *Appl. Sci.*, vol. 10, no. 7, pp. 1–18, 2020, doi: 10.3390/app10072360.
- [10] W. Zeng, J. He, and F. Liu, "Preparation and properties of antibacterial ABS plastics based on polymeric quaternary phosphonium salts antibacterial agents," *Polym. Adv. Technol.*, vol. 30, no. 10, pp. 2515–2522, 2019, doi: 10.1002/pat.4653.
- [11] I. Tse *et al.*, "Antimicrobial activity of 3d-printed acrylonitrile butadiene styrene (Abs) polymer-coated with silver nanoparticles," *Materials (Basel)*, vol. 14, no. 24, 2021, doi: 10.3390/ma14247681.
- [12] M. Cobos, I. De-La-Pinta, G. Quindós, M. J. Fernández, and M. D. Fernández, "One-step eco-friendly synthesized silver-graphene oxide/poly(vinyl alcohol) antibacterial nanocomposites," *Carbon N. Y.*, vol. 150, pp. 101–116, 2019, doi: 10.1016/j.carbon.2019.05.011.
- [13] F. N. J. Abedin *et al.*, "The effect of graphene oxide and sebs-g-mah compatibilizer on mechanical and thermal properties of acrylonitrile-butadiene-styrene/talc composite," *Polymers (Basel)*, vol. 13, no. 18, pp. 1–20, 2021, doi: 10.3390/polym13183180.
- [14] R. Mahendran, D. Sridharan, K. Santhakumar, T. A. A. Selvakumar, P. Rajasekar, and J.-H. Jang, "Graphene Oxide Reinforced Polycarbonate Nanocomposite Films with Antibacterial Properties," *Indian J. Mater. Sci.*, vol. 2016, pp. 1–10, 2016, doi: 10.1155/2016/4169409.
- [15] S. Liu *et al.*, "Antibacterial Activity of Graphite, Graphite Oxide, Graphene Oxide, and Reduced Graphene Oxide: Membrane and Oxidative Stress," *ACS Nano*, vol. 5, no. 9, pp. 6971–6980, 2011, doi: <https://doi.org/10.1021/nn202451x>.

***The International Symposium on Polymeric Materials 2022***

- [16] R. Mahendran, D. Sridharan, K. Santhakumar, T. A. Selvakumar, P. Rajasekar, and J.-H. Jang, "Graphene Oxide Reinforced Polycarbonate Nanocomposite Films with Antibacterial Properties," 2016, doi: 10.1155/2016/4169409.



## MECHANICAL PROPERTIES AND CONDUCTIVITY OF POLYANILINE-CELLULOSE-LATEX HYBRID

M. F. Banjar<sup>1</sup>, A. N. A. Yahaya<sup>1</sup>, N. A. Khalil<sup>1</sup>, A. A. Al-Dulaimi<sup>3</sup>, M. Singh<sup>4</sup>, M. Zulkifli<sup>2\*</sup>

<sup>1</sup>Universiti Kuala Lumpur, Branch Campus Malaysian Institute of Chemical and BioEngineering Technology, 78000 Alor Gajah, Melaka, Malaysia

<sup>2</sup>Green Chemistry and Sustainability Cluster, Universiti Kuala Lumpur, Branch Campus Malaysian Institute of Chemical and Bioengineering

<sup>3</sup>Department of Dental Technology, Al-Turath University College, Baghdad, Iraq.

<sup>4</sup>Malaysian Rubber Board, RRIM Research Station, 47000 Sungai Buloh, Selangor, Malaysia

---

### ABSTRACT

Composite films of polyaniline (PANI)-cellulose and prevulcanised latex (PVL) were prepared and studied extensively to understand the impact on mechanical properties and conductivity. PANI promotes conductive properties in any host matrix to form blends or composites. Usage of cellulose was intended to supplement the poor mechanical properties showed by PANI and further improve composite films. Alpha cellulose (AC) and microcrystalline cellulose (MCC) were applied to elucidate the significant effect of different particle size of celluloses. PANI-AC and PANI-MCC templates were synthesized through chemical oxidative polymerization with sodium dodecyl sulphate (SDS) as surfactant and mixed with PVL in different concentrations. Films were obtained by casting method and characterized by FTIR (Fourier Transform Infrared), TGA (Thermogravimetric Analysis) and tensile test. The results revealed that these templates improved the mechanical performance of PVL at 3 g and 5 g loading but further increase the loading led to a declining trend. The TGA revealed that increasing the amount of PANI-AC and PANI-MCC loading in PVL resulted in improved conductivity.

*Keywords:* polyaniline, latex, polyaniline-latex composite, cellulose, mechanical properties.

---

### INTRODUCTION

Polyaniline (PANI) is one of conductive polymers that attracted many researchers to work on due to its low cost, ease of synthesis, good environmental stability and reversible conduction mechanism [1]. PANI is conductive when doped with salt that protonate double bond imine nitrogen on the polymer chain, meanwhile can be dedoped by base to its insulating form. However, the poor mechanical property of PANI is unfavorable for advancement in materials technology and other potential applications. The beneficial characteristics driven the effort to fabricate PANI as filler in composite especially with natural rubber latex [2]–[4]. Cellulose is a biopolymer derived from plants well-known for its mechanically strong properties which are capable of being used as matrices with PANI. This material combined of conducting PANI, good mechanical-strength cellulose and non-conducting latex as the host, for instance covers the intrinsic brittle pure PANI. This research was carried out to develop PANI and PANI-cellulose template and disperse it into latex formulation. The performance of composite films was reported in mechanical properties as, Tensile strength and Young's modulus while TGA shows the thermal stability of films which have relationship with the conductivity.

### MATERIALS AND METHODS

#### *Materials*

Aniline (>99.5 %) and APS as the oxidizing agent were purchased from Bendosen. Anionic surfactant (SDS), hydrochloric acid (HCl, 37% fuming), potassium hydroxide pellet (KOH), microcrystalline cellulose powder (MCC) and alpha cellulose powder (AC) purchased from R&M Chemicals. The prevulcanised latex (Givul MRT, TSC:60%) was purchased from Getahindus, Malaysia. All chemicals were analytical grade and used as received.

#### *Methods*

---

#### *Article history:*

Received: 10 March 2022

Accepted: 7 June 2022

Published: 14 June 2022

#### *E-mail addresses:*

faizar.banjar16@s.unikl.edu.my (M. F. Banjar)

ahmadnaim@unikl.edu.my (A. N. A. Yahaya)

norafifah@unikl.edu.my (N. A. Khalil)

manroshan@lgm.gov.my (M. Singh)

muzafar@unikl.edu.my (M. Zulkifli)

\*Corresponding Author

#### *Synthesis of PANI-cellulose template and neat PANI*

0.2 M aniline solution was prepared by mixing 36.6 ml aniline in 2.0 L 1.0 M HCl and stirred using mechanical stirrer with stirring speed of 800 rpm for 15 minutes. Ice-water bath implemented along the polymerization process to maintain low temperature condition of 0 to 5 °C. Then, 30 g SDS and 60 g MCC were added into the solution and vigorously stirred (1200 rpm) for 45 minutes. 2.0 L of 0.2 M APS solution added afterwards via dropwise to initiate polymerization of aniline. The colour changes were observed from milky to dark green solution. As whole APS has been added, the solution was stirred for another 5 hours, then filtered using vacuum pump and washed using excess distilled water till colourless filtrate was obtained. PANI precipitate dried in oven at 60 °C for 24 hours. Entire synthesis flow was repeated using AC and

without celluloses, producing three types of samples, neat PANI and two PANI-cellulose template samples, indicated as PANI-MCC and PANI-AC. Lastly, dried samples were grinded using grinder and sieve to obtain fine powder.

*Synthesis of PANI-celluloses-PVL composite*

Different loadings (3 g, 5 g and 10 g) of PANI powder samples were dispersed in 0.1 % KOH solution to obtain 10 w/w % PANI dispersion. The dispersion then homogenized using Silverson Homogenizer and mixed with distilled water and PVL according to formulation as displayed in TABLE 1. Prepared samples then casted onto 50 mm × 50 mm × 10 mm casting plate. The film kept dry at ambient temperature for 24 hours.

TABLE 1: Formulation for PANI-cellulose-PVL composite

Substances	PANI-cellulose loading		
	3 g	5 g	10 g
60% PV Latex	100	100	100
10 % PANI-cellulose	3	5	10
Total (dry weight)	<b>103</b>	<b>105</b>	<b>110</b>
60% PV Latex	33.4	33.4	33.4
10 % PANI-cellulose	6	10	20
Distilled water	29.29	26.62	19.94
Total (wet weight)	<b>68.89</b>	<b>70.02</b>	<b>73.34</b>

*Characterization*

Neat PANI and PANI-cellulose powder were characterized by FTIR (Nicolet i10s) to investigate the functional group presence. The spectral range applied was 4000 to 400 cm<sup>-1</sup> at resolution of 2 cm<sup>-1</sup>. Mechanical performance of pure PVL and fabricated PANI-cellulose-PVL film were determined using Lloyds Universal Testing Machine with ASTM D3909 tensile test standard. These films were cut into dumbbell shapes with 1 kN load cell and performed at ambient temperature, 23 ± 2 °C as well as 50 ± 5 % relative humidity. Thermal gravimetry analysis (TGA) of films was conducted to interpret the thermal properties.

**RESULTS AND DISCUSSION**

*FTIR*

The chemical compositions of PANI, PANI-MCC and PANI-AC were displayed in Fig. 1 where several changes in peaks were observed. The spectrum of neat PANI shows characteristics peaks of PANI at 1207.00 cm<sup>-1</sup>, 1285.69 cm<sup>-1</sup> and 1548.41 cm<sup>-1</sup>, corresponding to C=C stretching vibration of quinoid ring, benzenoid ring and C-N stretching, respectively. These peaks diminished in PANI-cellulose samples indicating formation of the template [5]. Meanwhile, cellulose key peaks were at 1048.91 cm<sup>-1</sup> and 1102.36 cm<sup>-1</sup> denoting C-O-C stretching and glucose ring skeletal vibration, respectively.

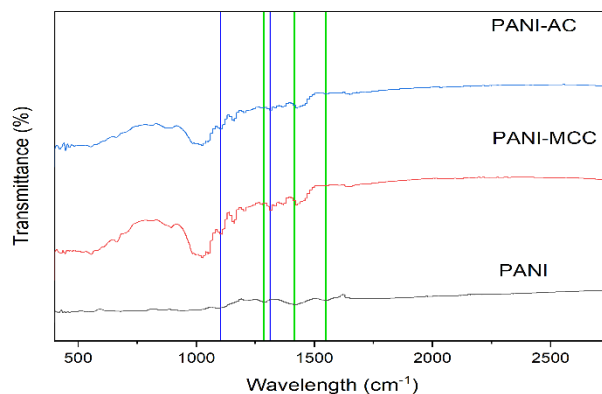


Fig. 1: FTIR of PANI, PANI-MCC and PANI-AC

*Mechanical Performance*

The mechanical performances of the films were monitored in tensile strength (TS) and Young’s modulus (YM). Tensile strength performance displayed in Fig. 2a where significant improvement shown as PANI and PANI-cellulose filler incorporated into PVL, indicating the reinforcement effect and rigidity of these fillers [6]. Compared to pure PVL (17.39 MPa), tensile strength improvement showed by 5 g loading of neat PANI (36.37 MPa) with 109.14 % gain. Meanwhile, TS deteriorated at 10 g loading of PANI-MCC (14.20 MPa) and PANI-AC (15.33 MPa) with decrement by 18.34 % and 11.84 %, respectively. This response can be related with amount of water absorbed due to hygroscopic of PANI and PANI-cellulose template [7], [8]. Both PANI and PANI-cellulose as filler enhance the TS up to 5 g loading and appear to decline at 10 g loading. Similar trend demonstrated in Fig. 2b, YM performance of the film where the ideal improvement obtained at 5 g loading and further loading of PANI-cellulose tend to reduce the value. The results indicated that reinforcement of neat PANI is much better filler for PVL due to the high strength and modulus.

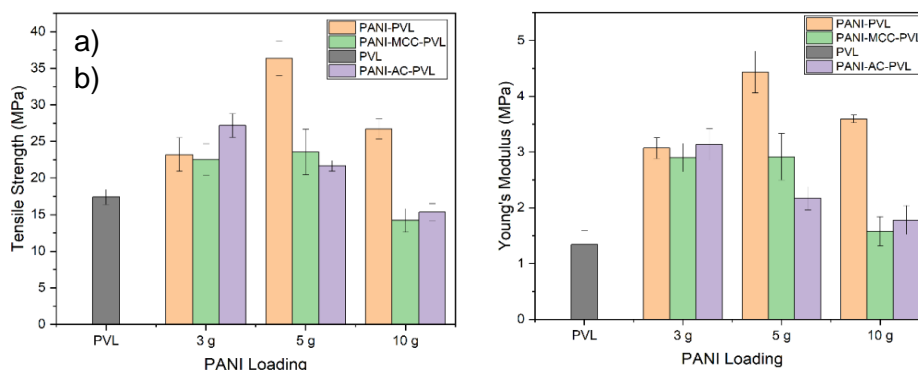


Fig. 2: Tensile strength (a) and Young's Modulus (b) of PANI-PVL composites

#### Thermogravimetric Analysis (TGA)

TGA was carried out between neat PVL as control sample, PANI-PVL, PANI-MCC-PVL and PANI-AC-PVL. TABLE 2 display the inflection point and the residual content of samples. As PANI was added into PVL, the inflection point was increase significantly, indicating enhancement of thermal properties. The conductivity of the composite has a correlation to its inflection point. Higher inflection point indicates higher conductivity. Hence, addition of PANI believe to improve the conductivity of film. Similar trend was observed by F.Ammar et al., where addition of PANI as filler in PVL resulted in increase of inflection point compared to blank PVL. [9]

TABLE 2: Thermogravimetric Analysis Data of PVL, PANI-PVL, PANI-MCC-PVL and PANI-AC-PVL

Sample	Inflection Point (°C)	Residue Content
PVL	300.16	3.51
PANI-PVL	389.60	2.00
PANI-MCC-PVL	386.85	1.43
PANI-AC-PVL	389.38	1.75

#### CONCLUSIONS

PANI and PANI-celluloses template reinforced in PVL have improved its mechanical properties and conductivity. The results revealed a clear comparison in terms of TS and YM between neat PANI, PANI MCC and PANI AC, with dominance by PANI as the filler in PVL. However, adding cellulose into the composite reduces the mechanical properties owing to its hygroscopic properties. The increment of inflection points as PANI and PANI-filler incorporated into PVL was correlated to enhancement conductivity.

#### ACKNOWLEDGEMENTS

The authors would like to thank Universiti Kuala Lumpur Malaysian Institute of Chemical and Bioengineering Technology (UniKL MICET) and Ministry of Higher Education (MoHE), Malaysia under Fundamental Research Grant Scheme (FRGS/1/2020/TK0/UNIKL/02/4).

#### REFERENCES

- [1] S. I. Abd Razak, W. A. Wan Abdul Rahman, S. Hashim, and M. Y. Yahya, "Polyaniline and their Conductive Polymer Blends: A Short Review," *Malaysian J. Fundam. Appl. Sci.*, vol. 9, no. 2, pp. 74–80, 2014.
- [2] P. Sukitpaneenit, T. Thanpitcha, A. Sirivat, C. Weder, and R. Rujiravanit, "Electrical Conductivity and Mechanical Properties of Polyaniline/Natural Rubber Composite Fibers," *J. Appl. Polym. Sci.*, vol. 106, pp. 4038–4046, 2007.
- [3] M. N. Kalasad et al., "Synthesis and characterization of polyaniline rubber composites," *Compos. Sci. Technol.*, vol. 68, no. 7–8, pp. 1787–1793, 2008.
- [4] M. M. Anisha, N. M. Faseena, and P. Predeep, "Electrochemical synthesis of conducting natural rubber nanocomposite films," *Plast. Rubber Compos.*, vol. 42, no. 6, pp. 264–267, 2013.
- [5] N. P. Putri, D. H. Kusumawati, N. Widiyanti, and Munasir, "Synthesis of polyaniline/cellulose composite as humidity sensor," *J. Phys. Conf. Ser.*, vol. 997, no. 1, 2018.
- [6] X. Wu, C. Lu, H. Xu, X. Zhang, and Z. Zhou, "Biotemplate synthesis of polyaniline@cellulose nanowhiskers/natural rubber nanocomposites with 3D hierarchical multiscale structure and improved electrical conductivity," *ACS Appl. Mater. Interfaces*, vol. 6, no. 23, pp. 21078–21085, 2014.
- [7] M. J. Da Silva, A. O. Sanches, L. F. Malmonge, and J. A. Malmonge, "Electrical, mechanical, and thermal analysis of natural rubber/polyaniline-Dbsa composite," *Mater. Res.*, vol. 17, pp. 59–63, 2014.
- [8] M. M. Ostwal, M. Sahimi, and T. T. Tsotsis, "Water harvesting using a conducting polymer: A study by molecular dynamics simulation," *Phys. Rev. E - Stat. Nonlinear, Soft Matter Phys.*, vol. 79, no. 6, pp. 1–16, 2009.
- [9] F. Ammar et al., "Preparation and characteristics of doped polyaniline in latex article," in *International Conference on Multifunctional and Hybrid Composite Materials for Energy, Environment And Medical Applications (ICMHCEE 2019)*, 2019.

## SUCCESSFUL COMMERCIALIZATION OF NATURAL FIBRE REINFORCED COMPOSITES

S.F.K. Sherwani<sup>1</sup>, S. M. Sapuan<sup>1,2\*</sup>, E.S. Zainudin<sup>1,2</sup>, Z. Leman<sup>2</sup>, A. Khalina<sup>2</sup>

<sup>1</sup>Advanced Engineering Materials and Composites Research Centre (AEMC), Department of Mechanical and Manufacturing Engineering, Universiti Putra Malaysia, 43400 UPM Serdang, Selangor, Malaysia

<sup>2</sup>Laboratory of Biocomposite Technology, Institute of Tropical Forestry and Forest Products (INTROP), Universiti Putra Malaysia, 43400 UPM Serdang, Selangor, Malaysia

---

### ABSTRACT

The growing environmental devastation ascribed to the disposal of packaging plastic waste has led to an urgent need to develop environmentally friendly packaging materials to rescue our ecosystem. In an effort to resolve the ongoing environmental crisis caused by non-biodegradable plastics, natural biopolymers have been considered as potential alternatives to conventional plastics. Biodegradable films for packaging have been reported to have low water barrier resistance. Such drawback strongly limit their wide application, especially for food packaging purposes. Many studies have been undertaken by scientists to improve the water sensitivity of starch-based materials without compromising their biodegradability. The reinforcement of natural biopolymers with nanocellulose has been shown to be beneficial for water transmission properties of biodegradable film.

*Keywords:* natural fibre, commercial, natural composites , biodegradable.

---

### INTRODUCTION

Natural biopolymers have been studied as viable replacements to conventional plastics in an effort to tackle the ongoing ecological disaster created by non-biodegradable plastics. The increasing environmental destruction caused by the disposal of packaging plastic waste has necessitated the development of ecologically friendly packaging materials in order to save our ecosystem.

### APPLICATION OF NATURAL FIBRE REINFORCED COMPOSITES (NFRCS)

1. Oil Catcher (Natural Fiber)  
Sheet-type adsorbent made of natural fiber that absorbs oil contents as shown in Fig. 1. Particularly excellent in oil absorption, absorbs oil approximately 30 times its own weight. Both adsorption force and adsorption speed are 3 times higher compared to chemical fiber products. The hollow fiber in the macaroni structure prevents the dripping of oil after adherence. Natural fibers are used as the primary material for minimal deterioration over time and for excellence in stockpiling.  
Applications: Can be used for oil leakages around facilities for metalworking, etc., and for adsorption of floating oil inside coolant tanks of machine tools or small grease traps. Ideal for stockpiling earthquake preparedness goods at corporate offices (BCP measures).
2. Natural fiber disc  
Fiber disc boasting long operation life and excellent grinding force as shown Fig. 2. In addition to the product having a long lifespan, replacement is made as easy as possible due to possible use without a back pad. The performance will not significantly deteriorate even under high temperature and high humidity. It is flexible and suitable for grinding rough workpieces. Applications: For grinding general steel, stainless steel, etc.
3. Natural bamboo fiber paper cup disposable as shown in Fig 3.
4. Plant-based Kitchen Brush Set Biodegradable Natural fiber Wooden Dish Brush, Bottle Brush, Pot Brush, Vegetable Brush as shown in Fig 4.
5. Coconut fiber mat as shown in Fig 5.
6. 10M Coco Liner Roll Basket Flower Basket Flowerpot Hanging Pad Coco Fiber Liner as shown in Fig 6.
7. Biodegradable lunch box as shown in Fig 7.
8. Biodegradable paper pulp peat pots plant seed nursery cup tray cultivation as shown in Fig 8.
9. 15 x 15 Biodegradable Hypermarket Plastic Bag as shown in Fig 9
10. Bamboo utensils as shown in Fig 10, [10].

Large scale development in the making of parts such as the interior panels of car, engines cover, handles, body parts etc, have improved the scope of the use of natural fibers as a building material for such components so as to boost the industry sector keeping in mind the KYOTO Protocols in minimizing the carbon footprints involved in the industry. Development of such kind of materials would meet the growing demands of this sector without disturbing the protocol. Use of such kind of material is not only sustainable because of its ease of production but also due to its ability to maintain the graded strength, thus not compromising with the security and safety of the passengers.

---

#### Article history:

Received: 10 March 2022

Accepted: 7 June 2022

Published: 14 June 2022

---

#### E-mail addresses:

Faisalsherwani786@gmail.com (S.F.K. Sherwani)

sapuan@upm.edu.my (S.M. Sapuan)

\*Corresponding Author



Fig. 1 [1]

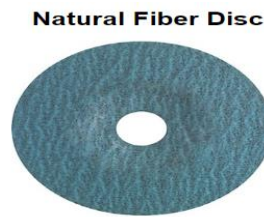


Fig. 2 [2]



Fig. 3 [3]



Fig. 4 [4]



Fig. 5 [5]



Fig. 6 [6]



Fig. 7 [7]



Fig. 8 [8]



Fig. 9 [9]



Fig. 10: Bamboo utensils [10]

## CONCLUSIONS

The study found that the usage of biodegradable materials is essential for both humans and the environment. As time goes on, these biomaterials grow increasingly ubiquitous in everyday life, but there is still a need for new materials as well as an awareness campaign to commercialize biomaterials derived from natural fibre composites.

## ACKNOWLEDGEMENTS

The authors gratefully thank Universiti Putra Malaysia (UPM) for funding this research through Geran Putra Berimpak (GPB), UPM.RMC.800-3/3/1/GPB/2020/9694500.

## REFERENCES

- [1] <https://my.misumi-ec.com/vona2/detail/223000702860/>.
- [2] <https://my.misumi-ec.com/vona2/detail/223006694765/>.
- [3] <https://shopee.com.my/Natural-bamboo-fiber-paper-cup-disposable-hospitality-thickened-home-office-wholesale-i.187412176.6737229258>.

- [4] <https://shopee.com.my/Plant-based-5pcs-Kitchen-Brush-Set-Biodegradable-Natural-Fibre-Wooden-Dish-Brush-Bottle-Brush-Pot-Brush-Vegetable-Brush-and-Replaceable-Head-Eco-friendly-Plastic-Free-product-i.288974453.7450748209>.
- [5] “[https://www.lazada.com.my/products/10pcspack-liner-permeable-non-toxic-reptile-habitat-home-office-round-for-hanging-basket-outdoor-garden-hotel-coconut-fiber-mat-i932362784-s2343700655.html?exlaz=d\\_1:mm\\_150050845\\_51350205\\_2010350205::12:1032211143!544000](https://www.lazada.com.my/products/10pcspack-liner-permeable-non-toxic-reptile-habitat-home-office-round-for-hanging-basket-outdoor-garden-hotel-coconut-fiber-mat-i932362784-s2343700655.html?exlaz=d_1:mm_150050845_51350205_2010350205::12:1032211143!544000).”
- [6] [https://www.lazada.com.my/products/10m-coco-liner-roll-basket-flower-basket-flowerpot-hanging-pad-coco-fiber-liner-i1220790987-s3606968719.html?spm=a2o4k.pdp.recommendation\\_2.1.62001651yhNScu&mp=1&scm=1007.16389.126158.0&clickTrackInfo=8200d6a1-4e4d-440c-](https://www.lazada.com.my/products/10m-coco-liner-roll-basket-flower-basket-flowerpot-hanging-pad-coco-fiber-liner-i1220790987-s3606968719.html?spm=a2o4k.pdp.recommendation_2.1.62001651yhNScu&mp=1&scm=1007.16389.126158.0&clickTrackInfo=8200d6a1-4e4d-440c-)
- [7] [https://www.lazada.com.my/products/biodegradable-lunch-box-beigebrown-800-piecescarton-i350063388-s492839167.html?exlaz=d\\_1:mm\\_150050845\\_51350205\\_2010350205::12:1032211143!54400014687!!!pla-296303633664!c!296303633664!492839167!135728067&gclid=Cj0KCQjw8fr](https://www.lazada.com.my/products/biodegradable-lunch-box-beigebrown-800-piecescarton-i350063388-s492839167.html?exlaz=d_1:mm_150050845_51350205_2010350205::12:1032211143!54400014687!!!pla-296303633664!c!296303633664!492839167!135728067&gclid=Cj0KCQjw8fr).
- [8] [www.lazada.com.my/products/zhang-50pcs-biodegradable-paper-pulp-peat-pots-plant-seed-nursery-cup-tray-cultivation-i1215240899-s3582692652.html?exlaz=d\\_1:mm\\_150050845\\_51350205\\_2010350205::12:1032211143!54400014687!!!pla-296303633664!c!296303633664!](http://www.lazada.com.my/products/zhang-50pcs-biodegradable-paper-pulp-peat-pots-plant-seed-nursery-cup-tray-cultivation-i1215240899-s3582692652.html?exlaz=d_1:mm_150050845_51350205_2010350205::12:1032211143!54400014687!!!pla-296303633664!c!296303633664!)
- [9] [https://www.lazada.com.my/products/15-x-15-biodegradable-hypermarket-plastic-bag-i597478566-s1213146210.html?exlaz=d\\_1:mm\\_150050845\\_51350205\\_2010350205::12:1032211143!54400014687!!!pla-368231893610!c!368231893610!1213146210!142650005&gclid=Cj0KCQjw8fr7BRD](https://www.lazada.com.my/products/15-x-15-biodegradable-hypermarket-plastic-bag-i597478566-s1213146210.html?exlaz=d_1:mm_150050845_51350205_2010350205::12:1032211143!54400014687!!!pla-368231893610!c!368231893610!1213146210!142650005&gclid=Cj0KCQjw8fr7BRD).
- [10] S. M. Sapuan, M. R. Ishak, and E. S. Zainudin, “Development and characterization of sugar palm nanocrystalline cellulose reinforced sugar palm starch bionanocomposites,” *Carbohydr. Polym.*, vol. 202, pp. 186–202, Dec. 2018, doi: 10.1016/j.carbpol.2018.09.002.

## **A COMPOSITE HYDROGEL BEADS BIO-SORBENT FOR REMOVAL OF COPPER: EFFECT OF pH OF COPPER SOLUTION**

A.S.A. Rahman<sup>1\*</sup>, N.A. Khalil<sup>1</sup>, M.S. Hossain<sup>2</sup>, A.N.A. Yahaya<sup>3</sup>, M. Zulkifli<sup>3\*</sup>

<sup>1</sup>Universiti Kuala Lumpur, Branch Campus Malaysian Institute of Chemical and Bioengineering Technology, 78000 Alor Gajah, Melaka, Malaysia

<sup>2</sup>School of Technology Industry, Universiti Sains Malaysia, Penang, Malaysia

<sup>3</sup>Green Chemistry and Sustainability Cluster, Universiti Kuala Lumpur, Branch Campus Malaysian Institute of Chemical and Bioengineering Technology, 78000 Alor Gajah, Melaka, Malaysia

---

### **ABSTRACT**

An environmentally friendly composite hydrogel beads bio-sorbent is being introduced by cross-linking cellulose, chitosan, magnetite, and alginate (CCMA) through a facile cross-linking method for the removal of copper. The effect of pH of copper (Cu) solution for the removal of Cu by CCMA was investigated through this study. Other than that, the net surface charge of CCMA hydrogel beads was characterized by zeta potential measurement. Besides that, the possible adsorption mechanism by CCMA was also proposed in this study. Based on the result, the best percentage of copper removal by CCMA was obtained at 91.29% at pH 6. A negatively charged CCMA was also proven at -16.3mV, which indicates a successful adsorbent for application in heavy metal removal.

*Keywords:* composite hydrogel beads bio-sorbent, cellulose, chitosan, magnetite, alginate, copper.

---

### **INTRODUCTION**

A significant increase in heavy metal pollution in groundwater as a result of wastewater from manufacturing and industrial activities has been one of the most serious global issues for the past two decades [1]. Common heavy metals in industrial wastewater such as copper, lead, chromium, zinc, and nickel are non-biodegradable and was proven to be toxic to human and living being[2]. Copper (Cu) metal, commonly associated with electroplating manufacturing industries is hazardous and will cause concerning health issues in human such as kidney and liver failure[3]. Therefore, a safe and proper heavy metal removal from wastewater should be implemented. Common heavy metal removal methods are membrane filtration, chemical precipitation, ion exchange, and adsorption process[4]. Adsorption process especially had gained mass interest among researchers due to its simple operation[3]. Currently, researchers had been focusing on the development of adsorbent by using bio-degradable and available materials such as cellulose, alginate, and chitosan[3–5].

Cellulose is a linear polymer  $\beta$ -1,4-linked anhydro-D-glucose with an abundant hydroxyl group (-OH) on its surface that is linked by intramolecular and intermolecular hydrogen bonds. This property of cellulose contributes to its high flexibility, mechanical properties, hydrophilicity, and affinity for heavy metal ions[6]. Chitosan, on the other hand, is a natural polysaccharide derived from crab or shrimp shells that is composed of poly [ $\beta$  -(1-4)-linked-2-amino-2-deoxy-D-glucose]. Chitosan, which has an abundance of hydroxyl groups (-OH) and amine groups (-NH<sub>2</sub>), has also demonstrated a high affinity for heavy metal ions through electrostatic interaction, ion exchange, and complexation with the heavy metal ions [3]. Aside from that, alginate's remarkable properties, such as its ability to instantly form solid gels upon interaction with divalent ions such as calcium cations, as well as its ability to serve sorption sites for heavy metal ions, make it a promising candidate for adsorbent development [3,7]. Alginate, a natural polysaccharide derived from brown marine algae, is composed of -L-guluronic acid and 1-4 linked -D-mannuronic acid, and it contains an abundant carboxyl group (-COOH), which facilitates interactions with heavy metal ions [3].

Through this study, a composite hydrogel beads adsorbent was developed by a one-step cross-linking method of cellulose, chitosan, magnetite, and alginate (CCMA). Surprisingly, there have not been much research that incorporate cellulose, chitosan, alginate, and magnetite in hydrogel beads form and its ability to remove heavy metal in variation of pH of adsorbate solution. Other than that, the effect of pH of heavy metal copper solution on the performance of copper metal removal by CCMA was also studied. The net surface charge of CCMA hydrogel beads was also characterized through zeta potential measurement in this study.

---

#### *Article history:*

Received: 10 March 2022

Accepted: 7 June 2022

Published: 14 June 2022

---

#### *E-mail addresses:*

aida.syafiqah@s.unikl.edu.my (A. S. A. Rahman)

muzafar@unikl.edu.my (M. Zulkifli)

\*Corresponding Author

## MATERIALS AND METHODS

### Materials

Microcrystalline cellulose powder, sodium alginate powder, and copper (II) sulphate anhydrous were provided by R&M Chemicals. Iron (II, III) oxide magnetite was provided by Sigma Aldrich. Chitosan with a De-acetylation degree of greater than 90%, was acquired from Bio Basic and calcium chloride anhydrous was acquired from Merck. All chemicals used were of analytical grade and were not modified or purified in any way.

### Methods

#### Development of CCMA Hydrogel Beads

First, an alginate solution was made by gradually incorporating 4g of sodium alginate powder into 200mL of ultrapure water while constantly stirring at 45°C for 1 hour. The solution was then supplemented with 2g of microcrystalline cellulose powder and 0.4g iron (II, III) oxide magnetite powder under the same conditions and stirred for another 2 hours. The well-mixed solution was then supplemented with 2g of chitosan powder, which was stirred for 2 hours. To ensure consistent sizes and shapes of the hydrogel beads, the composite bio-sorbent solution was dropped into a 0.2M calcium chloride solution using a burette at a constant 10 cm distance from the solution. The hydrogel beads were cured in the calcium chloride solution for 24 hours at room temperature. The hydrogel beads were then filtered and rinsed with deionized water several times to remove the residues of calcium chloride before stored in ultrapure water for further analysis. Fig. 1 shows the CCMA hydrogel beads in this study.



Fig. 1: CCMA Hydrogel Beads

#### Effect of pH of Copper Solution in Removal of Copper

250 mL conical flasks containing 100 mL of 100 mg/L Cu (II) solutions was used to investigate the performance of CCMA in copper removal. The effect of pH of copper solution on copper removal was studied by varying the pH at pH 3-6 in the thermoshaker incubator under constant shaking at 150 rpm at room temperature. Then, an adequate amount of samples were drawn and filtered with a 0.45 micron syringe filter after 24 hour. Furthermore, all flasks were sealed to prevent copper solution from evaporating into the surrounding environment. In addition, a 100 mL blank solution of 100 mg/L Cu (II) solution without CCMA hydrogel beads was prepared to ensure that no copper adsorption onto the flask wall occurred.

## RESULTS AND DISCUSSION

#### Effect of pH of Heavy Metal Copper Solution

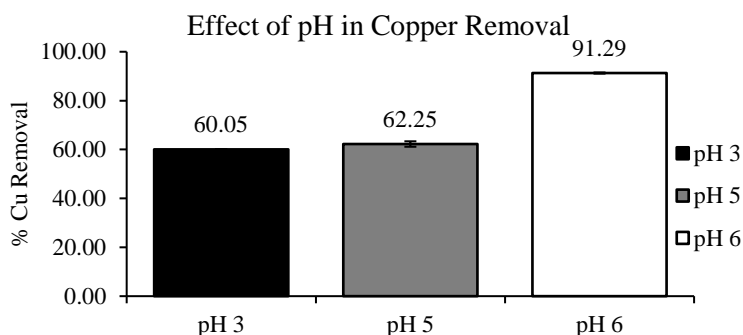


Fig. 2: Effect of pH of Copper Solution on Copper Removal [Contact time: 24hour, Temperature: 30°C, 150 rotating speed, 100 mg/L initial concentration of copper, CCMA dosage of 1.5g]

Variation of pH 3-6 was chosen and studied due to precipitation of metal oxides that would occur at higher pH [8]. The pH is one of main factor that affects the metal adsorption by adsorbent due to existence of ions in adsorbate solution and functional groups on the surface of adsorbent. Fig. 2 depicts the percentage removal of copper ions from copper solution as a function of pH. The percentage removal of copper increases as the pH rises. The low copper removal percentage at pH 3 may be due to the presence of



hydronium ion, H<sup>+</sup>, which competes with copper ion, Cu<sup>2+</sup>, for active sites on adsorbent surfaces [3]. This leads to a less interaction between copper ions and active sites on the adsorbent, thus decreasing the percentage of copper removed from copper solution. Aside from that, as the pH range increases, there will be stronger electrostatic interactions between copper ions, Cu<sup>2+</sup>, and active sites in functional groups -COOH- in alginate, -NH<sub>2</sub>- in chitosan, and -OH- in both chitosan and cellulose, resulting in a higher copper removal percentage from copper solution. This is because as the pH range increases, deprotonation occurs on the adsorbent's surface, leaving vacant active sites for interactions with copper ions [9].

Generally, the adsorption mechanism by adsorbent and heavy metal is by electrostatic interaction due to presence of different charges exist between the adsorbent and the heavy metal ion [10]. Therefore, the negatively charged functional groups exists on surface of CCMA may have been responsible for adsorption of positively charged copper metal ions, as supported by findings from Hu et al., 2017 and Wang et al., 2019 [9, 11]. This is further supported from the zeta potential measurement done in this study.

#### Zeta Potential

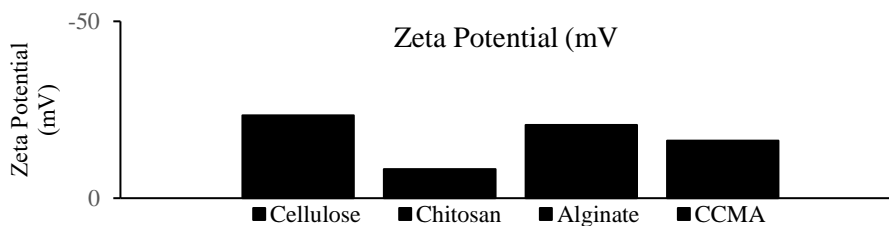


Fig. 3: Zeta Potential of Cellulose, Chitosan, Alginate and CCMA

Fig. 3 shows zeta potential of cellulose powder, chitosan powder, alginate, and CCMA hydrogel beads done at pH 5 to prove the negative potential value of CCMA. Zeta potential measurement shows all sample possess negative potential value. This proven that the CCMA hydrogel bead is negatively charged, thus making it favorable for electrostatic interaction with the positively charged copper metal ions [8]. However, a slight decrease in zeta potential value in CCMA at -16.3 mV compared to cellulose and alginate is possibly due to strong Van Der Waals forces between inter particles, which also leads to particles aggregation in the sample [12]. Other than that, particles aggregation could occur due to addition of magnetite in the sample [13].

#### CONCLUSIONS

Through this study, the development of CCMA hydrogel beads bio-sorbent was successfully done and introduced by using a one-step cross-linking method. Other than that, the effect of pH of copper solution in performance of CCMA for removal of heavy metal copper ions shows that the highest copper removal by CCMA was achieved at 91.29% at pH 6. Moreover, based on zeta potential measurement done, it was revealed that CCMA possess negative surface charge at -16.3 mV, thus indicates a favorable electrostatic interaction and adsorption of copper metal ions.

#### ACKNOWLEDGEMENTS

The authors would like to thank the Malaysian Ministry of Higher Education (MoHE) for providing financial support through the Fundamental Research Grant Scheme (FRGS/1/2018/STG07/UNIKL/03/1).

#### REFERENCES

- [1] F. N. Muya, C. E. Sunday, P. Baker, and E. Iwuoha, "Environmental remediation of heavy metal ions from aqueous solution through hydrogel adsorption: A critical review," *Water Science and Technology*, vol. 73, no. 5, pp. 983–992, 2016.
- [2] M. S. Samuel, S. S. Shah, J. Bhattacharya, K. Subramaniam, and N. D. Pradeep Singh, "Adsorption of Pb(II) from aqueous solution using a magnetic chitosan/graphene oxide composite and its toxicity studies," *International Journal of Biological Macromolecules*, vol. 115, pp. 1142–1150, 2018.
- [3] X. Yi *et al.*, "Encapsulating Fe<sub>3</sub>O<sub>4</sub> into calcium alginate coated chitosan hydrochloride hydrogel beads for removal of Cu (II) and U (VI) from aqueous solutions," *Ecotoxicology and Environmental Safety*, vol. 147, pp. 699–707, 2018, doi: 10.1016/j.ecoenv.2017.09.036.
- [4] Z. Wu, W. Deng, W. Zhou, and J. Luo, "Novel magnetic polysaccharide/graphene oxide @Fe<sub>3</sub>O<sub>4</sub> gel beads for adsorbing heavy metal ions," *Carbohydrate Polymers*, vol. 216, no. January, pp. 119–128, 2019.
- [5] X. Luo, X. Lei, N. Cai, X. Xie, Y. Xue, and F. Yu, "Removal of heavy metal ions from water by magnetic cellulose-based beads with embedded chemically modified magnetite nanoparticles and activated carbon," *ACS Sustainable Chemistry and Engineering*, vol. 4, no. 7, pp. 3960–3969, 2016, doi: 10.1021/acssuschemeng.6b00790.
- [6] S. Thomas, K. Joseph, S. K. Malhotra, K. Goda, and M. S. Sreekala, *Polymer Composites*, Volume 3. Weinheim, Germany: Wiley-VCH, 2014.

- [7] I. O. P. C. Series and M. Science, "Effect of magnetite on alginate-based hydrogel beads composite bio-sorbent for copper removal Effect of magnetite on alginate-based hydrogel beads composite bio-sorbent for copper removal," 2021, doi: 10.1088/1757-899X/1195/1/012052.
- [8] H. Zhang, A. M. Omer, Z. Hu, L. Y. Yang, C. Ji, and X. kun Ouyang, "Fabrication of magnetic bentonite/carboxymethyl chitosan/sodium alginate hydrogel beads for Cu (II)adsorption," *International Journal of Biological Macromolecules*, vol. 135, pp. 490–500, 2019, [Online]. Available: <https://doi.org/10.1016/j.ijbiomac.2019.05.185>
- [9] X. Wang, S. Jiang, S. Cui, Y. Tang, Z. Pei, and H. Duan, "Magnetic-controlled aerogels from carboxylated cellulose and MnFe<sub>2</sub>O<sub>4</sub> as a novel adsorbent for removal of Cu(II)," *Cellulose*, vol. 26, no. 8, pp. 5051–5063, 2019, [Online]. Available: <https://doi.org/10.1007/s10570-019-02444-7>
- [10] Z. Yu, X. Zhang, and Y. Huang, "Magnetic chitosan-iron(III) hydrogel as a fast and reusable adsorbent for chromium(VI) removal," *Industrial and Engineering Chemistry Research*, vol. 52, no. 34, pp. 11956–11966, 2013, doi: 10.1021/ie400781n.
- [11] H. Zhang *et al.*, "Removal of methyl orange from aqueous solutions by adsorption on cellulose hydrogel assisted with Fe<sub>2</sub>O<sub>3</sub> nanoparticles," *Cellulose*, vol. 24, no. 2, pp. 903–914, 2017, doi: 10.1007/s10570-016-1129-1.
- [12] E. Joseph and G. Singhvi, *Multifunctional nanocrystals for cancer therapy: A potential nanocarrier*. Elsevier Inc., 2019. doi: 10.1016/B978-0-12-816505-8.00007-2.
- [13] A. M. Khalid *et al.*, "Isolation and characterization of magnetic oil palm empty fruits bunch cellulose nanofiber composite as a bio-sorbent for Cu(II) and Cr(VI) removal," *Polymers (Basel)*, vol. 13, no. 1, pp. 1–22, 2021.

## **POLYMER MATRIX MATERIAL SELECTION FOR SUSTAINABLE TWO-STROKE MARINE DIESEL ENGINE CROSSHEAD BEARING DESIGN USING TOPSIS METHOD**

R.V. Yiow<sup>1,2\*</sup>, M.R. Mansor<sup>1</sup>

<sup>1</sup>*Fakulti Kejuruteraan Mekanikal, Universiti Teknikal Malaysia Melaka, Hang Tuah Jaya, 76100 Durian Tunggal, Melaka, Malaysia.*

<sup>2</sup>*Marine Engineering Department, Akademi Laut Malaysia, Batu 30, Kampung Tanjung Dahan, 78200 Kuala Sungai Baru, Melaka, Malaysia*

---

### **ABSTRACT**

Present two-stroke marine diesel engine crosshead bearing designs are similar to conventional tin-based journal bearings. The potential of natural fibre composites (NFC) as bearing material lead to the ideation of a geometric design of the crosshead bearing. The study focused on the selection of the best polymer matrix using the Technique for Order of Preference by Similarity to Ideal Solution (TOPSIS) method. Simulation results were obtained for Maximum Stress (von Mises), Maximum Deformation and Weight. Using TOPSIS, the best polymer matrix was determined to be Polyhydroxybutyrate (PHB), garnering a Relative closeness to ideal solution score of 0.928. These results show the potential of using polymer as bearing material in highly rated marine diesel engines.

*Keywords:* two-stroke marine diesel engine, natural fibre composite, polymer.

---

### **INTRODUCTION**

The two-stroke marine diesel engine is commonly known as a crosshead type engine due to the presence of a crosshead assembly connecting the piston to the connecting rod via a piston rod. The crosshead assembly is responsible for taking up the side thrust due to the connecting rod angularity similar to that of the piston skirt in conventional trunk type engines. The crosshead bearing is similar to conventional journal bearings which are steel backed with tin alloyed overlays [1]. A visualization of the crosshead as part of the running gear in the engine and an exploded view are illustrated in Fig. 1.

With increased pressure from environmental policies globally, focus has begun to shift to more sustainable sources of material. Natural fibre composites (NFC) provides such an option and has been widely researched in various industries [2]. NFC consists of natural fibres, which often are plant based, bonded together by a polymer matrix, either natural or synthetic [3]. To consider the use of NFC as potential bearing material requires careful analysis of capabilities of the fibres and matrices in providing the necessary attributes to withstand loads of the engine.

Hence, a new geometrical design of the crosshead bearing was ideated to accommodate NFC as its main material. In this study, the selection of polymer matrices is of interest as the selection of natural fibres was performed in another research. The selection exercise of the best polymer matrix was done using the Technique for Order of Preference by Similarity to Ideal Solution (TOPSIS) method. Data necessary for the selection was obtained through simulation of the crosshead bearing design using the ANSYS software.

---

#### *Article history:*

Received: 10 March 2022

Accepted: 7 June 2022

Published: 14 June 2022

---

#### *E-mail addresses:*

yiowruvern@alam.edu.my (R.V.Yiow)

muhd.ridzuan@utem.edu.my (M.R.Mansor)

\*Corresponding Author

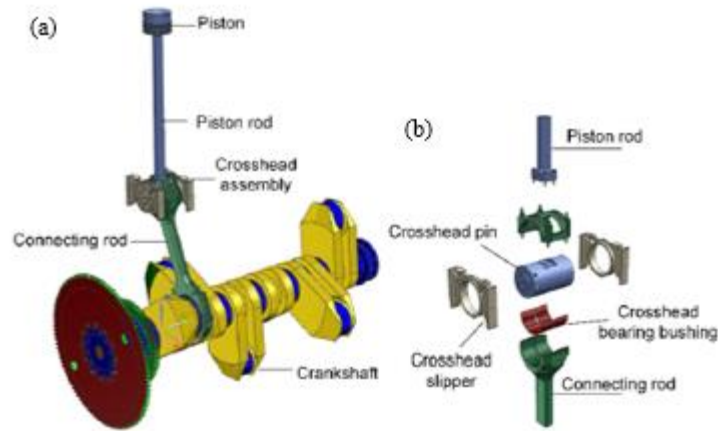


Fig.1: (a)Main running gear in a two-stroke marine diesel engine and (b) an exploded view of the crosshead assembly [4]

### MATERIAL SELECTION METHOD

The steps in selecting the best polymer matrix began with design ideation of the crosshead bearing, followed by the simulation setup. In the setup, the load on the bearing was applied at 1469 kg in the negative Y direction, similar to the combined weight of the piston and piston rod of a 60 cm bore engine [5]. Mechanical characteristics of the selected polymers, i.e., Young’s moduli (GPa), Density ( $\text{g/cm}^3$ ) and Tensile Strength (MPa), were keyed in as engineering data [6], [7]. The model was simulated with each polymer to obtain the Maximum Stress (von Mises) (MPa), Maximum Deformation (mm) and Weight (kg). The results of simulation were then given numerical weightage to rank their significance in the decision-making process. The values for the weightage were determined based on the author’s sea going experience while serving onboard crude oil tankers equipped with two-stroke marine diesel engines of similar bore size.

TABLE 1 shows the results with the respective weightage used in the TOPSIS method. For comparison, simulation values obtained for Structural Steel are also included.

TABLE 1: Simulation results for polymers and structural steel including the weightage allocated

Weightage	0.4	0.35	0.25
	Maximum Stress (von Mises) (MPa)	Maximum Deformation (mm)	Weight (kg)
Structural Steel	0.700	9.38E-05	4.882
TP	0.650	1.03E-02	0.746
PLA	0.634	2.60E-03	0.765
PLLA	0.634	2.72E-03	0.790
PHB	0.632	1.39E-03	0.759
PHBV	0.639	5.07E-03	0.771
PP	0.635	3.77E-03	0.641
HDPE	0.640	5.33E-03	0.591
LDPE	0.659	2.34E-02	0.571
PU	0.634	3.00E-03	0.734

Note: TP: Thermoplastic starch, PLA: Polylactic acid, PLLA: Poly-L-Lactic acid, PHB: Polyhydroxybutyrate, PHBV: Poly(3-hydroxybutyrate-co-3-hydroxyvalerate), PP: Polypropylene, HDPE: High-density polyethylene, LDPE: Low-density polyethylene, PU: Polyurethane

### RESULTS AND DISCUSSION

The selection of the best polymer matrix was performed using the simulation results (TABLE 1) of the crosshead bearing design. Previous research involving material selection showed the use of material data, such as the values of tensile strength and Young’s

modulus as criteria in the TOPSIS method. In the opinion of the authors, this particular step in material selection would prove more accurate as it utilizes results that are specific to the design of the crosshead bearing.

From the selection exercise using the TOPSIS method, the ranking of the polymer matrix was obtained as listed in TABLE 2. With a relative closeness to the ideal solution score of 0.928, Polyhydroxybutyrate (PHB) was determined to be the best polymer matrix to meet the requirements of the two-stroke marine diesel engine crosshead bearing based on the results of simulation. Polylactic acid (PLA) and Polyurethane (PU) make up the top three spots with values of 0.907 and 0.903, respectively.

TABLE 2: Overall ranking of polymer matrix material selection

	Positive ideal solution	Negative ideal solution	Relative closeness to the ideal solution	Rank
TP	0.116	0.168	0.591	8
PLA	0.027	0.266	0.907	2
PLLA	0.031	0.265	0.896	4
PHB	0.022	0.282	0.928	1
PHBV	0.053	0.235	0.817	7
PP	0.032	0.252	0.889	5
HDPE	0.051	0.233	0.821	6
LDPE	0.282	0.026	0.083	9
PU	0.028	0.261	0.903	3

## CONCLUSIONS

The material selection process showed the potential of polymer matrices in crosshead bearing technology. Results obtained showed favourable comparison with Structural Steel for Maximum Stress (von Mises) and Weight, however Maximum Deflection was much greater. This however should not be held as a deterrent, as polymer matrices are ‘bond’ for natural fibres in NFC. The capability of the polymer matrix is demonstrated here, giving the authors reason to further study the potential of NFC as bearing material in highly rated marine diesel engines.

## ACKNOWLEDGEMENT

The authors would like to thank Akademi Laut Malaysia (ALAM) and Universiti Teknikal Malaysia Melaka (UTeM) for the opportunity and support given throughout the duration of this study.

## REFERENCES

- [1] M. Lata arche, *Introduction*, 10th ed. Oxford: Elsevier Ltd., 2021.
- [2] E. Omrani, P. L. Menezes, and P. K. Rohatgi, “State of the art on tribological behavior of polymer matrix composites reinforced with natural fibers in the green materials world,” *Eng. Sci. Technol. an Int. J.*, vol. 19, no. 2, pp. 717–736, 2016, doi: 10.1016/j.jestch.2015.10.007.
- [3] Y. K. Kim, “Natural fibre composites (NFCs) for construction and automotive industries,” in *Handbook of Natural Fibres*, no. 2000, Woodhead Publishing Limited, 2012, pp. 254–279.
- [4] R. Li, X. Meng, J. Dong, and W. Li, “Transient tribo-dynamic analysis of crosshead slipper in low-speed marine diesel engines during engine startup,” *Friction*, vol. 9, no. 6, pp. 1504–1527, 2021, doi: 10.1007/s40544-020-0433-9.
- [5] “Volume II: Maintenance,” in *Electronic Instruction Manual for Engine Type: 6S60MC*, Kyungnam: HSD Engine Co., Ltd., 2003, p. Data 1(1).
- [6] G. Koronis, A. Silva, and M. Fontul, “Green composites: A review of adequate materials for automotive applications,” *Compos. Part B Eng.*, vol. 44, no. 1, pp. 120–127, 2013, doi: 10.1016/j.compositesb.2012.07.004.
- [7] M. T. Mastura, S. M. Sapuan, M. R. Mansor, and A. A. Nuraini, “Materials selection of thermoplastic matrices for ‘green’ natural fibre composites for automotive anti-roll bar with particular emphasis on the environment,” *Int. J. Precis. Eng. Manuf. - Green Technol.*, vol. 5, no. 1, pp. 111–119, 2018, doi: 10.1007/s40684-018-0012-y.

## **A COMPARATIVE REVIEW OF THE EFFECTS OF DIFFERENT FIBRE CONCENTRATIONS ON ARROWROOT FIBRE AND OTHER FIBRE-REINFORCED COMPOSITE FILMS**

J. Tarique<sup>1</sup>, S.M. Sapuan<sup>1,2,\*</sup>, E.S. Zainudin<sup>1,2</sup>, K.Z. Hazrati<sup>1,6</sup>, A. Khalina,<sup>2,3</sup>, R.A. Ilyas<sup>4,5</sup>, I. Aliyu<sup>1</sup>

<sup>1</sup>*Advanced Engineering Materials and composites Research Centre (AEMC), Department of Mechanical and Manufacturing Engineering, Universiti Putra Malaysia, 43400 UPM Serdang, Selangor, Malaysia*

<sup>2</sup>*Laboratory of Biocomposite Technology, Institute of Tropical Forest and Forest Products (INTROP), Universiti Putra Malaysia, 43400 UPM Serdang, Selangor, Malaysia*

<sup>3</sup>*Department of Biological and Agricultural Engineering, Universiti Putra Malaysia, 43400 UPM Serdang, Selangor, Malaysia*

<sup>4</sup>*School of Chemical and Energy Engineering, Faculty of Engineering, Universiti Teknologi Malaysia, 81310 UTM Johor Bahru, Johor, Malaysia*

<sup>5</sup>*Centre for Advanced Composite Materials (CACM), Universiti Teknologi Malaysia, 81310 UTM Johor Bahru, Johor, Malaysia*

<sup>6</sup>*German Malaysian Institute, Jalan Ilmiah, Taman Universiti, 43000, Kajang, Selangor, Malaysia*

---

### **ABSTRACT**

In recent years, there has been an increase in the development of composites reinforced with materials derived from renewable resources. Renewable resources are suitable materials for replacing synthetic compounds. The use of natural fibres as reinforcement during the production of starch-based composites is an effective method for improving the functional properties of composite films. This review has therefore been undertaken, focusing on more recent natural fibres-based composite films such as arrowroot fibre, *Dioscorea hispida*, corn husk, cassava bagasse, sugar palm, Nile rose, and kenaf fibre. The reinforcement of thermoplastic starch by different fibre concentrations improves the mechanical properties and promotes the suitability of starch-based composites as eco-friendly materials.

*Keywords:* natural fibre, arrowroot fibre, biopolymer composites, mechanical properties.

---

### **INTRODUCTION**

One of the most prominent materials used in the packaging industry, which has long been a source of concern for the global ecosystem, is polymers derived from fossil fuels. The substantial amount of environmentally hazardous plastic trash has motivated the research for polymers derived from natural sources that are renewable, sustainable, and biodegradable [1]. As a result, natural polymers are a viable option in the packaging sector for reducing the dependence on non-biodegradable and non-renewable resources [9].

Starch has attracted a lot of attention among the biopolymers being studied as potential alternative raw materials for plastics. Starch is appealing because it is biodegradable, renewable, affordable, and, for the most part, easily handled. Starch, on the other hand, has poor processability, dimension stability, and mechanical characteristics for its final products. As a result, native starch cannot be used as a packaging material. Arrowroot (*Maranta arundinacea*) tuber belongs to the *Marantaceae* family and is the source of a significant amount of starch, fiber, and carbohydrates [2]. Arrowroot starch is a locally produced native starch in Indonesia and Malaysia derived from arrowroot tubers with unique properties such as digestibility and gel-forming ability, as well as the highest amylose content (40.86%), competing with corn starch (28–33%), cassava starch (16–19%), wheat starch (30–32%), and potato (18–20%), which are all required for film production.

This review presents the recent developments of thermoplastics derived from starch and their potential in the industry. Starch modification is also highlighted, including blending with other naturally derived materials, which seem to further improve the mechanical and physical properties of the resulting biocomposite.

---

#### *Article history:*

Received: 10 March 2022

Accepted: 7 June 2022

Published: 14 June 2022

---

#### *E-mail addresses:*

sapuan@upm.edu.my (S.M. Sapuan)

\*Corresponding Author

TABLE 1: Comparison of properties of arrowroot-based composites films with other lignocellulosic fibers-based composites.

No.	Author	Starch	Fiber	Loading	Tensile strength	Water barrier	Thermal property
1.	Tarique et al. [3]	Arrowroot	Arrowroot fiber	2, 4, 6, 8, and 10 (wt.%)	<ul style="list-style-type: none"> <li>The tensile and tear strengths of TPAS/AF composites were increased significantly from 4.77 to 15.22 MPa and 0.87 to 1.28 MPa, respectively, as compared to the control TPAS films.</li> <li>While elongation was significantly decreased from 25.57 to 6.21%</li> </ul>	<ul style="list-style-type: none"> <li>The water contents of TPAS/AF films were significantly enhanced from (9.77 to 12.71%) by increasing fiber loadings from (2 to 10%).</li> <li>The TPAS/AF-10 demonstrated the lowest solubility of 22.56%, indicating that the films possessed good water stability.</li> </ul>	<ul style="list-style-type: none"> <li>An increase in arrowroot fiber concentration lowered the weight loss of biocomposites at temperatures above 300 °C, leading to an improvement in the thermal stability of biocomposites.</li> </ul>
2.	Ibrahim et al. [4]	Corn	Corn husk	2, 4, 6, 8 (wt.%)	<ul style="list-style-type: none"> <li>The higher concentration 8% revealed higher tensile strength and modulus of 12.84 Mpa and 639.62 MPa, respectively.</li> <li>2% concentration shows the lowest tensile and modulus.</li> </ul>	<ul style="list-style-type: none"> <li>The concentration of husk fiber of 8% indicates lower solubility in water (20.51%) and density (1.30 g/cm<sup>3</sup>). Contrary, 2% concentration high solubility and density of the composites.</li> </ul>	<ul style="list-style-type: none"> <li>The concentration of 6% shows high thermal stability and degradation started at 203.92 °C while 8% concentration at 197.93 °C.</li> </ul>
3.	Edhirej et al. [5]	Cassava	Cassava bagasse	3, 6, and 9% w/w dry starch	<ul style="list-style-type: none"> <li>A significant increase in tensile strength of the cassava starch-based films was observed with an increase in fibre content from 3 % to 6 % but there was a reduction at 9 % loading.</li> <li>It can be seen that the highest tensile stress (10.78 MPa) observed for 6% which was greater than the control film (4.7 MPa).</li> <li>The stiffness of film determined by elastic modulus.</li> <li>The addition of 3 and 6 % fibre (bagasse) resulted in increasing tensile stress and young's modulus.</li> <li>However, increasing bagasse content from 6 % to 9 % resulted</li> </ul>	<ul style="list-style-type: none"> <li>The moisture content of cassava composites were about 10.97 to 12.23 %, which were greater than the moisture content of the control film (10.96%).</li> <li>A significant decrease in the moisture content and solubility in the water of films was observed when the concentrations of bagasse fiber were amplified from 3 to 9 % (w/w).</li> </ul>	<ul style="list-style-type: none"> <li>Variances in mass residue for films containing bagasse fiber ranged from 24.41 to 32.07 % as increased concentration from 3 to 9%.</li> <li>Therefore, high thermal stability occurred on low fiber concentration.</li> </ul>

					in films with lower tensile stress and young's modulus. Decrease		
3.	M.M. Ibrahim et al. [6]	Corn starch	Nile rose fiber	0, 20, 40, 60, and 80 (wt.%)	<ul style="list-style-type: none"> <li>The higher tensile strength (18 Mpa) and maximum elongation at break (15.90 %) of NRF/starch biocomposites observed at 60% and 20% concentration, respectively.</li> <li>Contrarily, the elongation at break decreased because of the capacity of NRF blocking the stretching of the polymer chain.</li> </ul>	<ul style="list-style-type: none"> <li>Water uptake was increased with increasing fiber content.</li> <li>This phenomenon was ascribed with NRF in composite, the explanation for this phenomenon may be due to the nature of Nile roses as an aquatic plant.</li> </ul>	-
4.	Travalini et al. [7]	Cassava starch	Cassava bagasse (Lignocellulose nanofibers)	0.65, and 1.3% w/w	<ul style="list-style-type: none"> <li>An increase in tensile stress for all films was observed compared with the cassava starch sample (4.8 MPa), with the highest value for LCNF 1.3 sample (6.6 MPa) (37.5% improvement).</li> <li>It is indicating good intermolecular interaction between cassava starch and LCNF.</li> </ul>	<ul style="list-style-type: none"> <li>A reduction in water vapour permeability values was observed with LCNF and Nclay addition, at both 0.65 and 1.3 % levels, respectively.</li> <li>The reduction in permeability is strongly associated with a decrease in diffusion coefficient imposed by the presence of nanoparticles</li> </ul>	<ul style="list-style-type: none"> <li>The onset temperature of LCNF at 0.65% was higher than at 1.3%.</li> <li>The mass residue at 400 °C was 9.1 % and 11.3% for 0.65 and 1.3% respectively.</li> </ul>
5.	Babae et al. [8]	Kenaf bast fiber	Corn starch	10 wt.%	<ul style="list-style-type: none"> <li>The tensile properties showed that an increased modulus and strength of both nanocomposites with 10 wt.% nanofibers compared to the pure TPS.</li> <li>The Young's modulus and tensile strength increased from 16.6 and 8.6MPa to 141 and 38 MPa for the CNFs/TPS, respectively</li> </ul>	<ul style="list-style-type: none"> <li>The water uptake of the obtained composites reinforced with 10 wt.% of fiber and ACNFs was significantly reduced compared to the neat TPS.</li> <li>The WVP of composite films show a lower value than control thermoplastic.</li> <li>The addition of the CNFs to the polymer matrix presumably leads to denser and less porous materials.</li> </ul>	<ul style="list-style-type: none"> <li>The used nanofibers restricted the movement of the molecular chain of the TPS, thereby improving its thermal stability.</li> </ul>



## CONCLUSIONS

This paper compares biopolymers and the potential of starch-derived thermoplastics as replacements for present petroleum-based plastics. Blending starch with other biopolymers was suggested as a promising solution to solve native starch's limitations. However, the degree of compatibility between starch and other biopolymers varies greatly depending on the specific biopolymer. Concerning the worldwide environmental issue, biodegradable material properties are critical and should be taken into account. Although starch/biodegradable blends are an effective solution for environmental problems, their mechanical qualities frequently have an inverse relationship with their degradability. Another option is to use natural fibers as fillers in the starch matrix. As a result, optimizing their mechanical qualities necessitates additional research.

## ACKNOWLEDGEMENTS

Authors gratefully acknowledge Universiti Putra Malaysia for their financial support for this project through Geran Putra Berimpak (GPB) project number UPM.RMC.800-3/3/1/GPB/2020/9694500.

## REFERENCES

- [1] J. Tarique, S.M. Sapuan, A. Khalina, R.A. Ilyas, E.S. Zainudin, Thermal, flammability, and antimicrobial properties of arrowroot (*Maranta arundinacea*) fiber reinforced arrowroot starch biopolymer composites for food packaging applications, *Int. J. Biol. Macromol.* 213 (2022) 1–10. <https://doi.org/10.1016/j.ijbiomac.2022.05.104>.
- [2] J. Tarique, S.M. Sapuan, A. Khalina, S.F.K. Sherwani, J. Yusuf, R.A. Ilyas, Recent developments in sustainable arrowroot (*Maranta arundinacea* Linn) starch biopolymers, fibres, biopolymer composites and their potential industrial applications: A review, *J. Mater. Res. Technol.* 13 (2021) 1191–1219. <https://doi.org/10.1016/j.jmrt.2021.05.047>.
- [3] J. Tarique, E.S. Zainudin, S.M. Sapuan, R.A. Ilyas, A. Khalina, Physical, Mechanical, and Morphological Performances of Arrowroot (*Maranta arundinacea*) Fiber Reinforced Arrowroot Starch Biopolymer Composites, *Polymers (Basel)*. 14 (2022) 388. <https://doi.org/10.3390/polym14030388>.
- [4] M.I.J. Ibrahim, S.M. Sapuan, E.S. Zainudin, M.Y.M. Zuhri, Potential of using multiscale corn husk fiber as reinforcing filler in cornstarch-based biocomposites, *Int. J. Biol. Macromol.* 139 (2019) 596–604. <https://doi.org/10.1016/j.ijbiomac.2019.08.015>.
- [5] A. Edhirej, S.M. Sapuan, M. Jawaid, N.I. Zahari, Preparation and characterization of cassava bagasse reinforced thermoplastic cassava starch, *Fibers Polym.* 18 (2017) 162–171. <https://doi.org/10.1007/s12221-017-6251-7>.
- [6] M.M. Ibrahim, H. Moustafa, E.N.A. El Rahman, S. Mehanny, M.H. Hemida, E. El-Kashif, Reinforcement of starch based biodegradable composite using Nile rose residues, *J. Mater. Res. Technol.* 9 (2020) 6160–6171. <https://doi.org/10.1016/j.jmrt.2020.04.018>.
- [7] A.P. Travalini, B. Lamsal, W.L.E. Magalhães, I.M. Demiate, Cassava starch films reinforced with lignocellulose nanofibers from cassava bagasse, *Int. J. Biol. Macromol.* 139 (2019) 1151–1161. <https://doi.org/10.1016/j.ijbiomac.2019.08.115>.
- [8] M. Babae, M. Jonoobi, Y. Hamzeh, A. Ashori, Biodegradability and mechanical properties of reinforced starch nanocomposites using cellulose nanofibers, *Carbohydr. Polym.* 132 (2015) 1–8. <https://doi.org/10.1016/j.carbpol.2015.06.043>.
- [9] A. S. Norfarhana, R. A. Ilyas, and N. Ngadi, “A review of nanocellulose adsorptive membrane as multifunctional wastewater treatment,” *Carbohydr. Polym.*, vol. 291, p. 119563, Sep. 2022, doi: 10.1016/j.carbpol.2022.119563.

## **GREEN FIBRES AS SUSTAINABLE AND RENEWABLE RESOURCE FOR DEVELOPMENT OF BIONANOCOMPOSITE: A REVIEW**

R.M.O. Syafiq<sup>1</sup>, S.M. Sapuan<sup>1,2\*</sup>, M.Y.M. Zuhri<sup>1,2</sup>, S.H. Othman<sup>3</sup>, R.A. Ilyas<sup>4,5</sup>, K.Z. Hazrati<sup>2,6</sup>, A. Nazrin<sup>1</sup>, S.F.K. Sherwani<sup>2</sup>, J. Tarique<sup>2</sup>, M.M. Harussani<sup>2</sup>, M.D. Hazrol<sup>2</sup>

<sup>1</sup>Laboratory of Biocomposite Technology, Institute of Tropical Forestry and Forest Products (INTROP), Universiti Putra Malaysia, 43400 UPM Serdang, Selangor, Malaysia

<sup>2</sup>Advanced Engineering Materials and Composites Research Centre (AEMC), Department of Mechanical and Manufacturing Engineering, Universiti Putra Malaysia, 43400 UPM Serdang, Selangor, Malaysia

<sup>3</sup>Department of Process and Food Engineering, Universiti Putra Malaysia, 43400 UPM Serdang, Selangor, Malaysia

<sup>4</sup>School of Chemical and Energy Engineering, Faculty of Engineering, Universiti Teknologi Malaysia, 81310 Johor Bahru, Johor, Malaysia

<sup>5</sup>Center of Advanced Centre for Advanced Composite Materials (CACM), Universiti Teknologi Malaysia, 81310 Johor Bahru, Malaysia

<sup>6</sup>German Malaysian Institute, Jalan Ilmiah, Taman Universiti, 43000, Kajang, Selangor, Malaysia

---

### **ABSTRACT**

As people become more aware of the environmental damage caused by synthetic materials, green fibre bionanocomposite materials are being developed. Researchers have expressed a strong interest in creating materials that can replace synthetic materials. There has been a growth in demand for green fibres-bionanocomposite for commercial usage in many industrial sectors in recent years. The sustainability of green fibres-bionanocomposite materials has led to an increase in their use in a variety of industries. Green fibres have a wide range of applications, including their usage as reinforcement in polymer composite materials. The green fibres are introduced instead of synthetic fibres to make the composites lighter. In this paper, the diverse green fibres sources, their qualities, green fibres modification, and the effects of treatments on green fibres, among other things had been reviewed.

*Keywords:* fibre, bionanocomposite, renewable resource.

---

### **INTRODUCTION**

All green nanocomposites are low-cost materials. These low-cost green composites were found to have mechanical strength and properties suitable for applications in housing construction materials, furniture and automotive parts. Studies carried out in the past decades have demonstrated that green composites materials should combine high mechanical and other essential operational and technological properties (e.g. stability, low gas permeability, environmental safety, easy moulding) with biodegradability [1], [2]. In order to be competitive, eco-friendly composites must have the same desirable properties as obtained in conventional plastics [3], [4]. The most important factors to the formation of a successful green composites material industry include cost reduction as well as public and political acceptance. Existing green and environmental friendly composites materials are mainly blended with different materials with an aim to reduce cost and to tailor the product for some specific applications.

### **DIVERSE GREEN FIBRES SOURCES AND THEIR APPLICATIONS IN BIONANOCOMPOSITE**

Application of green composites in natural fibre-reinforced composites will broaden their uses. The demand for green and renewable materials continues to rise. Polymeric composites from renewable resources have occupied major applications in green packaging. Although these are emerging as alternatives to existing petroleum derived plastics; the present low level production and high costs restrict their widespread applications. The barrier properties of such degradable polymers can be improved through nano reinforcements [5]. The incorporation of nanoparticles in a polymer matrix reduces the permeability of penetrant molecules and thus develops high barrier composites [6]. Nanocomposites especially green nanocomposites or nanocomposites obtained from renewable resources are an emerging new class of materials, total environmental/economic impacts of which need to be studied to prove the industrial and environmental potential of targeted nanocomposites for automotive applications [7]. The bionanocomposites can be defined as the materials that comprise of particles with at least one dimension in the range of 1–100 nm and a constituent(s) of the biological origin or may be biopolymers [8, 9]. One of the major differences between bionanocomposites and biocomposites is that the latter may be constituted of biopolymers, but they

do not have the nanosized additives as seen in Fig.. 1. The need of green and biodegradable plastics has been increased during the past decades not only due to the increasing environmental concerns but also for its biomedical applications. It is now well evident that polymer/plastics waste management through biodegradation or bio-conversion is the most suitable solution for 'Plastic Waste Management' among the other traditional methods like incineration, pyrolysis and landfilling. Several means have been used to achieve the biodegradability in polymers

---

*Article history:*

Received: 10 March 2022

Accepted: 7 June 2022

Published: 14 June 2022

---

*E-mail addresses:*

sapuan@upm.edu.my (S.M. Sapuan)

\*Corresponding Author

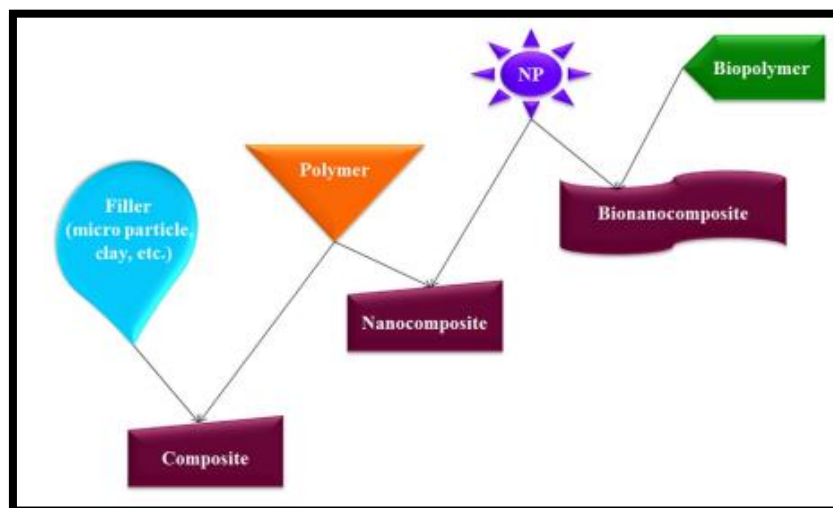


Fig. 1: Comparison of composite, nanocomposite and bionanocomposite [8]

## CONCLUSION

As a result of environmental awareness and the international demand for green technology, green composites have the potential to replace present petro chemical-based materials. They represent an important element of future waste disposal strategies. In true green nanocomposites, both the reinforcing material (such as a natural fibre) and the matrix are biodegradable. Cellulose, chitin and starch are the most abundant organic compounds in nature: they are also green, inexpensive, biodegradable and renewable. They obviously receive a great attention for non-food applications. The use of natural fibres instead of traditional reinforcement materials, such as glass fibres, carbon and tale, provides several advantages including low density, low cost, good specific mechanical properties, reduced tool wear and biodegradability. Important applications include packaging, wide-ranging uses from environmentally friendly biodegradable composites to biomedical composites for drug gene delivery, tissue engineering applications and cosmetic orthodontics. They often mimic the structures of the living materials involved in the process in addition to the strengthening properties of the matrix that was used but still providing green and biocompatibility, e.g., in creating scaffolds in bone tissue engineering. Bionanocomposites combine plant and animal nanofibres (derived from waste and biomass) with resins and other polymers, such as plastics and rubbers, to create natural-based composite materials. A variety of plant fibres with high tensile strength can be used including kenaf, industrial hemp, flax, jute, sisal, coir, etc. Green fibres can be combined with traditional resins or newer plant based resins. The result is a plant-based alternative for many traditional steel and fibreglass applications. Advantages of green nanocomposites over traditional composites are reduced weight, increased flexibility, greater mould ability, reduced cost, better sound insulation and their renewable nature.

## ACKNOWLEDGEMENT

The authors would like to thank Universiti Putra Malaysia for the financial support through Inisiatif Pemerkasaan Penerbitan Jurnal Tahun 2020 (Vot number: 9044033), Ministry of Higher Education Malaysia Grant scheme HICoE (6369107), Fundamental Research Grant Scheme (FRGS): FRGS/1/2017/TK05/UPM/01/1 (5540048) and Special Graduate Research Assistantship (SGRA) Geran Putra Berimpak (GPB), UPM/800-3/3/1/GPB/2019/9679800. Grant Inisiatif Putra Siswazah GP-IPS/2021/9697100.

## REFERENCES

- [1] R. Syafiq, S. M. Sapuan, and M. R. M. Zuhri, "Antimicrobial activity, physical, mechanical and barrier properties of sugar palm based nanocellulose/starch biocomposite films incorporated with cinnamon essential oil," *J. Mater. Res. Technol.*, vol. 11, pp. 144–157, Mar. 2021, doi: 10.1016/j.jmrt.2020.12.091.
- [2] L. Cao, W. Liu, and L. Wang, "Developing a green and edible film from Cassia gum: The effects of glycerol and sorbitol," *J. Clean. Prod.*, vol. 175, pp. 276–282, 2018, doi: 10.1016/j.jclepro.2017.12.064.
- [3] R. M. O. Syafiq, S. M. Sapuan, and M. R. M. Zuhri, "Effect of cinnamon essential oil on morphological, flammability and thermal properties of nanocellulose fibre-reinforced starch biopolymer composites," *Nanotechnol. Rev.*, vol. 9, no. 1, pp. 1147–1159, Nov. 2020, doi: 10.1515/ntrev-2020-0087.
- [4] S. Ketkaew et al., "Effect of Oregano Essential Oil Content on Properties of Green Biocomposites Based on Cassava Starch and Sugarcane Bagasse for Bioactive Packaging," *J. Polym. Environ.*, vol. 26, no. 1, pp. 311–318, 2018, doi: 10.1007/s10924-017-0957-x.
- [5] L. Thompson, J. Azadmanjiri, M. Nikzad, I. Sbarski, J. Wang, and A. Yu, "Cellulose nanocrystals: Production, functionalization and advanced applications," *Rev. Adv. Mater. Sci.*, vol. 58, no. 1, pp. 1–16, 2019, doi: 10.1515/rams-2019-0001.
- [6] R. Syafiq et al., "Antimicrobial activities of starch-based biopolymers and biocomposites incorporated with plant essential oils: A review," *Polymers (Basel)*, vol. 12, no. 10, pp. 1–26, 2020, doi: 10.3390/polym12102403.
- [7] S. P. Bangar and W. S. Whiteside, "Nano-cellulose reinforced starch bio composite films- A review on green composites," *Int. J. Biol. Macromol.*, vol. 185, no. July, pp. 849–860, 2021, doi: 10.1016/j.ijbiomac.2021.07.017.

***The International Symposium on Polymeric Materials 2022***

- [8] B. Arora, R. Bhatia, and P. Attri, *Bionanocomposites: Green materials for a sustainable future*. Elsevier Inc., 2018. doi: 10.1016/B978-0-12-811033-1.00027-5.
- [9] A. S. Norfarhana, R. A. Ilyas, and N. Ngadi, "A review of nanocellulose adsorptive membrane as multifunctional wastewater treatment," *Carbohydr. Polym.*, vol. 291, p. 119563, Sep. 2022, doi: 10.1016/j.carbpol.2022.119563.

## **ELECTROMAGNETIC WAVE REDUCTION OF MULTIWALLED CARBON NANOTUBES MIXED NANOMETER CoFe<sub>2</sub>O<sub>4</sub> AT HIGHER FREQUENCY RANGE**

F. M. Idris<sup>1\*</sup>, H. Kaco<sup>1</sup>, S. M. Mohd<sup>1</sup>, N. M. Jan<sup>1</sup>, M. S. E. Shafie, F. Esa<sup>2</sup>, Z. M. Idris<sup>3</sup>

<sup>1</sup>Kolej GENIUS Insan, Universiti Sains Islam Malaysia, Bandar Baru Nilai, 71800 Nilai, Negeri Sembilan, Malaysia

<sup>2</sup>Faculty of Sciences, Technology and Human Development, Universiti Tun Hussein Onn Malaysia, 86400 Batu Pahat, Malaysia

<sup>3</sup>IPG Kampus Pendidikan Teknik, Kompleks Pendidikan Nilai, Bandar Enstek, 71760 Nilai, Negeri Sembilan

---

### **ABSTRACT**

Traditional granular electromagnetic wave absorbers such as spinel ferrites are well known because of its high saturation magnetization and electrical resistivity. However, ferrite absorbent has a higher density and low environmental stability, limiting their use as an electromagnetic wave absorber. Thus, multiwalled carbon nanotubes (MWCNTs) were introduced to enhance the electromagnetic wave absorbing performances. Different weight percentages of MWCNTs were mixed with nanometer-size CoFe<sub>2</sub>O<sub>4</sub> and being used as fillers and further incorporated into epoxy resin as polymer matrix. The reflectivity and morphological study of the prepared samples were studied in the frequency range of 8 – 18 GHz. The results reveal that varying the amount of MWCNT content has influence the performance of the processed electromagnetic wave absorber. For thicknesses of 1 mm, 2 mm and 3 mm, the reflection loss peak shifted towards lower frequency as the amount of MWCNTs increased. The highest reflection loss was achieved at 9 GHz when the MWCNTs content was 2 wt% for a thickness of 3 mm, with the reflection loss of -28 dB.

*Keywords:* reflection loss, MWCNTs, cobalt ferrite, nanometer, electromagnetic wave absorber.

---

### **INTRODUCTION**

The development of new materials for various application with tight requirements in microwave reflection suppression is directly related to the production of electromagnetic wave absorbing material (EAM). The rapid development of electronic and telecommunication systems has resulted in an increase in electromagnetic pollution, which is known as electromagnetic interference (EMI) [1,2], prompting a greater number of investigations utilizing electromagnetic wave absorbing material technologies. To treat electromagnetic wave absorbing materials, numerous criteria must be considered. Weight, thickness, microwave absorption, environmental resistance, and mechanical strength are all important parameter that need to be taken into considerations [3,4]. An electromagnetic wave absorber's dielectric and/or magnetic losses cause microwave energy to be attenuated. The electric (E) field is affected by dielectric loss, which is found in the imaginary component of the complex permittivity. On the other hand, magnetic loss is found in the imaginary component of the permeability and acts on the magnetic (H) field.

Thus, this research focused on the effect of incorporating magnetic (Cobalt-Ferrite, CoFe<sub>2</sub>O<sub>4</sub>) and dielectric material (multiwalled carbon nanotubes, MWCNTs) into polymer matrix at different weight percentages of MWCNTs on magnetic property and electromagnetic wave absorbing property of the composites.

### **MATERIALS AND METHODS**

#### *Synthesis of CoFe<sub>2</sub>O<sub>4</sub> nanoparticles*

Cobalt ferrite (CoFe<sub>2</sub>O<sub>4</sub>) was prepared by using a mechanical alloying technique with starting raw materials from Alfa Aesar, which included Cobalt Oxide (Co<sub>3</sub>O<sub>4</sub>) 99.8% and Iron (III) Oxide (Fe<sub>2</sub>O<sub>3</sub>) 99.5%. The Cobalt Ferrite (CoFe<sub>2</sub>O<sub>4</sub>) phase was then formed by sintering it at 900°C for 10 hours at a rate of 4°C/min by using open tube furnace.

#### *Incorporation of fillers into polymer matrix*

The total weight percentages (wt%) of synthesized CoFe<sub>2</sub>O<sub>4</sub> sample mixed with commercial multiwalled carbon nanotubes (MWCNTs) were fixed at 60 wt%. On the other hand, the amount of epoxy resin as polymer matrix was fixed at 40 wt%. The polymer composite samples were made by mixing varying amounts of MWCNTs (0.5, 2, and 4 wt%) with cobalt ferrite and dispersing them in an epoxy resin matrix. The mixtures were then dispersed and uniformly mixed for 20 minutes using a high-speed mixer set to 3000 rpm. After that, the prepared samples were poured into sample holders of varying dimensions (for X-band and Ku-band) and thicknesses of 1mm, 2mm, and 3mm. Finally, the polymer composite samples were left overnight to cure at room temperature.

---

#### *Article history:*

Received: 10 March 2022

Accepted: 7 June 2022

Published: 14 June 2022

---

#### *E-mail addresses:*

fadzidahmohdidris@usim.edu.my (F.M. Idris)

\*Corresponding Author

#### *Materials' Characterization*

An X-Pert PANalytical diffractometer (PW3050/60) was used to investigate the phase analysis from X-ray diffraction (XRD) spectra in the 2θ range 20° to 70°. The cross-section surface morphology was determined from Field Emission Scanning Electron Microscope (FeSEM) micrographs

collected, while the initial diameter size of carbon nanotubes was evaluated using a Transmission Electron Microscope (TEM). Energy Dispersive X-ray (EDX) was used to study the elemental analysis. The magnetic properties of the material were determined at room temperature using a Vibrating Sample Magnetometer (VSM).

The electromagnetic parameters and absorption properties of the composites were investigated using a Vector Network Analyzer (VNA) in the frequency range of 8 to 18 GHz.

## RESULTS AND DISCUSSION

Fig. 1 shows the reflection loss of 60wt%  $\text{CoFe}_2\text{O}_4$ , 0.5wt%, 2wt% and 4wt% MWCNTs mixed with  $\text{CoFe}_2\text{O}_4$  and being incorporated into epoxy matrix.

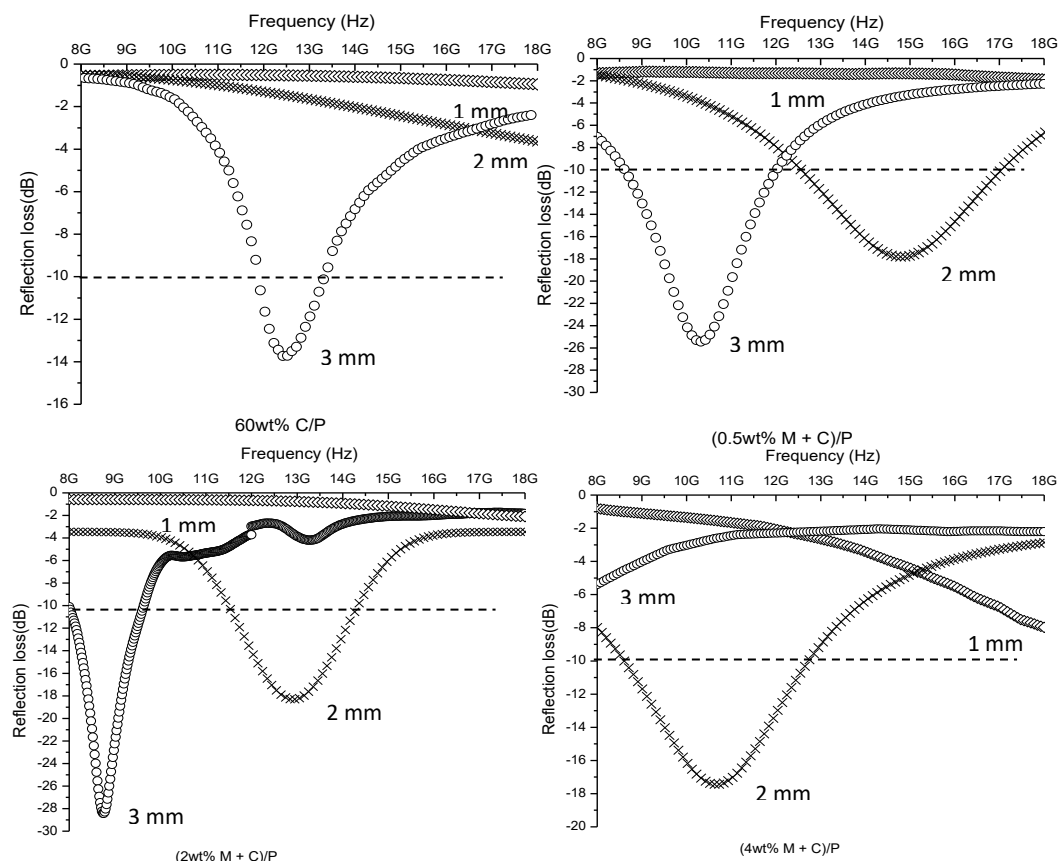


Fig. 1: Reflection loss of 60wt%  $\text{CoFe}_2\text{O}_4$ , 0.5wt%, 2wt% and 4wt% MWCNTs mixed with  $\text{CoFe}_2\text{O}_4$  and being incorporated into epoxy matrix.

The reflection loss (RL) for 60wt%  $\text{CoFe}_2\text{O}_4/\text{P}$  obtained for thickness 3 mm was -14 dB at frequency 12.5 GHz. As for composite samples with thickness of 1 mm, 2 mm, 3 mm, the addition of 0.5 wt%, 2 wt% and 4 wt% of MWCNTs shows that the resonance peaks shift towards lower frequency range. Adding MWCNTs into cobalt ferrite may reduce the working frequency range of the composite sample so that it can be used for lower frequency devices. The minimum RL shown by 0.5 wt% MWCNTs-  $\text{CoFe}_2\text{O}_4/\text{P}$  was -18 dB (14.7 GHz) and -25 dB (10.5 GHz) for thickness 2 mm and 3 mm respectively. As for 2 wt% MWCNTs-  $\text{CoFe}_2\text{O}_4/\text{P}$ , the RL was -18 dB (13 GHz) and -28 dB (9 GHz) for thickness 2 mm and 3 mm respectively. Reflection loss of -17 dB (10.5 GHz) for thickness 2 mm was given by sample with 4 wt% addition of MWCNTs.

## CONCLUSIONS

In conclusion, 3-dimensional network with varied weight percentages of MWCNTs mixed with  $\text{CoFe}_2\text{O}_4$  were synthesized and uniformly mixed and dispersed in the epoxy matrix. It demonstrates that adding just 0.5 wt% MWCNT to the mixture, improves the electromagnetic wave absorption ability. The dielectric loss contributed to the electromagnetic wave absorption of pure MWCNTs, while the influence of magnetic loss, such as eddy current and other magnetic losses, becomes dominant over the dielectric loss for pure  $\text{CoFe}_2\text{O}_4$  particles. This research indicates that adding magnetic (Cobalt-Ferrite) and dielectric (MWCNTs) materials into polymer matrix can improve the composites' electromagnetic wave absorption properties. The correlation of the data demonstrates that the number of MWCNTs introduced influences the performance of the processed electromagnetic wave absorber. As the number of MWCNTs increased, the reflection loss peak shifted to a lower frequency range. As a result, it can be demonstrated that the working frequency can be tuned simply by adding MWCNTs according to the application requirements for a specific frequency range. With a MWCNTs content of 2 wt% and a thickness of 3 mm, a reflection loss of -28 dB at 9 GHz was attained. However, a sample with a thickness of 2 mm for 0.5 wt% MWCNTs- $\text{CoFe}_2\text{O}_4/\text{P}$

## ***The International Symposium on Polymeric Materials 2022***

provided a broader bandwidth of 4.5 GHz, correspond to a reflection loss of less than -10 dB (90% absorption). Our research suggests that the samples could be used as an electromagnetic wave absorber in various applications.

### **ACKNOWLEDGEMENTS**

The research was supported by Ministry of Education Malaysia through Fundamental Research Grant Scheme (FRGS/1/2020/STG05/USIM/02/3) (USIM/FRGS/KGI/KPT/52020). The authors also express deepest gratitude and pleasure towards Institute of Nanoscience and Nanotechnology (ION2, UPM) and Kolej GENIUS Insan for providing the apparatus and equipment used in the laboratory.

### **REFERENCES**

- [1] N. Yusoff, M. H. Abdullah, A. A. Mansor, S. A. A. Hamid. "Electromagnetic and absorption properties of some microwave absorbers". *Journal of Applied Physics*, vol. 92(2), pp. 876-880, 2002, <https://doi.org/10.1063/1.1489092>
- [2] S. M. Lee. *International Encyclopedia of Composites*. New York: VHC Publishers, 1991.
- [3] J. H. Oh, K. S. Oh, C. G. Kim, C. S. Hong. "Design radar absorbing structures using glass/epoxy composite containing carbon black in the X frequency ranges". *Composites Part B: Engineering*, vol. 35 (1), pp. 49-56, 2004.
- [4] Y. M. M. Antar, H. W. Liu. "Effect of radar absorbing materials on RCS of partially coated targets". *Microwave and Optical Technology Letters*, vol. 17(5), pp. 281-284, 1998.

## APPLICATIONS OF NANOCELLULOSE AND ITS COMPOSITES IN BIO PACKAGING-BASED STARCH

M. Mahardika<sup>1\*</sup>, D. Amelia<sup>2</sup>, Azril<sup>3</sup>, E. Syafri<sup>4\*</sup>

<sup>1</sup>Research Center for Biomass and Bioproducts, National Research and Innovation Agency (BRIN), Bogor 16911, Indonesia

<sup>2</sup>Department of Chemical Engineering, Universitas Indonesia, Depok 16424, Indonesia

<sup>3</sup>Department of Biomedical Engineering National Cheng Kung University, Republic of China

<sup>4</sup>Department of Agricultural Technology, Politeknik Pertanian Negeri Payakumbuh, West Sumatra 26271, Indonesia

---

### ABSTRACT

This mini-review discusses existing technology and future issues in applying nanocellulose as a starch-based packaging of food material. Biopolymers, mainly starch as packaging materials, are increasingly replacing petroleum plastics. This mini-review encompasses applying the commonly used nanocellulose starch-based bio packaging material, focusing on production processes, properties, and analysis of potential uses in starch-based bio packaging. The use of nanocellulose as an alternative material for starch-based bio packaging substitutes conventional polymers for food packaging and its entirely new properties and characterization. Microorganisms can produce cellulose biopolymers through the fermentation process of various biological resources (e.g., bacterial cellulose). Biomass can be produced directly from various plants (pineapple, water hyacinth, and others). Researchers are currently focused on reducing the problem of pollution due to conventional plastics produced from fossil fuels.

*Keywords:* bio packaging, biopolymer, nanocellulose, starch.

---

### INTRODUCTION

Conventional plastic polymers produced from fossil fuels have been used for food packaging. Plastic is utilized to assure the safety and integrity of packaged food items, from production, handling, and storage to final usage by consumers. In particular, plastics play an essential role in avoiding rapid deterioration in product safety and quality, which influences the overall usage of packaged foods during their lifespan and ultimately avoids product spoilage losses. The interconnections among food, packaging materials, and environmental conditions focus on food packaging. Conventional plastics as food packaging materials have caused environmental pollution on land and sea, showing synthetic plastic pollution. Therefore, using environmentally friendly materials such as starch-based bio packaging with nanocellulose filler is an alternative solution to replace synthetic plastic.

Starch is the most widely used renewable raw material for bio packaging. Starch consists of glucose, amylose and amylopectin. Its chemical and physical characteristics are unique compared to all other carbohydrates. Sources of starch are obtained from whole grains, legumes, cereals, potatoes and fruits [1]. Starch polymers are susceptible to moisture, with high water vapour permeability and poor mechanical properties limiting the application of bio packaging. Several previous studies using starch as bio packaging are yam starch [2], cassava starch [3], sugar palm starch [4], corn starch [5], tapioca starch [6], sago starch [7], rice starch [8], and potato starch [9]. Starch derivatives are the most interesting and used in the food sector because they can be combined with various fillers, types and amounts of plasticizers used during starch-based bio packaging. To obtain superior properties that determine the final product's physical, chemical, and thermal properties. Its main utilization in the food sector is inflexible and solid packaging (bio-film, packaging, bio-coating, lamination, and others). The properties of starch-based bio packaging generated are biodegradable and it has good properties as a barrier to oxygen, moisture, and amylose content is a strong restrictive factor, related to the mechanical qualities of the starch film [10]. In many cases, to modify the properties of starch-based films, fillers or reinforcing agents have been added to the starch-polymer matrix, such as microcrystalline cellulose (MC), fiber, nano-clay, carboxymethylcellulose (CMC), carbon nanotubes, and nanocellulose [11]. Of several cellulose derivatives that have been produced commercially, such as cellulose acetate, it is widely used for food packaging (baked foods and fresh products) [12]. The properties of cellulose acetate are low resistance to gas and moisture and use the plasticization process when used for film development. Several previous studies using cellulose in food packaging based on yam starch films with nanocellulose from pineapple leaves [2], cassava starch with oil palm mesocarp cellulose nanowhiskers [13], bacterial cellulose nanofibers/starch/chitosan for a food packaging alternative [14], and potato starch/cellulose for sustainable packaging [9]. The film-forming properties have many cellulose derivatives, so the cost is too high for wider industrial use. In order to produce lower-cost cellulose packaging materials, processing technology for the production of cellulose derivatives is required. Nano-cellulose fiber reinforced with starch through film casting technique

processing has resulted in very successful bio packaging [15]. In this way, bio packaging improves its mechanical properties. In addition to this combination, starch mixed chitosan in the amount of 30% significantly increased the mechanical properties of the bio packaging by 97.8% [15]. Various types of starch reinforced with nanocellulose have been used in packaging applications for bread, vegetables and meat products stored under standard conditions [16].

---

*Article history:*

Received:

Accepted:

---

*E-mail addresses:*

edisyafril1@gmail.com (E. Syafri)



Bio packaging made of tapioca starch with bacterial cellulose nanofibers and filler chitosan as reinforcement has excellent mechanical properties, processability, water and gas vapour resistance and thermal resistance [14]. Fully biodegradable polymers are not recyclable from currently applied technology used in recycling conventional petroleum-based polymers. Starch-based biopolymer with nanocellulose filler can be used for wrapping food products. In this way, non-biodegradable plastic materials will no longer be needed. Biopolymers provide attractive functionality while maintaining the environmentally friendly characteristics of the material. Chitosan [17], carrageenan [18], and starch [19] have become a commonly researched and applied material as a biomaterial for bio packaging. Previous studies have found that the use of starch-based nanocomposite films modified by nano-cellulose and chitosan for food packaging applications showed significant performance improvements (reduced moisture permeability, improved mechanical, anti-fungal and waterproof properties). Balakrishnan et al. (2017) wrote about making sustainable packaging based on potato starch with added pineapple leaf nanofiber reinforcement to obtain extraordinary results because the bio packaging has better barrier properties in UV resistance and higher transparency [9]. In addition, any given bio packaging material must fulfil requirements related to conventional packaging materials. It refers to the permeability properties (permeability to water vapour and gases, aroma substances, and light) and mechanical and optical properties (e.g., transparency) [20].

### STARCH-BASED BIO PACKAGING PRODUCTION PROCESS AND ITS COMPOSITES

Previous research conducted by Marichelvam et al. made alternative packaging materials from corn and rice starch [19]. In rice and cornstarch-based bio packaging, glycerol was used as a plasticizer due to its better mechanical properties and good water solubility [19]. The bio-plastics produced by the solution casting method were prepared according to the following procedure: starch, glycerol, and citric acid were added to distilled water in various ratios. The mixture was stirred and heated on a hot plate under certain conditions [19]. Then it was poured into a Teflon-coated glass mold, leveled and dried. Saoza et al. 2020 reported Films for possible applications in food packaging prepared through the casting method [21]. Starch was dispersed in distilled water and continuously stirred to achieve starch gelatinization (see Fig. 1). Then, the mixture was added to the nanocrystalline glycerol cellulose, which is stirred and dried in the oven [21].

Abral et al. 2021 reported a method of making the edible antimicrobial film using starch/chitosan gel mixed with bacterial cellulose suspension [14]. Each gel suspension was sonicated under certain conditions, then poured into a petri dish and dried in the oven [14]. Film packaging was made through solution casting [15]. A certain amount of chitosan was dissolved in acetic acid while stirring to produce a transparent solution [15]. Then, a certain amount of nano-cellulose was dispersed in 20 mL of distilled water and sonicated to produce a homogeneous dispersion. Starch or gelatin is added to the mixed solution, heated and stirred to produce a gel solution. Chitosan and glycerol were added to the mixture, ultra-sonicated and dried in an oven until a film was formed [15]. Preparation of thermoplastics starch (TPS)/nanocellulose fiber (NCF) films was done through solution casting [22]. NCF was dispersed into distilled water with stirring. After that, glycerol and acetic acid were mixed and heated, stirring until the mixture was gelatinized. After that, it was poured into an acrylic mold and dried until a dry film was formed [22]. The corn starch and glycerol mixture were added to the distilled water, heated and stirred until gelatinization [23]. After plasticization was completed, nanocellulose was blended into the mixture to produce nanocomposite films using the casting method and dried in an oven [23].

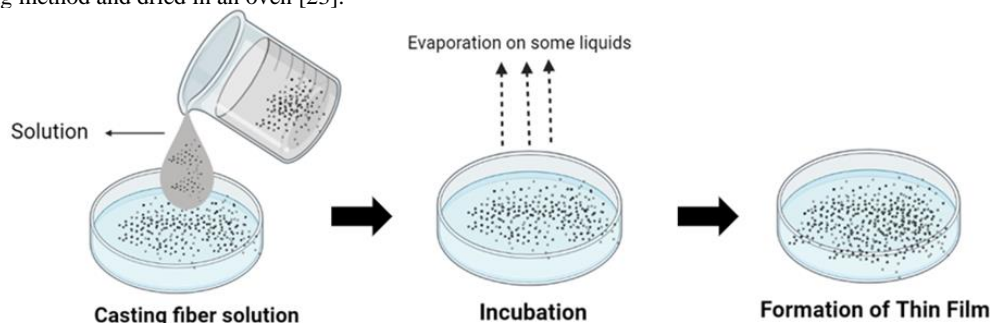


Fig. 1: Simple Illustration method of solution casting in manufacturing bioplastics

### PROPERTIES IN BIO PACKAGING

The film from corn and rice starch with glycerol and citric acid can increase the tensile properties after rice starch [19]. Then, the water absorption and water solubility are also reduced [19]. Starch-based films with nanocellulose-stabilized Pickering emulsions of ho-wood (*Cinnamomum camphora*) exhibited strong chemical interactions, which significantly increased the mechanical resistance of the films [21]. The films exhibit high thermal stability due to strong molecular interactions between starch chains and Pickering emulsions [21]. In addition, the film exhibits a lower rate of water vapour transmission. The starch-based film having good thermal stability is an indication that it can be safely applied in the food industry. Previous studies reported the highest tensile strength and high thermal resistance after nanofiber addition [14]. In addition, nanofibers also increase moisture resistance, water barrier, increase in the content of nano-cellulose and chitosan results in an increase in Young's modulus, tensile strength, elongation at break, transparency [15]. Characteristics of NCF in TPS film-based biocomposite showed high tensile strength; the percentage of elongation at break is reduced; reduction in water vapour rate transmission and oxygen transmission rate compared to TPS control films [22]. It is due to factors such as the nanometer size effect of NCF, the content of crystalline regions of cellulose, the homogeneous dispersion of NCF in TPS, and the strong interaction between NCF and TPS matrix [22].

Bamboo, cotton linter, and sisal fibers are a source of nanocellulose used as reinforcement in corn starch films [23]. The addition of nanocellulose did not affect the morphology and transparency of the three types of composite films but improved

the mechanical and barrier properties. As the number of nanocellulose increases, the thermal stability and elongation at the break of the composite film decrease [23, 24]. Savadeker et al. 2012 discussed the Differential scanning calorimeter (DSC) of Thermoplastic starch (TPS) and Nano-Cellulose fibers (NCF) film. The relative thermal capacity is the utmost result as the relative heat between references and samples was measured in the DSC. Over a quite broad temperature range transition.

## CONCLUSIONS

In industrialized countries, biopolymer materials such as starch and nanocellulose largely replaced conventional polymers as food packaging materials, mainly natural, organic, and functional food packaging. Biopolymers were many produced for various uses, ranging from food packaging to high technology. Despite biopolymers' benefits, many drawbacks limit the wide industrial use of these materials, especially in food packaging. It is generally due to higher efficiency and price when compared to petroleum-based polymer. Biopolymers can be classified into various groups and quality categories according to the production method and applied in the food sector. Cellulose-based biopolymers occupy the most extensive industrial application in the food packaging sector. Only a few additional biobased polymers are used industrially in the packaging of traditional foods. Material technology improvements have been made in generating industrial solutions utilizing starch-based biomaterials for many types of food packaging. Accordingly, biopolymers have grown in importance in food applications. The leading cause is that bio packaging is made from renewable resources and reused via recycling. Researchers focusing on biopolymers have demonstrated that they have features suited for a greater variety of usage in the food sector to attain commercially acceptable prices. In the future, when comparing bio packaging with recycled petroleum plastics, packaging materials created from sustainable biological resources will soon have economic cost and appropriate quality for the application of food packaging.

## ACKNOWLEDGEMENTS

The authors are thankful to the National Research and Innovation Agency for the kind support.

## REFERENCES

- [1] F. Fahma, T. C. Sunarti, S. M. Indriyani, and N. Lisdayana, "Thermoplastic cassava starch-PVA composite films with cellulose nanofibers from oil palm empty fruit bunches as reinforcement agent," *Int. J. Polym. Sci.*, vol. 2017, 2017.
- [2] M. Mahardika, H. Abral, A. Kasim, S. Arief, F. Hafizulhaq, and M. Asrofi, "Properties of cellulose nanofiber/bengkoang starch bionanocomposites: Effect of fiber loading," *LWT*, p. 108554, 2019.
- [3] E. Syafri, A. Kasim, A. Asben, P. Sentharamaikkannan, and M. R. Sanjay, "Studies on Ramie cellulose microfibrils reinforced cassava starch composite: influence of microfibrils loading," *J. Nat. Fibers*, pp. 1–10, 2018.
- [4] R. A. Ilyas, S. M. Sapuan, M. R. Ishak, and E. S. Zainudin, "Development and characterization of sugar palm nanocrystalline cellulose reinforced sugar palm starch bionanocomposites," *Carbohydr. Polym.*, vol. 202, pp. 186–202, 2018.
- [5] M. J. Fabra, A. López-Rubio, J. Ambrosio-Martín, and J. M. Lagaron, "Improving the barrier properties of thermoplastic corn starch-based films containing bacterial cellulose nanowhiskers by means of PHA electrospun coatings of interest in food packaging," *Food Hydrocoll.*, vol. 61, pp. 261–268, 2016.
- [6] H. Abral et al., "Characterization of Tapioca Starch Biopolymer Composites Reinforced with Micro Scale Water Hyacinth Fibers," *Starch-Stärke*, p. 1700287, 2018.
- [7] L. Nouri and A. Mohammadi Nafchi, "Antibacterial, mechanical, and barrier properties of sago starch film incorporated with betel leaves extract," *Int. J. Biol. Macromol.*, vol. 66, pp. 254–259, 2014.
- [8] S. Mathew, A. Jayakumar, V. P. Kumar, J. Mathew, and E. K. Radhakrishnan, "One-step synthesis of eco-friendly boiled rice starch blended polyvinyl alcohol bionanocomposite films decorated with in situ generated silver nanoparticles for food packaging purpose," *Int. J. Biol. Macromol.*, vol. 139, pp. 475–485, 2019.
- [9] P. Balakrishnan, S. Gopi, and S. Thomas, "UV resistant transparent bionanocomposite films based on potato starch/cellulose for sustainable packaging," *Starch-Stärke*, vol. 70, no. 1–2, p. 1700139, 2018.
- [10] O. Rompothi, P. Pradipasena, K. Tananuwong, A. Somwangthanaroj, and T. Janjarasskul, "Development of non-water soluble, ductile mung bean starch based edible film with oxygen barrier and heat sealability," *Carbohydr. Polym.*, vol. 157, pp. 748–756, 2017.
- [11] T. G. Ambaye, M. Vaccari, S. Prasad, E. D. van Hullebusch, and S. Rtimi, "Preparation and applications of chitosan and cellulose composite materials," *J. Environ. Manage.*, vol. 301, p. 113850, 2022.
- [12] D. A. Marrez, A. E. Abdelhamid, and O. M. Darwesh, "Eco-friendly cellulose acetate green synthesized silver nanocomposite as antibacterial packaging system for food safety," *Food Packag. Shelf Life*, vol. 20, p. 100302, 2019.
- [13] A. de Campos et al., "Bionanocomposites produced from cassava starch and oil palm mesocarp cellulose nanowhiskers," *Carbohydr. Polym.*, vol. 175, pp. 330–336, 2017.
- [14] H. Abral et al., "Antimicrobial Edible Film Prepared from Bacterial Cellulose Nanofibers/Starch/Chitosan for a Food Packaging Alternative," *Int. J. Polym. Sci.*, vol. 2021, p. 6641284, 2021.
- [15] S. M. Noorbakhsh-Soltani, M. M. Zerafat, and S. Sabbaghi, "A comparative study of gelatin and starch-based nanocomposite films modified by nano-cellulose and chitosan for food packaging applications," *Carbohydr. Polym.*, vol. 189, pp. 48–55, 2018.
- [16] A. K. Bharimalla, P. G. Patil, S. Mukherjee, V. Yadav, and V. Prasad, "Nanocellulose-polymer composites: novel materials for food packaging applications," in *Polymers for agri-food applications*, Springer, 2019, pp. 553–599.
- [17] S. Yadav, G. K. Mehrotra, and P. K. Dutta, "Chitosan based ZnO nanoparticles loaded gallic-acid films for active food packaging," *Food Chem.*, vol. 334, p. 127605, 2021.
- [18] A. Farhan and N. M. Hani, "Characterization of edible packaging films based on semi-refined kappa-carrageenan plasticized with glycerol and sorbitol," *Food Hydrocoll.*, vol. 64, pp. 48–58, 2017.

## ***The International Symposium on Polymeric Materials 2022***

- [19] M. K. Marichelvam, M. Jawaid, and M. Asim, "Corn and rice starch-based bio-plastics as alternative packaging materials," *Fibers*, vol. 7, no. 4, p. 32, 2019.
- [20] S. Jafarzadeh and S. M. Jafari, "Impact of metal nanoparticles on the mechanical, barrier, optical and thermal properties of biodegradable food packaging materials," *Crit. Rev. Food Sci. Nutr.*, vol. 61, no. 16, pp. 2640–2658, 2021.
- [21] A. G. Souza, R. R. Ferreira, L. C. Paula, S. K. Mitra, and D. S. Rosa, "Starch-based films enriched with nanocellulose-stabilized Pickering emulsions containing different essential oils for possible applications in food packaging," *Food Packag. Shelf Life*, vol. 27, p. 100615, 2021.
- [22] N. R. Savadekar and S. T. Mhaske, "Synthesis of nano cellulose fibers and effect on thermoplastics starch based films," *Carbohydr. Polym.*, vol. 89, no. 1, pp. 146–151, 2012.
- [23] Q. Chen, Y. Liu, and G. Chen, "A comparative study on the starch-based biocomposite films reinforced by nanocellulose prepared from different non-wood fibers," *Cellulose*, vol. 26, no. 4, pp. 2425–2435, 2019.
- [24] A. S. Norfarhana, R. A. Ilyas, and N. Ngadi, "A review of nanocellulose adsorptive membrane as multifunctional wastewater treatment," *Carbohydr. Polym.*, vol. 291, p. 119563, Sep. 2022, doi: 10.1016/j.carbpol.2022.119563.

## STUDY OF INPUT PARAMETER CHANGES TOWARD LOW DENSITY POLYETHYLENE'S PRODUCT PROPERTIES

N. L. Bekri<sup>1</sup>, I. Idris<sup>1\*</sup>, A. M. Som<sup>1</sup>, M. N. Murat<sup>2</sup>, F. S. Rohman<sup>2,3</sup>, R. A. Ilyas<sup>4</sup>, A. Azmi<sup>1\*</sup>

<sup>1</sup>School of Chemical Engineering, College of Engineering, Universiti Teknologi MARA, 40450, Shah Alam Selangor, Malaysia

<sup>2</sup>School of Chemical Engineering, Engineering Campus, Universiti Sains Malaysia, 14300 Nibong Tebal, Pulau Pinang, Malaysia

<sup>3</sup>Department of Chemical Engineering, Universitas Brawijaya, Jalan Mayjen Haryono 167, Malang 65145,

<sup>4</sup>School of Chemical and Energy Engineering, Faculty of Engineering, Universiti Teknologi Malaysia (UTM), Johor Bahru, Johor 81310, Malaysia

### ABSTRACT

Low-density polyethylene (LDPE) is one of the most widely used polymers in the world. It is produced in a high pressure tubular reactor. The significance of the LDPE polymerization process has created numerous works of modelling and simulation of LDPE tubular reactors. A thoroughly mathematical model for LDPE should be capable of presenting the profiles of initiator conversion, monomer conversion, reaction mass temperature and product quality. It has been proven that mathematical models are helpful for evaluating and developing the control, performance, and outline of chemical processes. The sensitivity study is the observation of the relationship between information flowing in and out of the model. The main point of sensitivity study is to determine the relative importance of model parameters and inputs in deciding output. In this work, the sensitivity study of input parameters in industrial LDPE tubular reactors is discussed by manipulating several input parameters. The inclusion of LDPE melt flow index in the reactor output is the novelty of this work. Based on the sensitivity studies, initial concentration of initiator and solvent are identified to give significant effect to the performance of LDPE process in tubular reactor.

**Keywords:** Low Density Polyethylene, polymerization, modelling, monomer conversion, tubular reactor.

### INTRODUCTION

Low-Density Polyethylene (LDPE) is a semi-rigid and lightweight plastic material. The majority of LDPE applications mainly focus on manufacturing containers, dispensing bottles, plastic bags for computer components and various moulded laboratory equipment. The importance of the LDPE polymerization process has led to various studies of modelling and simulation of LDPE tubular reactors. The studies are carried out with the goal of increasing the monomer conversion and reducing the unwanted products while keeping the polymer product quality with respect to its melt flow indexes (MFI) [1]. Melt flow indexes are the important product quality criteria a manufacturer needs to abide by [2]. A typical simplified flow-diagram of low-density polyethylene production is shown in Fig. 1.

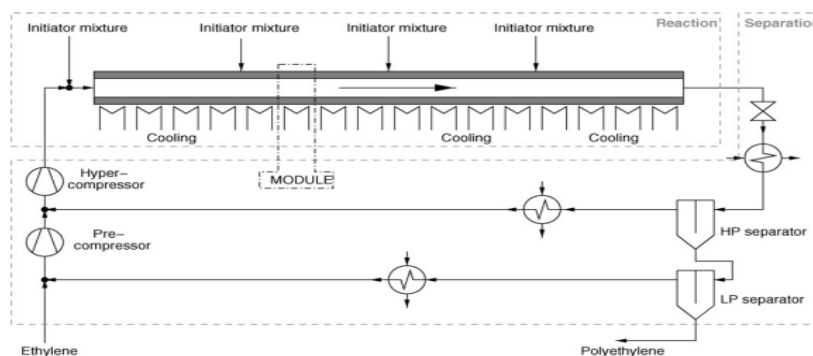


Fig. 1: Simplified flow-sheet of LDPE production [3].

Prior to the optimization work which is aimed to increase the monomer conversion, a sensitivity study needs to be conducted. The sensitivity study is observation of the relationship between information flowing in and out of the model[1]. The main point of sensitivity study is to determine the relative importance of model parameters and inputs in determining output. Considering that most of the published work didn't incorporate the melt flow indexes (MFI) in their works, thus, in this work, the sensitivity study of input parameters in industrial LDPE tubular reactors incorporating MFI is presented. The sensitivity studies are conducted by manipulating several input parameters namely the initial concentration of initiator and initial concentration of solvent.

#### Article history:

Received: 10 March 2022

Accepted: 7 June 2022

Published: 14 June 2022

#### E-mail addresses:

iyliaidris@uitm.edu.my (I. Idris)

ashraf.azmi@uitm.edu.my (A. Azmi)

\*Corresponding Author

METHODOLOGY

Reaction Mechanisms

The main reactions that are common to free radical polymerization are initiator decomposition, thermal initiation, propagation, termination by combination and termination by disproportionation. Beside the main reactions that occur in the free polymerization process, there are also some side reactions such as Chain transfer to monomer, Chain transfer to polymer, Chain transfer to modifier, Propagation of second radicals, Back biting and Beta Scission. These reaction mechanisms refer to [4].

Mathematical Model

The dynamic model of the LDPE process is derived based on the mass, momentum, and energy balances. The equations are developed for one module of the tubular reactor which comprises one coolant cycle. The developed model which consists of ODEs listed in TABLE 1 are solved using MATLAB R2021®. The differential equations are solved using ode15s solver due to its suitability for stiff differential equations. The values of parameters used in this simulation are taken from [5].

TABLE 1: Model Equations for LDPE Tubular Reactor

Description	Equation	No.
Mass Balance for Initiator	$v \frac{dC_{Ii}}{dz} + 2f_{di}K_{di}C_{Ii} = 0$	(1)
Mass Balance for Monomer	$v \frac{dC_M}{dz} + K_p C_M \lambda_0 = 0$	(2)
Mass Balance for Solvent (CTA)	$v \frac{dC_s}{dz} + K_{ts} C_s \lambda_0 = 0$	(3)
Energy Balance	$\frac{dT}{dz} = \frac{1}{\rho C_p v} \left[ -\Delta H K_p C_M \lambda_0 - \frac{4U(T - T_j)}{D_i} \right]$	(4)

RESULTS AND DISCUSSION

Initial Concentration of Initiator's Effect

It is observed from ss 2-5, higher initial concentration of initiator increases the reactor temperature and monomer conversion. The peak temperature is around 320°C while the monomer conversion is 10.70%. The value of MFI for after increment and reduction of initial concentration of monomer is 13.90 g/10 min and 18.64 g/10min respectively.

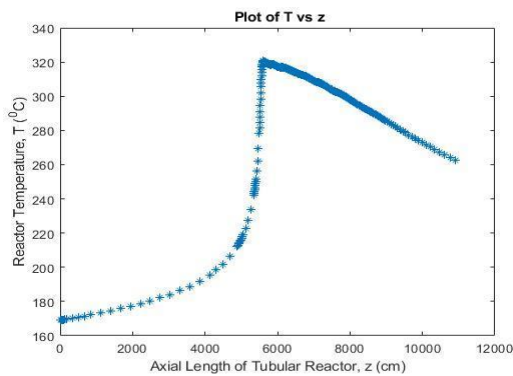


Fig. 2: Temperature profile after increment of  $Cl_0$

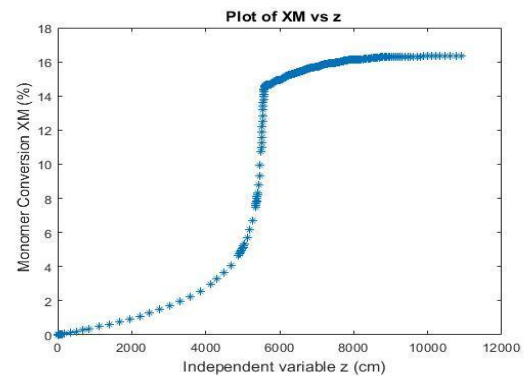


Fig. 3: Monomer conversion after increment of  $Cl_0$

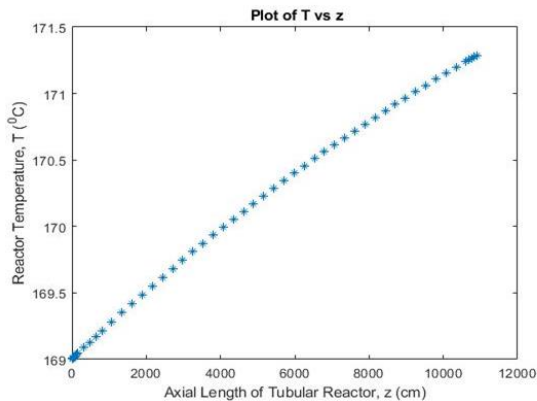


Fig. 4: Temperature profile after reduction of  $Cl_0$

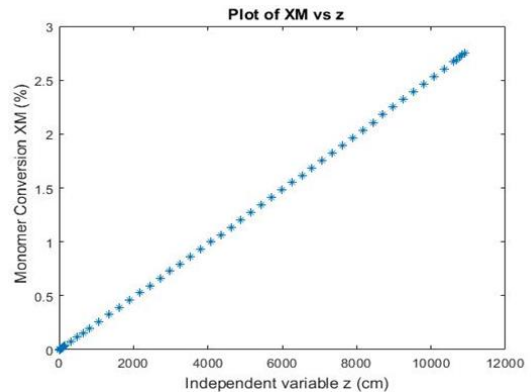


Fig. 5: Monomer conversion after reduction of  $Cl_0$

Initial Concentration of Solvent's Effect

It can be observed from ss 6-9 that after increment of initial solvent concentration, the temperature profile and monomer conversion does not show a noticeable change compared to reference condition. Previously the peak temperature for reference

conditions was also around 250°C and the monomer conversion also does not show any significant changes which is 9.62%. The only significant change in this analysis is the MFI value. The MFI value for initial solvent concentration after increment and reduction is 14.81 g/10min and 2.39 g/10min respectively.

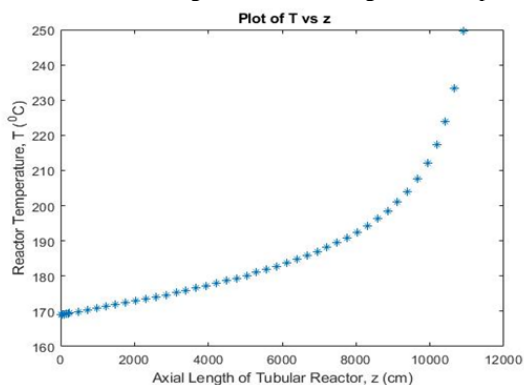


Fig. 6: Temperature profile after increment of  $CS_0$

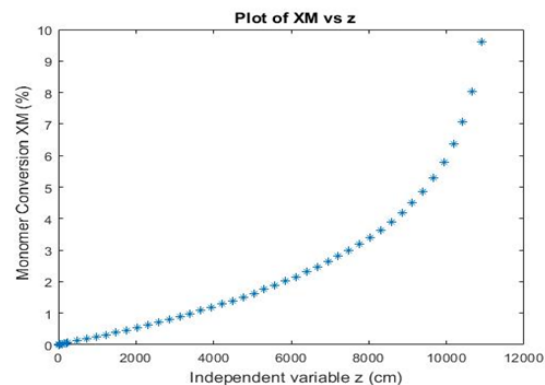


Fig. 7: Monomer conversion after increment of  $CS_0$

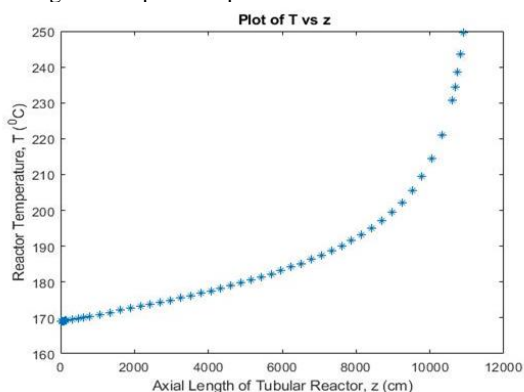


Fig. 8: Temperature profile after reduction of  $CM_0$

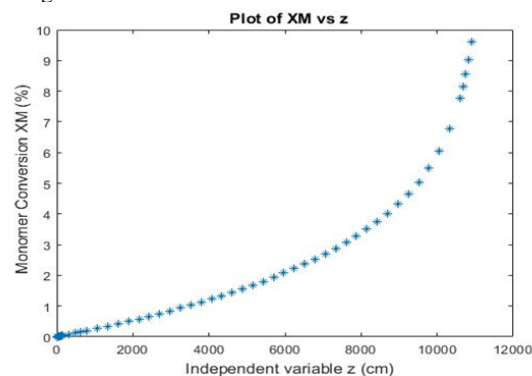


Fig. 9: Monomer conversion after reduction of  $CS_0$

## CONCLUSIONS

The present study reveals that the higher initial concentration of initiator and monomer contributes to greater monomer conversion and higher reactor temperature while there are no significant changes for initial concentration of solvent. As for solvent, it gives significant effect to the MFI of LDPE produced. Increment in initial concentration of solvent increases the MFI and vice versa for reduction in initial concentration of solvent.

## ACKNOWLEDGEMENTS

Financial support from College of Engineering, Universiti Teknologi MARA, Shah Alam through Synergy 2021 Grant No. 600-TNCPI 5/3/DDF (FKK) (009/2021).

## REFERENCES

- [1] M. L. Dietrich, A. Brandolin, C. Sarmoria, and M. Asteasuain, "Mathematical modelling of rheological properties of low-density polyethylene produced in high-pressure tubular reactors," in *IFAC-PapersOnLine*, Jun. 2021, vol. 54, no. 3, pp. 378–382. doi: 10.1016/j.ifacol.2021.08.271.
- [2] A. Azmi, S. Abdul Sata, F. S. Rohman, and N. Aziz, "Optimization studies of low-density polyethylene process: Effect of different interval numbers," *Chemical Product and Process Modeling*, vol. 15, no. 4, Dec. 2020, doi: 10.1515/cppm-2019-0125.
- [3] M. Häfele, A. Kienle, M. Boll, and C. U. Schmidt, "Modeling and analysis of a plant for the production of low density polyethylene," *Computers and Chemical Engineering*, vol. 31, no. 2, pp. 51–65, 2006, doi: 10.1016/j.compchemeng.2006.05.001.
- [4] F. Sholahudin Rohman, D. Muhammad, Sudibyoy, M. Nazri Murat, and A. Azmi, "Application of feed forward neural network for fouling thickness estimation in low density polyethylene tubular reactor," *Materials Today: Proceedings*, Feb. 2022, doi: 10.1016/j.matpr.2022.02.037.
- [5] A. Azmi, S. A. Sata, F. S. Rohman, and N. Aziz, "Dynamic optimization of low-density polyethylene production in tubular reactor under thermal safety constraint," *Chemical Industry and Chemical Engineering Quarterly*, vol. 27, no. 1, pp. 85–97, 2021, doi: 10.2298/CICEQ190108027A.

## **CUTTING FORCE MEASUREMENT OF OIL PALM EMPTY FRUIT BUNCH FIBER REINFORCED POLYMER MATRIX COMPOSITES**

M. K. Wahid<sup>1,\*</sup>, R. Jumaidin<sup>1</sup>, M. H. Osman<sup>1</sup>, A. Rahman, M. H<sup>1</sup>

<sup>1</sup>*Fakulti Teknologi Kejuruteraan Mekanikal dan Pembuatan, Universiti Teknikal Malaysia Melaka, Hang Tuah Jaya, 76100 Durian Tunggal Melaka, Malaysia*

---

### **ABSTRACT**

Malaysia is among the producers and exporters of palm oil in the world. Thus, this study aims on using oil palm empty fruit bunch (OPEFB), to be the reinforcement phase material for a polymer matrix composite. As a result, oil palm empty fruit bunch (OPEFB) fiber polymer matrix composite with different fiber to epoxy ratio has successfully been fabricated. As a composite, the material must undergo secondary process after the process is done to eliminate flashes/burrs that occurs during the machining process, and to ensure the correct dimensions. Thus, the cutting force of the composite samples of different fiber ratio are measured by using dynamometer. The cutting force data were analyzed and it is shown that the weight percentage of material plays a huge part in the cutting force of the composite. The higher the OPEFB fiber content, the lower the cutting force is.

*Keywords:* oil palm empty fruit bunch, fiber, cutting force, polymer.

---

### **INTRODUCTION**

Several research had been conducted on the use of OPEFB fiber as the reinforcing material in a polymer composite. Most of the researchers focus on the mechanical properties of such materials such as its tensile strength and impact toughness. [1][2] Processes such as trimming, and drilling are the most typical secondary processes that are done to any composites. These machining operations are completed mostly by conventional machining techniques. However, very few of these researches focusing on the machinability of the natural fiber composite, especially OPEFB fiber reinforced polymer composite. In order to apply these materials into their maximum potential, machining properties, such as the cutting force needed, must also be studied. In order to fabricate a fiber reinforced composite (FRP), there have to be a mixture between reinforcement (fiber) phase and matrix (polymer) phase. The ratio between reinforcement and matrix phase can affect the outcome of the product in terms of visual properties, mechanical properties etc. This ratio is typically denoted by the weight percentage (wt. %) of fiber. This study focuses only on a few fiber weight percentages, namely 30 wt.%, 40 wt.%, and 50 wt.% of fiber in a composite. These ratios of fiber and polymer are chosen based on the findings on various study, that states that these values have the most effect on the composite properties. Furthermore, there are arguably a lot of factors that will affect the cutting force of a composite. However, only two factors that will be the focus of this study, that are the fiber weight percentage and machining feed rate because these factors are considered as the most influential to the cutting force by past research and studies [3].

There is few research conducted concerning the cutting force of the natural fiber composite, let alone OPEFB fiber composite. The strength, rigidity, and elasticity of a composite materials are affected by its fiber ratio and their orientation. [4] Fibers oriented parallel to the force direction possess greater resistance to distortion from these forces and vice versa. Since it is practically very hard to produce a unidirectional composite by using natural fiber such as OPEFB fiber, only fiber to epoxy ratio will be varied in this experiment. Thus, there are three variations of fiber weight percentage, wt.% that has been chosen to be the focus for this study, that is 30, 40 and 50 wt.%. These values are chosen based on the previous study [2] that concludes that the mechanical properties of the natural fiber composites are inversely proportional to its fiber orientation. Cutting speed is the speed of a tool whilst it is cutting the work piece whereas feed rate is defined as tool's distance travelled during one spindle revolution. In this study, feed rate will be the focus of the experimental design since it is considered as one of the major factor influencing cutting force. [5] The variations of feed rate chosen for the study are 100 mm/min, 150 mm/min and 200 mm/min. These values are chosen based on a previous study [6] where they found out that the machining quality for the CFRP are similar between 100 and 150 mm/min parameter, but the quality dropped significantly once its feed rate is set to 200 mm/min. The study can give better understanding of machining natural fiber composite, in contrast to synthetic fiber composite. The aims of this study are to fabricate oil palm empty fruit bunch (OPEFB) fiber reinforced polymer matrix composites and to measure the cutting force required to machine the OPEFB fiber reinforced polymer matrix composite.

### **MATERIALS AND METHODS**

#### *Materials*

The type of fiber that was used in the fabrication of the composite is empty fruit bunch (EFB) fiber. OPEFB fibers are the byproduct of the crude palm oil extraction and are mostly considered as a waste. Thus, the OPEFB fiber is an abundant raw material and can be acquired from oil palm plantations.

#### *Methods*

Remove impurities such as particles and oil residues from the

---

#### *Article history:*

Received: 10 March 2022

Accepted: 7 June 2022

Published: 14 June 2022

---

#### *E-mail addresses:*

mohammadkhalid@utem.edu.my (M. K. Wahid)

\*Corresponding Author

OPEFB fibers by washing it using distilled water. Then, the fibers were allowed to dry for 20 hours in room temperature. The fibers were then soaked in a 1% sodium hydroxide solution for 1 hour, before it was dried in room temperature for another 24 hours. The fibre treatment was performed in order to roughen the fiber surface which consequently contribute to a better interfacial attachment with the matrix. The dried fibers were then straightened using a comb and by applying pressure at both ends of the fiber while securing them in straight position for approximately 8 hours duration. Compression molding is the process of molding in which a preheated polymer is placed into an open, heated mold cavity. The mold is then closed with a top plug and compressed in order to have the material contact all areas of the mold. The model of hot press compression mold that was used is GT-7014-H300, which is capable of applying for up to 30 ton of force. Thus, there are three variations of fiber weight percentage, wt.% that has been chosen to be the focus for this study, that is 30, 40 and 50 wt.% as shown in Fig. 1.



Fig 1: Fiber weight percentage in composite 30 wt.% 40 wt.% 50 wt.%

A computer numerical control (CNC) router is a computer-controlled cutting machine related to the hand-held router. Additionally, the CNC router helps in the thermoforming of plastics by automating the trimming process. A dynamometer as shown in Fig. 2 is a device for measuring force and torque. The type of dynamometer that was used in the study is cutting force dynamometer, manufactured by Kistler. The 9257BA 3-Component Dynamometer can be used to measure 3-component force measurement (dynamic and quasistatic), cutting force measurements for optimization of the manufacturing process (temporary measurement), and the cutting force measurements (turning, milling, grinding) for training purposes.

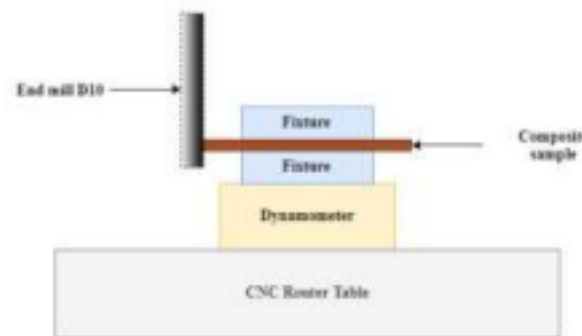


Fig 2: Cutting force measurement set up

**RESULTS AND DISCUSSION**

*Cutting force of OPEFB polymer matrix composite machining*

By using Taguchi method as shown in TABLE 1, the study found that the cutting force is inversely proportional to the weight percentage of fiber in the composite, whereas the relationship between the cutting force and machining feed speed is directly proportional. Furthermore, Taguchi method analysis also calculates that fiber weight percentage plays a bigger role in determining the cutting force. Lastly, the study found that for side milling the OPEFB fiber reinforced composite, the samples with 50 wt.% of fiber and 200 mm/min feed speed will need the least cutting force among all other parameters within this scope of study

TABLE 1: Taguchi L9 cutting force measurement

Run	Weight Percentage (wt.%)	Feed Rate (mm/min)	Cutting Force, Fx (N)		SN Ratio	Standard Deviations	Mean
			Sample 1	Sample 2			
1	50	200	8.26	9.02	-18.7387	0.5374	8.64
2	50	150	11.42	12.03	-21.3852	0.43134	11.725
3	50	100	10.26	8.71	-19.5696	1.09602	9.485
4	40	200	11.19	11.83	-21.2249	0.45255	11.51
5	40	150	13.57	11.66	-22.0426	1.35057	12.615
6	40	100	13.15	12.17	-22.0552	0.69296	12.66
7	30	200	16.54	16.55	-24.3733	0.00707	16.545
8	30	150	20.93	15.39	-25.2822	3.91737	18.16
9	30	100	19.6	19.07	-25.7277	0.37477	19.335



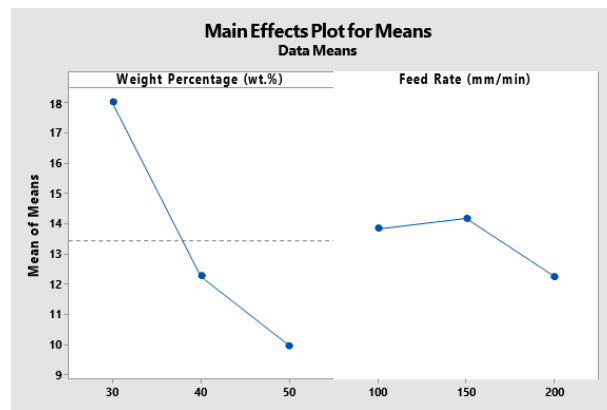


Fig 3: Main effects plot for means

Referring to the Fig. 3, the higher the weight percentage of fiber in the composite sample, the lower the cutting force obtained. This may be caused by several factors such as the incorporation of more natural fiber that is known to be non-abrasive material causes the material to be easier to machine. The relationship between machining feed rate and cutting force is inversely proportional. The higher the feed rate of the side milling process, the lesser the amount of force needed to machine the material. In conclusion, by using Taguchi method the best parameters in terms of minimizing cutting force can be predicted. Based on the data discussed earlier, the parameters are to side mill a composite with 50 wt.% of fibers at 200 mm/min.

## CONCLUSIONS

As conclusion, this study is done to measure the cutting force required to machine the OPEFB fiber reinforced polymer matrix composite. This aim has been accomplished by measuring the cutting force of the composite during side milling process using a dynamometer. In order to get a robust design of experiment, Taguchi method has been applied in order to determine the number of runs it need. The minimum cutting force are obtained when the parameter of composite is 50 wt.% with machining feed rate of 200 mm/min.

## ACKNOWLEDGEMENTS

The authors would like to thank Universiti Technical Malaysia Melaka for the financial support through research grant PJP/2021 /FTKMP/S01815 to corresponding author and hence for sponsoring this paper.

## REFERENCES

- [1] Bakri, M. K. Bin et al. (2015) 'Reinforced Oil Palm Fiber Epoxy Composites: An Investigation on Chemical Treatment of Fibers on Acoustical, Morphological, Mechanical and Spectral Properties', *Materials Today: Proceedings*, 2(4–5), pp. 2747–2756. doi: 10.1016/j.matpr.2015.07.266.
- [2] Saepulloh, D. R. and Nikmatin, S. (2017) 'Mechanical properties of unidirectional oil palm empty fruit bunch ( OPEFB ) fiber reinforced epoxy composite. doi: 10.1088/1757-899X/206/1/012045.
- [3] Patel, P. et al. (2018) 'Milling of Polymer Matrix Composites : A Review', 13(10), pp.7455–7465. *International Journal of Applied Engineering Research* ISSN 0973-4562 Volume 13, Number 10 (2018) pp. 7455-7465 © Research India Publications. <http://www.ripublication.com>
- [4] Sapuan, S. M. (2017) 'Natural Fiber-Reinforced Composites : Types , Development , Manufacturing Process , and Measurement', in. doi: 10.1016/B978-0-12-803581- 8.09183-9.
- [5] Attia, H., Sadek, A. and Meshreki, M. (2012) 'High speed machining processes for fiber-reinforced composites', in *Machining Technology for Composite Materials*. Woodhead Publishing, pp. 333–364. doi: <https://doi.org/10.1533/9780857095145.3.333>.
- [6] Zitoune, R. and Bougherara, H. (2015) 'Machining and drilling processes in composites manufacture: Damage and material integrity', (2010).

## **TENSILE PROPERTIES OF A HYBRID KENAF-GLASS FIBRE REINFORCED UNSATURATED POLYESTER COMPOSITE SHAFT**

N. A. Zakaria<sup>1</sup>, M. R. Ishak<sup>1,2,3\*</sup>, F. Mustapha<sup>1</sup>, N. Yidris<sup>1,3</sup>

<sup>1</sup>Department of Aerospace Engineering, Universiti Putra Malaysia, 43400 UPM Serdang, Selangor, Malaysia

<sup>2</sup>Laboratory of Biocomposite Technology, Institute of Tropical Forestry and Forest Products, Universiti Putra Malaysia, 43400 UPM Serdang, Selangor, Malaysia

<sup>3</sup>Aerospace Malaysia Research Centre, Universiti Putra Malaysia, 43400 UPM Serdang, Selangor, Malaysia

---

### **ABSTRACT**

Natural fibre is often used as reinforcement in polymeric materials, however research on long fibre reinforced polymeric materials, particularly kenaf fibre, is still lacking. In this paper, the experimental results of tensile tests conducted on continuous kenaf fibres reinforced unsaturated polymer produced the hollow and solid shaft composites with two different fibre orientation (0° and 45°). The fibre orientation of composite material might affect its mechanical properties. Two types of fabrication methods, namely filament winding and pultrusion method were used to fabricate the kenaf shaft composite. The effect of fibre orientation (0° and 45°) of kenaf reinforced unsaturated polymer was analyzed. It was found that the 0° orientation angle exhibit higher strength compared to the 45° orientation, where the tensile strength is 39.16MPa for 0° orientation and 18.97MPa 45° orientation. Then, the solid and hollow shaft of 0° orientation angle were compared and it shows that solid have higher strength value than hollow shaft, 83.44MPa. The solid shaft than latter been reinforced with a glass fibre material to produce a hybrid composite. It was discovered that the tensile properties of the hybrid shaft composite were improved by 96.29% compared to the kenaf shaft composite. Consequently, the failure mechanism and the adhesion between fibres were examined using the scanning electron micrographs. In conclusion, the mechanical properties of both fibres into unsaturated polyester shows a regular increasing trend.

*Keywords* : kenaf; fibre orientation, tensile properties, pultrusion, filament winding

---

### **INTRODUCTION**

Kenaf is a popular plant in southern Asia, associated to jute and has similar characteristics and properties. Kenaf fibre have a number of advantages which are low cost and high raw material availability that makes it good for a variety of composites applications. The ecological responsibility have grown the interest in natural and compostable material which bring upon the importance of biodegradability and environmental safety [1]. This research will focus on the kenaf as a natural fibre due to its economic and ecological advantages such as light weight, fast growing plant and low manufacturing cost [2]. Broadly, composite material such as glass is a hard material that is commonly used in the industry because it's excellent characteristics and properties that can withstand with compressive environment. However, glass fibre can cause irritations to the eyes, respiratory tracts when inhaled, and with glass fibre also can cause itching and skin rash due to the mechanical action of the fibre against skin. Aware to that, it is crucial to replace the existing glass fibre with safer and eco-environmental based material. Hence, hybrid of natural fibre reinforced with glass fibre is suggested in this study to enhance the quality of the natural fibre. Biocomposites can help the environmental by reducing energy use, light in weight and low in cost. The advantages were proven in the latest innovation in the constructions industry where the usage of concrete is reinforced with kenaf gives a reduction in cost by 40% and it is more sustain than the concrete alone. An efficient design of hybrid shaft can be achieved by selecting the proper variables, which can be identified for safe structure against failure and to meet the performance requirements. Hence, to enhance the structural properties of the biocomposite materials, the manufacturing method which are pultrusion and filament winding method is also acknowledged in this study. Besides the ability to produce excellent mechanical properties, for both methods, the desired winding angle may be achieved through out the manufacturing process. After that, the natural fibre, composites and reinforced specimens are evaluated in tensile experiments where seven specimens included.

### **MATERIALS AND METHODS**

#### *Materials*

The composite shafts were fabricated using the long kenaf fibre yarn and roving glass fibre purchased from Innovative Pultrusion Sdn. Bhd. The unsaturated polyester resin was used in this study as a reinforcement with the fibres.

#### *Methods*

The samples with different fibre orientations (0° and 45°) were prepared using the pultrusion and filament winding method. In pultrusion method, the continuous roll of fibre were pulled through a resin and then into a heated die where the resin undergoes polymerization. The process for filament winding was where the fibres were pulled through a resin bath

---

#### *Article history:*

Received: 10 March 2022

Accepted: 7 June 2022

Published: 14 June 2022

#### *E-mail addresses:*

afifahz89@gmail.com (N.A.Zakaria)

mohdridzwan@upm.edu.my (M.R.Ishak)

faizalms@upm.edu.my (F.Mustapha)

nyidris@upm.edu.my (N.Yidris)

\*Corresponding Author

and then wound onto the mandrel. Tensile tests were carried out using an INSTRON 3382 Floor Model Universal Testing Machine with the capacity of 10 kN.

## RESULTS AND DISCUSSION

Two different orientation angle ( $0^\circ$  and  $45^\circ$ ) used to produce the hollow shafts and shows that orientation angle give effect to the properties of shaft. The mechanical performances of the shaft were monitored in term of tensile strength. The  $0^\circ$  shaft which were produced by pultrusion method shows better strength compared to  $45^\circ$  shaft. The pultrusion method then were used to produce hollow and solid shaft which both of the shaft has the same content of fibres. The comparison results showed that solid shaft have better strength (72.23%) compared to hollow shaft. Lastly, the solid shaft been choose as the final type of shaft for hybridization. Solid shaft of hybrid kenaf and glass fibre were produced and the properties were compared to kenaf and glass fibre. Thus, the hybrid shaft is comparable to the glass fibre in term of tensile properties.

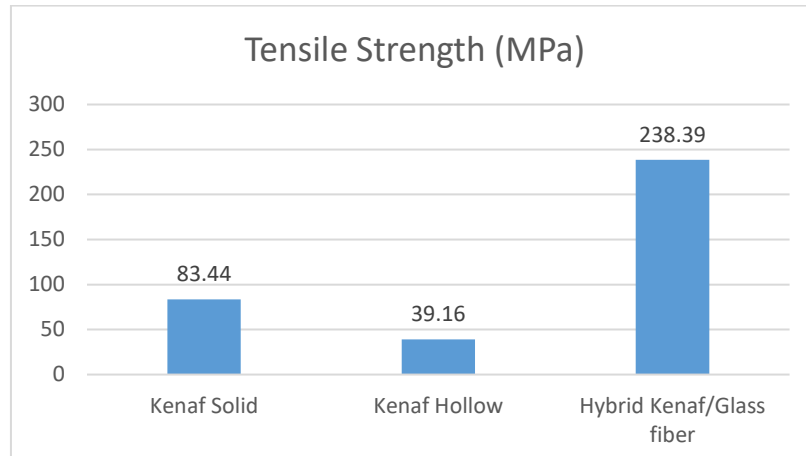


Fig. 1: Tensile strength data of kenaf solid, kenaf hollow and hybrid kenaf/glass fiber

## CONCLUSIONS

The hybridization of kenaf and glass fibre shaft enhanced the mechanical properties and strength of kenaf shaft by 96.29%.

## ACKNOWLEDGEMENTS

The authors would like to thank Universiti Putra Malaysia for providing research grants for this research work, GP-IPS/2015/9486800.

## REFERENCES

- [1] Roy, S. B., Shit, D. S. C., Gupta, D. R. A. S., & Shukla, D. P. R. (2014). A Review on Bio-Composites: Fabrication, Properties and Applications. *International Journal of Innovative Research in Science, Engineering and Technology*, 03(10), 16814–16824.
- [2] Akil, H., Omar, M., Mazuki, A., Safiee, S., Ishak, Z., & Abu Bakar, A. (2011). Kenaf fiber reinforced composites: A review. *Materials & Design*, 32(8–9), 4107–4121.
- [3] Saba, N., Paridah, M., & Jawaid, M. (2015). Mechanical properties of kenaf fibre reinforced polymer composite: A review. *Construction and Building Materials*, 76, 87–96.
- [4] Rasoul GM, A. (2013). Some Health Disorders among Workers in a Glass Factory. *Occupational Medicine & Health Affairs*, 01(02).
- [5] Ochi, S. (2008). Mechanical properties of kenaf fibers and kenaf/PLA composites. *Mechanics of Materials*, 40(4–5), 446–452.
- [6] Misri, S., Sapuan, S., Leman, Z., & Ishak, M. (2014). Tensile Properties of Kenaf Yarn Fibre Reinforced Unsaturated Polyester Composites at Different Fibre Orientations. *Applied Mechanics and Materials*, 564, 412–417.

## **THE EFFECT OF DIFFERENT PULPING TIME ON DEGRADATION OF LIGNIN IN KAPOK FIBER (*CEIBA PENTANDRA*, L.)**

F. A. Rezekinta<sup>1</sup>, A. Kasim<sup>2\*</sup>, E. Syafri<sup>3</sup>, I. Chaniago<sup>1</sup>, F. Ridwan<sup>4</sup>

<sup>1</sup>*Department of Agriculture, Andalas University, West Sumatra 25175, Indonesia*

<sup>2</sup>*Department of Agricultural Technology, Andalas University, West Sumatra 25175, Indonesia*

<sup>3</sup>*Department of Agricultural Technology, Politeknik Pertanian Negeri Payakumbuh, West Sumatra 26271, Indonesia*

<sup>4</sup>*Department of Mechanical Engineering, Andalas University, West Sumatra 25175, Indonesia*

---

### **ABSTRACT**

One of the surface modifications used to improve the performance of lignocellulosic fibers and promote better adhesion between the natural reinforcement and the polymeric matrix is the removal of lignin. Lignin removal is critical due to the complexity of the chemical structure and interaction with polysaccharides, which resulted in lignin embedding cellulose microfibrils in an amorphous matrix in the plant cell wall. Kapok fiber has a high lignin content of around 14 percent but also a high cellulose content of up to 64 percent. It has the potential to be used as a raw material for cellulose. This study used a variety of pulping times (60, 70, 80, 90, and 100 minutes) to determine the optimal lignin degradation on kapok fiber. The pulping process was carried out at a temperature of 105°C in a room atmosphere. As a result, the optimal pulping time was 70 minutes, with 3.57 percent lignin remaining in the fiber and a yield of 69.87 percent.

*Keywords* : lignin, degradation, kapok fiber, pulping, yield

---

### **INTRODUCTION**

Kapok fiber as a source of cellulose is a plant that grows in tropical areas such as Indonesia. Kapok fiber contains cellulose and lignin up to 64% and 21%, respectively [1][2][3]. Locally, kapok fiber is used as a filling material for pillows, dolls and bolsters. Kapok fiber is getting more attention with some amazing properties in it [4]. For cellulose used of kapok fiber, the presence of high enough lignin will affect the cellulose yield obtained. Hence, it is necessary to remove lignin in kapok fiber for further implementations.

Lignin is a phenolic compound formed by the combination of p-hydroxy cinnamyl alcohol and related compounds such as guaiacyl (G), syringyl (S), and p-hydroxyphenyl (H) propanol monolignol which are cross-linked by various bonds. The aryl ether bonds in lignin form non-condensable bonds which are relatively easier to break [5]. Lignin as a protective plant cell wall can inhibit the hydrolysis process [6], removing of lignin in lignocellulosic materials is important to release cellulose and hemicellulose for further processing.

Isolation of lignin from lignocellulosic materials can be accomplished by chemical or enzymes treatments, one of the most widely used chemical treatments is alkaline treatment using sodium hydroxide (NaOH) [6][7][5][8]. Treatment with NaOH is a treatment of lignocellulosic material to eliminate lignin by hydrolysing an ester in lignocellulosic materials which makes it easier for polysaccharides to be accessed by enzymes for hydrolysis [9]. In addition, treatment with NaOH uses lower temperatures and pressures more than other treatment methods [10]. The removal of lignin with NaOH was accomplished at various concentrations [11][5][12]. Therefore, the length of the process required for pulping was carried out to determine the optimum time for lignin degradation using NaOH.

### **NaOH TREATMENT (PULPING)**

Kapok fiber is a source of cellulose that can be found in the tropical area. Presented as a source of cellulose with a high cellulose content reaching 64% [1], kapok fiber has a high lignin content of up to 21% [2]. In obtaining cellulose from cotton wool, the lignin content must be removed. The lignin in the fiber is tightly bound together with cellulose and hemicellulose [13] therefore chemical solution is needed in the removal process.

NaOH treatment or pulping of lignocellulosic materials removes hemicellulose and lignin by breaking the ether and ester bonds in the lignin-carbohydrate complex [14][15][16]. Pulping of the fiber can improve the mechanical properties of the composite [13]. The breaking of bonds between lignin,

---

#### *Article history:*

Received: 1 March 2022

Accepted: 10 March 2022

Published: 14 June 2022

---

#### *E-mail addresses:*

angelinarezekinta@gmail.com (F. A. Rezekinta)

\*Corresponding Author

hemicellulose, and cellulose caused by NaOH will cause swelling of the cell walls so that the fibers will become softer and have better flexibility [17]. Kapok fiber that treated with NaOH will removed the lignin from the fiber. NaOH treatment using 105°C temperature with different pulping time. The bonds between lignin and holocellulose will break with high temperature of NaOH hence cause lignin degradation. Time different for the pulping process of fiber effected the yield of lignin degradation. The damage of the lignin bonds in cell wall will stop if the pulping time is stopped, furthermore the lignin will be not optimally degraded.

REFERENCES

- [1] J. Wang, Y. Zheng, and A. Wang, "Effect of kapok fiber treated with various solvents on oil absorbency," *Ind. Crops Prod.*, vol. 40, no. 1, pp. 178–184, 2012, doi: 10.1016/j.indcrop.2012.03.002.
- [2] E. Bozaci, "Optimization of the alternative treatment methods for Ceiba pentandra (L.) Gaertn (kapok) fiber using response surface methodology," *J. Text. Inst.*, vol. 110, no. 10, pp. 1404–1414, 2019, doi: 10.1080/00405000.2019.1602897.
- [3] T. Dong, G. Xu, and F. Wang, "Adsorption and adhesiveness of kapok fiber to different oils," *J. Hazard. Mater.*, vol. 296, pp. 101–111, 2015, doi: 10.1016/j.jhazmat.2015.03.040.
- [4] R. H. Sangalang, "Kapok Fiber-Structure, Characteristics and Applications : (A Review)," *Orient. J. Chem.*, vol. 37, no. No. 3, pp. 513–523, 2021.
- [5] W. Jung, D. Savithri, R. Sharma-Shivappa, and P. Kolar, "Changes in lignin chemistry of switchgrass due to delignification by sodium hydroxide pretreatment," *Energies*, vol. 11, no. 2, pp. 1–12, 2018, doi: 10.3390/en11020376.
- [6] C. Arslan, M. Javed, A. Sattar, F. Ilyas, W. Tariq, and S. H. Gillani, "Optimizing the Effect of Chemical Pretreatment on Lignocellulosic Properties of Wheat Straw," *J. Wastes Biomass Manag.*, vol. 2, no. 2, pp. 28–32, 2020, doi: 10.26480/jwbm.02.2020.28.32.
- [7] A. A. Modenbach and S. E. Nokes, "Effects of sodium hydroxide pretreatment on structural components of biomass," *Trans. ASABE*, vol. 57, no. 4, pp. 1187–1198, 2014, doi: 10.13031/trans.56.10046.
- [8] N. S. Hassan and K. H. Badri, "Lignin recovery from alkaline hydrolysis and glycerolysis of oil palm fiber," *AIP Conf. Proc.*, vol. 1614, no. February 2015, pp. 433–438, 2014, doi: 10.1063/1.4895236.
- [9] Z. Liu *et al.*, "Two-step delignification of miscanthus to enhance enzymatic hydrolysis: Aqueous ammonia followed by sodium hydroxide and oxidants," *Energy and Fuels*, vol. 28, no. 1, pp. 542–548, 2014, doi: 10.1021/ef401317z.
- [10] M. Han, G.-W. Choi, Y. Kim, and B. Koo, "Bioethanol production by Miscanthus as a lignocellulosic biomass: Focus on high efficiency conversion to glucose and ethanol," *Bioresources*, vol. 6, no. Lynd 1996, pp. 1939–1953, 2011.
- [11] D. Ciftci, R. A. Flores, and M. D. A. Saldaña, "Cellulose Fiber Isolation and Characterization from Sweet Blue Lupin Hull and Canola Straw," *J. Polym. Environ.*, vol. 26, pp. 2773–2781, 2018.
- [12] D. Jiang *et al.*, "Effect of alkaline pretreatment on photo-fermentative hydrogen production from Giant Reed: Comparison of NaOH and Ca(OH)<sub>2</sub>," *Bioresour. Technol.*, p. 123001, 2020, doi: 10.1016/j.biortech.2020.123001.
- [13] A. Oushabi, S. Sair, F. Oudrhiri Hassani, Y. Abboud, O. Tanane, and A. El Bouari, "The effect of alkali treatment on mechanical, morphological and thermal properties of date palm fibers (DPFs): Study of the interface of DPF–Polyurethane composite," *South African J. Chem. Eng.*, vol. 23, pp. 116–123, 2017, doi: 10.1016/j.sajce.2017.04.005.
- [14] J. Kim, M. Sunagawa, S. Kobayashi, T. Shin, and C. Takayama, "Developmental localization of calcitonin gene-related peptide in dorsal sensory axons and ventral motor neurons of mouse cervical spinal cord," *Neurosci. Res.*, pp. 1–7, 2015, doi: 10.1016/j.neures.2015.09.003.
- [15] L. C. Malucelli, L. G. Lacerda, and M. Aure, "Preparation , properties and future perspectives of nanocrystals from agro-industrial residues : a review of recent research," *Rev. Environ. Sci. Bio/Technology*, vol. 16, pp. 131–145, 2017, doi: 10.1007/s11157-017-9423-4.
- [16] C. Gao, J. Yang, and L. Han, "Bioresource Technology Systematic comparison for effects of different scale mechanical-NaOH coupling treatments on lignocellulosic components , micromorphology and cellulose crystal structure of wheat straw," vol. 326, no. December 2020, 2021.
- [17] H. Chen, J. Wu, J. Shi, W. Zhang, and G. Wang, "Industrial Crops & Products Strong and highly flexible slivers prepared from natural bamboo culm using NaOH pretreatment," *Ind. Crop. Prod.*, vol. 170, no. March, p. 113773, 2021, doi: 10.1016/j.indcrop.2021.113773.

## **EXPERIMENTAL ANALYSIS OF KERF TAPER ANGLE IN CUTTING PROCESS OF SUGAR PALM FIBER REINFORCED UNSATURATED POLYESTER COMPOSITES WITH ABRASIVE WATER JET CUTTING TECHNOLOGY**

F. Masoud<sup>1</sup>, S. M. Sapuan<sup>1,2\*</sup>, M. K. A. M. Ariffin<sup>1</sup>, Y. Nukman<sup>3</sup>, E. Bayraktar<sup>4</sup>

<sup>1</sup>*Department of Mechanical and Manufacturing Engineering, University Putra Malaysia, Serdang 43400, Selangor, Malaysia*

<sup>2</sup>*Laboratory of Biocomposite Technology, Institute of Tropical Forestry and Forest Products (INTROP), University Putra Malaysia, 43400 UPM, Serdang 43400, Selangor, Malaysia*

<sup>3</sup>*Department of Mechanical Engineering, University of Malaya, Kuala Lumpur 50603, Malaysia*

<sup>4</sup>*School of Mechanical and Manufacturing Engineering, Supmeca-Paris, 3 rue Fernand Hainaut, 93400 Saint Ouen, France*

---

### **ABSTRACT**

In this research, the effect of processing input parameters on the kerf taper angle response of three various material thicknesses of sugar palm fiber reinforced unsaturated polyester composite was investigated as output parameter from abrasive water jet cutting technique. The main purpose of the study is to obtain data that includes the optimum input parameters in cutting the composite utilizing this unconventional technique to avoid some defects that arise when using traditional cutting methods for cutting the composites. In abrasive water jet cutting process, traverse speed, water pressure, and stand-off-distance were selected as the variable input parameters to optimize the kerf taper angle with fixing all of the other input parameters. The levels of the input parameters that provide the optimal response of the kerf taper angle were determined using Taguchi's approach, and the significance of input parameters was determined by computing the max-min variance of the average of the signal to-noise ratio (S/N) for each parameter. The contribution of each input processing parameter to the effects on kerf taper angle was determined using analysis of variation (ANOVA). Compared with the results that were extrapolated in the previous studies, the processes achieved acceptable results in terms of the response of the kerf taper angle.

*Keywords* : abrasive water jet; natural fiber; composite; kerf taper angle

---

### **INTRODUCTION**

Natural fibers have been primarily viewed as waste and remnants until recently, as they were not efficiently exploited. However, its use is spreading due to the advantages of natural fibers that made them to be an acceptable alternative to synthetic fibers in many applications, especially considering the property of natural decomposition of natural fibers, which makes them environmentally friendly materials [1][2], in addition to that they are extracted from renewable resources that require no energy consumption to produce them unlike the synthetic fibers production processes. They also have certain other advantages, such as low density, low cost, enhanced recovery, and flexibility [3][4]. Owing to mentioned benefits, natural fibers have attracted a lot of attention in advanced polymeric composites field for a variety of engineering applications as a reinforcement material for a broad spectrum of matrices [5][6]. Although composites are formed close to near-net shape, final processes such as drilling, cutting, trimming, and profiling are still required [7]. Due to the cutting forces associated with conventional cutting methods and the heterogeneous nature of composites, in addition to specimen fixing that requires a relatively large clamping force, several serious defects appear with the application of traditional cutting techniques in the composites cutting processes, such as, material damage, poor surface quality, delamination, fiber fraying, and dimensional instability [8][9]. In order to avert these flaws, non-traditional techniques were considered [7]. Abrasive water jet machining (AWJ) is the most prominent unconventional technology utilized in cutting composites due to their high efficiency and productivity [6][7]. In this context, the current study investigates and analyzes the influence of significant input parameters on the kerf taper angle response in cutting three different material thicknesses (2, 4, and 6 mm) of sugar palm fiber reinforced unsaturated polyester (SPF-UPE) composite cut with Abrasive water jet machining technique. As one of the most interesting composite materials reinforced with sugar palm fibers is the sugar palm fibers reinforced unsaturated polyester (SPF-UPE), on which several studies have been conducted regarding the evaluation of its physical and chemical properties [10]. In this study, the focus was on testing the SPF-UPE under unconventional cutting conditions, as the principle target is to collect data that involves the optimum input

---

#### *Article history:*

Received: 10 March 2022

Accepted: 7 June 2022

Published: 14 June 2022

---

#### *E-mail addresses:*

fathimasoud77@gmail.com (F. Masoud)

sapuan@upm.edu.my (S. M. Sapuan)

faizalms@upm.edu.my (M. K. A. M. Ariffin)

nyidris@upm.edu.my (Y. Nukman)

bayraktar@supmeca.fr (E. Bayraktar)

\*Corresponding Author

parameters in cutting the composite using abrasive water jet technology to prevent or limit the defects that emerge with using conventional machining processes for cutting the SPF-UPE. The data provided in this research would contribute to the exploitation of natural fiber composites, especially the material under study in various applications, such as automobiles, aerospace, construction industries, marine applications, packaging, sporting products, and electronic industries applications.

MATERIALS AND METHODS

Materials

Fabrication of Composite

Sugar palm fiber reinforced unsaturated polyester (SPF-UPE) composite was used for the research. Sugar palm fibers (SPFs) were cleaned with pure water, dried by hot air, and then treated with 0.25 M/L NaOH with one-hour immersion duration, as this treatment demonstrated good improvement in the mechanical and physical properties of SPF [10]. The fibers have been cut manually with lengths from 5 to 10 mm (average aspect ratio 25). The matrix used is unsaturated polyester (UPE) with fiber loading by 30%, as this fiber content showed good mechanical and physical properties [11]. Three molds with three different depths were utilized to make three different types of specimens with thicknesses of 2, 4, and 6 mm and lengths of 210 mm and widths of 120 mm. The hand lay-up technique was used to perform the composite specimens. The molds were subsequently disassembled and the specimens were removed after 24 hours of being covered with a 40 kg weight

Methods

Abrasive water jet cutting experiments were carried out using Flow Mach2 1313B CNC Waterjet machine with operating water pressure up to 60 K psi and Traverse speed up to 10m/min, 80 mesh (177microns) garnet abrasive size was used for all of experiments as it gave the best results based on previous studies. The diameter of the nozzle was 1 mm and impact angle was 90°. Traverse speed, water pressure, and stand-off-distance were chosen as the input parameters as they showed a significant influence on the kerf taper angle. With varied input parameter levels, three distinct material thicknesses of 2, 4, and 6 mm were examined under abrasive water jet machining conditions.

RESULTS AND DISCUSSION

For optimizing kerf taper angle response of sugar palm reinforced unsaturated poly-ester composite cut with abrasive waterjet technology, the ranges of input parameters that produced the flaws shown in Fig. 1 were excluded

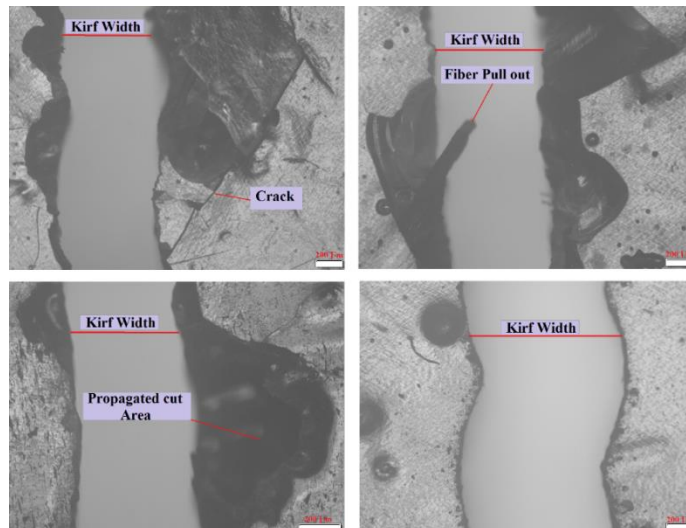


Fig 1. (a) Damages and cracks at cutting kerf. (b) Incomplete cut and pull out of fibers. (c) High propagated cutting area. (d) uneven cut.

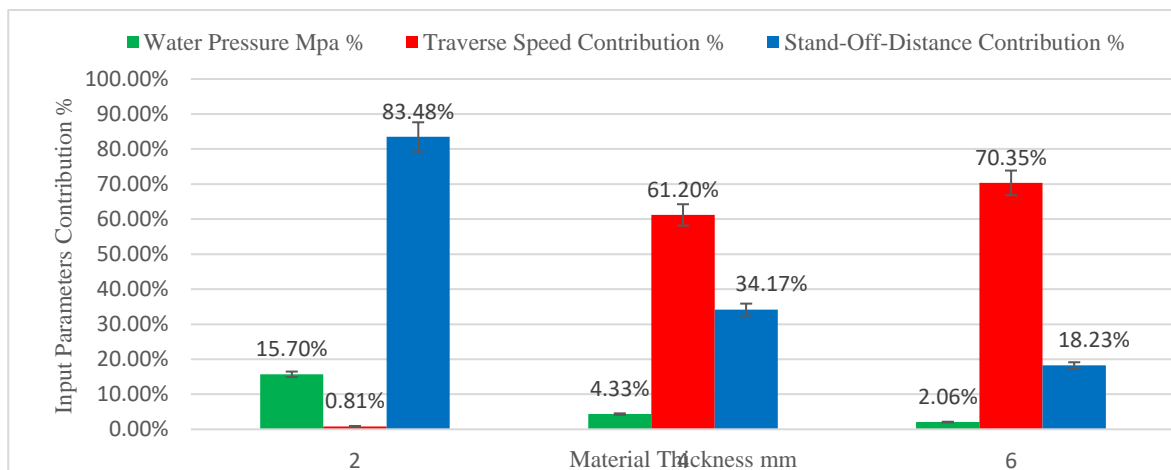


Fig. 2: Input parameter contributions to kerf taper angle of the various material thick-nesses of SPF-UPE composite cut with waterjet cutting technology.

## CONCLUSIONS

The abrasive water jet cutting process of sugar palm fiber reinforced unsaturated polyester composite is completed satisfactorily, with the following findings:

- In waterjet cutting process, stand-off-distance has the largest influence on the kerf taper angle response, followed by water pressure with small contribution of traverse speed, for 2 mm material thicknesses, while traverse speed has the greatest influence on the kerf taper angle, followed by stand-off-distance and water pressure, respectively, in the cases of 4 mm and 6 mm specimen thicknesses.
- Optimum input parameters that gave the best response of kerf taper angle in waterjet cutting technology were, 3 mm stand-off-distance, 2400 mm/min traverse speed, and 340 MPa water pressure for 2mm material thickness. In the case of 4 mm material thickness the optimum input parameters were, 1 mm stand-off-distance, 1800 mm/min traverse speed, and 320 MPa water pressure, while the optimum input parameters for 6 mm specimen thickness were, 1 mm stand-off-distance, 1200 mm/min traverse speed, and 300 MPa water pressure.

## ACKNOWLEDGMENTS

The authors would like to thank the support of Universiti Putra Malaysia for considerably assisting in the completion of this study. The authors would like to thank Technical University of Malaysia Malacca (UTeM) for facilitating the completion of this study.

## REFERENCES

- [1] M. H. Alaaeddin, S. M. Sapuan, M. Y. M. Zuhri, E. S. Zainudin, and F. M. AL- Oqla, "Physical and mechanical properties of polyvinylidene fluoride - Short sugar palm fiber nanocomposites," *J. Clean. Prod.*, vol. 235, pp. 473–482, 2019.
- [2] S. N. Monteiro *et al.*, "Fique fabric: A promising reinforcement for polymer composites," *Polymers (Basel)*, vol. 10, no. 3, pp. 1–10, 2018.
- [3] A. Lotfi, H. Li, and D. V. Dao, "Drilling Behavior of Flax/Poly(Lactic Acid) Bio-Composite Laminates: An Experimental Investigation," *J. Nat. Fibers*, vol. 17, no. 9, pp. 1264–1280, 2020.
- [4] E. Sarikaya, H. Çallioğlu, and H. Demirel, "Production of epoxy composites reinforced by different natural fibers and their mechanical properties," *Compos. Part B Eng.*, vol. 167, no. 15, pp. 461–466, 2019.
- [5] P. Khalili, X. Liu, K. Y. Tshai, C. Rudd, X. Yi, and I. Kong, "Development of fire retardancy of natural fiber composite encouraged by a synergy between zinc borate and ammonium polyphosphate," *Compos. Part B Eng.*, vol. 159, pp. 165–172, 2019.
- [6] F. Masoud, S. M. Sapuan, M. K. A. Mohd Ariffin, Y. Nukman, and E. Bayraktar, "Cutting processes of natural fiber-reinforced polymer composites," *Polymers (Basel)*, vol. 12, no. 6, pp. 15–17, 2020.
- [7] A. Lotfi, H. Li, D. V. Dao, and G. Prusty, "Natural fiber-reinforced composites: A review on material, manufacturing, and machinability," *J. Thermoplast. Compos. Mater.*, 2019.
- [8] J. L. Mercy, P. Sivashankari, M. Sangeetha, K. R. Kavitha, and S. Prakash, "Genetic Optimization of Machining Parameters Affecting Thrust Force during Drilling of Pineapple Fiber Composite Plates—an Experimental Approach," *J. Nat. Fibers*, vol. 00, no. 00, pp. 1–12, 2020.
- [9] S. P. Jani, A. S. Kumar, M. A. Khan, and M. U. Kumar, "Machinability of Hybrid Natural Fiber Composite with and without Filler as Reinforcement," *Mater. Manuf. Process.*, vol. 31, no. 10, pp. 1393–1399, 2016.
- [10] M. R. Ishak, S. M. Sapuan, Z. Leman, M. Z. A. Rahman, U. M. K. Anwar, and J. P. Siregar, "Sugar palm (*Arenga pinnata*): Its fibres, polymers and composites," *Carbohydr. Polym.*, vol. 91, no. 2, pp. 699–710, 2013.
- [11] M. N. Norizan, K. Abdan, M. S. Salit, and R. Mohamed, "Physical, mechanical and thermal properties of sugar palm yarn fibre loading on reinforced unsaturated polyester composites," *J. Phys. Sci.*, vol. 28, no. 3, pp. 115–136, 2017.



## CONCEPTUAL DESIGN OF THE CAR GEAR CONSOLE PANEL MADE BY GLASS/NATURAL FIBER REINFORCED HYBRID POLYMER COMPOSITE

J. Yusuf<sup>1</sup>, Z. Leman<sup>1,2\*</sup>, S.M. Sapuan<sup>1,2</sup>

<sup>1</sup>Department of Mechanical and Manufacturing Engineering, Faculty of Engineering, Universiti Putra Malaysia, 43400, UPM, Serdang, Selangor, Malaysia

<sup>2</sup>Advanced Engineering Materials and Composites Research Centre (AEMC), Department of Mechanical and Manufacturing Engineering, Faculty of Engineering, Universiti Putra Malaysia, 43400, UPM, Serdang, Selangor, Malaysia

---

### ABSTRACT

This study was conducted in order to enhance the car gear console panel with environmentally friendly aspects by making it from glass/coir fiber-reinforced polypropylene hybrid composite. The functions and competitive benchmarking criteria were compiled and merged with the environmental requirements to produce the Product Design Specifications (PDS). The chosen polymer was compared to a benchmark material, Acrylonitrile Butadiene Styrene (ABS), using the Weighted Evaluation Matrix (WEM). Coir fiber and Polypropylene (PP) were found to be effective bio-composites for car gear console panel. After that, using an integrated Theory of Inventive Problem Solving (TRIZ) and Morphological Chart, the conceptual design development of a coir fiber-reinforced polypropylene gear console panel was carried out, followed by final conceptual design selection utilising an integrated Pugh Chart. The new design concept has less annular snaps, position of the screws are also changed. Coir fiber-reinforced polypropylene hybrid composites were found to be an alternate material for eco-friendly car gear panel.

*Keywords:* Morph Chart, Pugh scoring method, coir fiber, conceptual design, PDS, TRIZ

---

### INTRODUCTION

Composites are made up of at least two materials that have different properties than the constituent materials acting alone [1]. In order to replace the material in cost effective manner Conceptual design is used. The Conceptual design only requires 5 % of the budget and it was also found out that 75 % of the budget of any project is decided in the initial stage [2]. The use of bio-based composite materials in automotive parts was initially considered by Ford Motor Company in the early 1930s. Furthermore, in the search for environmentally acceptable light-bodied cars, these materials promised to reduce weight and emissions. As a result, the Ford Motor Company embarked on an intense research programme into the widespread usage of natural fiber in automobiles, culminating in the 1941 introduction of the T concept car [3][4]. A flax/sisal fiber mat-reinforced epoxy matrix was used to make the door, which resulted in a 20 % weight decrease [5]. The automobile industries are manufacturing cars with increased performance and aesthetics by continuing to develop composite materials technologies. The ability to use this type of lightweight material provides a competitive edge that will benefit future automobiles as well as the manufacturing process [1]. Natural fiber composites are commonly used in interior components.

### FUNCTION ANALYSIS

The functions of Car Gear Console Panel are written in form of verb and noun. The higher order role of a car gear console panel is to improve the biodegradability by using bio composite panel. In this regard, the primary function of panel is to "prevent contact". When the secondary functions of "conceal area" are completed, the basic function is completed. At the same time, concealing the region can improve the appearance of the car gear console panel.

### COMPETITIVE BENCHMARKING INFORMATION

In the product design mechanical properties play a crucial role. In car gear console panel the required properties include low density, low moisture content etc. because it will conceal all mechanical components. ABS has adequate heat resistant to prevent heat distortion. In order to maintain the aesthetics the door panels are tailored and painted as per requirements. It also provides additional protection to the component, for an example UV protection, water repellent, weather resistant and protection from plastic corrosion.

### ENVIRONMENTAL REQUIREMENT

Environmentally conscious products should be able to identify potential environmental problems. According to the product should be able to be recovered at the end of its life cycle by simplifying material separation, facilitating material recycling, and lowering the amount of trash that needs to be burnt or disposed of in landfills. Natural fibers such as jute, sisal, kenaf, hemp, oil palm, date palm, rami, and flax have emerged as eco-friendly product alternatives.

---

#### Article history:

Received: 10 March 2022

Accepted: 7 June 2022

Published: 14 June 2022

---

#### E-mail addresses:

zleman@upm.edu.my (Z. Leman)

\*Corresponding Author

**PRODUCT DESIGN SPECIFICATIONS (PDS)**

The design goal and design objectives are decided as below:

- a. Design Goal
  - Environmentally friendly car gear console panel
- b. Design Objective
  - To conceptually design car gear console panel with natural fiber composites without compromising the existing product characteristic. Based on the inputs from side cover functions, benchmarking characteristic and environmental requirement, the decided PDS and its criteria.

**CONCEPTUAL DESIGN DEVELOPMENT**





The Theory of Inventive Problem Solving was used to produce a conceptual design for a composite car gear console panel. The PDS is suitable for the TRIZ 39 engineering parameters [5]. The goal of the concept is to replace the ABS car gear console panel with a coir/PP composite car gear console panel to improve biodegradability and reduce pollution. However, as compared to ABS, the chosen material is projected to improve coir density. As a result, #31 is the improving parameter. The deteriorating parameter is #2 weight of stationary object. TABLE 1 shows relationship between PDS and TRIZ 39 engineering parameter which are required in car gear console panel.

TABLE 1: Relationship between PDS and TRIZ 39 engineering parameter

PDS Main Criteria	TRIZ 39 engineering parameter
Strength	#14 Strength
Concealing	#29: Accuracy of manufacturing
Asthetics	#32: Change the colour

Contradiction matrix is created to identify the appropriate solution principles for each worsening parameter that corresponds to the issues encountered in attaining the design purpose. The #35 parameter changes found from 40 innovative concepts to counteract the increase of #20 weight of stationary object.

TABLE 2: Morphological chart of TRIZ solution principle and their related design where L,R,T and B represents left, right, top and bottom position of screws

TRIZ solution principles and design strategy	Design Blocks	Conceptual Designs			
		Benchmark	1	2	3
					
#35 Parameter Changes	No. of annular snap fitted	4	<u>2</u>	6	7
	No. of Screws	2	<u>4</u>	1	4
	Screw positions	L=1 & R=1 T=0 & B=0	<u>L=1&amp; R=1</u> <u>T=1&amp; B=1</u>	L=1 & R=1 T=0 & B=1	L=0 & R=0 T=1 & B=1
	Assembly structures	<u>3</u>	<u>3</u>	2	4
	Shape	trapezoidal	<b>rectangular</b>	Circular	oval

## ***The International Symposium on Polymeric Materials 2022***

According to TRIZ solution principles and design strategy parameter changes were done on the design block. The changes were as follows:

- Number of annular snap fitted was changed from 4 to 2.
- Number of Screws was changed from 2 to 4.
- Screw positions were distributed evenly on top, bottom, left and right positions. · Assembly structures were kept same as 3.
- The shape was suggested rectangular from trapezoidal shape. Ranking was done for each natural fiber properties along with their selecting criteria. The final material is selected by Pugh Matrix. When deciding, the Pugh Matrix is a straightforward way to take these various aspects into account [16].

Coir fiber has been selected as the most suitable material for car gear console panel compared to hemp, sisal, flax, kenaf and jute.

### **CONCLUSIONS**

The glass/coir fiber-reinforce polypropylene hybrid composites was replaced by ABS material for the car gear console panel. Coir fiber displayed the highest score as compared to its counter materials which were Hemp, Sisal, Flax, Kenaf and Jute fiber. It shows the suitability of PP matrix in place of ABS.

### **REFERENCES**

- [1] Fentahun MA, Savas MA. Materials <https://doi.org/10.5923/j.ijme.20180803.02>.
- [2] S.M.Sapuan. Composite Materials. vol. 53. 2013.
- [3] Siti S, Abdul HPS, Wan WO, Jawai M. Bamboo Based Biocomposites Material, Design and Applications. Mater Sci - Adv Top 2013. <https://doi.org/10.5772/56057>.
- [4] Mohammed L, <https://doi.org/10.1155/2015/243947>.
- [5] Akampumuza O, Wambua PM, Ahmed A, Li W, Qin XH.

## NATURAL FIBER REINFORCED POLYMER COMPOSITES: OPPORTUNITIES, CHALLENGES, AND ITS APPLICATIONS

N.A. Maidin<sup>1,3</sup>, S.M. Sapuan<sup>1,2\*</sup>, M.T. Mastura<sup>3</sup>, M.Y.M. Zuhri<sup>1</sup>

<sup>1</sup>Department of Mechanical and Manufacturing Engineering, Faculty of Engineering, Universiti Putra Malaysia, 43400 UPM Serdang, Selangor Darul Ehsan, Malaysia.

<sup>2</sup>Laboratory of Biocomposite Technology, Institute of Tropical Forestry and Forest Products (INTROP), Universiti Putra Malaysia, 43400 UPM Serdang, Selangor, Malaysia

<sup>3</sup>Department of Manufacturing Engineering Technology, Faculty of Mechanical and Manufacturing Engineering Technology, Universiti Teknikal Malaysia Melaka, 76100 Durian Tunggal, Melaka, Malaysia

---

### ABSTRACT

Nowadays, the use of natural fiber reinforced polymer-based composites gradually increases day by day because of their many advantages. Polymer-based composite materials are widely used in civil construction, automotive, aerospace, and many others. Natural fibers such as jute, kenaf, pineapple, sugarcane, hemp, oil palm, flax, leaf, etc., are cheap, environmentally friendly, renewable, entirely and partially biodegradable, and can be utilized to obtain new high-performance polymer materials. These composites have good mechanical properties (i.e., tensile properties, flexural stress-strain behavior, fracture toughness, and fracture strength), making them more attractive than other composites. Due to easy availability and renewability, natural fibers can be used as an alternative to synthetic fibers as a reinforcing agent. This paper reviews the potential different natural fibers reinforced based polymer composites mechanical characterization, opportunities, challenges, and future demand, especially in sports applications because these materials are rarely used in this area.

*Keywords:* natural fiber reinforced polymer composites, biodegradable, environmentally friendly, applications.

---

### INTRODUCTION

The expanding environmental damage ascribed to depend on composite materials, and they started to utilize composite material in different aspects. Natural fiber composite materials are eco-friendly, lightweight, strong, renewable, affordable, biodegradable and sustainable. Natural fiber offers good qualities compared to synthetic fiber [1]. Recently, natural fibers have been employed as an alternative reinforcement in polymer composites which has received interest among many academics and scientists due to its advantages over standard synthetic materials [2]. These natural fibers include jute, hemp, sisal, kenaf, coir, banana, bamboo, sugarcane, flax, and many others [3], which provide better mechanical properties than manufactured fibers. Their cost is reasonable, recyclable and renewable, reduce energy consumption, less health risk and nonabrasive to the equipment, and non-irritation to the skin [4]. The most prevalent and economically natural fibers in the world and world production have been shown in TABLE 1.

TABLE 1: Natural fibers in the world and their world production [4-5]

Fiber source	World production (10 <sup>3</sup> ton)
Hemp	214
Coir	100
Jute	2300
Kenaf	970
Flax	830
Bamboo	30000
Grass	700
Ramie	100
Sugar cane bagasse	75000
Abaca	70
Sisal	375

---

#### Article history:

Received: 10 March 2022

Accepted: 7 June 2022

Published: 14 June 2022

---

#### E-mail addresses:

ain2513@gmail.com (N.A. Maidin)

sapuan@upm.edu.my (S.M. Sapuan)

mastura.taha@utem.edu.my (M.T. Mastura)

zuhri@upm.edu.my (M.Y.M Zuhri)

\*Corresponding Author

It can be utilized as a reinforced material due to its thermoplastic and thermosetting characteristics. Thermosetting resins such as epoxy, unsaturated polyester resin, polyester, polyurethane, and phenolic are often used to make a composite material that delivers superior performance in many applications. They give good mechanical qualities, and their pricing is reasonable. Natural fibres attract more attention among academics, researchers, and students because of their good features, such as high strength, low density, and ecological advantages over conventional composites. Due to their non-carcinogenic and bio-degradable, the use of natural composites is rising day by day [6]. In addition to this, the

energy consumption by natural fibres during their manufacture is only 17 percent as opposed to synthetic fibres like glass fibres [7-10]. The use of these composites in many sectors has tremendous potential to improve the pace of manufacturing and recycling with environmental friendliness [10]. Natural fiber polymer composites (NFPC) are a composite material consisting of a polymer matrix interwoven with high strength natural fibers, like jute, oil palm, sisal, kenaf, and flax [10]. Usually, polymers can be divided into two types, thermoplastics and thermosets. The structure of thermoplastic matrix materials comprises one or two-dimensional molecules. Therefore, these polymers tend to make softer at a high heat range and roll back their qualities throughout cooling. On the other hand, thermosets polymer can be characterized as strongly cross-linked polymers cured using only heat, heat and pressure, or light irradiation. This structure contributes to the thermoset polymer's good qualities, such as high flexibility for customizing desired ultimate properties, tremendous strength, and modulus [11, 13]. Thermoplastics extensively employed for biofibers are polyethylene [11], polypropylene (PP) [12], and polyvinyl chloride (PVC), whereas phenolic, polyester, and epoxy resins are mostly utilized in thermosetting matrices [10]. Different factors can alter the features and performance of NPCs. The hydrophilic nature of the natural fiber [14] and the fiber loading both impact the composite characteristics [13]. Usually, considerable fiber loading is needed to acquire good attributes of NPCs [14]. Generally, notice that the increase in fiber content improves the tensile properties of the composites [8]. Another crucial component that greatly affects the properties and surface features of the composites is the process parameters utilized. For that reason, relevant process procedures and parameters should be thoroughly chosen to acquire the best qualities of manufacturing composite [10]. The chemical composition of natural fibers also has a large effect on the qualities of the composite expressed by the percentage of cellulose, hemicellulose, lignin, and waxes.

**NATURAL FIBER POLYMER COMPOSITES APPLICATIONS**

The applications of NFPCs are expanding rapidly in several technical domains. The numerous kinds of natural fibers such as jute, hemp, kenaf, oil palm, and bamboo reinforced polymer composite have great relevance in diverse automotive applications, structural components, packing, and building [14-15]. NFPCs are found in electrical and electronic industries, aerospace, sports, recreation equipment, watercraft, machinery, office items, etc. The widespread application of NFPCs in polymer composites due to its low specific weight, relatively high strength, relatively low production cost, resistance to corrosion and fatigue, totally biodegradable, improving the surface finish of molded part composites, relatively good mechanical properties, available and renewable sources as compared to synthetic fibers [14, 16]. On the other hand, there are physical disadvantages of the NFPCs, such as moisture absorption, restricted processing temperature, and fluctuating quality, which restrict their performance [17].

TABLE 2: Natural fiber composite applications in industry [12-13, 18-20].

<b>Fiber</b>	<b>Applications</b>
Ramie fiber	Use in products as industrial sewing thread, packing materials, fishing nets, and filter cloths. It is also made into fabrics for household furnishings (upholstery, canvas) and clothing, paper manufacture.
Cotton fiber	Furniture industry, textile and yarn, goods, and cordage
Jute fiber	Building panels, roofing sheets, door frames, door shutters, transport, packaging, geotextiles, and chip boards.
Coir fibers	Building panels, flush door shutters, roofing sheets, storage tank, packing material, helmets and postboxes, mirror casing, paper weights, projector cover, voltage stabilizer cover, a filling material for the seat upholstery, brushes and brooms, ropes and yarns for nets, bags, and mats, as well as padding for mattresses, seat cushions
Stalk fiber	Building panel, furniture panels, bricks, and constructing drains and pipelines
Bagasse fiber	Window frame, panels, decking, railing systems, and fencing
Kenaf fiber	Packing material, mobile cases, bags, insulations, clothing-grade cloth, soilless potting mixes, animal bedding, and material that absorbs oil and liquids
Sisal fiber	In construction industry such as panels, doors, shutting plate, and roofing sheets; also, manufacturing of paper and pulp
Flax fiber	Window frame, panels, decking, railing systems, fencing, tennis racket, bicycle frame, fork, seat post, snowboarding, and laptop cases
Oil palm fiber	Building materials such as windows, door frames, structural insulated panel building systems, siding, fencing, roofing, decking, and other building materials
Rice husk fiber	Building materials such as building panels, bricks, window frame, panels, decking, railing systems, and fencing
Hemp fiber	Construction products, textiles, cordage, geotextiles, paper & packaging, furniture, electrical, manufacture bank notes, and manufacture of pipes
Wood fiber	Window frame, panels, door shutters, decking, railing systems, and fencing

**ADVANTAGES OF NATURAL FIBER COMPOSITES**

TABLE 3: Advantages of natural fiber composites.

<b>Advantages</b>	
<b>Dimensional stability</b>	Composites constantly stay in stable conditions. Their shape and size do not change with weather or temperature. On the other hand, wood shrinks and swells when the temperature changes. Therefore, composites have outstanding properties to fit in every environment. That's why it is utilized to make aircraft wings so that wings' shape and size do not alter in any weather or hot or cool.
<b>Strength related to weight</b>	Strength-to-weight ratio is a material feature of the composite material, which offers us information about the material. It gives us a concept of how much that material is strong, heavy or light. Composite materials are not only strong materials but also light materials. That's why composite materials can be employed in aerospace design and automotive industries.
<b>High strength</b>	Metals such as steel or aluminium are employed in construction sectors which are supplied strong strength in all directions. Composite materials can be stronger than other materials and must be designed in a specific direction.
<b>Nonconductive</b>	Composites have non-conductive characteristics. That means composites are unable to conduct electricity. Because of this property, composite materials are utilized to construct electrical utility poles and circuit boards. Sometimes electrical conductivity is needed in the composite materials, and then it is so easy to transform their qualities into conductive materials.
<b>Low thermal conductivity</b>	Natural fiber composites are employed as a good insulator. They are used indoors, windows, and panel structures to protect the buildings from the elements because natural fibre-based composites do not easily conduct cold or heat.
<b>Radar transparent</b>	Composites are used to construct radar equipment, whereas composites material is employed in radar for passing signals on the ground or in the air. Composites play an essential part in manufacturing aircraft such as the U.S. Air Force's B-2 stealth bomber, and this stealth bomber is utilized for transferring signals.
<b>Nonmagnetic</b>	Composites have nonmagnetic qualities, and that is the sole reason composite materials can be utilized in creating houses and tables, used around the electronic equipment, and used as a reinforced material used to build concrete walls and floors in the hospital.
<b>Corrosion resistance and high-impact strength</b>	Composites have good corrosion-resistant and high impact strength qualities. It can absorb any items, and also it can prevent damage from the weather. Composite has strong chemical resistance qualities. It can become severe in any temperature or condition. Composite materials can be able to absorb any unexpected force. Because of this ability, composites are used to manufacture bulletproof jackets and panels and to screen aeroplanes, buildings, and military vehicles from explosions.
<b>Durable</b>	When composites are utilized to build a structure, they have a long life and need little upkeep. Many composites can serve roughly half a century. But we do not know how long a composite structure can be demonstrated its endurance, and we do not know when original composites have ended.
<b>Light weight</b>	Composites are lightweight materials that's why it is employed in aerospace and automotive applications. Composite materials' weight is lighter than many other materials such as wood and metals. Nowadays, composite materials are used in building modern aeroplanes (i.e. Boeing 787 Dreamliner, Cockpit) since they are now more worried about fuel efficiency, which is only achievable if we use lightweight composite material.

**CHALLENGES IN USING NATURAL FIBRES**

Among so many positives, natural fibers also hold some downsides when they are utilized to build composite materials. Natural fibers have several shortcomings regarding their performance. The behaviour is changed when the polymer is added for manufacturing and processing new composite. The physical properties of the natural fiber are not uniform. Their physical attributes vary with harvesting season and harvesting reign. Natural fibers attribute variance depends on the harvesting procedure, locale, and maturity of the plant and manufacturing process of the fibers, woven or unwoven. All these elements affect the characteristics of the natural fiber composites. [21] The manufacturing cost of the products created from natural fibers is often high. When natural fiber composites are used as construction materials, it also shows several faults such as inferior durability due to high moisture, chemical absorption, concrete fractures due to swelling and volume fluctuations, and poor compatibility with polymeric or cementitious matrices. Their low compatibility with numerous polymeric matrices yields non-uniform results. To overcome these limitations, certain modifications of the natural fibers are needed, such as treatment with alkali, saline, and water-repelling agents, to promote adhesion between matrix chemical coupling or compatibilism [22] methods many researchers have been already used plasma modification of natural fibers. These methods help reduce the water absorption of the natural fiber by removing hemicellulose and lignin or by imparting hydrophobicity and also help to improve the interface between natural fiber and the polymeric matrix. Chemical coupling agents are utilized to treat the surface of the matrix. Another issue is the less rigidity of the composite materials. In the construction industry, the stiffness of the materials or composites is a vital aspect of designing any civil engineering project. Though natural fiber composites have excellent strength, their stiffness is lower than other composites. Overdesigned structures are necessary to tackle the problem. [23-24] Another significant downside of the usage of fibers is inadequate temperature stability. Natural fibers can sustain temperatures

up to 2000 C. Over this temperature, natural fibers are begun to decay and shrink, and because of low thermal stability, natural fiber composites show worse performance than other materials. To avoid this problem, the range of processing time and the temperature has to be controlled. [25-27]

## CONCLUSION

Natural fiber is a biodegradable, eco-friendly and renewable raw material. Natural fiber provides strong thermal insulating capabilities and good mechanical properties. But the strength of the natural fiber relies on the loading applied to the fiber and the young modulus of the fiber. It also depends on the fiber weight ratio, cultivation process, fiber extracting procedure from the plant, harvesting period, manufacturing process, and the fabrication methods of the natural fiber with polymeric matrices. Natural fiber composites combine two different materials that generate new versatile materials in industrial, engineering and technology. This study presents an overview of the natural fibers, varieties of natural fiber, physical and mechanical properties, and advantages of the natural fiber. It discusses the natural fibres' limitations over other materials. In a nutshell, natural fiber is rising hastily in industrial use. Already much research work is done, but still, further research and investigation are required to overcome the limitations of the natural fiber such as stiffness of composites, moisture effect, an alkaline solution, fatigue, creep and physical degradation, moisture absorption toughness and reduced long term stability for outdoor application. Many academics are greatly interested in completing their study work on natural fiber and natural fibre-based composites. Therefore, the research effort on the natural fiber-based composite materials has risen by leaps and bounds over the past few years because of their durability, renewable, entirely or partially recyclable qualities. Despite all of these abovementioned concerns, some sectors are employing natural fibers to build innovative products. The automotive and aerospace industries are the most active users of natural fibre-based composites, which manufactures non-structural and semi-structural parts; other industries are gradually paying more attention to making products using natural fiber composites, such as sports, medical, furniture, packaging materials, among others.

## REFERENCES

- [1] May-Pat A, Valadez-Gonzalez A and Herrera-Franco P J. 'Effect of fiber surface treatments on the essential work of fracture of HDPE continuous henequen fiber-reinforced composites. *Polymer Testing*, 2013, 32(6): 1114-1122. <https://doi.org/10.1016/j.polymertesting.2013.06.006>
- [2] Saira T, Munawar MA and Khan S. Natural Fiber Reinforced Polymer Composites. *Proceedings of the Pakistan Academy of Sciences*, 2007, 44(2): 129-144
- [3] Faruk O, Bledzki AK, Fink HP, et al. Biocomposites Reinforced with Natural Fibers: 2000-2010. *Progress in Polymer Science*, 2012, 37(11): 1552-1596. <https://doi.org/10.1016/j.progpolymsci.2012.04.003>
- [4] Nguong CW, Lee SNB and Sujun D. A Review on Natural Fibre Reinforced Polymer Composites. *International Journal of Materials and Metallurgical Engineering*, 2013, 7(1): 52-59
- [5] Shalwan, A., and B. F. Yousif. 2013. "In State of Art: Mechanical and Tribological Behaviour of Polymeric Composites Based on Natural Fibres." *Materials & Design* 48: 14–24. doi:10.1016/j.matdes.2012.07.014.
- [6] Keya, K. N., Kona, N. A., Koly, F. A., Maraz, K. M., Islam, M. N., & Khan, R. A. (2019). Natural fiber reinforced polymer composites: history, types, advantages, and applications. *Materials Engineering Research*, 1(2), 69–87. <https://doi.org/10.25082/mer.2019.02.006>
- [7] Holbery, J., and D. Houston. 2006. "Natural-Fiber-Reinforced Polymer Composites in Automotive Applications." *JOM Journal of the Minerals, Metals and Materials Society* 58 (11): 80–86. doi:10.1007/s11837-006-0234-2.
- [8] Dhakal, H. N., Z. Y. Zhang, and M. O. W. Richardson. 2007. "Effect of Water Absorption on the Mechanical Properties of Hemp Fibre Reinforced Unsaturated Polyester Composites." *Composites Science and Technology* 67 (7–8): 1674–1683. doi:10.1016/j.compscitech.2006.06.019.
- [9] Kumar, R., Ul Haq, M. I., Raina, A., & Anand, A. (2019). Industrial applications of natural fiber-reinforced polymer composites challenges and opportunities. *International Journal of Sustainable Engineering*, 12(3), 212–220. <https://doi.org/10.1080/19397038.2018.1538267>
- [10] Bledzki, A. K., and J. Gassan. 1999. "Composites Reinforced with Cellulose Based Fibres." *Progress in Polymer Science* 24 (2): 221–274. doi:10.1016/S0079-6700(98)00018-5.
- [11] O. Faruk, A. K. Bledzki, H.-P. Fink, and M. Sain, "Biocomposites reinforced with natural fibers: 2000–2010," *Progress in Polymer Science*, vol. 37, no. 11, pp. 1552–1596, 2012
- [12] Mohammed, L., Ansari, M. N. M., Pua, G., Jawaid, M., & Islam, M. S. (2015). A Review on Natural Fiber Reinforced Polymer Composite and Its Applications. *International Journal of Polymer Science*, 2015. <https://doi.org/10.1155/2015/243947>
- [13] A. Ticoalu, T. Aravinthan, and F. Cardona, "A review of current development in natural fiber composites for structural and infrastructure applications," in *Proceedings of the Southern Region Engineering Conference (SREC '10)*, pp. 113–117, Toowoomba, Australia, November 2010.
- [14] A. Shalwan and B. F. Yousif, "In state of art: mechanical and tribological behaviour of polymeric composites based on natural fibres," *Materials & Design*, vol. 48, pp. 14–24, 2013.
- [15] E. Sassoni, S. Manzi, A. Motori, M. Montecchi, and M. Canti, "Novel sustainable hemp-based composites for application in the building industry: physical, thermal and mechanical characterization," *Energy and Buildings*, vol. 77, pp. 219–226, 2014.
- [16] S. Shinoj, R. Visvanathan, and S. Panigrahi, "Towards industrial utilization of oil palm fibre: physical and dielectric characterization of linear low density polyethylene composites and comparison with other fibre sources," *Biosystems Engineering*, vol. 106, no. 4, pp. 378–388, 2010.
- [17] E. Gallo, B. Scharrel, D. Acierno, F. Cimino, and P. Russo, "Tailoring the flame retardant and mechanical performances of natural fiber-reinforced biopolymer by multi-component laminate," *Composites Part B: Engineering*, vol. 44, no. 1, pp. 112–119, 2013.

## ***The International Symposium on Polymeric Materials 2022***

- [18] T. Sen and H. N. Reddy, "Various industrial applications of hemp, kinaf, flax and ramie natural fibres," *International Journal of Innovation, Management and Technology*, vol. 2, pp. 192–198, 2011.
- [19] U. S. Bongarde and V. D. Shinde, "Review on natural fiber reinforcement polymer composite," *International Journal of Engineering Science and Innovative Technology*, vol. 3, no. 2, pp. 431–436, 2014.
- [20] L. Mwaikambo, "Review of the history, properties and application of plant fibres," *African Journal of Science and Technology*, vol. 7, no. 2, p. 121, 2006.
- [21] O'Donnell A, Dweib MA and Wool RP. Natural fiber composites with plant oilbased resin. *Composites Science and Technology*, 2004, 64: 1135-1145. <https://doi.org/10.1016/j.compscitech.2003.09.024>
- [22] Bismarck A, Mishra S and Lampke T. Plant fibers as reinforcement for green composites, In: Mohanty AK, Misra M, Drzal TL, editors. *Natural fibers, biopolymers, and biocomposites*, Boca Raton: Crc Press-Taylor & Francis Group. 2005.<https://doi.org/10.1201/9780203508206.ch2>
- [23] Fan M. Future scope and intelligence of natural fibre based construction composites. *Advanced High Strength Natural Fibre Composites in Construction*, 2017, 545-556. <https://doi.org/10.1016/B978-0-08-100411-1.00022-4>
- [24] Nagavally RR. *Composite Materials - History, Types, Fabrication Techniques, Advantages, and Applications*. *International Journal of Mechanical And Production Engineering*, 2017, 5(9): 2320-2092.
- [25] Charoenvaisarocha AC, Jongjit H and Joseph K. Materials and mechanical properties of pretreated coir-based green composites. *Composites: part B*, 2009, 40: 633-637. <https://doi.org/10.1016/j.compositesb.2009.04.009>
- [26] Chadramohan D and Marimuthu k. Tensile and Hardness Tests on Natural Fiber Reinforced Polymer Composite Material. *International Journal of advanced engineering science and technologies*, 2011, 6(1): 97-104.
- [27] A. S. Norfarhana, R. A. Ilyas, and N. Ngadi. A review of nanocellulose adsorptive membrane as multifunctional wastewater treatment, *Carbohydr. Polym.*, 2022, 291: 119563. <https://doi.org/10.1016/j.carbpol.2022.119563>.



## TEMPORARY SOUND BARRIER SYSTEM FROM RICE HUSK POLYMERIC COMPOSITE

H. M. Ariff<sup>1,2\*</sup>, D. W. Jung<sup>3</sup>, T. H. Rafin<sup>1</sup>, Z. Leman<sup>1,2</sup>, K. A. M. Rezali<sup>1</sup>, R. Calin<sup>4</sup>.

<sup>1</sup>Department of Mechanical and Manufacturing Engineering, Faculty of Engineering, Universiti Putra Malaysia, Serdang 43400, Selangor, Malaysia.

<sup>2</sup>Advance Engineering Materials and Composites Research Center, (AEMC), Faculty of Engineering, Universiti Putra Malaysia, Serdang 43400, Selangor, Malaysia.

<sup>3</sup>Department of Mechanical Engineering, Jeju National University, 1 Ara I-dong, Jeju 690-756, Korea.

<sup>4</sup>Material Engineering Department, Engineering Faculty, Kirikkale University, Kirikkale, Turkey.

---

### ABSTRACT

Sound barriers, rather than shutting off the source of noise, are the most effective method for reducing noise pollution and reducing the intensity from diverse sources. Because of low toxicity and environmental safety, natural fiber may be a good and prominent source for sound absorption material. The sound barrier's efficacy will be improved by using natural fiber-reinforced composite material. This method has the benefit of not only reducing noise transmissibility but also potentially lowering the cost of sound barriers, which is particularly advantageous in the Malaysian context. The main aim of this research is to develop a sound barrier made of rice husk which can reduce the transmission of noise by reinforcing the PU polymeric materials in the design. The scope of this research is to perform Harmonic Analysis through ANSYS to know the sound absorbing coefficient and transmission loss. To have better understanding on the sound absorption coefficient and transmission loss the frequency range on the simulation was set between 0 to 4000 Hz. The result showed better sound absorption coefficient on the lower frequency region while showing higher transmission loss at a higher frequency region since high frequency means high sound intensity level.

*Keywords:* temporary sound barrier, rice husk, polymeric composite, harmonic analysis.

---

### INTRODUCTION

In populated areas, noise pollution is one of the contaminants which has a significant effect on the public environment. Noise pollution nearby housing area especially can disrupt every day's life. Construction is one of the key contributors to noise emissions. Machine sounds such as stacking, welding, banging, hammering, or even shipping of goods cause noise. To avoid noise emissions, a permitted noise cap is necessary. Various sound barriers are used nowadays to assist in reducing the noise to a permissible level. From mineral wool to fiberglass, various ranges of sound barriers can be made. Due to technology development and public awareness about noise in daily life, the use of a variety sound-absorbing materials has increased significantly [1,2]. Natural fiber can be an excellent and sustainable source for sound absorption material because of its low toxicity, sustainability, abundance, renewable, and most importantly, it is biodegradable. Apart from that, the manufacturing of natural fibrous sound absorbers involves a significantly lower carbon footprint compared to conventional synthetic sound absorbers. Researchers have now been drawn to apply natural fibers as sound absorption composites. Natural fibers are entirely biodegradable, and new technological advances will make its manufacturing process economical. Kenaf, bamboo, cotton, cork, cane, cardboard, sheep-wool pineapple fibers, Arenga Pinata fiber, coconut coir fiber, and rice-husk grains are few examples of natural fibers with strong potency to be grown as a sonorous product [1,2].

Palm oil fiber, rice husk, and kenaf are the three natural fibers found abundant in Malaysia. Natural fiber has attributes to be used as sound absorbing material due to its porous nature, rigid and the cross section of the fiber have cavities which when connected to the porosity of the surface, can be used entirely to trap and absorb the sound wave inside the structure [2]. Porous materials function well for medium to high-frequency sound absorption. Few scientists have researched the possibility of using natural fiber as sound-absorbing material worldwide due to its low density and its high porosity, which is very critical for the

---

#### *Article history:*

Received: 10 March 2022

Accepted: 7 June 2022

Published: 14 June 2022

---

#### *E-mail addresses:*

azmah@upm.edu.my (A. H. M. Ariff)

jungdw77@naver.com (D. W. Jung)

tahrim.rafin@gmail.com (T. H. Rafin)

zleman@upm.edu.my (Z. Leman)

khairilanas@upm.edu.my (K. A. M. Rezali)

recepcalin@gmail.com (R. Calin)

\*Corresponding Author

process of sound absorption to dissipate acoustic energy within the structure. In order to achieve a sound barrier made of natural fiber, the polymeric composite of the natural fiber needs to be fabricated with suitably selected fiber size with reduced diameter, which increases sound absorption at low frequencies by having a more tortuous route and a larger surface area, which improves the fibrous material's airflow resistivity. The increase in airflow resistivity induces sound energy loss by sound wave friction with air molecules, improving low-frequency sound absorption [2, 3].

This study will focus on the simulation of an acoustic panel that is made from rice husk polymeric composite. The simulation process involves the measurement of the sound absorption coefficient (SAC), which will help to develop and analyze the best sound barrier. The simulation will also help

to get comparative results on the sound barrier for various ranges of frequencies. The aim is to evaluate the possibility of using rice husk as a candidate material for temporary sound barrier in housing construction.

**MATERIALS AND METHODS**

*Materials*

The material selected for this study is rice husk reinforced PU polymer. TABLE 1 is showing the values of the porosity, density, fiber diameter, and SAC for rice husk taken from published literature [1, 4].

TABLE 1: Porosity, Density, Fiber Diameter, and SAC of rice husk.

Natural Fiber	Porosity (%vol)	Density (Kg/m <sup>3</sup> )	Fiber diameter (µm)	SAC @250Hz
Rice Husk	70%	300	250 to 380	0.889

In this study, there is only one design and ratio of the material in mind. According to some literature, it was studied that rice husk with polyurethane foam shows the best sound absorption coefficient. It was also found that rice husk, when used in 25% of the mixture with the polyurethane foam, shows the best SAC than any other percentage of rice husk. For this reason, the rice husk in this study is 25% along with 75% polyurethane foam. The ratio of the materials was kept at 1:3 in designing the panel.

*Methods*

The numerical analysis was performed in the ANSYS platform with the Harmonic Analysis. The noise barrier was modeled in SOLIDWORKS, and then later, the geometry was shifted to ANSYS for further analysis. Dimension of the panel used in the simulation is 30 mm thickness x 500 mm width x 1980 mm length. In the Material Library of ANSYS, the material composite rice husk with polyurethane foam were not found due to the shortage of data in the ANSYS Material library. For this, the data of the materials were added manually to run the simulation with our selected materials.

Harmonic analysis simulation was done in Modal, Harmonic response, and Harmonic Acoustic analysis to find the transmission loss, and sound absorption coefficient. For the Modal analysis, the analysis settings and Fixed support were set up for the frequency ranging from 100 Hz to 4000 Hz. Subsequently, this setup was done after meshing. The meshing was done with 3756 nodes and 528 elements. Further, the simulation was run with necessary acoustic boundary conditions (Radiation Boundary and Port Inlet and Outlet) and acoustic excitation (Mass source and Surface Velocity), where the acoustic region is the enclosure and physics region is the panel. The acoustic medium surrounding the sound barrier and the sound source was created as the domain in which acoustic waves propagate. Zero pressure was applied on the outer faces to ensure absorption of outgoing waves, whereby no reflection will be considered in the simulation. The sound pressure level in the computational domain was then calculated, representing the effect of sound isolation of a particular noise barrier.

**RESULTS AND DISCUSSION**

*Sound absorption coefficient*

The SAC is usually evaluated to know how much energy is absorbed by the material compared to the incident energy. Sound or noise, which is a form of energy, can lose some of its strength while passing through a material which defines its sound absorbing quality. Material with good sound absorbent quality has more sound absorption coefficient. The higher value means that the material can easily absorb more of the sound energy, resulting in less noise or sound on the other side of the material. The sound absorption coefficient of this sound barrier panel is presented in the graph below in Fig. 1 in terms of various frequencies. With different frequency inputs, the sound absorption coefficient shows different values.

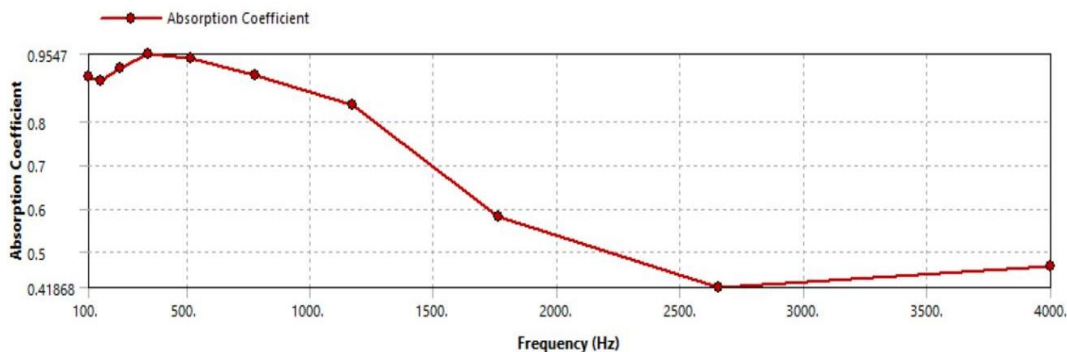


Fig. 1: Graph of SAC at different range of frequencies.

As seen in the graph, the SAC of the panel shows good SAC from the frequency ranging from 100Hz to 1500Hz. At 2700Hz, the panel shows the lowest frequency, which is almost 0.41, and from there, the SAC very slightly rises as the frequencies increases. The graph here shows how well the sound barrier material can absorb the sound energy at various frequencies. It can be concluded that the SAC showing peak values in the range between 100 Hz to 1500 Hz, can absorb the most sound or sound energy which is enough for the mentioned frequency region.

*Transmission loss*

Another critical factor in knowing how well a sound barrier perform in transmission loss. Transmission loss can vary at a different frequency depending on the intensity of the sound. Transmission loss means that the amount of sound intensity loss. The ratio of the transmitted power with the incident power shows how much transmission is being lost. Transmission loss in a sound-absorbing material is a prevalent factor where the more the loss, the more effective the material is for sound absorption. The transmission loss shows greater results at a greater sound intensity which is usually found in higher frequencies. The simulated transmission loss graph with frequency is shown below in Fig. 2

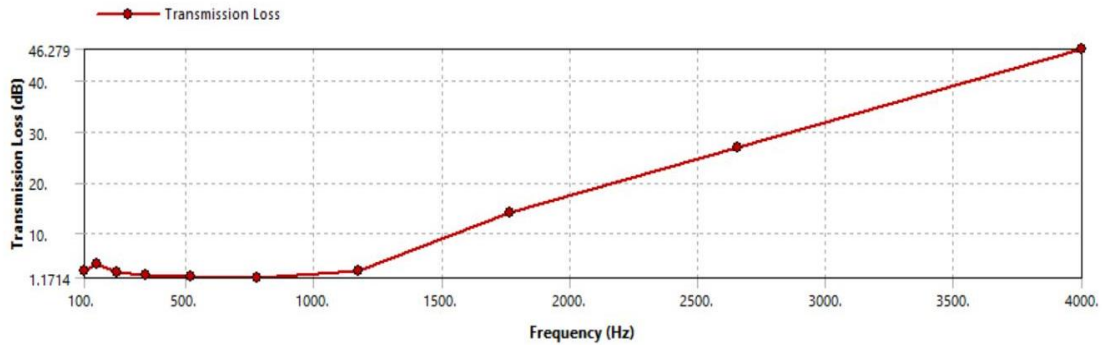


Fig. 2: Graph of Transmission loss at different ranges of frequencies.

The transmission loss shown in Fig. 2 has different transmission values at different frequencies. As it can be seen that ranging from 100Hz to 1200Hz, the transmission loss is very negligible and can be valued around 1.19 dB, but as the frequency increases from 1200Hz, the transmission loss increases and reaches a peak value of 46.27 dB at 4000Hz. The reason for showing less transmission loss at the beginning is that the sound ranging from 100Hz to 1200Hz has significantly less intensity which means the incident power of the sound is already low, and the transmitted power is 1.17 to 2 dB lower than the incident power. For this reason, the transmission loss at the beginning is shallow. When the frequency range gradually increases from 1200Hz, the transmission loss starts to increase with the frequency. It is because the higher frequency has higher sound intensity, which means the incident power is more and needs to be minimized to reach comfortable hearing range. For this reason, the transmission loss is higher at the end range of the frequency. It does not have to be consistently high transmission loss at all the frequency range. High transmission loss is required more when the sound intensity level is higher. Usually, the sound intensity levels for humans is considered as high from range 90 dB onwards.

**CONCLUSIONS**

The designs were made based on the concept of natural fiber composite. The natural fiber composite used in this research was Rice Husk-PU reinforced composite, which was designed and simulated using ANSYS software. An effective sound barrier was designed and modeled to achieve acceptable SAC and transmission loss. From the data analyzed, it can be concluded that the panel has higher transmission loss at a higher frequency which was explained in the discussion for what reason the transmission value needs to be higher at a specific frequency region. All the data were evaluated and analyzed in the frequency range of 100 Hz to 4000 Hz. The result showed better sound absorption coefficient on the lower frequency region while showing higher transmission loss at a higher frequency region since high frequency means high sound intensity level. This opens up the possibility for its utilization as a temporary natural sound barrier made of natural fiber composite.

**ACKNOWLEDGEMENTS**

The authors would like to thank Universiti Putra Malaysia for the financial support through the Research Management Center of Universiti Putra Malaysia (UPM/GP-IPB/2020/9688700).

**REFERENCES**

- [1] M. N. Yahya, M. Sambu, H. A. Latif, and T. M. Junaid, "A study of Acoustics Performance on Natural Fibre Composite," *IOP Conf. Ser. Mater. Sci. Eng.*, vol. 226, pp. 1-8, 2017, doi: 10.1088/1757-899X/226/1/012013.
- [2] P. Hassani, P. Soltani, M. Ghane, and M. Zarrebini, "Porous resin-bonded recycled denim composite as an efficient sound-absorbing material," *Applied Acoustics*, vol. 173, pp. 1-10, 2021, doi.org/10.1016/j.apacoust.2020.107710.
- [3] T. Yang, L. Hu, X. Xiong, M. Petr, M.T. Noman, R. Mishra, and J. Militký, "Sound absorption properties of natural fibers: A review," *Sustain.*, vol. 12, no. 20, pp. 1–25, 2020, doi: 10.3390/su12208477.
- [4] Z. Chen, Y. Xu, and S. Shivkumar, "Microstructure and tensile properties of various varieties of rice husk," *J. Sci. Food Agric.*, vol. 98, no. 3, pp. 1061–1070, 2018, doi: 10.1002/jsfa.8556.

## **BIODEGRADABLE SYNTHETIC POLYMER IN ORTHOPAEDIC APPLICATION: A REVIEW**

F. D. Al-shalawi<sup>1</sup>, M. A. A. Hanim<sup>1,4</sup>, M. K. A. Ariffin<sup>1</sup>, C. L. S. Kim<sup>2</sup>, D. Brabazon<sup>3</sup>, R. Calin<sup>5</sup>, M. O. Alosaimi<sup>6</sup>

<sup>1</sup>Department of Mechanical and Manufacturing Engineering, Faculty of Engineering, Universiti Putra Malaysia, 43400 Serdang, Selangor, Malaysia

<sup>2</sup>Department of Orthopaedic, Faculty of Medicine and Health Sciences, Universiti Putra Malaysia, 43400 Serdang, Selangor, Malaysia

<sup>3</sup>Advanced Manufacturing Research Centre, and Advanced Processing Technology Research Centre, School of Mechanical and Manufacturing Engineering, Dublin City University, Dublin, Ireland

<sup>4</sup>Research Center Advance Engineering Materials and Composites (AEMC), Faculty of Engineering, Universiti Putra Malaysia, Serdang 43400, Malaysia

<sup>5</sup>Material Engineering Department, Engineering Faculty, Kırıkkale University, Kırıkkale, Turkey.

<sup>6</sup>Department of Cell and Molecular Biology, Faculty of Biotechnology and Bimolecular Sciences, Universiti Putra Malaysia, 43400 Serdang, Selangor, Malaysia

---

### **ABSTRACT**

Every year, many people suffer from bone fractures because of accidents or diseases. Majority of these fractures are too complicated to be treated with conventional medicine and must be mended surgically using non-degradable metal implants. Such treatment can cause refusal and stress shielding but may also require a second surgery to remove the metal implants. In addition, biodegradable metals that can readily erode inside the human body come with certain complications. These aspects prompted scientists to find alternatives to metals. Some researchers began to focus on the field of polymers which have shown significant promise in replacing metals. In orthopedics, degradable polymeric fixation appliances are being studied to substitute metallic implants, eliminating stress shielding and evading a second operation for implant removal. The new generation of bioabsorbable and degradable polymeric implants are free of toxic and mutagenic effects. However, these implants have several issues, including mechanical stiffness and strength limitations, unfavourable tissue responses, foreign-body reactions, a late-degradation tissue response, and infection due to its crystallinity and hydrophobicity. This review discusses the alternative synthetic polymer implants materials available that can be employed and their properties.

*Keywords:* orthopedic, synthetic polymer, biodegradable, bioabsorbable.

---

### **INTRODUCTION**

Bone is a natural compound in living tissue that contains roughly 30% matrix, 60% minerals, and 10% water [1]. Bone submits numerous functions including major backing skeleton designed construction, the binding site for ligaments, muscles and tendons, mechanical support and protection of most vital tissues [2]. Every year, many people suffer from bone fractures because of accidents or diseases. Majority of these fractures are too complicated to be treated with conventional medicine and must be mended surgically using non-degradable metal implants. Such treatment can cause refusal and stress shielding but may also require a second surgery to remove the metal implants. In addition, this type of cure can worsen physical suffering and places a significant financial burden on patients [3, 4]. In addition, the metals readily corroded inside the human body and becomes toxic due to their ions if its available in high concentration [5, 6]. These aspects prompted scientists to research alternatives to metals. As a result, orthopaedic implants have progressed to steadily improve their interaction with surrounding bone tissue to ensure successful results for patients. The beneficial biological interaction between the implant and the surrounding bone relies on a mixture of physical, mechanical, and topological characteristics [7]. Some researchers began to focus on the field of polymers which have shown significant promise in replacing metals [8]. In orthopaedics, bioabsorbable polymeric fixation devices have been employed to substitute metallic implants, eliminating stress shielding and evading a second operation for implant removal [9]. The new generation of bioabsorbable and degradable polymeric implants are free of toxic and mutagenic effects. However, these implants have several issues, involving mechanical stiffness and strength restrictions, unfavourable tissue responses, foreign-body reactions, a late-degradation tissue response, and infection due to its crystallinity and hydrophobicity [10].

---

#### *Article history:*

Received: 10 March 2022

Accepted: 7 June 2022

Published: 14 June 2022

---

#### *E-mail addresses:*

faisalalshe22@gmail.com (F. D. Al-Shalawi)

azmah@upm.edu.my (M. A. A. Hanim)

\*Corresponding Author

#### *Biomaterial*

Biomaterials are defined as materials that interact with biological systems to repair, assess, or replace any tissue, organ, or system in the body [11]. The use of biomaterials to treat the human body is not new, as it dated back to ancient civilizations. Around 2000 BC, the Egyptians used elephant ivories to replace missing teeth [12]. Artificial legs, eyes, and teeth were employed, according to ancient Indian literature from the Vedic period (1800–1500 BC) [13].

### *Polymer*

The word "polymer" is a Greek term derived from poly and meros, meaning many and parts, respectively [14, 15]. Instead of polymer, some scientists prefer the term macromolecule or huge molecule [16]. Natural and synthetic polymers are the present and future biomaterials for orthopedic applications and bone tissue engineering; due to their capability to imitate the natural extracellular matrix (ECM) in future [17]. The utilization of polymer as a biomaterial was by chance. It was observed that World War II pilots who were wounded by slivers of polymethyl methacrylate (PMMA) did not suffer any negative established reactions from the existence of the plastic fragments [18]. Polymers were classified into two main categories, synthetic and natural, and each section was divided into two parts, biodegradable and non-degradable [19, 20].

### *Natural polymer*

The first biodegradable biomaterials used medically were natural polymers. Contrasted to traditional synthetic materials, natural polymers display excellent chemical versatility, superior biodegradability, and ameliorated biological performance [21]. The natural polymers include the following polymers: Chitosan, collagen, gelatin, silk, alginate, cellulose and hyaluronic acid. Collagen, Chitosan, and chitin are the most widely used natural polymers for bone tissue engineering applications [17].

### *Synthetic polymer*

Synthetic biopolymers might have better mechanical characteristics and thermal steadiness than natural polymers. Poly ( $\alpha$ -hydroxy acids) group of artificial biopolymers has been examined widely. The most extensively employed of these polymers are poly (lactic acid) (PLA), poly(glycolic acid) (PGA), and poly(lactic-co-glycolic acid) (PLGA) which are bioabsorbable or degradable under in vivo conditions and work as an appropriate matrix for regenerative medicine [22].

### *Poly (glycolic acid) (PGA)*

Polyglycolide was the first biodegradable polymer used as screws, plates, and nails in bone surgery. It is a stiff and rigid polymer with an average molecular weight ranging from  $2.0 \times 10^4$  to  $1.45 \times 10^5$ , melts at about 224 °C, and has a highly crystalline structure. Although its removal time is 6–12 months, due to its rapid deterioration characteristic, PGA shows an early loss of mechanical strength in vivo, approximately 4-7 weeks after transplantation. Moreover, when used in orthopedic surgery, ossification using PGA was correlated with adverse effects such as fluid accumulation, swelling, and sinus fashioning [23].

#### i. Poly (lactic acid) (PLA)

Poly (lactic acid) is a biodegradable, thermoplastic aliphatic polyester made from naturally occurring organic acid (lactic acid) [24]. PLA is a biopolymer with numerous unique properties, including good transparency, a glossy look, high stiffness, and outstanding processability, making it an environmentally and commercially appealing biopolymer. However, it has certain drawbacks, including intrinsic brittleness, weak toughness (less than 10% elongation at break), and a sluggish degradation rate, limiting its use [25]. PLA has shown its potential as a biomaterial in varied medical applications, such as tissue engineering, regenerative medicine, and orthopaedic. PLA has manifested helpful significance as a (3D) printable biopolymer [26].

#### ii. Poly (lactide-co-glycolide)

This co-polymer merges the advantages of PLLA and PGA with adjustable degradation, hydrolysis, and biocompatibility. PLGA experiences hydrolytic degradation into principle acidic components lactic and glycolic acid that is biologically harmful and have to be expelled to avert complications. To decrease the amount of acidic byproducts emitted, PLGA has been combined with ceramics such as  $\beta$ -tricalcium phosphate and hydroxyapatite [27].

#### iii. Poly(caprolactone)

PCL is a semicrystalline, biodegradable, non-toxic, aliphatic polyester, with a low melting point (59 - 64 °C) [28], which can be utilised for easy production of scaffolds for tissue engineering, bone and cartilage repair, surgical sutures, and drug-delivery systems. The main disadvantages of PCL are its hydrophobicity, which is detrimental to cell adhesion and penetration, and its slow degradation, which can last up to 3 or 4 years, despite the fact that it is more stable, cheaper, more readily available, and of greater quality than polyhydroxy acids. Amendment of its characteristics can be performed by co-polymerization or merging with other polymers [29].

## **CONCLUSIONS**

Degradable synthetic polymer implants are excellent alternative to metal implants, but the materials on its own need more research, analysis and improvement before it can be deemed safe to be use as orthopedic implants. Aspects that can be improved are the mechanical properties, rate of degradation and biocompatibility.

## **ACKNOWLEDGEMENTS**

The authors would like to acknowledge Universiti Putra Malaysia (UPM) for providing necessary resources, Research Grant (UPM/GP-IPB/2020/9688700).

REFERENCES

- [1] V. K. Bommala, M. G. Krishna, and C. T. Rao, "Magnesium matrix composites for biomedical applications: A review," *J. Magnes. Alloy.*, vol. 7, no. 1, pp. 72–79, 2019, doi: 10.1016/j.jma.2018.11.001.
- [2] J. Pajarinen *et al.*, "Mesenchymal stem cell-macrophage crosstalk and bone healing," *Biomaterials*, vol. 196, pp. 80–89, 2019.
- [3] D. Kudo *et al.*, "An epidemiological study of traumatic spinal cord injuries in the fastest aging area in Japan," *Spinal Cord*, vol. 57, no. 6, pp. 509–515, 2019.
- [4] C. Sukotjo, T. J. Lima-Neto, J. F. S. Júnior, L. P. Faverani, and M. Miloro, "Is there a role for absorbable metals in surgery? A systematic review and meta-analysis of Mg/Mg alloy based implants," *Materials (Basel)*, vol. 13, no. 18, 2020, doi: 10.3390/MA13183914.
- [5] A. Mirzajavadkhan, S. Rafieian, and M. H. Hasan, "Toxicity of Metal Implants and Their Interactions with Stem Cells: A Review," *Int. J. Eng. Mater. Manuf.*, vol. 5, no. 1, pp. 2–11, 2020, doi: 10.26776/ijemm.05.01.2020.02.
- [6] B. Priyadarshini, M. Rama, Chetan, and U. Vijayalakshmi, "Bioactive coating as a surface modification technique for biocompatible metallic implants: a review," *J. Asian Ceram. Soc.*, vol. 7, no. 4, pp. 397–406, 2019, doi: 10.1080/21870764.2019.1669861.
- [7] F. Bartolomeu, N. Dourado, F. Pereira, N. Alves, G. Miranda, and F. S. Silva, "Additive manufactured porous biomaterials targeting orthopedic implants: A suitable combination of mechanical, physical and topological properties," *Mater. Sci. Eng. C*, vol. 107, p. 110342, 2020, doi: 10.1016/j.msec.2019.110342.
- [8] S. Krishnakumar and T. Senthilvelan, "Polymer composites in dentistry and orthopedic applications—a review," *Mater. Today Proc.*, vol. 46, no. xxxx, pp. 9707–9713, 2019, doi: 10.1016/j.matpr.2020.08.463.
- [9] L. Figueiredo, R. Fonseca, L. F. V. Pinto, F. C. Ferreira, A. Almeida, and A. Rodrigues, "Strategy to improve the mechanical properties of bioabsorbable materials based on chitosan for orthopedic fixation applications," *J. Mech. Behav. Biomed. Mater.*, vol. 103, p. 103572, 2020, doi: 10.1016/j.jmbbm.2019.103572.
- [10] Y. Matsuda, M. Karino, T. Okui, and T. Kanno, "Complications of Poly-L-Lactic Acid and Polyglycolic Acid (PLLA/PGA) Osteosynthesis Systems for Maxillofacial Surgery: A Retrospective Clinical Investigation," *Polymers (Basel)*, vol. 13, no. 6, p. 889, 2021.
- [11] A. Mehboob, S. H. A. Rizvi, S. H. Chang, and H. Mehboob, *Comparative study of healing fractured tibia assembled with various composite bone plates*, vol. 197. Elsevier Ltd, 2020.
- [12] E. Marin, F. Boschetto, and G. Pezzotti, "Biomaterials and biocompatibility: An historical overview," *J. Biomed. Mater. Res. - Part A*, vol. 108, no. 8, pp. 1617–1633, 2020, doi: 10.1002/jbm.a.36930.
- [13] S. Ramakrishna, M. Ramalingam, T. S. Sampath Kumar, and W. O. Soboyejo, *Biomaterials: A nano approach*. 2016.
- [14] P. Yenagolla, K. Sandeep, and J. V. S. Sharma, "EPRA International Journal of Research and Development ( IJRD ) NATURAL POLYMERS AND ITS APPLICATIONS-A REVIEW EPRA International Journal of Research and Development ( IJRD )," vol. 7838, no. January, pp. 6–15, 2022.
- [15] V. Kumar, L. T. Jule, and K. Ramaswamy, "8 Conducting Polymers for," *Conduct. Polym. Adv. Energy Appl.*, p. 139, 2021.
- [16] A. M. Abbas, A. S. Mhammedtaib, and N. H. M. Saeed, "Synthesis and characterization of linear thermally stable polyester contain schiff bases," *Egypt. J. Chem.*, vol. 63, no. 8, pp. 2999–3013, 2020, doi: 10.21608/ejchem.2020.25217.2526.
- [17] S. Chahal, A. Kumar, and F. S. J. Hussian, "Development of biomimetic electrospun polymeric biomaterials for bone tissue engineering. A review," *J. Biomater. Sci. Polym. Ed.*, vol. 30, no. 14, pp. 1308–1355, 2019, doi: 10.1080/09205063.2019.1630699.
- [18] D. M. B. James, "Remodeling Life and Living - A Review of Advanced Polymeric Materials," *Int. J. Res. Appl. Sci. Eng. Technol.*, vol. 8, no. 5, pp. 396–400, 2020, doi: 10.22214/ijraset.2020.5066.
- [19] M. S. B. Reddy, D. Ponnamma, R. Choudhary, and K. K. Sadasivuni, "A comparative review of natural and synthetic biopolymer composite scaffolds," *Polymers (Basel)*, vol. 13, no. 7, 2021, doi: 10.3390/polym13071105.
- [20] M. C. Hacker, J. Krieghoff, and A. G. Mikos, "Synthetic polymers," in *Principles of regenerative medicine*, Elsevier, 2019, pp. 559–590.
- [21] G. Ramírez Rodríguez, T. Patrício, and J. Delgado López, *Natural polymers for bone repair*, Second Edi. Elsevier Ltd, 2019.
- [22] K. Budak, O. Sogut, and U. Aydemir Sezer, "A review on synthesis and biomedical applications of polyglycolic acid," *J. Polym. Res.*, vol. 27, no. 8, pp. 1–19, 2020, doi: 10.1007/s10965-020-02187-1.
- [23] S.-W. On, S.-W. Cho, S.-H. Byun, and B.-E. Yang, "Bioabsorbable osteofixation materials for maxillofacial bone surgery: a review on polymers and magnesium-based materials," *Biomedicines*, vol. 8, no. 9, p. 300, 2020.
- [24] Y. Liu, H. Cao, L. Ye, P. Coates, F. Caton-Rose, and X. Zhao, "Long-chain branched poly (lactic acid)-b-poly (lactide-co-caprolactone): Structure, viscoelastic behavior, and triple-shape memory effect as smart bone fixation material," *Ind. Eng. Chem. Res.*, vol. 59, no. 10, pp. 4524–4532, 2020.
- [25] R. Siakeng, M. Jawaid, H. Ariffin, S. M. Sapuan, M. Asim, and N. Saba, "Natural fiber reinforced polylactic acid composites: A review," *Polym. Compos.*, vol. 40, no. 2, pp. 446–463, 2019, doi: 10.1002/pc.24747.
- [26] V. DeStefano, S. Khan, and A. Tabada, "Applications of PLA in modern medicine," *Eng. Regen.*, vol. 1, no. April, pp. 76–87, 2020, doi: 10.1016/j.engreg.2020.08.002.
- [27] D. M. Ramos, R. Dhandapani, A. Subramanian, S. Sethuraman, and S. G. Kumbar, "Clinical complications of biodegradable screws for ligament injuries," *Mater. Sci. Eng. C*, vol. 109, p. 110423, 2020, doi: 10.1016/j.msec.2019.110423.
- [28] M. E. Hassan, J. Bai, and D. Q. Dou, "Biopolymers; Definition, classification and applications," *Egypt. J. Chem.*, vol. 62, no. 9, pp. 1725–1737, 2019, doi: 10.21608/EJCHEM.2019.6967.1580.
- [29] P. Chocholata, V. Kulda, and V. Babuska, "Fabrication of scaffolds for bone-tissue regeneration," *Materials (Basel)*, vol. 12, no. 4, 2019, doi: 10.3390/ma12040568.

## RECENT ADVANCES IN POLYMER AND PEROVSKITE BASED THIRD-GENERATION SOLAR CELL DEVICES

T. F. Alhamada<sup>1,2\*</sup>, M. A. A. Hanim<sup>2,3</sup>, A. A. Nuraini<sup>2</sup>, W. Z. Wan Hasan<sup>4</sup>, D. W. Jung<sup>5</sup>

<sup>1</sup>Northern Technical University, University Presidency, Mosul 41001, Iraq.

<sup>2</sup>Department of Mechanical and Manufacturing Engineering, Faculty of Engineering, Universiti Putra Malaysia, Serdang 43400, Selangor, Malaysia.

<sup>3</sup>Advance Engineering Materials and Composites Research Center, (AEMC), Faculty of Engineering, Universiti Putra Malaysia, Serdang 43400, Selangor, Malaysia.

<sup>4</sup>Department of Electrical and Electronic Engineering, Faculty of Engineering, UPM, Serdang 43400, Malaysia.

<sup>5</sup>Department of Mechanical Engineering, Jeju National University, 1 Ara I-dong, Jeju 690-756, Korea.

### ABSTRACT

This review article begins with a comparative overview of the configurations, materials, fabrication methods, and energy conversion efficiency of polymer and perovskite solar cells' photovoltaic performances. Firstly, there has been a significant increase in solar cells due to the growing need for renewable and clean energy. Among all Third-Generation photovoltaic technologies, polymer solar cells and perovskite solar cells have attracted significant interest due to their potential to be inexpensive, lightweight, simple to fabricate, and rapid charging. Polymer solar cells have been studied for over two decades, whereas perovskite solar cells have been in operation for less than eight years. As a basic comparison, the best power conversion efficiency results are 21.6 percent for a 1cm<sup>2</sup> perovskite solar cell and 15.2 percent for polymer solar cells. Finally, this article recommends necessary improvements and future research areas in polymer and perovskite solar cells.

*Keywords:* polymer and perovskite solar cells, power conversion efficiency, device fabrication .

### INTRODUCTION

The search for more efficient technologies that can deliver low-cost, clean, and renewable energy is critical for supporting society's economic progress, given the finite supply of fossil fuels and the significant concerns about global warming and environmental protection. Sunlight is the most abundant, cheapest, and cleanest source of energy for the long-term needs of society. The most effective and practical way to use solar energy is via solar cells, which convert sunlight directly into electricity [1]. PV technologies can be regarded as the greenest and most sustainable source of energy since sunlight is the most plentiful, unlimited, and pure source of energy on the planet. Polymer solar cells (PSCs) have emerged as one of the most promising PV technologies because of their unique characteristics, such as lightweight, variable form factors and the ability to produce huge quantities cost-effectively. It was established by Heeger and Friend et al. [2] that the bulk-heterojunction (BHJ) structure was a viable method for fabricating PSCs. An electron donor (D) and an electron acceptor (A) are mixed to form the photoactive layer that receives solar rays and turns them into electric power in a typical BHJ structure (PC61BM or PC71BM, respectively). Bicontinuous and interpenetrated nanoscale network topology generated by the blending components, providing dense D/A interfaces in bulk volume with easy solution processing, is a significant property of this kind of BHJ structure (Fig. 1) [3].

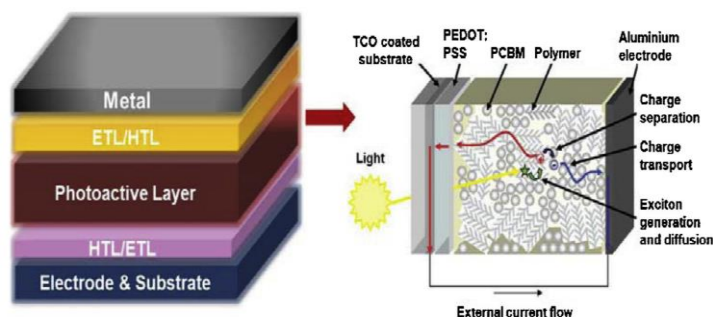


Fig. 1: Diagrammatic representation of bulk-heterojunction polymer solar cells (BHJ PSCs) [2].

#### Article history:

Received: 10 March 2022

Accepted: 7 June 2022

Published: 14 June 2022

#### E-mail addresses:

GS60180@student.upm.edu.my (T. F. Alhamada)

\*Corresponding Author

Polymer solar cells (PSCs) have garnered considerable interest because of their semitransparency, inexpensive solution processing costs, lightweight, and flexibility. Using these benefits, PSCs have a bright future in the domains of wearable electronics, portable electronics, and building-integrated photovoltaics [4]. Over the last two decades, numerous studies have shown an immediate increase in PSCs' power conversion efficiency (PCE). The PCE of PSCs based on fullerene and non-fullerenes small molecules has

achieved 11% and 18%, respectively, using suitable chemical methods and processing engineering [5]. Although PCE has made significant progress, morphological and mechanical stability have remained a barrier.

Perovskite solar cells (PKSCs) have advanced rapidly over the last decade, with power conversion efficiency (PCE) increasing from 3.8 percent to over 25% due to the advantages of metal halide perovskite materials such as long carrier diffusion lengths, low charge recombination loss, and high defect tolerance [6]. Perovskite solar cells must meet or surpass industry criteria for operational lifespan and reliability to be economically viable for commercial manufacture. By combining and comparing experimental and theoretical results, it is possible to understand how perovskite composition, film formation methods, additive and solvent engineering affect efficiency and stability, as well as identify future research directions for further improving both key performance metrics. PSCs' certified efficiency has increased to 25.2% by 2020 [7], making them an appealing alternative for standalone solar modules or as sub-cells in high-efficiency perovskite-silicon tandem solar cells [8]. The general structural formula for perovskites is  $ABX_3$ , where A is a monovalent organic [ $CH_3NH_3$  (MA: methylammonium),  $HC(NH_2)_2$  (FA: formamidinium)] or inorganic [Cs and Rb] cation, B is a divalent metal ion [Pb, Sn, and Bi], and X is a halogen anion [I, Br, or Cl] cation [9]. Two different kinds of third-generation solar cells, namely BHPSCs and PKSCs, have been introduced. The configurations, materials, mechanisms, and present state were summarized, revealing their similarities and differences.

*Device fabrication and measurements*

There are two groups of structures, processes, and materials that have been discussed before. After that, their parallels, linkages, and contrasts in these areas are outlined. Afterwards. Their photovoltaic capabilities are contrasted in this section. The value of the open-circuit current defines the photovoltaic performance of a solar cell ( $V_{oc}$ ), the short circuit current ( $J_{sc}$ ), the fill factor (FF), and the power conversion efficiency (PCE), which are taken from the current-voltage characteristics. PCE is mainly determined by solar cells'  $V_{oc}$ , a crucial photovoltaic property. It was previously shown that the  $V_{oc}$  is mainly determined by the difference between the donor's HOMO and acceptor's LUMO levels in heterojunction polymer devices [10]. Techniques for fabricating BHPSCs and PKSCs are available in various ways. Polymer and Perovskite films are often deposited using solution-processed techniques. Spin-coating, printing, or spray-coating are examples of processes that use solvents to dissolve and deposit precursors onto a substrate. Donor and acceptor are dissolved in a common solvent, such as chlorobenzene, in polymer devices before being deposited in a single step. In contrast, the absorbers in perovskite devices are deposited in a single or a two-step procedure, as shown in Fig. (2).

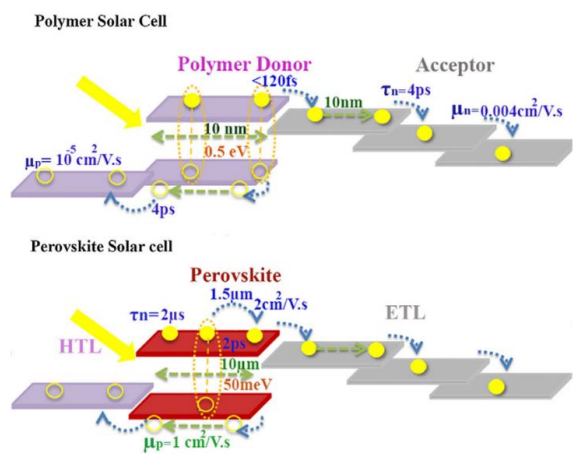


Fig 2. Schematic representation of exciton formation and dissociation in BHPSCs and PKSCs and their properties [10].

Integrating noble metal nanostructures into organic solar cells can enable them to function better by dispersing the incoming light to the active layer. Theoretically interpreted effects of gold (Au) and silver (Ag) metallic nanoparticles (NPs) integration on PSC performance are discussed. In addition to metallic nanoparticles, we explore the impact of metal oxide nanoparticle inclusion on organic solar cells, such as ZnO and TiO<sub>2</sub> [11]. Although perovskite materials have made enormous strides in solar cells, their sensitivity to water, oxygen, and ultraviolet irradiation, which reduces their long-term stability, has been a barrier to their successful commercialization. Perovskites are very hydrophilic materials that quickly absorb water from the environment to create hydrate products [12]. MXene 2D transition metal joined the solar cell manufacturing process in 2018 by improving the efficiency of energy generated and the stability of solar cells. The recent discovery of a PKSC efficiency of better than 23.3 percent by [1], [13].

**CONCLUSIONS**

BHPSCs and PKSCs, two types of third-generation solar cells, were presented in comparison. An overview of their configurations (materials, mechanisms and present condition) highlighted the connections and variations between them. The absorber layers' optical and electrical characteristics were the primary influence, and they were shown to have a significant impact on the device's performance. Nonetheless, careful production and tuning of noble nanostructures are required to have a meaningful effect on the PCE in SCs. For a long-term stable device, it was necessary to consider the effects of solar deterioration as well as hole/electron mobility and energy level misalignment. With the recent efficiency of more than 15.19% for PSC [14] and 23.3% for PKSC by [13], the resultant PSCs demonstrated a steady-state power conversion efficiency and exceptional stability against humidity and light soaking for the related solar cells. According to the results of this review:

1. The photo-absorption of BHJ PSCs can be improved by using noble metals and metal oxides, which have been shown to have excellent potential in terms of stability, efficiency, and cost-effectiveness.



2. Polymers interact with other materials to generate hybrids and nanocomposites with better or extra functionality. These novel materials might be employed in various applications, including renewable energy generation, energy storage, and conversion.
3. As a result of the excellent resistance to moisture, heat, and light and the superb crystallization and low density of defects in perovskite films, perovskite solar cells are being adopted for use in solar energy technology.
4. The incorporation of MXene into perovskite solar cells resulted in a steady-state energy conversion efficiency of 23.3% and exceptional stability.

## REFERENCES

- [1] T. F. Alhamada, M. A. Azmah Hanim, D. W. Jung, A. A. Nuraini, and W. Z. Wan Hasan, "A brief review of the role of 2D mxene nanosheets toward solar cells efficiency improvement," *Nanomaterials*, vol. 11, no. 10, pp. 1–19, 2021, doi: 10.3390/nano11102732.
- [2] D. M. Chapin, C. S. Fuller, and G. L. Pearson, "A New Silicon p-n Junction Photocell for Converting Solar Radiation into Electrical Power," *J. Appl. Phys.*, vol. 25, no. 5, p. 676, May 2004, doi: 10.1063/1.1721711.
- [3] Z. Li, C. C. Chueh, and A. K. Y. Jen, "Recent advances in molecular design of functional conjugated polymers for high-performance polymer solar cells," *Prog. Polym. Sci.*, vol. 99, 2019, doi: 10.1016/j.progpolymsci.2019.101175.
- [4] M. Riede, D. Spoltore, and K. Leo, "Organic Solar Cells—The Path to Commercial Success," *Adv. Energy Mater.*, vol. 11, no. 1, p. 2002653, Jan. 2021, doi: 10.1002/AENM.202002653.
- [5] C. Li *et al.*, "Non-fullerene acceptors with branched side chains and improved molecular packing to exceed 18% efficiency in organic solar cells," *Nat. Energy* 2021 66, vol. 6, no. 6, pp. 605–613, May 2021, doi: 10.1038/s41560-021-00820-x.
- [6] Q. Fu *et al.*, "Multifunctional Two-Dimensional Conjugated Materials for Dopant-Free Perovskite Solar Cells with Efficiency Exceeding 22%," *ACS Energy Lett.*, vol. 6, no. 4, pp. 1521–1532, 2021, doi: 10.1021/acsenerylett.1c00385.
- [7] "Best Research-Cell Efficiency Chart | Photovoltaic Research | NREL." <https://www.nrel.gov/pv/cell-efficiency.html> (accessed Apr. 02, 2022).
- [8] H. Shen *et al.*, "Monolithic Perovskite/Si Tandem Solar Cells: Pathways to Over 30% Efficiency," *Adv. Energy Mater.*, vol. 10, no. 13, p. 1902840, Apr. 2020, doi: 10.1002/AENM.201902840.
- [9] M. A. Mahmud *et al.*, "Origin of Efficiency and Stability Enhancement in High-Performing Mixed Dimensional 2D-3D Perovskite Solar Cells: A Review," *Adv. Funct. Mater.*, vol. 32, no. 3, p. 2009164, 2022, doi: 10.1002/adfm.202009164.
- [10] F. Arabpour Roghabadi *et al.*, "Bulk heterojunction polymer solar cell and perovskite solar cell: Concepts, materials, current status, and opto-electronic properties," *Sol. Energy*, vol. 173, no. August, pp. 407–424, 2018, doi: 10.1016/j.solener.2018.07.058.
- [11] P. J. Maake, A. S. Bolokang, C. J. Arendse, V. Vohra, E. I. Iwuoha, and D. E. Motaung, "Metal oxides and noble metals application in organic solar cells," *Sol. Energy*, vol. 207, no. October 2019, pp. 347–366, 2020, doi: 10.1016/j.solener.2020.06.084.
- [12] J. Huang, S. Tan, P. D. Lund, and H. Zhou, "Impact of H<sub>2</sub>O on organic–inorganic hybrid perovskite solar cells," *Energy Environ. Sci.*, vol. 10, no. 11, pp. 2284–2311, Nov. 2017, doi: 10.1039/C7EE01674C.
- [13] Y. Yang *et al.*, "Modulation of perovskite crystallization processes towards highly efficient and stable perovskite solar cells with MXene quantum dot-modified SnO<sub>2</sub>," *Energy Environ. Sci.*, vol. 14, no. 6, pp. 3447–3454, 2021, doi: 10.1039/d1ee00056j.
- [14] Z. Zhang *et al.*, "A dithienobenzothiadiazole-quaterthiophene wide bandgap polymer enables non-fullerene based polymer solar cells with over 15% efficiency," *Polymer (Guildf.)*, vol. 233, no. September, p. 124193, 2021, doi: 10.1016/j.polymer.2021.124193.

## FABRICATION OF HALOCHROMIC POLYLACTIC ACID (PLA) FILAMENT FOR 3D PRINTING

Q. H. Chan<sup>1</sup>, M. Z. Zamri<sup>1</sup>, A. Rusli<sup>1</sup>, Z. A. A. Hamid<sup>1</sup>, M. K. Abdullah<sup>1</sup>, M. D. Syafiq<sup>1</sup>, K. I. Ku Marsilla<sup>1\*</sup>

<sup>1</sup>*School of Materials and Mineral Resources Engineering, Engineering Campus, Universiti Sains Malaysia 14300 Nibong Tebal, Malaysia*

---

### ABSTRACT

With increasing concerns regarding plastic waste and pollution, researchers have been looking to develop advanced materials from biodegradable plastics. This study features the additive manufacturing of halochromic polylactic acid (PLA) filaments and the testing of halochromic properties of the specimens. PLA/polyethylene glycol (PEG)/bromocresol purple (BCP) compound was extruded and wound to produce a 3D printing filament. The halochromic responsiveness and colour reversibility were tested by exposing the samples to liquid and vaporized pH solutions for 30 minutes and then placing them back into ambient conditions for 48 hours. The compatibility of PLA, PEG and BCP were found to be good, and the halochromic compound formed was homogenous. Dumbbell-shaped and rectangular specimens were successfully fabricated from the compound through 3D printing. Overall, the 3D printed halochromic PLA specimens show promising results and have proven their functionality as pH sensors which offers wide applications in many industries such as medical, environmental and packaging.

*Keywords:* halochromic, polylactic acid, 3D printing, halochromic responsiveness, colour reversibility

---

### INTRODUCTION

Smart materials can aid in our daily lives by responding to external stimuli including moisture, magnetism, electricity and mechanical stimulus, as well as pH and temperature changes. The current work will attempt to tackle the mounting plastic wastes by featuring a biodegradable polymer while utilizing the advancements in additive manufacturing. Halochromic materials are a kind of smart materials that respond to pH changes by changing their colour. In this research, PLA was used as a polymer substrate to incorporate the halochromic dye. Being a biodegradable polymer, PLA offers an alternative to tackle the mounting plastic waste issue. From previous research, halochromic polylactic acid (PLA) films have been successfully fabricated through solution casting method which offers wide applications as good acid base sensors [1]. However, the technique used was a huge amount of solvent and only limited to film. In this work, 3D printing will be used as processing technique to produce halochromic PLA that can produce custom-made products such as pH sensitive films for medical and packaging and environmental applications [2]–[5]. As of the commencement of this work, no other works featuring 3D-printed halochromic PLA have been found.

### MATERIALS AND METHODS

#### *Materials*

Polylactic acid (PLA) pellets (3021D; 96% L, 4% D) was supplied by NatureWorks LLC. Polyethylene glycol (PEG) flakes ( $M_w$ : 6000 g/mol, CAS: 25322-68-3) were supplied by Sigma-Aldrich, Merck KGaA, Darmstadt, Germany. Bromocresol purple (BCP) powder ( $M_w$ : 540.22 g/mol, CAS: 115-40-2) was supplied by Gouden Sdn Bhd, Malaysia. Hydrochloric acid (HCl, aqueous) (CAS: 7647-01-0), ammonia solution ( $NH_3$ ,  $M_w$ : 17.031 g/mol), acetic acid ( $CH_3COOH$ ,  $M_w$ : 60.052 g/mol) and ethanol ( $CH_3CH_2OH$ ,  $M_w$ : 46.069 g/mol) was supplied by the School of Materials and Mineral Resources laboratory.

#### *Methods*

PLA pellets were dried in an oven at 50 °C overnight. To obtain PLA/PEG blends, PLA pellets and PEG flakes were compounded using two-roll mill at 160 °C for 20 minutes, based on the formulation shown in TABLE 1. The PLA/PEG flakes were then immersed in a solution mixture of BCP and ethanol for 24 hours before drying in an oven at 50 °C overnight. Filament extrusion was carried out using Brabender Kompaktextruder KE 19 with a filament die of diameter 1.75 mm. The extrusion parameters are shown in TABLE 2. Dumbbell-shaped (ASTM D638 Type I) and rectangular specimens (30mm x 10mm x 1mm) were designed in CAD software SolidWorks (Dassault Systèmes). Conversion software Creality was used to convert SolidWorks STL files into 3D-printer-compatible G-code files. The specimens were then printed using 3D printer Ender 6 FDM (Creality). The parameters for 3D printing are shown in TABLE 3. The printed rectangular specimens were exposed to liquids and vapours of hydrochloric acid (pH 3), acetic acid (pH 5) and ammonia (pH 11) respectively for 30 minutes to test the halochromic properties of the specimens. All specimens were then removed from the varying pH conditions and placed under ambient conditions for 48 hours.

---

#### *Article history:*

Received: 10 March 2022

Accepted: 7 June 2022

Published: 14 June 2022

---

#### *E-mail addresses:*

ku\_marsilla@usm.my (K. I. Ku Marsilla)

\*Corresponding Author

TABLE 1: Formulation of PLA/PEG/BCP compound, based on formulation [1].

Ingredient	Percentage in weight (wt.%)	Weight per 500g (g)
PLA	85	425
PEG	15	75
BCP	0.03	0.15

TABLE 2: Extrusion parameters for pure and compounded PLA filaments.

Filament type	Screw speed (rpm)	Pulling speed (rpm)	Temperature (°C)			
			Feed zone	Melting zone	Metering zone	Die zone
PLA/PEG/BCP	18	Manual	150	160	160	150

TABLE 3: Parameters used for 3D printing.

Filament	Print speed (mm/s)	Layer height (mm)	No. of top/bottom layers	Temperature (°C)		Nozzle diameter (mm)	Line width (mm)	Infill pattern	Infill density (%)
				Nozzle	Bed				
PLA/PEG/BCP	80	0.16	5	210	100	0.4	0.35	Concentric	100

**RESULTS AND DISCUSSION**

*Fabrication*

Fig. 1 shows the fabrication procedures of the halochromic PLA 3D printing filament. The resultant compound was homogenous. Upon completion of extrusion, the filament was observed to be uniform and homogenous.

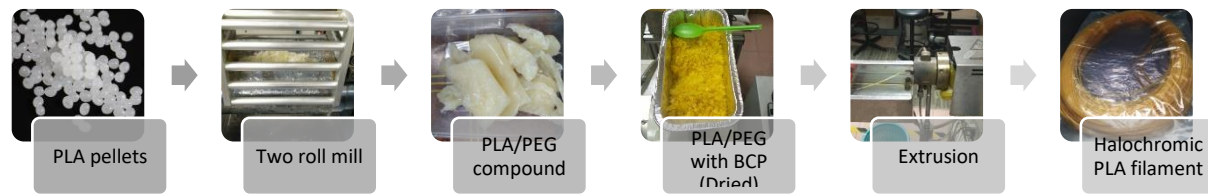


Fig. 1: Fabrication of halochromic PLA/PEG/BCP filament.

*Printing*

Fig. 2 illustrates the printing of a dumbbell-shaped specimen. All printed specimens were able to be printed with no error, signifying the potential for industrial 3D printing applications.

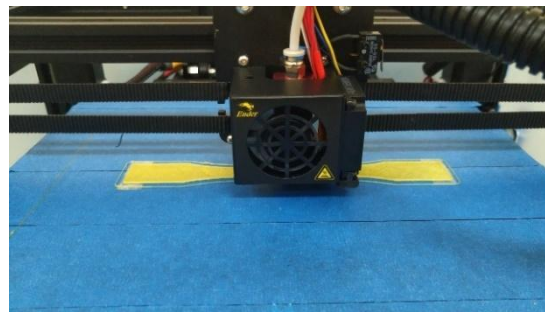





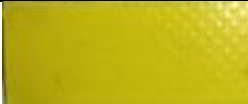
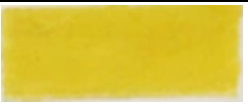
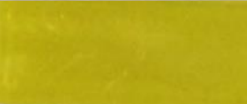

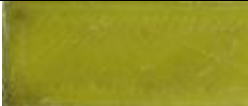




Fig. 2: 3D printing of a dumbbell specimen in progress.

*Halochromic Responsiveness and Colour Reversibility*

TABLE 4 shows the transitioned and reversed colours of the specimens under each condition. Upon exposure to acidic conditions, a darker shade of yellow is observed while a purple colouration can be seen in specimens exposed to alkaline conditions. Colour reversion is observed in the alkaline specimens but not the acidic specimens, possibly due to the slight initial colour change. Halochromic films produced in this work can be useful in detecting hazardous alkaline chemicals and gases.

TABLE 4: Colour changes and reversal of PLA halochromic specimens under different pH.

pH	Solution		Vapour	
	After exposure	Colour reversion	After exposure	Colour reversion
3				
5				
11				

**CONCLUSION**

Halochromic PLA/PEG/BCP specimens have been successfully fabricated through 3D printing. Compounding was carried out using a heated two-roll mill and the compound was crushed into flakes. A filament was produced through extrusion. Dumbbell-shaped and rectangular specimens were then printed from the filament. The compound appears to be homogenous and the filament was printable. The specimens indicate good halochromic response towards ammonia (pH 11) solution and vapour after an exposure time of 30 minutes. Acidic conditions change the specimens from yellow to a darker yellow while alkaline conditions change the specimens from yellow to purple. Only the specimens exposed to alkaline conditions showed obvious colour reversion upon placing in ambient conditions for 48 hours. The findings support the functionality of the fabricated PLA films as alkaline chemical and gas sensors.

**ACKNOWLEDGEMENT**

The authors would like to thank the School of Materials and Mineral Resources Engineering, Universiti Sains Malaysia for providing the facilities and laboratory equipment needed to accomplish this research. The authors are also thankful for the financial support from JICA Project, Grant 304/PBAHAN/6050450/A119.

**REFERENCES**

- [1] J. Y. Ng, A. Rusli, Z. A. A. Hamid, M. K. Abdullah, and K. I. K. Marsilla, "Halochromic poly (lactic acid) film for acid base sensor," *J. Appl. Polym. Sci.*, no. September, p. 50093, 2020.
- [2] C. Gamerith *et al.*, "pH-responsive materials for optical monitoring of wound status," *Sensors Actuators, B Chem.*, vol. 301, no. August, p. 126966, 2019, doi: 10.1016/j.snb.2019.126966.
- [3] W. Wang, D. Feng, Y. Zhang, L. Lin, and H. Mao, "Development of azobenzene-functionalized eco-friendly waterborne polyurethane with halochromic property," *Mater. Lett.*, vol. 268, p. 127561, 2020, doi: 10.1016/j.matlet.2020.127561.
- [4] E. Yildiz, G. Sumnu, and L. N. Kahyaoglu, "Monitoring freshness of chicken breast by using natural halochromic curcumin loaded chitosan/PEO nanofibers as an intelligent package," *Int. J. Biol. Macromol.*, vol. 170, pp. 437–446, 2021, doi: 10.1016/j.ijbiomac.2020.12.160.
- [5] M. Ghorbani *et al.*, "A halochromic indicator based on polylactic acid and anthocyanins for visual freshness monitoring of minced meat, chicken fillet, shrimp, and fish roe," *Innov. Food Sci. Emerg. Technol.*, vol. 74, no. September, p. 102864, 2021, doi: 10.1016/j.ifset.2021.102864.

## ISOLATION AND CHARACTERIZATION OF NANOCRYSTALLINE CELLULOSE FROM BIOFUEL WASTE BY ORGANIC ACID HYDROLYSIS

H. Holilah<sup>1,3\*</sup>, D. V. Ramadhani<sup>2</sup>, N. Jadid<sup>1</sup>, T. P. Oetami<sup>5</sup>, A. Asranudin<sup>1,3\*</sup>, R. Ediati<sup>1</sup>, D. Prasetyoko<sup>1\*</sup>

<sup>1</sup>Department of Chemistry, Faculty of Science and Data Analytics, Institut Teknologi Sepuluh Nopember Surabaya, Indonesia

<sup>2</sup>Department of Biology, Faculty of Science and Data Analytics, Institut Teknologi Sepuluh Nopember Surabaya, Indonesia

<sup>3</sup>Department of food science and technology, Faculty of Agriculture, Halu Oleo University

<sup>4</sup>PT. Agrindo, Raya Driyorejo Km. 19, Gresik, East Java, Indonesia

---

### ABSTRACT

Biofuel production generated unused seed shells from *Reutealis trisperma* (RTS). The shell wastes provide a large potential source of cellulose isolation. Nanocrystalline cellulose (NCs) were successfully isolated from biodiesel waste. Purification of cellulose from waste was done in two stages; alkalization and bleaching process to remove lignin and hemicellulose, respectively. The cellulose content of RTS after purification was  $63.9 \pm 0.8\%$ . NCs was prepared using organic acid hydrolysis and ultrasonication method. XRD analysis showed that NCs had the higher crystallinity than waste and cellulose. NCs obtained also had the high thermal stability than the waste. The temperature peak of NC-RTS was  $342.46^\circ\text{C}$ . Rod-like morphology structure was owned by NC-RTS. NC-RTS had the diameter and length of 24.3 nm and 350.2 nm, respectively. The isolated NCs may be potentially applied in various application, such as bio-nanocomposites, food, biomedicine, pharmacy, etc.

*Keywords:* nanocrystalline cellulose, biofuel waste, seed, organic acid hydrolysis.

---

### INTRODUCTION

*Reutealis trisperma* seed (RTS) oil is one of the sources for biofuel production and is widely cultivated in Indonesia. RTS as raw material for biodiesel can produce high by-products [1]. The shell of RTS is one of side waste from the processing of biodiesel production [2]. Several previous studies have used RTS oil for biofuel production [2]–[4]. Until now, the shell of RTS was used as activated carbon [1], [5]. Unused seed shell has a potential source of cellulose production. Various types of lignocellulosic wastes have been reported as sources of cellulose, namely Rice straw [6], pineapple crown [7], sago seed shell [8], Rosela fiber [9] [10], mango seed shell [11], mulberry waste [12], *Pyrus pyrifolia* pell (Chen *et al.*, 2019), rice husk (Rashid and Dutta, 2020b), tea stalk [14], *Cucumis sativus* pell [15], pepper waste [16]. Nanocellulose is a natural fiber that can be isolated from cellulose sources. The size of nanocellulose fibers generally has a diameter of less than 100 nm and a length in the micrometer scale. Nanocellulose is a biodegradable nanofiber with a light weight, low density (about 1.6 g/cm<sup>3</sup>) and has a modulus of elasticity up to 220 GPa greater than Kevlar fiber [17]. In addition, nanocellulose is transparent with a reactive surface due to the presence of hydroxyl groups that can be used for various surface properties [18].

Hydrolysis of cellulose to NC generally uses classical strong acid such as sulfuric acid [13], [14], [19], [20]. Based on their mechanical and morphological characteristics, NCs are utilized various application such as reinforcing materials, food, and pharmaceuticals. However, the use of sulfuric acid has several disadvantages such as thermal stability and environmental incompatibility [21]. In addition, sulfuric acid is corrosive to the environment and large amounts of water are used for the neutralization process [22]. To overcome this, exploration of alternatives to sulfuric acid needs to be carried out. Organic acid is a type of food grade and environmentally friendly acid that can be applied in the cellulose hydrolysis process. In the present work cellulose nanocrystal were isolated from biodiesel waste (RTS shell) by organic acid hydrolysis. Citric acid is a weak organic acid with no odor and a semi-transparent crystalline solid form among the numerous types of organic acids. Citric acid is a food grade material that widely used in the food, beverage and pharmaceutical fields [23], [24].

### MATERIALS AND METHODS

RTS shell wastes were obtained from PT. Agrindo, East Java, Indonesia. Hydrogen peroxide (H<sub>2</sub>O<sub>2</sub>, 30% (w/w) in H<sub>2</sub>O) was purchased from Merck, Germany. The sodium hydroxide (NaOH,  $\geq 99\%$ ) and citric acid monohydrate (C<sub>6</sub>H<sub>8</sub>O<sub>7</sub>,  $\geq 99.5\%$ ) were purchased from Sigma, Singapore. The isolation of cellulose from RTS waste was done by two step preparation namely alkalization and bleaching [25] Nanocrystalline cellulose was conducted based on the method from Holilah *et al.*, [16]. NCs was isolated by organic acid hydrolysis and ultrasonication. The determination of cellulose, hemicellulose, and lignin composition was conducted using neutral detergent fiber (NDF), acid detergent fiber (ADF), and acid detergent lignin (ADL) methods [26]. The RTS waste, cellulose and nanocellulose were characterized using FTIR (Fourier Transform Infrared), XRD (X-Ray Diffraction), SEM (Scanning Electron Microscope), TEM (Transmission Electron Microscope), TGA (Thermogravimetric analysis) to investigate the functional group, crystallinity, morphology, and the thermal stability, respectively.

---

#### Article history:

Received: 10 March 2022

Accepted: 7 June 2022

Published: 14 June 2022

---

#### E-mail addresses:

holilah.itp@uho.ac.id (H. Holilah)

\*Corresponding Author

## RESULTS AND DISCUSSION

The photograph of RTS was presented in Fig. 1 (a). The functional group investigation of RTS waste, C-RTS and NC-RTS was shown in Fig. 1 (b). NC-RTS and C-RTS had the peak characteristics of cellulose. There are six band characteristics of cellulose i.e. 897, 1060, 1430, 1640, 2905 and 3400  $\text{cm}^{-1}$ [7]. The peak at 1503, 1740 and 2860 were only detected on RTS. The peak indicated that the waste containing lignin and hemicellulose. Some properties of NC-RTS also presented in TABLE 1. The NC-RTS had the crystallinity index of 79.82%. The similar result was reported by Holilah et. al., [16] that produced NCs by citric acid hydrolysis from pepper waste. The NC had the crystallinity index of 76.4%. NC-RTS also had rod-shape morphology with the diameter of 24.3nm and the length of 275.5 nm.

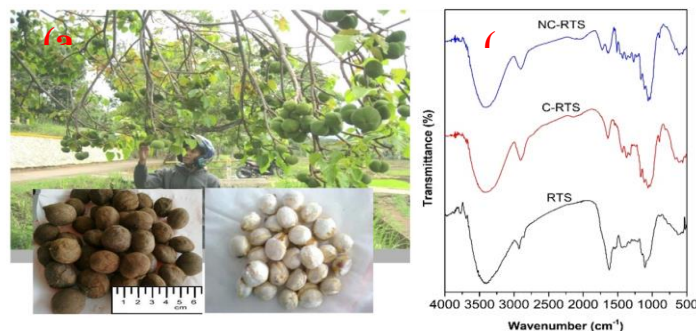


Fig. 1. The photograph of *Reutealis trisperma* seed [2] (a) and the FTIR spectra of RTS waste, C-RTS and NC-RTS (b).

TABLE 1. The properties of NC-RTS.

Properties	NC-RTS
Crystallinity (%)	79.82
Temperature peak (°C)	342.46
Particle size (nm)	D: 24.3; L: 275.5
Morphology	Rod shape

## CONCLUSIONS

Nanocellulose was isolated from RTS-waste using organic acid hydrolysis and ultrasonication. The XRD analysis showed that the crystallinity of obtained nanocellulose was higher than cellulose and waste. The crystallinity was reached by nanocellulose from RTS approximately 79.82%. Thermal analysis shows that the thermal stability of nanocrystalline cellulose was higher than waste and cellulose. TEM micrographs showed the morphological of nanocrystalline cellulose was rod-like structure. The diameter and length of NC-RTS was 24.3 nm and 275.5 nm. Based on the zeta potential value, NC-RTS had the good stability dispersion. Hydrolysis with organic acids is very promising in the future because the resulting nanocellulose is applied in various fields.

## ACKNOWLEDGEMENTS

The authors would like to acknowledge Kementerian Pendidikan Kebudayaan Riset dan Teknologi, Indonesia for the financial and technical support under Doctoral Research Grant (PDD) 2022 awarded to Holilah and Didik Prasetyoko.

## REFERENCES

- [1] H. Hutami, G. Rabelsa, Yohandri, and A. Putra, "Making an Active Carbon from Candlenut Shell for the Application of Electromagnetic Wave Absorbers," *Prog. Electromagn. Res. Symp.*, vol. 2019-June, pp. 1284–1286, 2019, doi: 10.1109/PIERS-Spring46901.2019.9017682.
- [2] H. Holilah et al., "The potential of *Reutealis trisperma* seed as a new non-edible source for biodiesel production," *Biomass Convers. Biorefinery*, vol. 5, no. 4, pp. 347–353, Dec. 2015, doi: 10.1007/s13399-014-0150-6.
- [3] Z. Rahmawati, H. Holilah, S. W. Purnami, H. Bahruji, T. P. Oetami, and D. Prasetyoko, "Statistical Optimisation using Taguchi Method for Transesterification of *Reutealis Trisperma* Oil to Biodiesel on CaO-ZnO Catalysts," *Bull. Chem. React. Eng. Catal.*, vol. 16, no. 3, pp. 686–695, Sep. 2021, doi: 10.9767/BCREC.16.3.10648.686-695.
- [4] R. E. Nugraha et al., "Lewis acid Ni/Al-MCM-41 catalysts for H<sub>2</sub>-free deoxygenation of *Reutealis trisperma* oil to biofuels," *RSC Adv.*, vol. 11, no. 36, pp. 21885–21896, Jun. 2021, doi: 10.1039/D1RA03145G.
- [5] Taslim, O. Bani, Iriany, N. Aryani, and G. S. Kaban, "Preparation of activated carbon-based catalyst from candlenut shell impregnated with KOH for biodiesel production," *Key Eng. Mater.*, vol. 777 KEM, pp. 262–267, 2018, doi: 10.4028/www.scientific.net/KEM.777.262.
- [6] V. A. Barbash, O. V. Yaschenko, and O. M. Shniruk, "Preparation and Properties of Nanocellulose from Organosolv Straw Pulp," *Nanoscale Res. Lett.*, vol. 12, no. 1, 2017, doi: 10.1186/s11671-017-2001-4.
- [7] M. Mahardika, H. Abral, A. Kasim, S. Arief, and M. Asrofi, "Production of nanocellulose from pineapple leaf fibers via high-shear homogenization and ultrasonication," *Fibers*, vol. 6, no. 2, pp. 1–12, 2018, doi: 10.3390/fib6020028.
- [8] S. Naduparambath, J. T.V., V. Shaniba, S. M.P., A. K. Balan, and E. Purushothaman, "Isolation and characterisation

- of cellulose nanocrystals from sago seed shells,” *Carbohydr. Polym.*, vol. 180, no. April 2017, pp. 13–20, 2018, doi: 10.1016/j.carbpol.2017.09.088.
- [9] L. K. Kian, M. Jawaid, H. Ariffin, and Z. Karim, “Isolation and characterization of nanocrystalline cellulose from roselle-derived microcrystalline cellulose,” *Int. J. Biol. Macromol.*, vol. 114, pp. 54–63, Jul. 2018, doi: 10.1016/j.ijbiomac.2018.03.065.
- [10] R. Poonguzhali, S. Khaleel Basha, and V. Sugantha Kumari, “Synthesis of alginate/nanocellulose bionanocomposite for in vitro delivery of ampicillin,” *Polym. Bull.*, vol. 75, no. 9, pp. 4165–4173, Sep. 2018, doi: 10.1007/s00289-017-2253-2.
- [11] A. P. M. Silva *et al.*, “Mango kernel starch films as affected by starch nanocrystals and cellulose nanocrystals,” *Carbohydr. Polym.*, vol. 211, pp. 209–216, May 2019, doi: 10.1016/j.carbpol.2019.02.013.
- [12] Z. Wang *et al.*, “Isolation and characterization of cellulose nanocrystals from pueraria root residue,” *Int. J. Biol. Macromol.*, vol. 129, pp. 1081–1089, 2019, doi: 10.1016/j.ijbiomac.2018.07.055.
- [13] Y. W. Chen, M. A. Hasanulbasori, P. F. Chiat, and H. V. Lee, “Pyrus pyrifolia fruit peel as sustainable source for spherical and porous network based nanocellulose synthesis via one-pot hydrolysis system,” *Int. J. Biol. Macromol.*, vol. 123, pp. 1305–1319, 2019, doi: 10.1016/j.ijbiomac.2018.10.013.
- [14] Y. Guo, Y. Zhang, D. Zheng, M. Li, and J. Yue, “Isolation and characterization of nanocellulose crystals via acid hydrolysis from agricultural waste-tea stalk,” *Int. J. Biol. Macromol.*, vol. 163, pp. 927–933, Nov. 2020, doi: 10.1016/j.ijbiomac.2020.07.009.
- [15] N. Sai Prasanna and J. Mitra, “Isolation and characterization of cellulose nanocrystals from Cucumis sativus peels,” *Carbohydr. Polym.*, vol. 247, p. 116706, Nov. 2020, doi: 10.1016/j.carbpol.2020.116706.
- [16] H. Holilah *et al.*, “Uniform rod and spherical nanocrystalline celluloses from hydrolysis of industrial pepper waste (*Piper nigrum* L.) using organic acid and inorganic acid,” *Int. J. Biol. Macromol.*, vol. 204, pp. 593–605, Apr. 2022, doi: 10.1016/J.IJBIOMAC.2022.02.045.
- [17] A. Demirbaş, “Estimating of structural composition of wood and non-wood biomass samples,” *Energy Sources*, vol. 27, no. 8, pp. 761–767, 2005, doi: 10.1080/00908310490450971.
- [18] R. J. Moon, A. Martini, J. Nairn, J. Simonsen, and J. Youngblood, “Cellulose nanomaterials review: Structure, properties and nanocomposites,” *Chem. Soc. Rev.*, vol. 40, no. 7, pp. 3941–3994, Jun. 2011, doi: 10.1039/c0cs00108b.
- [19] M. F. Rosa *et al.*, “Cellulose nanowhiskers from coconut husk fibers: Effect of preparation conditions on their thermal and morphological behavior,” *Carbohydr. Polym.*, vol. 81, no. 1, pp. 83–92, May 2010, doi: 10.1016/j.carbpol.2010.01.059.
- [20] B. S. Purkait, D. Ray, S. Sengupta, T. Kar, A. Mohanty, and M. Misra, “Isolation of cellulose nanoparticles from sesame husk,” *Ind. Eng. Chem. Res.*, vol. 50, no. 2, pp. 871–876, 2011, doi: 10.1021/ie101797d.
- [21] K. J. Nagarajan, A. N. Balaji, S. T. Kasi Rajan, and N. R. Ramanujam, “Preparation of bio-eco based cellulose nanomaterials from used disposal paper cups through citric acid hydrolysis,” *Carbohydr. Polym.*, vol. 235, May 2020, doi: 10.1016/j.carbpol.2020.115997.
- [22] X. Yang *et al.*, “Effects of preparation methods on the morphology and properties of nanocellulose (NC) extracted from corn husk,” *Ind. Crops Prod.*, vol. 109, pp. 241–247, Dec. 2017, doi: 10.1016/j.indcrop.2017.08.032.
- [23] C. R. Soccol, L. P. S. Vandenberghe, C. Rodrigues, and A. Pandey, “New perspectives for citric acid production and application,” *Food Technol. Biotechnol.*, vol. 44, no. 2, pp. 141–149, 2006.
- [24] V. C. Souza, E. Niehues, and M. G. N. Quadri, “Development and characterization of chitosan bionanocomposites containing oxidized cellulose nanocrystals,” *J. Appl. Polym. Sci.*, vol. 133, no. 7, p. n/a-n/a, Feb. 2016, doi: 10.1002/app.43033.
- [25] H. Holilah *et al.*, “Hydrothermal assisted isolation of microcrystalline cellulose from pepper (*Piper nigrum* L.) processing waste for making sustainable bio-composite,” *J. Clean. Prod.*, vol. 305, p. 127229, Jul. 2021, doi: 10.1016/J.JCLEPRO.2021.127229.
- [26] M. A. A. Mohammed, A. Salmiaton, W. A. K. G. Wan Azlina, and M. S. Mohamad Amran, “Gasification of oil palm empty fruit bunches: A characterization and kinetic study,” *Bioresour. Technol.*, vol. 110, pp. 628–636, Apr. 2012, doi: 10.1016/j.biortech.2012.01.056.

## FABRICATION OF PES/POM-TiO<sub>2</sub> MIXED MATRIX MEMBRANE WITH PHOTOCATALYTIC ACTIVITY FOR METHYLENE BLUE REMOVAL

S. Zhafiri<sup>1</sup>, T. Gunawan<sup>1</sup>, N. Widiastuti<sup>1\*</sup>

<sup>1</sup>*Department of Chemistry, Faculty of Science and Data Analytics, Institut Teknologi Sepuluh Nopember, Sukolilo, Surabaya 60111, Indonesia*

---

### ABSTRACT

Dyes is considered as a micropollutant for aquatic ecosystems since its presence can pollute the environment. Stable and complex structure of synthetic dyes making them difficult to degrade. Disposal of dyes into the environment continuously without going through a proper waste treatment process has the potential to cause long-term hazards. Membrane filtration process is widely used for the treatment of pollutants in commercial scale. However, fouling is the major obstacle of the membrane filtration process as it destructs the membrane performance. The combination of membrane process and photocatalysis can be a solution to this issue. Photocatalysis is a potential method for removing harmful contaminants from the aquatic environment, such as dyes. The fabricated PES/POM/TiO<sub>2</sub> membrane showed good performance against 5 mg/L methylene blue solution.

*Keywords:* mixes matrix membrane, photocatalytic membrane, polyoxometalate, methylene blue.

---

### INTRODUCTION

In recent years, population development, urbanization, and industrialization have increased industrial waste, especially pollution from the dye use sector. Disposal of dyes into the environment continuously without going through a sewage treatment process can increase water quality degradation such as causing unpleasant odors, discoloration and turbidity as well as long-term potential hazards such as accumulation of carcinogenic waste [1]. Thus, processing dye pollutants from water sources is an important thing to do. Membrane technology has developed significantly in recent decades due to its benefits in water treatment. Membrane technologies, especially ultrafiltration, nanofiltration and reverse osmosis, can be used to treat dye wastewater. However, this method does not degrade the dye but only lowers its concentration in the water by filtration [2][3], so that it can cause fouling on the surface of the membrane which results in a decrease in the effectiveness and efficiency of the membrane [4]. To overcome these problems, combining membrane filtration processes with photocatalytic processes to produce photocatalytic membranes can be an effective solution [5]. Photocatalytic degradation is considered a favorable method to be used in dye wastewater treatment because of its effectiveness, environmental friendliness, low cost and does not produce secondary pollutants [6]. One of the photocatalyst materials is polyoxometalate (POM) which has various types of atomic structure and arrangement [7]. The most commonly studied POM structures are Keggin, such as PW<sub>12</sub>O<sub>40</sub> [8]. PW<sub>12</sub>O<sub>40</sub> (PW<sub>12</sub>) is reported to have a bandgap of 3.32 eV [9]. A large bandgap energy is considered less effective in photocatalytic reactions because it requires a larger photon energy [7]. Another type of POM, P<sub>2</sub>W<sub>18</sub>O<sub>62</sub> (P<sub>2</sub>W<sub>18</sub>) with Wells-Dawson structure has a smaller bandgap which is 2.9 eV so that it has the potential to produce more effective photocatalytic reactions [9].

However, due to the poor specific surface area and high solubility, the use of POM becomes less effective [10]. Immobilization and solidification of other semiconductor matrices, such as TiO<sub>2</sub> can overcome these POM deficiencies and increase photocatalytic effectiveness by preventing electron and hole recombination [11]. The use of POM, especially PW<sub>12</sub> in dye degradation has been reported in a number of publications. Among them is a study by Lin and Huang [11] who reported that PW<sub>12</sub>/TiO<sub>2</sub> photocatalyst can degrade up to 95% of methylene blue dye. However, there are still few studies that study the use of P<sub>2</sub>W<sub>18</sub> as a photocatalyst. In this research, PES/POM/TiO<sub>2</sub> photocatalytic flat sheet will be fabricated using two types of POM, PW<sub>12</sub> and P<sub>2</sub>W<sub>18</sub> with a non-solvent phase inversion method, which is able to separate and degrade the pollutant dye methylene blue by increasing the fouling resistance of the solvent. membrane surface.

### MATERIALS AND METHODS

#### *Materials*

The materials used in this study include sodium tungstate dihydrate (Na<sub>2</sub>WO<sub>4</sub>·2H<sub>2</sub>O), phosphoric acid (H<sub>3</sub>PO<sub>4</sub>, 85%), disodium hydrogen phosphate dihydrate (Na<sub>2</sub>HPO<sub>4</sub>·2H<sub>2</sub>O), hydrochloric acid (HCl, 37%) potassium chloride (KCl), diethyl ether (100%), titanium (IV) isopropoxide (TTIP, 97%), isopropanol (C<sub>3</sub>H<sub>8</sub>O), N,N-dimethylacetamide (DMAC, 99.9%), aqua distillation, aqua bromine, polyethylene glycol (PEG), polyethersulfone (PES) and methylene blue (MB).

---

#### *Article history:*

Received: 10 March 2022

Accepted: 7 June 2022

Published: 14 June 2022

---

#### *E-mail addresses:*

nurul\_widiastuti@chem.its.ac.id (N. Widiastuti)

\*Corresponding Author

#### *Methods*

Photocatalyst PW<sub>12</sub> and P<sub>2</sub>W<sub>18</sub> was synthesized using the method by Dias et al [12] and Mbomekalle et al [13], respectively. POM/TiO<sub>2</sub> photocatalysts were synthesized by a combination of sol-gel and calcination methods by Hassan et al [14]. Photocatalytic membrane fabrication was carried out



using the non-solvent induced phase inversion (NIPS) method in order to obtain a membrane with a flat module (flat sheet) with a finger-like pore structure [15]. A total of 24.9 g of NMP was put into a Durant bottle and then 0.0255 g POM/TiO<sub>2</sub> photocatalyst was added while stirring for 1 hour and sonicated for 20 minutes. Then 0.051 g of PVP and 5.1 g of PES were added to the solution while stirring at room temperature for 24 hours to obtain a dope solution. Dope solution was then sonicated for 20 minutes to remove the gas in it. Next, the dope solution was poured onto a glass plate and leveled, then soaked for 2 minutes in a coagulant bath containing distilled water. The resulting membrane was then transferred to another coagulant bath containing distilled water and soaked for 24 hours.

## RESULTS AND DISCUSSION

### IR Spectrum

The vibration of the P-O bond obtained from the PO<sub>4</sub> tetrahedron shows at wavelength of 1080 cm<sup>-1</sup>. The wavelength of 982 cm<sup>-1</sup> is the absorption of the W-O bond and there are two absorption bands at 890 and 810 cm<sup>-1</sup> which are the vibrations of the W-O-W bridge structure [16]. The IR spectrum of P<sub>2</sub>W<sub>18</sub> shows strong absorption at wavelength 1091 cm<sup>-1</sup> obtained from the PO<sub>4</sub> tetrahedron. There is absorption from the W-O bond at 962 cm<sup>-1</sup> and vibrations from the W-O-W bridge structure at wavelengths 914 and 780 cm<sup>-1</sup> [17].

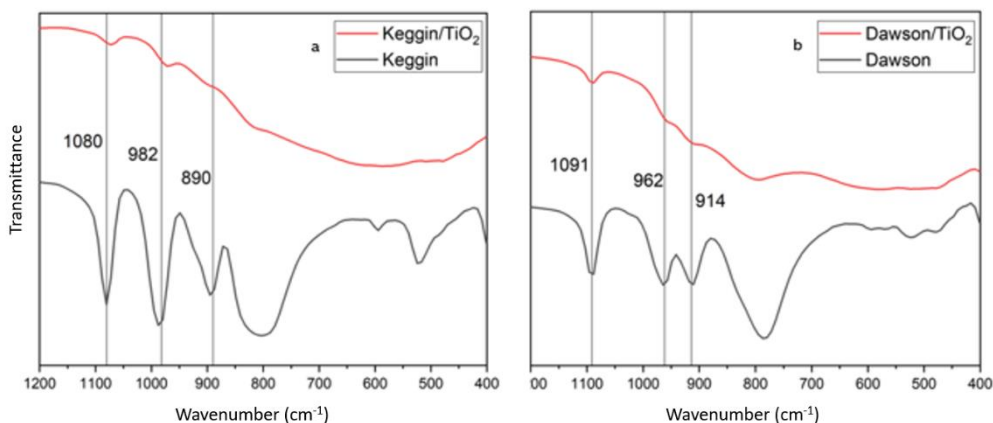


Fig. 1: FTIR spectra of (a) Keggin types POM PW<sub>12</sub> and PW<sub>12</sub>/TiO<sub>2</sub>; (b) Dawson type POM P<sub>2</sub>W<sub>18</sub> and P<sub>2</sub>W<sub>18</sub>/TiO<sub>2</sub>.

### Membrane Performance

The membrane permeability to MB 5 mg/L solution shown in the Fig. 2. Under no UV irradiation, the M0 membrane produced a MB flux of 10.8 kg/m<sup>2</sup>h, while M-K membrane produced 28.2 kg/m<sup>2</sup>h and M-D membrane with 31.5 kg/m<sup>2</sup>h.

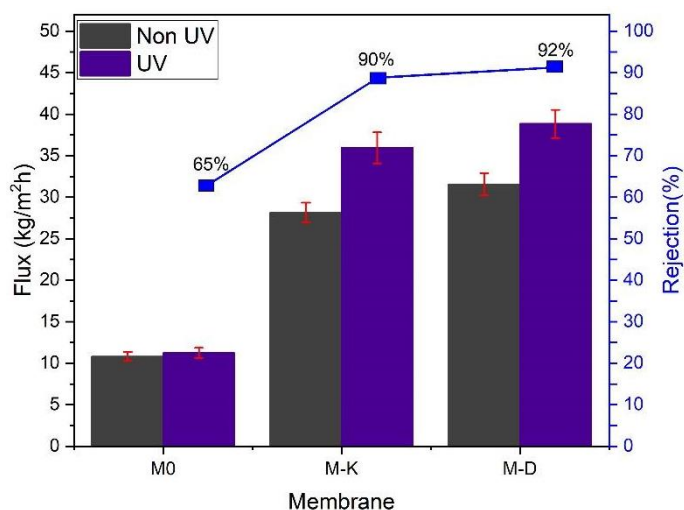


Fig. 2: Membranes flux to 5 mg/L methylene blue solution.

For filtration under UV irradiation, both of membranes with POM/TiO<sub>2</sub> addition showed an increase in flux compared to the no UV irradiation. This is due to the addition of POM/TiO<sub>2</sub> photocatalyst which works under UV light to break down the MB dye structure into simpler molecules (CO<sub>2</sub> and water) and prevent fouling formation on the membrane surface [11]. rejection of methylene blue solution showed the results reached 90%.

## CONCLUSIONS

Membrane technology is an efficient method for the removal of dyes from water. Fouling formation that commonly occurs in membrane surface can be overcome by the addition of photocatalyst materials such as POM/TiO<sub>2</sub>.

## REFERENCES

- [1] J. Sharma, S. Sharma, and V. Soni, "Classification and impact of synthetic textile dyes on Aquatic Flora: A review," *Regional Studies in Marine Science*, vol. 45. Elsevier, p. 101802, 01-Jun-2021.
- [2] E. O. Ezugbe and S. Rathilal, "Membrane technologies in wastewater treatment: A review," *Membranes*, vol. 10, no. 5. 2020.
- [3] S. Natarajan, H. C. Bajaj, and R. J. Tayade, "Recent advances based on the synergetic effect of adsorption for removal of dyes from waste water using photocatalytic process," *Journal of Environmental Sciences (China)*, vol. 65. Elsevier, pp. 201–222, 01-Mar-2018.
- [4] B. Zhang *et al.*, "Simultaneously enhanced permeability and anti-fouling performance of polyethersulfone ultrafiltration membranes by structural control and mixed carbon quantum dots," *J. Memb. Sci.*, vol. 641, p. 119931, Jan. 2022.
- [5] W. Li, T. Li, X. Ma, Y. Li, L. An, and Z. Zhang, "Electrospinning preparation of a H<sub>4</sub>SiW<sub>12</sub>O<sub>40</sub>/polycaprolactam composite nanofibrous membrane and its greatly enhanced photocatalytic activity and mechanism," *RSC Adv.*, vol. 6, no. 15, pp. 12491–12496, 2016.
- [6] A. Rafiq *et al.*, "Photocatalytic degradation of dyes using semiconductor photocatalysts to clean industrial water pollution," *Journal of Industrial and Engineering Chemistry*, vol. 97. Elsevier, pp. 111–128, 25-May-2021.
- [7] S. Y. Lai, K. H. Ng, C. K. Cheng, H. Nur, M. Nurhadi, and M. Arumugam, "Photocatalytic remediation of organic waste over Keggin-based polyoxometalate materials: A review," *Chemosphere*, vol. 263. Pergamon, p. 128244, 01-Jan-2021.
- [8] S. Rahut, S. S. Basu, and J. K. Basu, "An electron trapping protocol of FePW<sub>12</sub>O<sub>40</sub> microflowers with dual catalytic properties: visible light photodegradation of amphetamine and electrocatalytic oxygen evolution," *Chem. Commun.*, vol. 55, no. 33, pp. 4825–4828, 2019.
- [9] J. Gu *et al.*, "The roles of polyoxometalates in photocatalytic reduction of carbon dioxide," *Materials Today Energy*, vol. 21. Elsevier, p. 100760, 01-Sep-2021.
- [10] H. Shi *et al.*, "Pt/POMs/TiO<sub>2</sub> composite nanofibers with an enhanced visible-light photocatalytic performance for environmental remediation," *Dalt. Trans.*, vol. 48, no. 35, pp. 13353–13359, 2019.
- [11] Z. Lin and J. Huang, "A hierarchical H<sub>3</sub>PW<sub>12</sub>O<sub>40</sub>/TiO<sub>2</sub> nanocomposite with cellulose as scaffold for photocatalytic degradation of organic pollutants," *Sep. Purif. Technol.*, vol. 264, p. 118427, Jun. 2021.
- [12] J. A. Dias, S. C. L. Dias, E. Caliman, J. Bartis, and L. Francesconi, "Keggin Structure Polyoxometalates," in *Inorganic Syntheses*, vol. 36, 2014, pp. 216–222.
- [13] I. M. Mbomekalle, Y. W. Lu, B. Keita, and L. Nadjo, "Simple, high yield and reagent-saving synthesis of pure  $\alpha$ -K<sub>6</sub>P<sub>2</sub>W<sub>18</sub>O<sub>62</sub> · 14H<sub>2</sub>O," *Inorg. Chem. Commun.*, vol. 7, no. 1, pp. 86–90, 2004.
- [14] S. M. Hassan, A. I. Ahmed, and M. A. Mannaa, "Surface acidity, catalytic and photocatalytic activities of new type H<sub>3</sub>PW<sub>12</sub>O<sub>40</sub>/Sn-TiO<sub>2</sub> nanoparticles," *Colloids Surfaces A Physicochem. Eng. Asp.*, vol. 577, pp. 147–157, Sep. 2019.
- [15] H. Barzegar, M. A. Zahed, and V. Vatanpour, "Antibacterial and antifouling properties of Ag<sub>3</sub>PO<sub>4</sub>/GO nanocomposite blended polyethersulfone membrane applied in dye separation," *J. Water Process Eng.*, vol. 38, p. 101638, Dec. 2020.
- [16] G. Marci, E. I. García-López, F. R. Pomilla, L. F. Liotta, and L. Palmisano, "Enhanced (photo)catalytic activity of Wells-Dawson (H<sub>6</sub>P<sub>2</sub>W<sub>18</sub>O<sub>62</sub>) in comparison to Keggin (H<sub>3</sub>PW<sub>12</sub>O<sub>40</sub>) heteropolyacids for 2-propanol dehydration in gas-solid regime," *Appl. Catal. A Gen.*, vol. 528, pp. 113–122, 2016.
- [17] E. I. García-López, G. Marci, I. Krivtsov, J. Casado Espina, L. F. Liotta, and A. Serrano, "Local Structure of Supported Keggin and Wells-Dawson Heteropolyacids and Its Influence on the Catalytic Activity," *J. Phys. Chem. C*, vol. 123, no. 32, pp. 19513–19527, 2019.

## **TENSILE PROPERTIES OF SEA APPLE LEAF (SALF) FILLER REINFORCED POLYESTER COMPOSITE**

A.E. Hadi<sup>1\*</sup>, J.P. Siregar<sup>2</sup>, T. Cionita<sup>3</sup>, A.P. Irawan<sup>4</sup>, D.F. Fitriyana<sup>5</sup>, R. Junid<sup>2</sup>

<sup>1</sup>*Mechanical Engineering Department, Faculty of Engineering, Universitas Malahayati, Jl. Pramuka No. 27, Kemiling, Bandar Lampung 35153, Indonesia*

<sup>2</sup>*College of Engineering, Universiti Malaysia Pahang, Gambang 26300, Malaysia*

<sup>3</sup>*Faculty of Engineering and Quantity Surveying, INTI International University, Nilai 71800, Malaysia*

<sup>4</sup>*Faculty of Engineering, Universitas Tarumanagara, Jakarta 11480, Indonesia* <sup>5</sup>*Department of Mechanical Engineering, Universitas Negeri Semarang, Kampus Sekaran, Gunungpati, Semarang 50229, Indonesia*

---

### **ABSTRACT**

Environmental concerns have contributed to the production of natural fiber composites. This study aimed to investigate tensile properties of sea apple leaf filler as a reinforcement agent in polyester resin as a matrix. The sea apple leaf (SALF) was crushed and sieved into coarse (10 mesh) and fine (100 mesh) sizes. The tensile and flexural test specimens were produced using a hand lay-up technique and an open molding cast. Furthermore, the influence of sizing and loadings of sea apple leaf filler on the composite was investigated. The results showed that the fine filler achieved higher tensile and flexural properties of composites. The increase in filler content from 10% to 20% demonstrated that the optimum formula composition ratio between filler and matrix at 15%:85% wt.%, outperformed the others. Additionally, the fine SALF filler had more improved tensile properties than the coarse and neat polyester resin. As a result, the filler loadings and sizing significantly impacted the performance of natural filler reinforced polymer composites.

*Keywords:* sea apple leaf, filler, polyester, composite, natural filler.

---

### **INTRODUCTION**

In the last few decades, the development of natural fiber reinforced composites (NFRC) has been examined. The aim has always been to find a long-term solution to the solid waste of economic plant by-products [1]. For instance, palm plants are known for their high economic value due to their fruits. However, the other parts are disposed directly without proper treatment, increasing the amount of solid waste as products and hindering environmental protection. Therefore, various research have been conducted in attempting to utilize all the resources instead of discarding it in public [2].

Natural fiber composite is known for its unique properties, including low density or light weight. Furthermore, most of them have a desired value for low loading applications and some can replace synthetic fiber in the production of eco-friendly composites [3]–[5]. Most natural fiber materials are biodegradable, which promotes sustainable development in society from an engineering standpoint. Furthermore, due to their abundant renewable resources, most of them can be produced on a low budget. However, they have some limitations that make it undesirable to the society [6].

The natural fiber reinforced polymer composites (NFRPC) have different mechanical properties from the synthetic due to the nature of the fiber. This is because natural fibers are hydrophilic and the mechanical properties rely on the interaction of the hydrophilic fiber with the hydrophobic matrix [7], [8]. Previous studies stated that the fiber and the matrix requires a strong adhesion to produce high-performance composite materials. The mechanical properties of NFRPC are determined by the type of fiber, content, size, orientation, and processing method [3].

Singha and Rana's (2012) comprehensively reviewed agave fiber embedded with polystyrene matrix composite and found that the type of fiber, such as short or long, significantly impacted the mechanical properties. Subsequently, the tensile, compressive, and flexural strength of the composites can be improved by using fiber in particle form instead of short or long, unlike the impact strength. Particle reinforced composites have the highest mechanical properties compared to the short and long due to a greater surface area, which strengthens the matrix/fiber adhesion [9].

Youssef et al. (2015) studied the mechanical properties of corn husk fiber and low-density polyethylene matrix composites. The results showed that increasing the fiber content from 5% to 10%, increased the tensile modulus from 327 MPa to 457 MPa. This indicated that increasing the density of the composite improved the tensile modulus by 39.4%. As a result, the high density increased the amount of internal bonding in the composite. However, the tensile strength and modulus decreased above 10% fiber content due to insufficient LDPE matrix [10].

---

*Article history:*

Received: 10 March 2022

Accepted: 7 June 2022

Published: 14 June 2022

---

*E-mail addresses:*

efriyo@malahayati.ac.id (A.E. Hadi)

\*Corresponding Author

El-Shekeil et al. (2014) explored the properties of kenaf fiber reinforced poly (vinyl chloride)/thermoplastic polyurethane poly-blend (PVC/TPU/KF) composites. The results showed that the tensile strength decreased when the fiber loading was

increased from 20% to 30%. This demonstrated that increasing the percentage of kenaf fiber in the matrix reduced the tensile strength. This was supported by the morphological analysis, which revealed that the fiber and the matrix had a poor adhesion. In terms of morphological properties, an increase in fiber content created more stress failure points in the composite, resulting in visible fiber pull-outs and gaps using high magnification scanning electron microscopy of PVC/TPU/KF [11].

This study aimed to investigate the tensile properties of a sea apple leaf filler reinforced polyester composite. Furthermore, the effects of sizing and filler loadings in the composites were evaluated and compared.

## **MATERIALS AND METHODS**

### *Materials preparation*

The waste sea apple leaf used as filler reinforcement was collected in Universiti Malaysia Pahang, Malaysia, attempting to have a sufficient quantity. The preparations included cleaning, crushing, and sieving the material with various varying parameters. Furthermore, the filler requires two different particle sizes, namely fine (100 mesh) and coarse (10 mesh). The unsaturated polyester resin Reversol P9509 was purchased from Ize Solution Enterprise, Kuala Lumpur. The polyester hardener, methyl ethyl ketone peroxide (MEKP), was selected as the catalyst (1% total weight of polyester) to pre-promote ambient temperature for gel and cure.

### *Fabrication of specimen*

The hand lay-up method was used with an open mold solution casting. The composite mixture consisted of two parts of filler and matrix. The initial stage involved measuring and recording the sea apple leaves filler, epoxy, and hardener with different compositions based on their weight. The epoxy was poured into the hardener and stirred slowly and uniformly with a wooden stick for approximately 5 minutes. This was followed by partially adding a small batch of the filler into the mixture while continuously stirring for 5 minutes. The composite was put in the vacuum oven at 25°C room temperature for 5 minutes to remove the bubbles in the mixture before pouring it into the mold. The final stage involved pouring the composite mixture into the mold using a self-made funnel. The funnel was made of one-third of A4 PVC cone-shaped paper to help spread the mixture evenly into the mold. As a result, the specimens cured for at least 24 hours at a room temperature. TABLE 1 shows the formulation composition of filler sizes and loading.

TABLE 1. Composition mixture of filler and polyester.

SALF Filler Size	Filler Loading (wt.%)	Polyester (wt.%)
Fine (100 mesh)	10	90
	15	85
	20	80
Coarse (10 mesh)	10	90
	15	85
	20	80

### *Tensile properties*

The composites were tensile tested using an Instron 3369 universal testing machine based on the ASTM D 638 - IV specifications. Five sampled specimens were tested with a cross-head speed of 2 mm/min, while the composites' tensile strength and modulus were measured.

### *Flexural Properties*

The three-point bending flexural test was performed using a 50 kN Instron 3369 universal testing machine based on ASTM D790. The specimen span and compression rate were set at 50 mm and 2 mm/min, respectively. Five replicate samples of size 127 mm x 12.7 mm x 3 mm were tested, and the results averaged and analyzed.

### *Microscopy analysis*

The tensile fractured specimen of sea apple leaf filler reinforced polyester composite were analyzed under Meiji techno microscope.

## **RESULTS AND DISCUSSION**

The tensile test was conducted to determine the optimum fiber loading with two different fiber lengths. Fig. 1 depicts the comparison of tensile strength and modulus on different fiber loading of fine sea apple leaf filler (SALF) reinforced polyester composites.

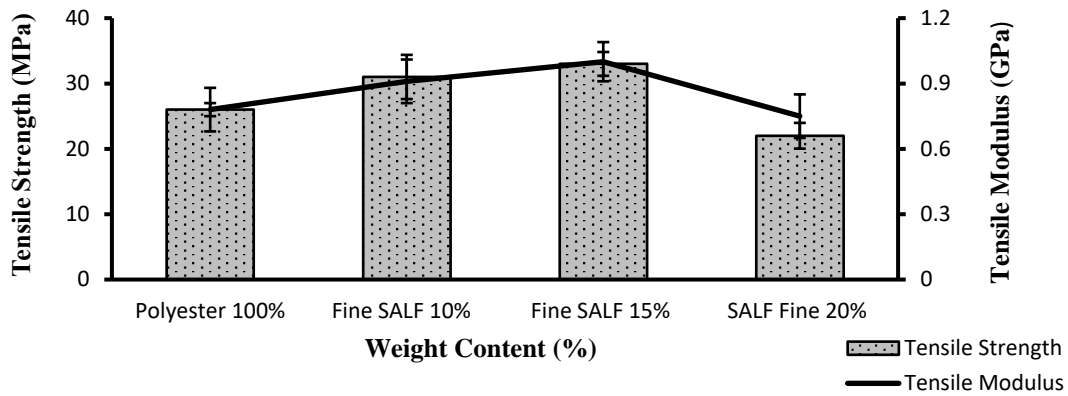


Fig. 1: Comparison tensile properties of SALF fine reinforced polyester composites against fibre loadings.

Fig. 1 shows that the tensile strength and modulus of neat polyester resin were 26 MPa and 0.78 GPa, respectively. Furthermore, an additional 10% of fine sea apple leaf filler to polyester resin increased the tensile strength and modulus by 19% and 16%, respectively. The optimum filler concentration of 15 wt.% achieved the highest tensile strength and modulus of 33 MPa and 1 GPa, respectively. Additionally, the tensile strength and modulus were lower in fine SALF concentrations of 20 wt.% than in the others. The influence of filler on matrix-filler bonding reduced the tensile strength. The interfacial bonding of matrix and filler was affected by adding filler to the resin, reducing the surface area [12]. Tensile strength of composites decreased with filler ratios of 20% of overall performance. This findings were similar to Sarikaya et al. (2019), who discovered that palm/epoxy, birch, and eucalyptus composites with a maximum fiber loading of 30% had lower tensile strength than virgin epoxy [13]. Hence, increasing the filler concentration above the limit decreased the tensile strength. There was a strong fiber-to-fiber interaction at higher filler loadings, resulting to poor wetting of fibers and fiber dispersion. This type of systems have easier crack initiation and propagation at higher loadings, as shown in Fig. 3 [14], [15].

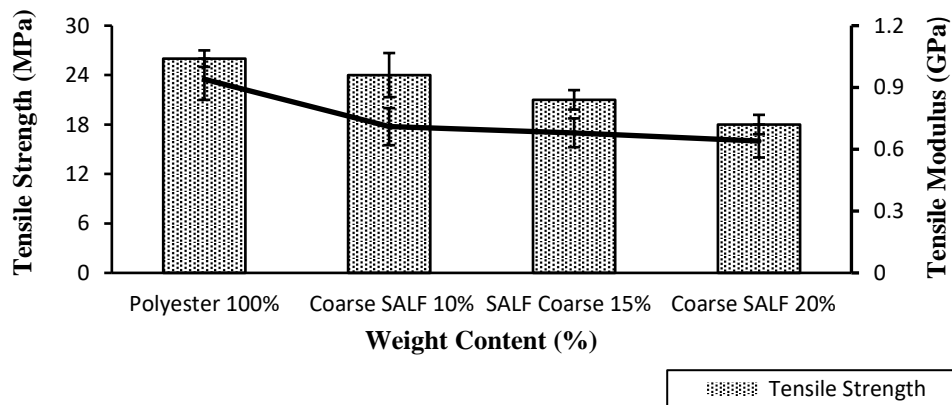


Fig. 2: Comparison tensile properties of SALF coarse reinforced polyester composites against fiber loadings.

Fig. 2 presents the comparison of tensile properties of the coarse SALF filler reinforced epoxy with different fiber loadings. The comparison of three type composition of SALF showed that the tensile strength and modulus values decreased from 24 MPa to 18 MPa and 0.71 GPa to 0.64 GPa, respectively. The addition of 10 wt.% coarse filler in the composite decreased the tensile strength and modulus by 8% and pf 28%, respectively, compared to the unfilled filer (neat polyester). This was supported by Sathiskumar et al (2012), which concluded that increasing the fiber length and loading significantly reduced the tensile strength and load transfer between fibers and matrix [16]. Furthermore, Zhang et al. (2018) concluded that the weak adhesion was caused by the interference of the hydrophilic fibers with the hydrophobic polymer, while the poor spreading was due to the heavy intermolecular bonding of the natural fibers that cause agglomeration [17]. Subrahmanyam et al (2019) showed that the increased fiber loading causing agglomeration lead to void formation within the composite, making the processing difficult. This indicated a similar finding image of optical microscope, as shown in Fig. 3. Furthermore, shrinkage and cooling rate cause the void formation during matrix curing [18].

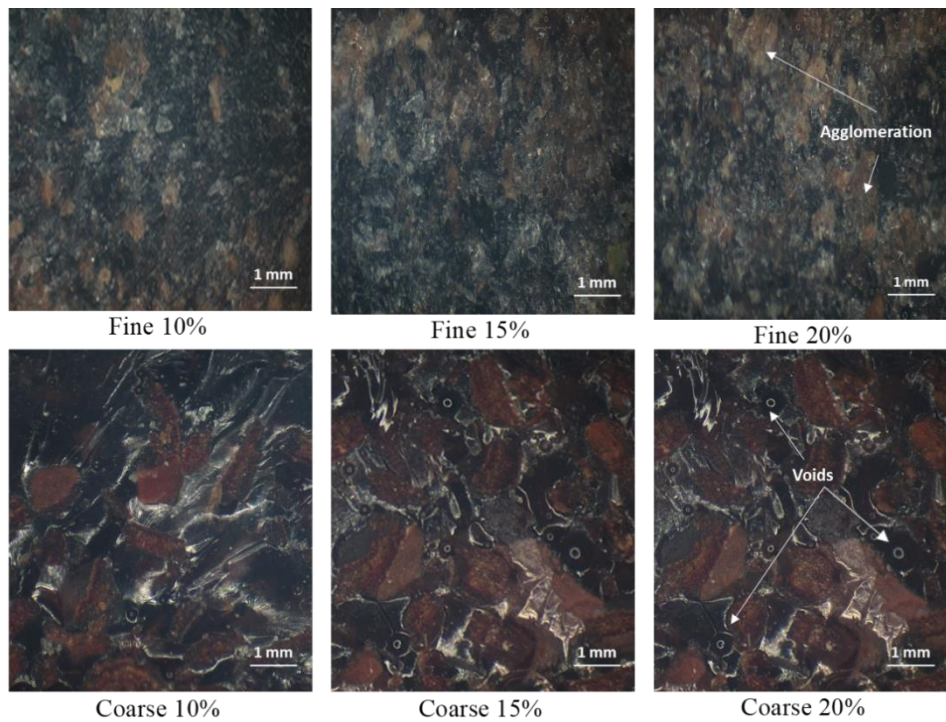


Fig. 3: Image of optical microscope of SALF filler reinforced polyester composite.

Fig. 4 shows a major comparison between fine SALF filler compositions compared to the coarse on the tensile properties. There was a significant difference on the tensile strength and modulus with 29% and 9%, respectively, on the fine SALF with 10 wt.% compared to the coarse with 10 wt.% filler. The 10% fine SALF indicated 31 MPa tensile strength and 0.91 GPa modulus compared to the coarse with 24 MPa and 0.71 GPa tensile strength and modulus, respectively. Similarly, the 15% SALF composition showed an outstanding difference between fine and coarse filler with 57% tensile strength and 47 % modulus. The tensile strength and modulus of fine SALF 15% presented the output of 33 MPa and 1.0 GPa. In contrast, the coarse SALF 15% showed a tensile strength and modulus of 21 MPa and 0.68 GPa, respectively. The filler increase of 20% significantly decreased the tensile properties for both sizes. This was caused by improper adhesion between the reinforcement agent and matrix composites. The finding supported Bisht et al. (2018), which stated that the filler load and length caused by inadequate adherence between the fibre and the matrix material, is attributed to the decrease of mechanical properties [19]. Subsequently, the air bubbles on the specimen surface during the hand lay-up process can affect the tensile properties of the composites (see in Fig. 3) [20], [21].

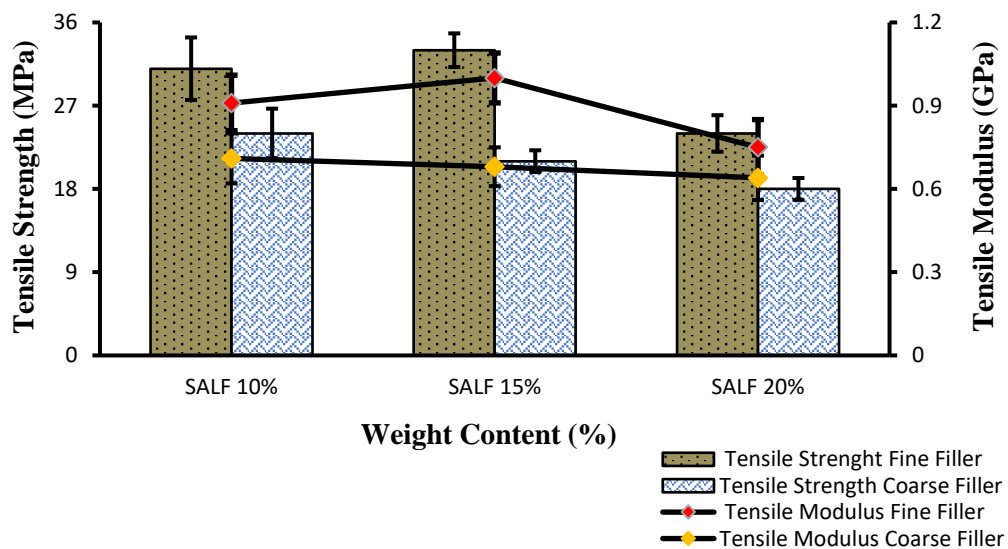


Fig. 4: Comparison tensile properties of different fiber size of SALF reinforced Epoxy composites against fiber loadings.

## CONCLUSION

This study successfully performed the tensile properties on sea apple leaf filler reinforced polyester composites. The objectives included evaluating and comparing the effects on fiber loading and the influence of fiber length on tensile properties. The fine sea apple leaf (SALF) filler at 15 wt.% concentration showed the optimum tensile properties of the composites. Furthermore, the addition of coarse filler from 10% to 20% decreased the tensile properties.

## ACKNOWLEDGMENT

The author expresses sincere gratitude to the Universitas Malahayati and Universiti Malaysia Pahang for their support, facilities, and equipment.

## REFERENCES

- [1] A. Lotfi, H. Li, D. V. Dao, and G. Prusty, "Natural fiber-reinforced composites: A review on material, manufacturing, and machinability," *Journal of Thermoplastic Composite Materials*, vol. 34, no. 2, pp. 238–284, 2021.
- [2] M. Safiuddin, M. Z. Jumaat, M. A. Salam, M. S. Islam, and R. Hashim, "Utilization of solid wastes in construction materials," *International journal of physical sciences*, vol. 5, no. 13, pp. 1952–1963, 2010.
- [3] C. Tezara *et al.*, "The effect of hybridisation on mechanical properties and water absorption behaviour of woven jute/ramie reinforced epoxy composites," *Polymers*, vol. 13, no. 17, Sep. 2021, doi: 10.3390/polym13172964.
- [4] A. E. Hadi *et al.*, "Application of Micromechanical Modelling for the Evaluation of Elastic Moduli of Hybrid Woven Jute–Ramie Reinforced Unsaturated Polyester Composites," *Polymers*, vol. 13, no. 15, 2021. doi: 10.3390/polym13152572.
- [5] J. P. Siregar *et al.*, "The effect of maleic anhydride polyethylene on mechanical properties of pineapple leaf fibre reinforced polylactic acid composites," *International Journal of Precision Engineering and Manufacturing-Green Technology*, vol. 6, no. 1, pp. 101–112, 2019.
- [6] J. Jaafar, J. P. Siregar, C. Tezara, M. H. M. Hamdan, and T. Rihayat, "A review of important considerations in the compression molding process of short natural fiber composites," *The International Journal of Advanced Manufacturing Technology*, vol. 105, no. 7–8, pp. 3437–3450, 2019.
- [7] M. H. M. Hamdan *et al.*, "Water absorption behaviour on the mechanical properties of woven hybrid reinforced polyester composites," *International Journal of Advanced Manufacturing Technology*, vol. 104, no. 1–4, 2019, doi: 10.1007/s00170-019-03976-9.
- [8] C. Tezara *et al.*, "Effect of Stacking Sequences, Fabric Orientations, and Chemical Treatment on the Mechanical Properties of Hybrid Woven Jute–Ramie Composites," *International Journal of Precision Engineering and Manufacturing-Green Technology*, pp. 1–13, 2021.
- [9] A. S. Singha and R. K. Rana, "Natural fiber reinforced polystyrene composites: Effect of fiber loading, fiber dimensions and surface modification on mechanical properties," *Materials & Design*, vol. 41, pp. 289–297, 2012.
- [10] A. M. Youssef, A. El-Gendy, and S. Kamel, "Evaluation of corn husk fibers reinforced recycled low density polyethylene composites," *Materials Chemistry and Physics*, vol. 152, pp. 26–33, 2015.
- [11] Y. A. El-Shekeil, S. M. Sapuan, M. Jawaid, and O. M. Al-Shuja'a, "Influence of fiber content on mechanical, morphological and thermal properties of kenaf fibers reinforced poly (vinyl chloride)/thermoplastic polyurethane polyblend composites," *Materials & Design*, vol. 58, pp. 130–135, 2014.
- [12] A. G. Adeniyi, S. A. Abdulkareem, S. A. Adeoye, and J. O. Ighalo, "Preparation and properties of wood dust (isoberlinia doka) reinforced polystyrene composites," *Polymer Bulletin*, pp. 1–19, 2021.
- [13] E. Sarikaya, H. Çallioğlu, and H. Demirel, "Production of epoxy composites reinforced by different natural fibers and their mechanical properties," *Composites Part B: Engineering*, vol. 167, pp. 461–466, 2019.
- [14] H. Ku, H. Wang, N. Pattarachaiyakoo, and M. Trada, "A review on the tensile properties of natural fiber reinforced polymer composites," *Composites Part B: Engineering*, vol. 42, no. 4, pp. 856–873, 2011.
- [15] S. F. K. Sherwani, S. M. Sapuan, Z. Leman, E. S. Zainudin, and A. Khalina, "Physical, mechanical and morphological properties of sugar palm fiber reinforced polylactic acid composites," *Fibers and Polymers*, vol. 22, no. 11, pp. 3095–3105, 2021.
- [16] T. P. Sathishkumar, P. Navaneethkrishnan, and S. Shankar, "Tensile and flexural properties of snake grass natural fiber reinforced isophthallic polyester composites," *Composites Science and Technology*, vol. 72, no. 10, pp. 1183–1190, 2012, doi: 10.1016/j.compscitech.2012.04.001.
- [17] W. Zhang, X. Yao, S. Khanal, and S. Xu, "A novel surface treatment for bamboo flour and its effect on the dimensional stability and mechanical properties of high density polyethylene/bamboo flour composites," *Construction and Building Materials*, vol. 186, pp. 1220–1227, 2018.
- [18] B. v Subrahmanyam, S. V. G. Krishna, R. J. Kumar, and S. B. R. Devireddy, "Experimental and micromechanical thermal characteristics of jute fiber reinforced polyester composites," *Materials Today: Proceedings*, vol. 18, pp. 350–356, 2019.
- [19] N. Bisht and P. C. Gope, "Effect of alkali treatment on mechanical properties of rice husk flour reinforced epoxy bio-Composite," *Materials Today: Proceedings*, vol. 5, no. 11, pp. 24330–24338, 2018.
- [20] B. Shivamurthy, K. Murthy, P. C. Joseph, K. Rishi, K. U. Bhat, and S. Anandhan, "Mechanical properties and sliding wear behavior of jatropa seed cake waste/epoxy composites," *Journal of Material Cycles and Waste Management*, vol. 17, no. 1, pp. 144–156, 2015.

***The International Symposium on Polymeric Materials 2022***

- [21] T. G. T. Pereira, J. F. Mendes, J. E. Oliveira, J. M. Marconcini, and R. F. Mendes, “Effect of reinforcement percentage of eucalyptus fibers on physico-mechanical properties of composite hand lay-up with polyester thermosetting matrix,” *Journal of Natural Fibers*, 2018.



## UTILIZATION OF POLYETHYLENE TEREPHTHALATE (PET) PLASTIC BOTTLE WASTE AS A MEMBRANE WITH SEVERAL MODIFICATIONS FOR THE REMOVAL OF CHROMIUM IONS IN WASTEWATER

B. T. I. Ali<sup>1</sup>, N. Widiastuti<sup>1\*</sup>, Y. Kusumawati<sup>1</sup>, J. Jaafar<sup>2</sup>

<sup>1</sup>Department of Chemistry, Faculty of Science and Data Analytics, Institut Teknologi Sepuluh Nopember, Sukolilo, Surabaya 60111, Indonesia

<sup>2</sup>Advanced Membrane Technology Research Centre (AMTEC), Universiti Teknologi Malaysia, 81310 Skudai, Johor Bahru, Malaysia

---

### ABSTRACT

The increasing demand for products that use the electroplating process has caused the growth of the electroplating industry in various countries to increase. This growth was followed by an increase in the amount of toxic and hazardous chromium waste in the water. Continuous technology development is needed to overcome these problems. One of the technologies that has been developed until now is membrane technology. On the other hand, plastic bottle waste, which increases every year (381.73 million tons), has the property of forming films or thin layers. Therefore, the use of plastic bottle waste into a low-cost, sustainable, and environmentally friendly membrane material has great potential. In this study, the immersion-precipitation phase inversion method was used in the membrane preparation process by modifying fillers (zeolite NaY) to improve membrane performance. Determination of fillers was studied. Furthermore, the fabricated membranes were tested for their performance in chromium ion contamination in wastewater. The results showed that the PET-W membrane could produce a water flux of 292.74 Lm<sup>-2</sup>h<sup>-1</sup>bar<sup>-1</sup> and a chromium ion flux of 544.94 Lm<sup>-2</sup>h<sup>-1</sup>bar<sup>-1</sup>. The addition of zeolite NaY increased the percent removal from PET-W membrane to 10 times (from 4.07 to 47.8).

*Keywords:* PET waste, membrane modification, chromium ions, wastewater treatment.

---

### INTRODUCTION

The increasing demand for products that use the electroplating process has caused the growth of the electroplating industry in various countries to increase. This growth was followed by an increase in the amount of toxic and hazardous chromium waste in the water. The Environmental Protection Agency (EPA) reports that high concentrations of chromium ions in waters (250 times higher than the WHO allowable limit of 50 µg/L) in India, America, Nepal, and Indonesia. Continuous technology development is needed to overcome these problems. One of the technologies that has been developed until now is membrane technology [1]. On the other hand, plastic waste has become a serious problem in various countries. Plastic is one of the low-cost membrane materials, and has the ability to form films, so that it can be used as a membrane material [2], [3]. Polyethylene terephthalate (PET) is a type of plastic that is widely used in bottled drinking water. PET membranes have been used for wastewater treatment and water purification. However, the use of plastic waste made from PET into membranes has not been developed much. Based on this background, this study utilizes PET plastic waste as a membrane material. The addition of Zeolite-Y as filler was used to increase the selectivity to chromium ion. Zeolite-Y is a type of filler that is simple to make and has been shown to outperform MOF, silica, and carbon in membrane performance [4]. The choice of zeolite is based on the nature of the zeolite, which has uniformly sized pores and is composed of aluminosilicate in a tetrahedral shape with high thermal and chemical stability and is composed of aluminosilicate in a tetrahedral shape with the oxygen atom in the corner of the geometric pattern. Furthermore, zeolites can overcome polymer membrane limits such as thermal breakdown or deformation at high temperatures and pressures [5]. The phase immersion inversion technique is used in the manufacture of membranes from PET waste because of the simplicity of the process. The cross flow module is used during filtration to prevent fouling of the membrane. This research is expected to overcome chromium ion contamination in wastewater by utilizing plastic waste in order to obtain sustainable technology. The wastewater used in this research comes from wastewater produced from the electroplating industry and synthetic wastewater (wastewater made by adding chromium ions in a certain concentration).

### MATERIALS AND METHODS

#### *Materials*

Polyethylene terephthalate (C<sub>10</sub>H<sub>8</sub>O<sub>4</sub>)<sub>n</sub> was obtained from drinking water bottle waste (Surabaya, Indonesia), Zeolite-Y was obtained from previous research [6], Phenol (C<sub>6</sub>H<sub>6</sub>O, 99%), and sodium dichromate (K<sub>2</sub>Cr<sub>2</sub>O<sub>7</sub>, 99%) (purchased from Merck, Germany).

#### *Methods*

The preparation of the membrane refers to a previous study conducted by Ali [3]. Waste PET plastic bottles are thoroughly cleaned before being dried for 30 minutes at 30 degrees Celsius. The dried plastic waste is cut into 1 x 1 cm squares using a cutter to make it simpler to dissolve. Plastic

---

#### *Article history:*

Received: 10 March 2022

Accepted: 7 June 2022

Published: 14 June 2022

---

#### *E-mail addresses:*

tamamali2308@gmail.com (B.T.I. Ali)

nurul\_widiastuti@chem.its.ac.id (N. Widiastuti)

y\_kusumawati@chem.its.ac.id (Y. Kusumawati)

juhana@petroleum.utm.my (J. Jaafar)

\*Corresponding Author

trash up to 17.12% (w/w) grams in weight was weighed and put in a Duran bottle holding 82.19% (w/w) of phenol. To avoid phenol's capacity to dissolve PET plastic bottle trash from being harmed, 0.68% (w/w) zeolite-NaY was dissolved separately in phenol with PET plastic bottle garbage. The homogenization process of the dope solution (14.6 mL) was carried out in complete darkness (no light) using a magnetic stirrer (speed 200 rpm, temperature 100 °C) until homogenous. The homogenous membrane imprint solution was poured onto a glass plate after remaining for a few minutes to eliminate any bubbles created by stirring. The glass plate was immersed in a coagulation bath containing ethanol and water in a 15:1 ratio for the phase transition technique. The membrane produced will be used to filter fluids containing chromium ions at a concentration of 10 parts per million. To keep the membrane from fouling, a cross flow module is employed. Within 40 minutes, the filtration process is completed.

RESULTS AND DISCUSSION

Fig. 1 a displays the FTIR spectra of the waste PET membrane (PET-W) before and after the addition of zeolite. Spectra were obtained at a frequency of 4000-400 cm<sup>-1</sup>. The FTIR measurements suggested the existence of stretched O-H bonds by the appearance of a peak at 3363 cm<sup>-1</sup>. Peak at 1578 cm<sup>-1</sup> confirms the existence of C=C bonds in the phenyl ring of PET. Peaks at 2967 cm<sup>-1</sup> and 737 cm<sup>-1</sup> were induced by the C-H stretching bond of the ethyl group of PET. The signal at 1742 cm<sup>-1</sup> suggests that the PET ester group is undergoing C=O stretching. In addition, the peaks at 1408 cm<sup>-1</sup> correspond to the C-O bond stretching of the PET ester group, whilst the peaks at 1021 cm<sup>-1</sup>, 1140 cm<sup>-1</sup>, and 1248 cm<sup>-1</sup> reveal the existence of the terephthalate group [3]. The area of the zeolite peak, 973.17 cm<sup>-1</sup>, differentiates it from PET (Si-O-Al) [7]. The addition of zeolite did not considerably alter the FTIR spectra of PET since the amount of zeolite applied was rather tiny. Fig. 1b displays the values of the PET-W membrane's water flux and chromium ion flux. The reduction in water and chromium ion flow values was caused by fouling during filtration. Due to lower ion particle size (2.5 μm) than water particle size, the chromium ion flux has a greater value than the water ion flux (4.9 μm). TABLE 1 displays the amount of Chromium ions removed by PET-W and PET-W/Zeolite membranes. The inclusion of zeolite as a filler in the membrane increased by ten times percentage of chromium ions removed. The increase in elimination percentage was attributed to the zeolite's capacity to absorb and interact effectively with chromium ions.

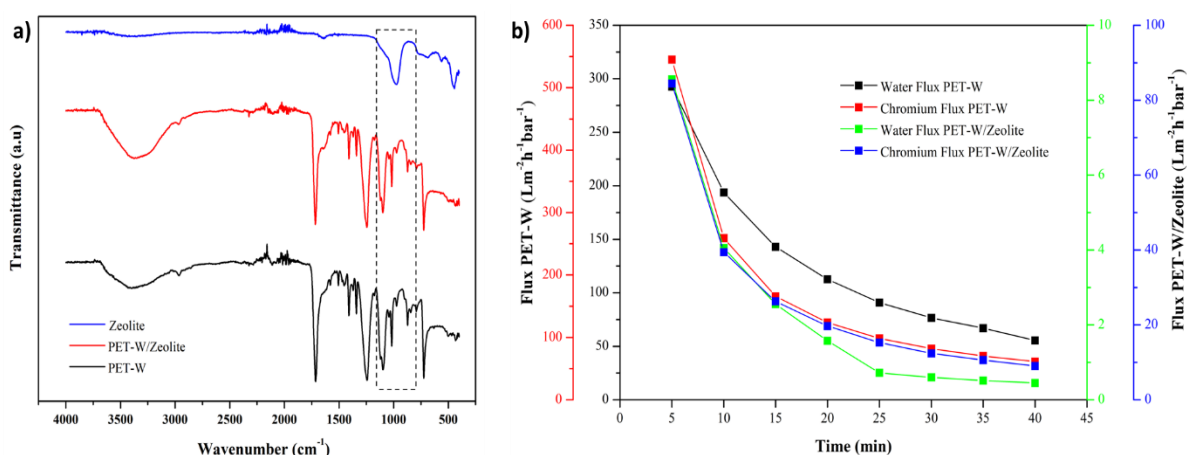


Fig 1. a) FTIR spectra, b) Water Flux and Chromium ion Flux

TABLE 1. Percent removal of chromium

Membrane	% Removal
PET-W	4.07
PET-W/Zeolite	47.8

CONCLUSIONS

Plastic bottle waste made of polyethylene terephthalate can be utilized as a membrane to lower ion chromium levels in wastewater. The use of zeolite-Y as a membrane filler can improve the performance of the membrane in removing chromium ions to 10 times.

ACKNOWLEDGEMENTS

The authors would like to thank Kementerian Pendidikan Kebudayaan Riset dan Teknologi, Indonesia for the financial support through the Doctoral Research Grant (PDD) and Kurita Water and Environment Foundation (KWEF) Grant No. 21Pid071-15R.

**REFERENCES**

- [1] A. Asad, D. Sameoto, and M. Sadrzadeh, "Overview of membrane technology," in *Nanocomposite Membranes for Water and Gas Separation*, Elsevier, 2020, pp. 1–28.
- [2] I. V Korolkov *et al.*, "Modification of PET ion track membranes for membrane distillation of low-level liquid radioactive wastes and salt solutions," *Sep. Purif. Technol.*, vol. 227, no. April, p. 115694, 2019, doi: 10.1016/j.seppur.2019.115694.
- [3] B. T. I. Ali, N. Widiastuti, Y. Kusumawati, and J. Jaafar, "Utilization of drinking water bottle waste as a sustainable and low-cost membrane material in water purification," *Mater. Today Proc.*, no. xxxx, 2022, doi: 10.1016/j.matpr.2022.03.581.
- [4] M. Vinoba, M. Bhagiyalakshmi, Y. Alqaheem, A. A. Alomair, A. Pérez, and M. S. Rana, "Recent progress of fillers in mixed matrix membranes for CO<sub>2</sub> separation: A review," *Sep. Purif. Technol.*, vol. 188, pp. 431–450, 2017, doi: 10.1016/j.seppur.2017.07.051.
- [5] M. R. A. Hamid and H. K. Jeong, "Recent advances on mixed-matrix membranes for gas separation: Opportunities and engineering challenges," *Korean J. Chem. Eng.*, vol. 35, no. 8, pp. 1577–1600, 2018, doi: 10.1007/s11814-018-0081-1.
- [6] N. Widiastuti, E. Sukma Ningtiar, F. Nafilah, B. Tamam Ibnu Ali, A. Setyo Purnomo, and T. Qodar Romadiansyah, "Enhancement of PVDF/LiCl membrane performance by modifying the membrane surface using zeolite NaY and ZCC spray coating method for *Dunaliella salina* microalgae dewatering," *Mater. Today Proc.*, no. xxxx, 2022, doi: 10.1016/j.matpr.2022.02.525.
- [7] A. Mekki *et al.*, "Michael Addition of 1,3-Dicarbonyl Derivatives in the Presence of Zeolite Y as an Heterogeneous Catalyst," *J. Inorg. Organomet. Polym. Mater.*, vol. 30, no. 7, pp. 2323–2334, 2020, doi: 10.1007/s10904-019-01424-5.

## LATEX DIPPING FILM OF CREAMED SKIM NATURAL RUBBER LATEX

P. Ramchan<sup>1</sup>, W. Taweepreda,<sup>1,2\*</sup> D. Veerasamy<sup>3</sup>

<sup>1</sup>*Polymer Science Program, Division of Physical Science, Faculty of Science, Prince of Songkla University, Hat-Yai, Songkhla 90110, THAILAND*

<sup>2</sup>*Tavorn Rubber Industry (1982) Co., Ltd., 33 Kanjanavanich Road, Sadao, Songkhla 90120, THAILAND*

<sup>3</sup>*19, Jalan KE 4/9 Kota Emerald, 48000 Rawang, Selangor, Malaysia*

---

### ABSTRACT

Skim natural rubber latex (SNRL) was recovered solid rubber by creaming process using hydroxyethyl cellulose (HEC). It was found that the amount of recovered skim rubber is independent of the dry rubber content and ammonia concentration in the SNRL but depended on the concentration and the viscosity of creaming agent used. The maximum recovered skim rubber was obtained when using 5.56 g/L of HEC. The dipped latex film was prepared by various ratio of creamed SNRL with concentrated high ammonia natural rubber latex (HA-NRL). The SNRL with high viscosity, contained high amount of protein, can be mixed with HA-NRL at the ratio 50:50 as maximum and give smooth film product. The protein of film product was removed by leaching process with hot water. The tensile strength and elongation at breakage of the rubber film decreased after leaching process.

*Keywords:* skim natural rubber latex, latex films, creaming, protein.

---

### INTRODUCTION

Natural rubber latex (NRL) is obtained from *Hevea Brasiliensis* trees. Field NRL is tapped from rubber trees and preserved with ammonia solution consisted of 30% rubber fraction and about 5% non-rubber such as proteins and lipids. It is well known that the commercial high ammonia natural rubber latex concentrate can be produced by centrifugation of field NRL, leaving behind a by-product with 4–6 wt% DRC of this process which consists highly of non-rubber and small rubber particles or skim natural rubber latex (SNRL) particles in dilution. Concentrated NRL is mainly used in dipping processes for the production of medical gloves, condoms, and other NRL products. In contrast, SNRL is processed into skim natural rubber (SNR) products such as skim crepe and skim blocks or is discarded as waste. Since increasing amounts of SNRL are being produced as an industrial by-product, characterization methods for SNRL and SNR were investigated. These materials contain a higher amount of proteins than does NRL, and the SNRL particles are smaller and can be more easily converted into a smooth film product [1,2]. Moreover, skim rubber exhibits good adhesion and has been studied for use as a urea encapsulant in controlled release applications [3].

### MATERIALS AND METHODS

#### *Materials*

Creaming agent hydroxyethyl cellulose (HEC) with viscosity 3800 – 5000 mPa.s Brookfield LV [25°C, 1% solution] was purchased from Phitsanuchemical Co., Ltd. Potassium laurate solution 20% and Potassium hydroxide solution 10% were purchased from Lucky four Co., Ltd (Thailand). All of compounding ingredients were supplied by Tiarco Chemical (M) Sdn Bhd., Malaysia. Precipitated calcium carbonate was obtained from Vicchi Enterprise Co., Ltd. Calcium nitrate liquid (55%) (DipCal LQ). and modified corn starch (GELATO USP) were supplied by Excelkos Sdh Bhd., Malaysia and General Starch Company Limited, Thailand, respectively.)

#### *Preparation of Dipped Latex Film*

The latex compound was prepared followed the compounding ingredients as shown in TABLE 1. The 20% potassium laurate solution was first added in to the latex, and then were all vulcanizing ingredients. Finally, the latex compound was diluted with deionized water to achieve the Total Solids Content at 30 % (w/w) TSC. The latex compound was kept under stirring at 120 rpm at ambient temperature for 48 hours.

---

#### *Article history:*

Received: 10 March 2022

Accepted: 7 June 2022

Published: 14 June 2022

---

#### *E-mail addresses:*

rpattadon@gmail.com (P. Ramchan)

\*Corresponding Author

TABLE 1. The ingredients of latex compound

Ingredients	Dry weight (pphr.)
NR Latex (HA-NRL and HA-NRL mixing with Creamed SNRL)	100
20% Potassium Laureate solution	1.6
10% Potassium hydroxide solution	0.1
50% Sulfur Dispersion	1.0
50% Zinc Oxide Dispersion	0.6
50% ZDEC Dispersion	0.8
50% ZDBC Dispersion	0.2
50% Antioxidant Dispersion	1.0
50% Titanium dioxide Dispersion	1.0

A cleaned former was first dipped into the coagulant solution with mixture of 8% calcium nitrate and 4% precipitated calcium carbonate by weight in distilled water, dried in hot air oven. After that was dipped in to NRL compound followed pre-leaching with hot water. The deposited latex film was then dried in hot air oven at 115-120 °C for 16 minutes to cure followed by post-leaching in hot water. Before stripping, the films were coated with modified corn starch to prevent sticking. The films were kept in desiccator for 7 days prior to further testing.

## RESULTS AND DISCUSSION

### *Creaming SNR latex by creaming agents*

When the SNR latex/creaming agent mixture was allowed to stand at room temperature in a separating funnel for 3 days, separation of rubber particles occurred. Formed rubber particles in the cream phase floated to the top of the latex mixture since density of rubber particle (0.93 g/cm<sup>3</sup>) is smaller than that of water. Creaming of SNR latex by using HEC as creaming agent was found to depend on their concentration and viscosity. They could be seen that %serum phase volume shown continuous decreases with increasing of creaming agent concentration. The observed creaming behavior of SNR latex at various concentration of creaming agent could be explained in relation to the viscosity of the mixture. It was found that the viscosity of the latex mixture increased rapidly with rising concentration of creaming agent. According to Stokes' Law

$$V = (2gR^2)(D_1 - D_2) / 9\eta$$

where V is the particle velocity, g is the acceleration of gravity, R is the particle diameter, D<sub>1</sub> is the density of particle, D<sub>2</sub> is the density of medium and η is the viscosity of medium, the rate of movement of a suspended spherical particle under gravity is inversely proportional to the viscosity of the dispersion medium. Thus, rapid creaming of the rubber particles will be favored by low viscosity medium. For this reason, separation of rubber particles will be slower at higher concentration of creaming agent, hence the observed decline in %serum phase volume with increasing concentration of creaming agent.

TABLE 2: The thickness of latex film from the mixing of various ratio between HA-NRL and SNRL

Proportion of Concentrated Latex And Creamed Skim Latex	Average Thickness (mm)
100/0	0.31 ± 0.03
90/10	0.26 ± 0.01
80/20	0.24 ± 0.02
70/30	0.22 ± 0.02

TABLE 3: Mechanical properties of latex films

Samples	Tensile Strength (MPa)	100% Modulus (MPa)	300% Modulus (MPa)	500% Modulus (MPa)	Elongation At Break (%)
100/0	18.69 ± 0.80	0.8 ± 0.02	1.50 ± 0.02	3.14 ± 0.28	696.40 ± 18.59
90/10	18.15 ± 1.66	0.75 ± 0.02	1.39 ± 0.02	2.43 ± 0.03	773.07 ± 22.76
80/20	17.37 ± 1.59	0.72 ± 0.02	1.34 ± 0.02	2.38 ± 0.28	775.92 ± 10.96
70/30	12.60 ± 1.73	0.71 ± 0.02	1.26 ± 0.15	2.35 ± 0.51	703.98 ± 22.55

TABLE 4: Mechanical properties of latex films after curing accelerate at 100°C for 24 hrs

Samples	Tensile Strength (MPa)	100% Modulus (MPa)	300% Modulus (MPa)	500% Modulus (MPa)	Elongation At Break (%)
100/0	11.31 ± 3.17	0.70 ± 0.03	1.34 ± 0.05	2.40 ± 0.09	700.08 ± 34.85
90/10	12.00 ± 0.97	0.72 ± 0.02	1.40 ± 0.02	3.00 ± 0.20	633.66 ± 18.56
80/20	11.80 ± 1.58	0.57 ± 0.06	1.21 ± 0.18	3.51 ± 0.30	645.71 ± 17.87
70/30	10.25 ± 1.92	0.64 ± 0.03	1.27 ± 0.03	2.76 ± 0.44	569.13 ± 62.50

TABLE 5: Mechanical properties of latex films after leaching to remove protein with various method

Sample	Tensile Strength (MPa)	100% Modulus (MPa)	300% Modulus (MPa)	500% Modulus (MPa)	Elongation At Break (%)
<b>Unleached (UL)</b>					
100/0	18.69 ± 0.80	0.8 ± 0.02	1.50 ± 0.02	3.14 ± 0.28	696.40 ± 18.59
90/10	18.15 ± 1.66	0.75 ± 0.02	1.39 ± 0.02	2.43 ± 0.03	773.07 ± 22.76
80/20	17.37 ± 1.59	0.72 ± 0.02	1.34 ± 0.02	2.38 ± 0.28	775.92 ± 10.96
70/30	12.60 ± 1.73	0.71 ± 0.02	1.26 ± 0.15	2.35 ± 0.51	703.98 ± 22.55
<b>Leached By Hot Water At 85 Degree Celsius, 5 Mins</b>					
100/0	25.42 ± 1.14	0.87 ± 0.02	1.58 ± 0.05	3.75 ± 0.20	688.27 ± 24.27
90/10	20.3 ± 1.37	0.81 ± 0.05	1.58 ± 0.13	3.60 ± 0.45	713.24 ± 16.90
80/20	26.65 ± 0.92	0.83 ± 0.02	1.57 ± 0.04	3.21 ± 0.17	808.64 ± 20.16
70/30	17.19 ± 0.74	0.83 ± 0.01	1.48 ± 0.05	2.75 ± 0.34	689.10 ± 7.83
<b>Leached By 0.2 M KOH Solution At 85 Degree Celsius, 5 Mins</b>					
100/0	18.58 ± 0.90	0.77 ± 0.03	1.48 ± 0.11	3.06 ± 0.24	701.66 ± 20.66
90/10	16.28 ± 1.02	0.74 ± 0.03	1.38 ± 0.05	3.03 ± 0.28	723.86 ± 20.66
80/20	14.76 ± 0.82	0.85 ± 0.02	1.52 ± 0.03	4.00 ± 0.40	691.89 ± 10.27

## CONCLUSIONS

The creaming of SNR latex can be achieved by using HEC as creaming agent. No coagulation of the rubber particles in the cream phase occurred after phase separation. The rubber-recovering efficiency is very high and this process is independent of the dry rubber content and ammonia concentration in the SNR latex. There is the best concentration and viscosity of the creaming agent in order to cream SNR latex effectively. 3.70 g/L of HEC yielded about 100% recovered skim rubber. The protein of film product was removed by leaching process with hot water. The tensile strength and elongation at breakage of the rubber film decreased after leaching process.

## ACKNOWLEDGEMENTS

This research project is supported by National Research Council of Thailand (NRCT): N41A640250. PR would like to thank TAVORN RUBBER INDUSTRY (1982) CO., LTD. and Faculty of Science, Prince of Songkla University for research supporting

## REFERENCES

- [1] Rippel MM, Lee LT, Leite CA, Galembek F. Skim and cream natural rubber particles: colloidal properties, coalescence and film formation. *J Colloid Interface Sci.* 2003; 268:330-40.
- [2] Tangboriboonrat P, Tanunchai, T, Tiyapiboonchaiya C. Creaming skim natural rubber latex for encapsulation of urea fertiliser. *Plast Rubber Compos.* 1999; 28:357-62
- [3] Sakdapipanich JT, Rojruthai P. Molecular structure of natural rubber and its characteristics based on recent evidence. In: Sammour R, editor. *Biotechnology-Molecular Studies and Novel Applications for Improved Quality of Human Life.* Croatia: InTech; 2012. p. 213-38

## MODIFICATION OF CHITOSAN-BASED MEMBRANE WITH EPOXIDIZED NATURAL RUBBER

A. Wichianchom<sup>1</sup>, W. Taweepreda,<sup>1\*</sup> Q. Ali<sup>2</sup>, M. Zulkifli<sup>3</sup>.

<sup>1</sup>Polymer Science Program, Division of Physical Science, Faculty of Science, Prince of Songkla University, Hat-Yai, Songkhla 90110, Thailand

<sup>2</sup>Sustainable Energy Management, Faculty of Environmental Management, Prince of Songkla University, Hat-Yai, Songkhla 90110 Thailand

<sup>3</sup>Green Chemistry and Sustainability Cluster, Universiti Kuala Lumpur, Branch Campus Malaysian Institute of Chemical and Bioengineering Technology, Taboh Naning, 78000 Alor Gajah, Melaka, Malaysia

---

### ABSTRACT

Fuel cell technology is a viable option to potentially overcome these challenges due to its high energy efficiency and eco-friendliness. Chitosan is considered one of the promising materials for polymer electrolyte membrane fuel cells (PEMFC) due to the high manufacturing cost of the commercial polymer electrolyte membrane (PEM). In this study, Chitosan (C-1), Epoxidized natural rubber (ENR), chitosan blended with ENR (CE-6 and CE-7) based membranes were prepared by solution casting technique. The optical contact angle (OCA) showed that the C-1 had the highest contact angle while ENR-41 with least contact angle. From the electrical measurements, the CE-7 showed highest resistance, resistivity, and the ENR-41 showed highest dissipation factor and dielectric constant. Finally, the results revealed that the CE-7 had the most suitable results, making it fit to use as a PEM.

*Keywords:* chitosan, epoxidized natural rubber, electrical conductivity, atomic force microscopy, contact angle, polymer electrolyte membrane fuel cell.

---

### INTRODUCTION

The fuel cell is an electrochemical device which converts chemical energy into electrical energy consists of an anode and a cathode and an electrolyte. It was discovered by William Grove in 1839 [1]. Among the different types of Fuel cells, polymer electrolyte membrane fuel cell (PEMFC) is a type of fuel cell which has been one of the trending research subjects for the researchers and engineers for decades and it has been used successfully as an energy source for submarines and spacecraft [2]. However, commercialization of PEMFC is still inhibited due to some major technical challenges, like the cost of the material, high methanol and water permeability as well as significantly electroosmotic drag. Therefore, the replacement of Nafion with cost-effective polymer materials is highly desirable [3], [4].

In this study, chitosan modified by chloroacetic acid to get chloroacetate chitosan, and the modified chitosan blended with epoxidized natural rubber for using as PEM for polymer electrolyte membrane fuel cells. The homogenous chitosan/ENR membrane was prepared by solution casting with different ratios. The membranes were crosslinked with sulfuric acid and sodium hydroxide and dried for at least 24hrs. The physical properties of the membranes were analyzed by the ATR-FTIR; the surface properties were characterized by using atomic force microscope (AFM) by imaging techniques. The hydrophobicity and hydrophilicity were checked by optical contact angle technique. An LCR meter used to analyze the electrical properties of the membranes.

### MATERIALS AND METHODS

#### *Materials*

Chitosan powder (Seafresh Industry Public Co. Ltd, Thailand) with the degree of deacetylation of 95% and the molecular weight of 500,000 gmol<sup>-1</sup>. CH<sub>3</sub>COOH (glacial 100%) was purchased from Merck KGaA, Germany. NaOH (≥ 99%) and H<sub>2</sub>SO<sub>4</sub> (95–97%) were obtained from Merck KGaA, Germany. ENR-50 Latex was purchased from Muang Mai Guthrie Public Co. Ltd.

#### *Methods*

The chitosan solution (0.5 wt%) was prepared by dissolving 0.5 g of chitosan powder in diluted acetic acid solution (96.5 g of water and 3 g of acetic acid) and vigorously stirred it with a magnetic stirrer until it was fully dissolved at ambient temperature. The chitosan/ENR (CS/ENR) solutions were prepared by blending the homogenous mixture of chitosan solution and ENR latex with different ratios. The chitosan solution used to prepare chitosan (C-1) membrane. Furthermore, chitosan solution blended with ENR latex to make CE-6 (chitosan-15g/ENR-3g) membrane and CE-7 (Chitosan-9g/ENR-9g) membrane. In addition, ENR latex (18g) used to prepare ENR-41 (epoxidized natural rubber membrane). To prepare the membranes the solutions poured

---

#### *Article history:*

Received: 10 March 2022

Accepted: 7 June 2022

Published: 14 June 2022

---

#### *E-mail addresses:*

wirach.t@psu.ac.th (W. Taweepreda)

\*Corresponding Author

onto glass plate and placed in oven for 30 hours for drying at 60 °C. The membranes crosslinked with aqueous NaOH and H<sub>2</sub>SO<sub>4</sub> for one and two hours, respectively. After that, the membranes were washed with distilled water and placed for final drying in the oven for 2 to 3 hours until dry completely at 40 °C. The hydrophobicity and hydrophilicity were checked by optical contact angle technique. An LCR meter was used to analyze the electrical properties of the membranes.

## RESULTS AND DISCUSSION

### Contact angle Measurements

The contact angles of sessile drops on the surface of membranes were elucidated by asymmetric shape analysis of drops. The contact angles of the drops and volume of the bubble are summarized in TABLE 1. The results showed that the C-1 membrane has the highest contact angle (87.5°), followed by CE-6 with 84.5°. The other membranes with major contact angles were CE-7 and ENR-41 with 75° and 56.5° respectively. While, it has been observed that when the membrane absorbs the water inside a fuel cell, it causes to activate the membrane by conducting protons through the membrane. In order to achieve this characteristic, the contact angle of a membrane needs to be in between the hydrophilic and hydrophobic regions [5]. In this study, we have two membranes (C-1 and CE-6) that gave contact angles that a PEM required to function, while the other membranes (CE-7 and ENR-41) showed relatively low contact angles showing hydrophilic properties.

TABLE 1: Contact angle and volume of drop of the membranes.

Membrane	Contact Angle (θ)	Bubble volume (μL)
C-1	87.5°	13.6
CE-6	84.5°	11
CE-7	75°	9.6
ENR-41	56.5°	10.9

### Electrical Properties

#### i. Capacitance

The capacitance of the polymeric membranes was plotted as a function of frequency with the range of 75 kHz to 1 MHz shown in Fig. 1(a). The results showed that the membranes based on chitosan without any blending (C-1) showed the highest capacitance values, on the other hand the membranes based on just ENR (ENR-41), chitosan/ENR (CE-6 and CE-7) showed relatively lower capacitance values. In the PEMFC the higher the membrane capacitance will have a better performance.

#### ii. Conductance (G)

The electrical conductance of the membrane given in Fig. 1(b) by plotting it against frequency with the range of 75 kHz to 1000 kHz. For comparison, several membranes used with different materials and blends with different concentrations. The results showed that the C-1, and ENR-41 which were based on just chitosan or ENR showed high conductance values. However, the membranes which are based on the blends of both ENR and chitosan gave the least result. At last, it is known the PEM has two functions: first is to conduct protons, and second is to insulate the anode and cathode, That's why it is important for a PEM to have low conductance [6], whereas in this study, blended membranes showed promising conductance values for using them as a PEM.

#### iii. Resistance (R)

Fig. 1(c) shows the results of electrical resistance versus frequency (75-975) kHz for the membrane samples. Among the different membrane samples, the CE-7 showed the highest resistance value of 3050 kΩ at initial frequency (75 kHz), and significantly decreased by the escalation of frequency with the resistance of 617 kΩ at final frequency value (975 kHz). The sample which showed the second highest resistance value at low to high frequency was CE-6 with (2780-633) kΩ at (75-975) kHz. The membranes (ENR-41 and C-1) showed the lower resistance values among all others. In addition, the membrane which were based on simple composition without any blends showed low resistance.

#### iv. Resistivity (Ω.cm)

Fig. 1(d) shows the resistivity vs frequency of membrane samples, the frequency range used in this study was 75-975 kHz. The CE-7 membrane showed the highest resistivity value of 750.3 Ω•cm at low frequency with a significant fall by the increase in frequency, and at 975 kHz, the resistivity of CE-7 became 151.78 Ω.cm. The CE-6 showed the second highest resistivity of (333.6-75.96) Ω.cm at low to high frequency with the similar trend as CE-7. The other major membranes (ENR-41) showed result of resistivity with (135.85-28.91) Ω.cm. Finally, the C-1 showed the lower resistivity at low to high frequency values with the least (1.1-0.24) Ω.cm.

#### v. Conductivity (S cm<sup>-1</sup>)

The results of conductivity against frequency given in Fig. 1(e). At low frequency, the conductivity of C-1 was highest with 0.30 S/cm at 75 kHz and escalated with the rise in frequency by 2.17 S/cm at 975 kHz, followed by ENR-41 with (0.0111-0.0450) S/cm at low to high frequency. The results showed that all the membranes based on ENR (ENR-41), chitosan/ENR (CE-6 and CE-7) gave low conductivity values and CE-7 gave the lowest values (0.0013-0.0066) S/cm at low to high frequency. Finally, the above results showed that the mixing of ENR can cause a significant change in conductivity values of the membranes caused to gain the conductivity values.

#### vi. Dissipation factor (tan δ)

Mostly, the polymer electrolyte membranes are aqueous electrolytes because they are operational only in the conditions in which they absorbed water around their sulfonic acid group structure, so it is very important to understand the water dynamics



of the membranes by the dielectric characterization [7]. Actually, the dissipation factor is the ratio of ohmic losses to capacitance reactance. The lower dissipation factor will have better capacitance [8]. The results show the dissipation factor versus frequency (Fig. 1(f)) of the membrane samples in which the ENR-41 showed the highest dissipation factor with 0.57 at 75 kHz, followed by CE-7 and CE-6 with 0.27-0.11 and 0.20-0.08 each at low to high frequency, respectively. Finally, the C-1 showed the least dissipation factor value (0.14-0.09).

vii. Dielectric constant ( $\epsilon_r$ )

The dynamics of water (molecules and protons) within the membrane, it is necessary to know the dielectric characteristics of the membrane. Furthermore, the dissipation factor affects the performance of PEMFC, which depends on the dielectric properties of the material and the frequency. Fig. 1(g) shows the results of dielectric constant against frequency results of the membranes. The ENR-41 showed the highest relative permittivity (18.43 F/m) at low frequency and 7.98 F/m at high frequency. The second highest was the CE-7 with 4.65 F/m at 75 kHz and fell down with the escalation in frequency by 3.67 F/m at 975 kHz. In all the cases the dielectric constant decreased with the increase in frequency. The membrane C-1 showed the lower values (2.56-2.16) at low to high frequency and CE-6 showed the least dielectric constant values (2.51-2.05) at 75-975 kHz.

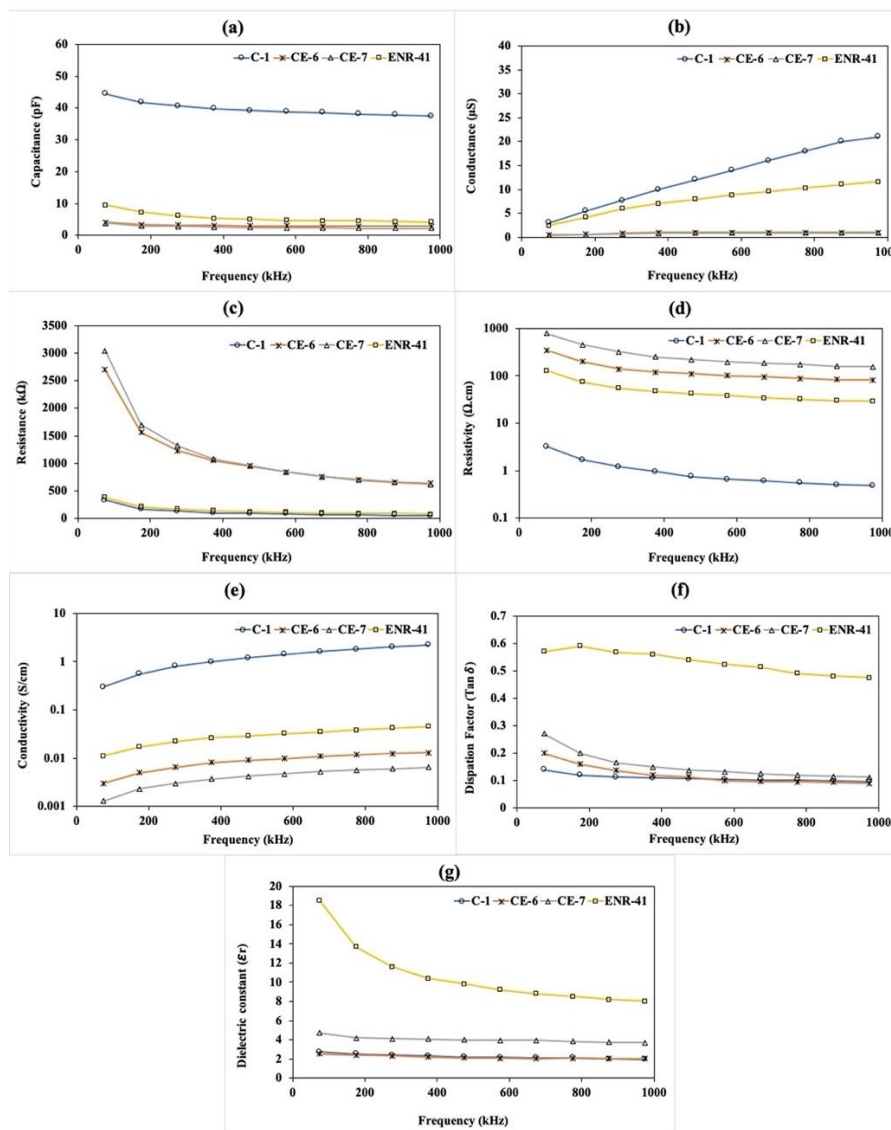


Fig. 1: Electrical properties of the membranes: (a) Capacitance; (b) Conductance; (c) Resistance; (d) Resistivity; (e) Conductivity; (f) Dissipation factor; (g) Dielectric constant.

CONCLUSIONS

In this work, the chitosan and ENR based membranes were prepared to use as PEM. The chitosan was blended with ENR with different amounts and wt%. The solution casting technique used to prepare the membranes. The optical contact angle (OCA) used to calculate the hydrophobicity and hydrophilicity of the membranes, the C-1 showed the highest contact angle followed by the CE-6. For the electrical measurements an LCR meter was used, the CE-7 showed highest resistance, resistivity, and the ENR-41 showed highest dissipation factor and dielectric constant. Finally, the results of LCR revealed that the blended membranes had most of the suitable characteristics which are required for a PEM and CE-7 was the most suitable among all.

## ACKNOWLEDGEMENTS

The authors were grateful for the financial support from the National Science and Technology Development Agency (NSTDA). Besides, this work was supported by the Higher Education Research Promotion and National Research University Project of Thailand, Office of the Higher Education Commission. Finally, our team research would like to thank the Graduate School and Faculty of Science, Prince of Songkla University for supporting budgets and locations during this research.

## REFERENCES

- [1] Inc. S. A. I. C. E. S. Parsons, *Fuel cell handbook*, 5th ed., vol. 5, no. 1. West Virginia, 2000. doi: 10.5860/CHOICE.26-6292.
- [2] B. Smitha, S. Sridhar, and A. A. Khan, "Chitosan–poly(vinyl pyrrolidone) blends as membranes for direct methanol fuel cell applications," *Journal of Power Sources*, vol. 159, no. 2, pp. 846–854, Sep. 2006, doi: 10.1016/j.jpowsour.2005.12.032.
- [3] P. D. Beattie *et al.*, "Ionic conductivity of proton exchange membranes," *Journal of Electroanalytical Chemistry*, vol. 503, no. 1–2, pp. 45–56, 2001, doi: 10.1016/S0022-0728(01)00355-2.
- [4] M. M. Hasani-Sadrabadi, N. M. Dorri, S. R. Ghaffarian, E. Dashtimoghadam, K. Sarikhani, and F. S. Majedi, "Effects of organically modified nanoclay on the transport properties and electrochemical performance of acid-doped polybenzimidazole membranes," *Journal of Applied Polymer Science*, vol. 117, no. 2, pp. 1227–1233, Jul. 2010, doi: 10.1002/app.31974.
- [5] D. E. Moilanen, I. R. Piletic, and M. D. Fayer, "Water dynamics in nafion fuel cell membranes: The effects of confinement and structural changes on the hydrogen bond network," *Journal of Physical Chemistry C*, vol. 111, no. 25, pp. 8884–8891, 2007, doi: 10.1021/jp067460k.
- [6] S. M. J. Zaidi, "Preparation and characterization of composite membranes using blends of SPEEK/PBI with boron phosphate," *Electrochimica Acta*, vol. 50, no. 24, pp. 4771–4777, Aug. 2005, doi: 10.1016/j.electacta.2005.02.027.
- [7] Z. Lu, M. Lanagan, E. Manias, and D. Macdonald, "Dielectric properties of polymer electrolyte membranes measured by two-port transmission line technique," in *The Electrochemical Society*, 2010, vol. 28, no. 29, pp. 95–105. doi: 10.1149/1.3502448.
- [8] I. D. Gimba, A. S. Abdulkareem, A. Jimoh, and A. S. Afolabi, "Theoretical Energy and Exergy Analyses of Proton Exchange Membrane Fuel Cell by Computer Simulation," *Journal of Applied Chemistry*, vol. 2016, pp. 1–15, 2016, doi: 10.1155/2016/2684919.

## THE EFFECT OF CHEMICAL TREATMENT TOWARDS PHYSICAL DIMENSIONS OF SUGAR PALM FIBER/PLA COMPOSITE FILAMENT FOR FDM

M. H. M. Nasir<sup>1</sup>, M. M. Taha<sup>2\*</sup>, Nadlene R.<sup>1</sup>

<sup>1</sup>*Faculty of Mechanical Engineering, Universiti Teknikal Malaysia Melaka, Hang Tuah Jaya, 76100 Durian Tunggal, Melaka, Malaysia.*

<sup>2</sup>*Faculty of Mechanical and Manufacturing Engineering Technology, Universiti Teknikal Malaysia Melaka, Hang Tuah Jaya, 76100 Durian Tunggal, Melaka, Malaysia.*

---

### ABSTRACT

A study on the effect of chemical treatment towards the physical dimension of sugar palm fiber (SPF)/Polylactic Acid (PLA) composite filament for FDM is presented in this paper. The fiber was treated with three different chemical treatments which are alkaline, silane, and a combination of alkaline and silane treatment. The composite filaments were extruded using a twin-screw extruder with a 2.5% presence of SPF. The fabricated filaments were used to prepare all samples of tensile and flexural tests which were printed using a 3D printing machine. The sample physical dimension was evaluated to determine the differences (error %) compared with designated drawing dimensions. As a result, the untreated samples show bigger dimensions compared with other samples which are -1.56 % and -0.94% error on thickness while the pure PLA filament shows the largest difference with a 6.25% error which means lower than drawing dimensions. However, the different treatments of the composite did not show any significant effect towards the physical dimensions of the printed sample which are below 5% error.

*Keywords:* sugar palm fiber, fused deposition modeling, natural composite filament.

---

### INTRODUCTION

Over the last two decades, 3D printing technology has progressed from a costly, high-end luxury item to an affordable, dependable, and low-cost appliance, making significant contributions to science, engineering, and manufacturing. The mechanism is composed of numerous components. The mechanism incorporates three technologies: computer-aided design (CAD), computer-aided manufacturing (CAM), and Fused Deposition Modeling (FDM), a filament-extrusion-based technology. The designed CAD model is exported as a stereolithography (STL) format file before being printed. Following that, slicing software from a 3D printer's manufacturer is used to horizontally separate the 3D model into thin layers and manage the FDM machine. Thermoplastic filaments are fed into the heated extrusion print head in FDM, allowing for three-dimensional (3D) dispensing of polymer melts on a platform [1].

Currently, various thermoplastic polymer materials such as Polypropylene (PP), Acrylonitrile Butadiene Styrene (ABS), Polylactic Acid (PLA), and others are used for FDM filament. FDM is a reliable method for rapid prototyping because it does not require the use of expensive moulds and tools. There is a demand for composite filaments by incorporating certain fillers into polymer matrices due to their improved mechanical characteristics, biocompatibility, and conductivity [3]. Sugar palm fiber (SPF) has been utilized in conjunction with polymeric materials as a reinforcing material. Numerous investigations have been conducted by previous researchers using SPF as a polymer composite, as shown in the TABLE 1 below.

TABLE 1: A synopsis of a prior study on SPF composites.

Authors	Fiber	Polymer	Sampling Method
[4]	Sugar palm	Epoxy	Hand lay-up
[5]	Sugar palm	TPU	Hot-press moulding
[6]	Sugar palm	TPU	Composite board
[7]	Sugar palm	PU	Composite board
[8]	Sugar palm	Epoxy	Composite board
[9]	Sugar palm, Roselle	PU	Sheet form
[10]	Sugar palm nanocellulose	TPS/PLA	Compression moulding

---

#### Article history:

Received: 10 March 2022

Accepted: 7 June 2022

Published: 14 June 2022

---

#### E-mail addresses:

mastura.taha@utem.edu.my (M. M. Taha)

\*Corresponding Author

The employment of natural fiber with polymer matrix has posed a compatibility issue due to the hydrophilic of natural fibers and the polymer matrix is hydrophobic which can cause interfacial incompatibilities and wettability. With this issue, many researchers had performed chemical treatments on the fiber surface to improve the adhesion between natural fibers and polymer matrix [9].

Printing parameters such as nozzle temperature, bed temperature, layer thickness, building orientation, and printing speed normally will contribute to the printing quality of parts. The mechanical properties of FDM printed components are significantly influenced by the design and processing conditions of the process, often exhibiting anisotropic mechanical properties due to the choice of specific orientation of the infill layer [11]. Several factors lead to the accuracy of the printed parts such as the mechanical properties of materials, which can affect how a print is wrapped, the post-curing process that could cause shrinkage, and post-processing tools that can contribute to reliable results. The effect of the FDM process parameters on the mechanical properties of fabricated parts was investigated in [12], and [13]. However, limited research has studied the effect of chemical treatment towards dimensional accuracy of SPF/PLA composite for FDM 3D printing.

**MATERIALS AND METHODOLOGY**

*Material*

In this study, the filament used to print the sample is from Sugar Palm Fiber (SPF) reinforced with Polylactic Acid (PLA) with 2.5 % fiber loading. Several surface treatments of SPF have been executed using 3 different processes such as alkaline treatment (NaOH), silane treatment (3-Aminopropyltriethoxysilane), and a combination of alkaline with silane treatment. SPF reinforced PLA filament was prepared using a twin-screw extruder with a diameter of 1.75mm; a desired diameter of filament to be used at the FDM machine.

*Printing Process*

All samples were printed using *Creativity Ender-3* with four different types of filaments according to the dimension as shown in Fig. 1. The filament from pure 100% PLA also has been printed as a comparison to composite samples. The printer is equipped with a 0.8mm diameter nozzle to ensure no clogging issues occur during the printing process. The printing parameter is set up as shown in TABLE 2.

TABLE 2: Printing process parameter.

Ind.	Temperature	Infill	Speed	Resolution
1.	Printing 190 °C	Density 100 %	Print 50mm/s	High
2.	Bed 80 °C	Pattern Line	Travel 80mm/s	Brim

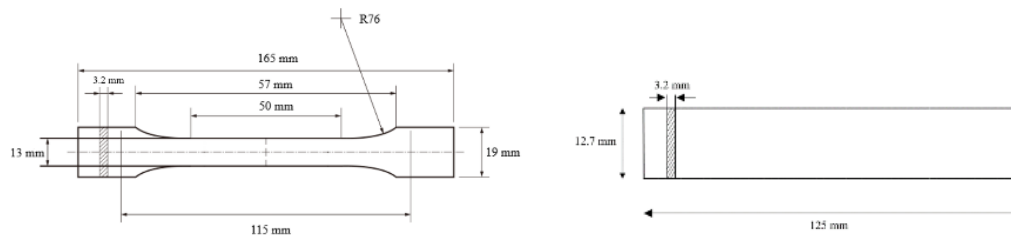


Fig. 1: Dimension of tensile and flexural samples.

*Measurement.*

The measurement of all samples was conducted by using a Digital Caliper from *Mitutoyo*.

**RESULT AND DISCUSSION**

*Dimension measurement using Vernier Caliper.*

All samples were printed using a 3D printer machine with parameters as TABLE 2 accordingly. The brim of all samples was removed and the surface of the sample was clean to ensure no debris or defect would affect the reading of the vernier caliper during measurement.

In the measurement of samples, the values of all samples were recorded. Three main parts have been measured which are width, length, and thickness. Four samples from each type of treatment were taken to determine the accuracy of printed samples. The relative error is evaluated to compare the difference between the dimensions of the drawing and the dimensions of printed parts. The error % was calculated as *Equation 1*.

$$\frac{\text{Drawing dimension} - \text{Actual dimension}}{\text{Drawing dimension}} \times 100 \%$$

(Equation 1)

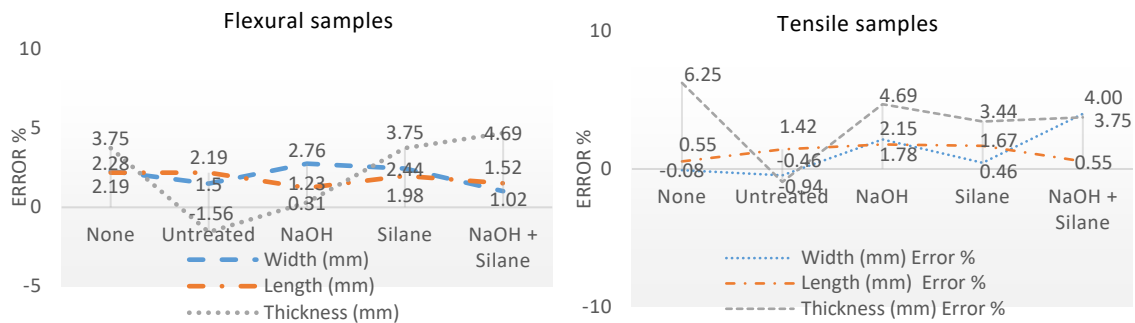


Fig. 2: Flexural and tensile samples

As a result, the 3D printer has printed out all samples with below 5% error compared to the drawing dimensions. The different types of fiber treatment were not contributing to the dimension differences in the sample. Moreover, pure samples of 100 % PLA show a huge error for thickness even though without the presence of SPF in the filament. However, the thickness dimension of untreated samples shows slightly higher than other treated samples. It may be due to the poor adhesion of the printed layer that might bring a huge void inside the printed parts.

In conclusion, SPF/PLA composite filament extruded by an FDM machine is printable and suitable to be used as filament composite for FDM. Further investigation of its characteristics needs to be performed to ensure the reliability of the produced filament to be used in various applications.

#### ACKNOWLEDGEMENTS

The authors would like to thank Universiti Teknikal Malaysia, Melaka, and the Ministry of Education, Malaysia for the financial support through the grant scheme FRGS/1/2020/FTKMP-CARE/F00456 for this project and Jabatan Perkhidmatan Awam (JPA) for providing financial support through scholarship Hadiah Latihan Persekutuan (HLP) to the principal author.

#### REFERENCES

- [1] G. Cicala, D. Giordano, C. Tosto, G. Filippone, A. Recca, and I. Blanco, "Polylactide (PLA) filaments a biobased solution for additive manufacturing: Correlating rheology and thermomechanical properties with printing quality," *Materials (Basel)*, vol. 11, no. 7, 2018, doi: 10.3390/ma11071191.
- [2] T. Yao, J. Ye, Z. Deng, K. Zhang, Y. Ma, and H. Ouyang, "Tensile failure strength and separation angle of FDM 3D printing PLA material: Experimental and theoretical analyses," *Compos. Part B Eng.*, vol. 188, no. January, p. 107894, 2020, doi: 10.1016/j.compositesb.2020.107894.
- [3] T. N. A. T. Rahim, A. M. Abdullah, and H. Md Akil, "Recent Developments in Fused Deposition Modeling-Based 3D Printing of Polymers and Their Composites," *Polym. Rev.*, vol. 59, no. 4, pp. 589–624, 2019, doi: 10.1080/15583724.2019.1597883.
- [4] D. Bachtiar, S. M. Sapuan, and M. M. Hamdan, "The effect of alkaline treatment on tensile properties of sugar palm fibre reinforced epoxy composites," *Mater. Des.*, vol. 29, no. 7, pp. 1285–1290, 2008, doi: 10.1016/j.matdes.2007.09.006.
- [5] A. Atiqah, M. Jawaid, S. M. Sapuan, and M. R. Ishak, "Physical properties of silane-treated sugar palm fiber reinforced thermoplastic polyurethane composites," *IOP Conf. Ser. Mater. Sci. Eng.*, vol. 368, no. 1, 2018, doi: 10.1088/1757-899X/368/1/012047.
- [6] A. Atiqah, M. Jawaid, S. M. Sapuan, and M. R. Ishak, "Properties of Sugar Palm / Glass Fiber-reinforced," no. April, 2017.
- [7] A. A. Mohammed, D. Bachtiar, J. P. Siregar, and M. R. M. Rejab, "Effect of sodium hydroxide on the tensile properties of sugar palm fibre reinforced thermoplastic polyurethane composites," *J. Mech. Eng. Sci.*, vol. 10, no. 1, pp. 1765–1777, 2016, doi: 10.15282/jmes.10.1.2016.2.0170.
- [8] D. Bachtiar, S. M. Sapuan, and M. M. Hamdan, "The influence of alkaline surface fibre treatment on the impact properties of sugar palm fibre-reinforced epoxy composites," *Polym. - Plast. Technol. Eng.*, vol. 48, no. 4, pp. 379–383, 2009, doi: 10.1080/03602550902725373.
- [9] A. M. Radzi, S. M. Sapuan, M. Jawaid, and M. R. Mansor, "Effect of Alkaline Treatment on Mechanical, Physical and Thermal Properties of Roselle/Sugar Palm Fiber Reinforced Thermoplastic Polyurethane Hybrid Composites," *Fibers Polym.*, vol. 20, no. 4, pp. 847–855, 2019, doi: 10.1007/s12221-019-1061-8.
- [10] A. Nazrin, S. M. Sapuan, and M. Y. M. Zuhri, "Mechanical, physical and thermal properties of sugar palm nanocellulose reinforced thermoplastic starch (Tps)/poly (lactic acid) (pla) blend bionanocomposites," *Polymers (Basel)*, vol. 12, no. 10, pp. 1–18, 2020, doi: 10.3390/polym12102216.
- [11] M. M. Hanon, L. Zsidai, and Q. Ma, "Accuracy investigation of 3D printed PLA with various process parameters and different colors," *Mater. Today Proc.*, vol. 42, pp. 3089–3096, 2021, doi: 10.1016/j.matpr.2020.12.1246.
- [12] S. Bakrani Balani, F. Chabert, V. Nassiet, and A. Cantarel, "Influence of printing parameters on the stability of deposited beads in fused filament fabrication of poly(lactic acid)," *Addit. Manuf.*, vol. 25, no. July 2018, pp. 112–121, 2019, doi: 10.1016/j.addma.2018.10.012.
- [13] X. Wang, M. Jiang, Z. Zhou, J. Gou, and D. Hui, "3D printing of polymer matrix composites: A review and prospective," *Composites Part B: Engineering*. 2017, doi: 10.1016/j.compositesb.2016.11.034.

## STARCH-BASED PLASTICS: A BIBLIOMETRIC ANALYSIS (1990-2021)

A.H. Nordin<sup>1</sup>, R.A. Ilyas<sup>1, 2\*</sup>, N. Ngadi<sup>1</sup>

<sup>1</sup>*School of Chemical and Energy Engineering, Faculty of Engineering, Universiti Teknologi Malaysia (UTM), Skudai 81310, Malaysia*

<sup>2</sup>*Centre for Advanced Composite Materials (CACM), Universiti Teknologi Malaysia (UTM), Skudai 81310, Malaysia*

---

### ABSTRACT

Plastics have been extensively utilized primarily for food packaging as they are cheap, lightweight and easy in the process of manufacture and use. Nonetheless, the characteristic of plastic (such as non-biodegradable) remains challenging. Following that, researchers have been investigating to substitute conventional petroleum-based plastics with biodegradable plastics. Bioplastics are the best substitute as they are biodegradable and green which can minimize environmental pollution. Biodegradable plastics made from starch have gained great attention as they are natural polysaccharides made by plants. In this study, the bibliometric analysis was conducted to understand and predict the direction of future studies for starch-based plastics research. All reported articles regarding “Starch-based plastics” from the WoS database were analyzed using the VOS viewer to develop visualization maps. The analysis of the data shows that starch-based plastics research is a new but essential field of study, and more research is expected in the years ahead. The most active countries were China, USA, Brazil, France and Malaysia, while Averous L (from France) was the most active author who had made valuable contributions related to starch-based plastics research with 36 published documents from 2000 to 2021. Keyword plus co-occurrence analysis reveals a rapid investigation on the improvement of starch-based plastics properties to ensure the stability and quality of the materials for replacing conventional petroleum-based plastics.

*Keywords:* starch, natural polymers, plastics, packaging purpose.

---

### INTRODUCTION

Plastics are used in a wide range of sectors, including food packaging, automotive, construction, healthcare, and recreation [1]. Plastic usage has increased as the global population has expanded, resulting in negative environmental consequences. Due to concerns about global climate change caused by massive quantities of plastic waste generation, biobased and biodegradable polymeric materials may be among the most acceptable substitutes for existing petroleum-based plastics [10]. Starch has been viewed as the best choice for creating bioplastics since it is plentiful in nature, green, and affordable [2, 3]. The characteristics of starch-based bioplastics have been studied extensively [4, 5]. Mose and Maranga [6] pointed out that the significant elements of outstanding bioplastic depended on their mechanical and thermoforming qualities, gas and water vapor permeability, transparency and accessibility. Starch-based plastics are an intriguing part of material engineering research. Therefore, a thorough examination of research and publishing patterns on starch-based plastic would greatly assist scientists in this area in planning and determining the direction of future research. This work uses a bibliometric analysis of scientific publications published between 1990 and 2021 to look into the trends in starch-based plastics research. Annually, the overall trends in reported research publications and proceedings (collectively referred to as documents in this study) were examined. The visualisation maps were created to show productivity and cooperation at the author and nation levels, as well as the co-occurrence of keywords in the chosen texts. To the best of the authors' knowledge, this is the first bibliometric analysis on starch-based plastics research that provides readers with a current overview of the research and publishing landscape on the topic.

### METHODOLOGY

Web of Science (WoS) database and search key string of TS= (Starch-based plastic\*) was applied on 08/03/2022 for the selection of the documents. Only the articles and conference proceedings (from 1990 to 2021) were comprised in the analysis as these documents present original findings on the topic of starch-based plastics [7, 8]. A total of 2292 documents were analyzed using a method adapted from Wu *et al.*, [9]. The analysis was divided into three phases: (1) quantitative analysis on the publication trend on starch-based plastics research; (2) social network analysis to demonstrate the research collaborations among countries and authors, and (3) co-occurrence analysis of Keywords to determine the research focus.

### RESULTS AND DISCUSSION

#### *General publication trend*

As shown in Fig. 1a, the number of articles related to starch-based plastics increased significantly from 2 (in 1990) to 245 (in 2021) due to the increased research funding by many agencies, starting in 2017 (14) and continuing through 2021 (319), on starch-based plastics research as a replacement for conventional plastics. The National Natural Science Foundation of China is the largest funder, followed by the National Council for Scientific and Technological Development and the CAPES Foundation of Brazil, the

---

#### *Article history:*

Received: 10 March 2022

Accepted: 7 June 2022

Published: 14 June 2022

---

#### *E-mail addresses:*

abuhassannordin@gmail.com (A.H.Nordin)

Ahmadilyasrushman@yahoo.com (R.A.Ilyas)

norzita@cheme.utm.edu.my (N.Ngadi)

\*Corresponding Author

European Commission, and Argentina's National Scientific and Technical Research Council. In contrast to the enormous expansion in the number of research articles published annually, yearly proceedings output fluctuated between 1 and 30, with no clear trend. According to the findings, starch-based plastics research is a relatively young but important research issue, with greater research output projected in the coming years.

*Contribution and collaboration among countries*

People from many nations and continents may now collaborate on research projects more easily because of advancements in communication technologies. This allows for cross-border knowledge and technology transfer. Collaborations from forty nations resulted in a large number of papers on starch-based polymers, as seen in Fig. 1b (minimum number: 10 articles per country). China disclosed the most papers (287), followed by the United States (246), Brazil (202), France (166), and Malaysia (165). (166). (147). For example, early international collaboration research on starch-based polymers included China, France, Finland, and Greece. More nations began to use green plastics as time went on, and information was shared via international partnerships. Most recent research partnerships were led by Indonesian, Pakistani, Polish, and Nigerian professionals.

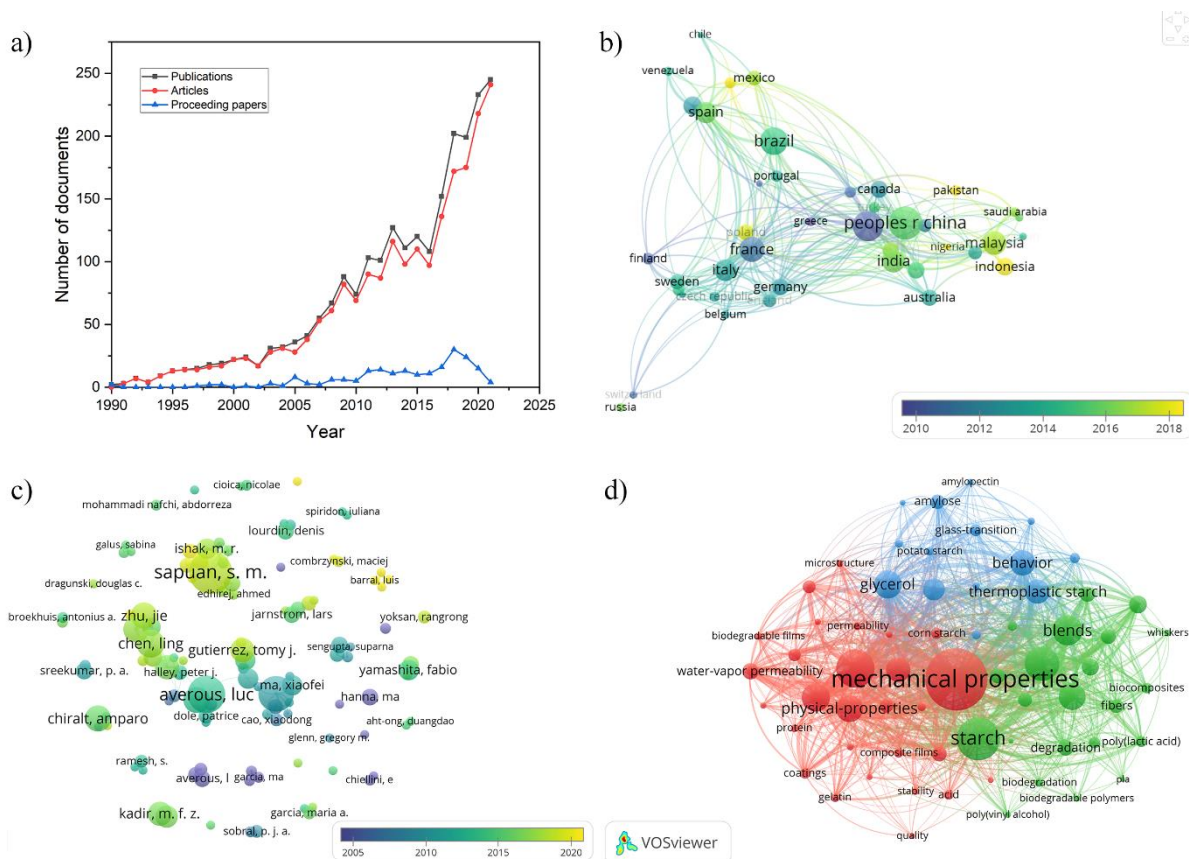


Fig. 1: a) annual publication from 1990-2021, b) international collaboration among countries, c) co-authorship network among authors and d) keyword co-occurrence networks involved in starch-based plastics research.

*Most productive authors*

The overlay visualization network in Fig. 1c shows that there are several author cooperation networks, which are primarily clustered by institutional affiliations. During the study period, 6970 authors were active in starch-based plastics research, with 114 of them publishing 5 or more publications. Averous L is the most prolific author in starch-based plastics research and has written 36 papers with an average of 98.97 citations per item and an h-index of 23. The author's research focuses on developing starch-based nanocomposites as bio-sourced polymers (bioplastics) to replace traditional plastics.

*Keyword co-occurrence analysis*

Keyword analysis exposes researchers' interest in a certain study subject, making it an essential aspect of bibliometric analysis. The VoSviewer visualization network map (Fig. 1d) was created to investigate the co-occurrence connection between the keywords retrieved from publications on starch-based plastics research. In the keyword map, three overlapping clusters with unique colors were discovered. The core subject at the heart of the keyword map is "mechanical characteristics". It is grouped with 27 other terms in cluster 1 (in red). Cluster 1 (in red) denotes investigations on the qualities of starch-based polymers, with "mechanical properties" as the biggest node. This conclusion suggests that many studies have focused on the mechanical qualities of starch-based polymers. Cluster 2 (in green) focuses on creating biodegradable polymers generated from starch composites (such as polylactic acid). Various studies have looked at combining starch with polymers and fibers to enhance the characteristics of starch films. The conversion of starch to thermoplastic starch is the subject of Cluster 3 (in blue). In general, starch is made up of amylose and amylopectin components that may be thermoplasticized with the addition of a plasticizer (such as glycerol and water). Plasticizers may form hydrogen bonds with starch molecules, weakening the hydroxyl group interactions and making starch thermoplastic.

## CONCLUSIONS

The analysis result revealed rapid progress in the development of biodegradable plastics using starch from 1990 to 2021. In this topic, a study on the mechanical properties of starch-based plastics has gained lots of concern from researchers. The most active countries were China, USA, Brazil, France and Malaysia. The leading author in the research regarding starch-based plastics was Averous L from France, with 36 documents published, 98.97 citations (average per item) and 23 h-index. The study could also assist ambitious scientists in locating collaborators, trends and resources for strategic planning of high-risk or high-reward investigations that expand the research frontier.

## ACKNOWLEDGEMENTS

The first author, Abu Hassan Nordin is also thankful for the support from Universiti Teknologi Malaysia in the form of Zamalah Scheme.

## REFERENCES

- [1] Al-Salem, S., Antelava, A., Constantinou, A., Manos, G., and Dutta, A. A review on thermal and catalytic pyrolysis of plastic solid waste (PSW). *Journal of Environmental Management*. 2017; 197: 177-198.
- [2] Huang, M.-F., Yu, J.-G., and Ma, X.-F. Studies on the properties of montmorillonite-reinforced thermoplastic starch composites. *Polymer*. 2004; 45(20): 7017-7023.
- [3] Marichelvam, M., Jawaid, M., and Asim, M. Corn and rice starch-based bio-plastics as alternative packaging materials. *Fibers*. 2019; 7(4): 32.
- [4] Kasmuri, N. and Zait, M.S.A. Enhancement of bio-plastic using eggshells and chitosan on potato starch based. *Int J Eng Technol*. 2018; 7(3): 110-115.
- [5] Tan, S.X., Ong, H.C., Andriyana, A., Lim, S., Pang, Y.L., Kusumo, F., and Ngoh, G.C. Characterization and Parametric Study on Mechanical Properties Enhancement in Biodegradable Chitosan-Reinforced Starch-Based Bioplastic Film. *Polymers*. 2022; 14(2): 278.
- [6] Mose, B.R. and Maranga, S.M. A review on starch based nanocomposites for bioplastic materials. *Journal of Materials Science and Engineering. B*. 2011; 1(2B): 239.
- [7] Song, Y., Chen, X., Hao, T., Liu, Z., and Lan, Z. Exploring two decades of research on classroom dialogue by using bibliometric analysis. *Computers & Education*. 2019; 137: 12-31.
- [8] Xing, Y., Zhang, H., Su, W., Wang, Q., Yu, H., Wang, J., Li, R., Cai, C., and Ma, Z. The bibliometric analysis and review of dioxin in waste incineration and steel sintering. *Environmental science and pollution research*. 2019; 26(35): 35687-35703.
- [9] Wu, H., Zuo, J., Zillante, G., Wang, J., and Yuan, H. Construction and demolition waste research: a bibliometric analysis. *Architectural Science Review*. 2019; 62(4): 354-365.
- [10] A. S. Norfarhana, R. A. Ilyas, and N. Ngadi. A review of nanocellulose adsorptive membrane as multifunctional wastewater treatment. *Carbohydr. Polym.*, 2022; 291; 119563. doi: 10.1016/j.carbpol.2022.119563.



## COMPRESSION PROPERTIES OF SQUARE CORE SANDWICH STRUCTURE MADE OF KENAF/PLA COMPOSITE

M.A.H.M. Yusri<sup>1\*</sup>, M.Y.M. Zuhri<sup>1,2\*</sup>, M.R. Ishak<sup>2,3</sup> and M.A. Azman<sup>1</sup>

<sup>1</sup>Advanced Engineering Materials and Composites, Department of Mechanical and Manufacturing Engineering, Universiti Putra Malaysia, 43400 UPM Serdang, Selangor, Malaysia

<sup>2</sup>Laboratory of Biocomposite Technology, Institute of Tropical Forestry and Forest Products, Universiti Putra Malaysia, 43400 UPM Serdang, Selangor, Malaysia

<sup>3</sup>Department of Aerospace Engineering, Universiti Putra Malaysia, 43400 UPM Serdang, Selangor, Malaysia

---

### ABSTRACT

This study aims to develop and identify the characteristics and properties of square core sandwich structure made of natural fibre. Here, kenaf fibre reinforced polylactic acid (kenaf/PLA) composites are selected as the core material. A quasi-static compression testing has been conducted to investigate the compression strength and energy-absorbing capability of the kenaf/PLA sandwich structure. The square core is fabricated by cutting the composite panel into a small rectangular strip and interlocking it using the simple slotting technique. It is found that the maximum loading of the square core sandwich structure with 20 mm cell size reach at approximately 30.17 kN with specific energy absorption of 6.907 kJ/kg.

*Keywords:* kenaf fibre, square core, sandwich structure.

---

### INTRODUCTION

Over the last few years, the application of a sandwich structure made of composite materials has grown rapidly due to its high stiffness to weight ratio characteristics. A wide variety of industrial material applications such as automotive, aerospace and marine have already utilised this sandwich structure application [1]. Sandwich structures are known for their low weight, high energy absorption, and high strength-to-weight ratios; these structures allow the elimination of unnecessary parts while maintaining a high stiffness-to-weight ratio. The emergence of environmental awareness has triggered the increase in using natural fibre composite or biocomposite in many applications. There are many studies that have been conducted on the natural fibre composite as well as testing it in an actual application due to its advantages of environmental acceptability and commercial viability [1,2, 3]. In addition, previous studies also discovered that combining synthetic and natural fibres with the polymer can improve the mechanical properties of its composite, especially in the application of sandwich structure [4, 5, 6]. However, the application of kenaf fibre composites in sandwich structures is still at its lowest and needs further investigation. In this study, the capability of a kenaf composite as core structure material has been investigated. A quasi-static compression testing is conducted to determine the compression strength as well as its energy-absorbing capability.

### MATERIALS AND METHODS

Firstly, woven kenaf and non-woven kenaf mat with a size of 350 mm x 350 mm are prepared. The composite panel is prepared by two plies of woven kenaf, one ply of non-woven kenaf mat, and 40 plies of PLA film. Here, a flat mould is used for the fabrication. The materials are then placed in the hot-press machine with a heat range between 170 °C – 180 °C and a pressure of 2.0 bar. The pressing time is set to 7 minutes. The flat composite panel is then cut into small rectangular strips and interlocked by using a simple slotting technique to form the square core structure. Finally, the core is bonded to the balsa wood which acts as the skin by using epoxy. The core structure consists of 4 cells with a cell size of 20 mm between the cell webs. Fig. 1 shows the complete fabrication of the kenaf/PLA square core sandwich structure.

---

#### Article history:

Received: 10 March 2022

Accepted: 7 June 2022

Published: 14 June 2022

---

#### E-mail addresses:

Hakimi.arif98@gmail.com (M.A.H.M. Yusri)

zuhri@upm.edu.my (M.Y.M. Zuhri)

mohdridzwan@upm.edu.my (M.R. Ishak)

amin.azman@upm.edu.my (M.A. Azman)

\*Corresponding Author

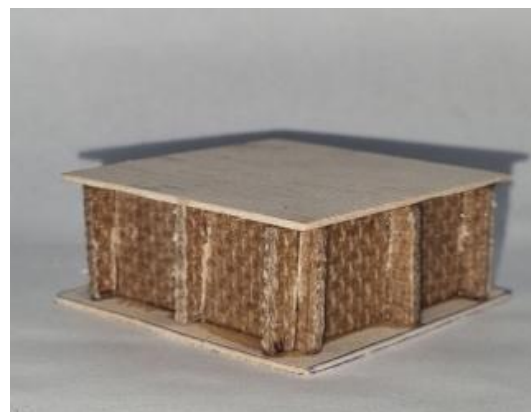


Fig. 1: The image of the square core sandwich structure of kenaf/PLA

## RESULTS AND DISCUSSION

Fig. 2 shows the typical load-displacement curve of the kenaf/PLA square core structure. At first, the core structure demonstrated a non-linear elastic behavior until it reached its peak load at approximately 30.17 kN before having a failure at a displacement close to 3 mm. After a sudden drop in load, the core experiences a plateau loading averaging 11 kN. It is observed that the square core sandwich structure is having a failure from buckling to composite breaking. Here, the average SEA values are calculated at around 6.91 kJ/kg.

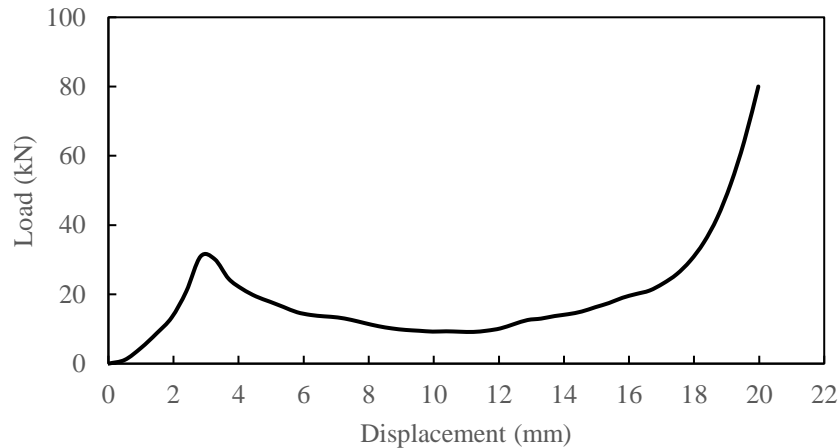


Fig. 2: Typical load-displacement curve of the kenaf/PLA square core structure.

## CONCLUSIONS

The compressive properties of square core structures made of kenaf/PLA composite have been investigated. The square core sandwich structure made of kenaf/PLA composite offers a SEA value of approximately 6.91 kJ/kg. Finally, the structure is observed to failed from buckling to composite breakage.

## ACKNOWLEDGEMENTS

The authors would like to thank the Ministry of Higher Education Malaysia for funding this work through the Fundamental Research Grant Scheme (FRGS/1/2021/TK0/UPM/02/21).

## REFERENCES

- [1] Cinar, K. (2020). Evaluation of sandwich panels with composite tube-reinforced foam core under bending and flatwise compression. *Journal of Sandwich Structures and Materials*, 22(2), 480–493. <https://doi.org/10.1177/1099636218798161>
- [2] Sharba, M. J., Leman, Z., Sultan, M. T. H., Ishak, M. R., & Azmah Hanim, M. A. (2016). Effects of kenaf fibre orientation on mechanical properties and fatigue life of glass/kenaf hybrid composites. *BioResources*, 11(1), 1448–1465. <https://doi.org/10.15376/biores.11.1.1448-1465>
- [3] Tay, C. H., Mazlan, N., Hameed Sultan, M. T., Abdan, K., & Lee, C. H. (2021). Mechanical performance of hybrid glass/kenaf epoxy composite filled with organomodified nano clay. *Journal of Materials Research and Technology*, 15, 4415–4426. <https://doi.org/10.1016/j.jmrt.2021.10.062>
- [4] Ashraf, W., Ishak, M. R., M.Y.M, Z., Yidris, N., & Ya'Acob, A. M. (2021). Investigation of Mechanical Properties of Honeycomb Sandwich Structure with Kenaf/glass Hybrid Composite Facesheet. *Journal of Natural Fibers*, 00(00), 1–15. <https://doi.org/10.1080/15440478.2020.1870637>
- [5] Khan, T., Hameed Sultan, M. T. Bin, & Ariffin, A. H. (2018). The challenges of natural fibre in manufacturing, material selection, and technology application: A review. *Journal of Reinforced Plastics and Composites*, 37(11), 770–779. <https://doi.org/10.1177/0731684418756762>
- [6] Stocchi, A., Colabella, L., Cisilino, A., & Álvarez, V. (2014). Manufacturing and testing of a sandwich panel honeycomb core reinforced with natural-fibre fabrics. *Materials and Design*, 55, 394–403. <https://doi.org/10.1016/j.matdes.2013.09.054>

## PHYSICOCHEMICAL PROPERTIES OF PVC RESIN MEMBRANE BLENDING WITH PEG

S. Seansukato<sup>1</sup>, W. Taweepreda<sup>1\*</sup>, S. Lamlong<sup>1</sup>, A. Gangasalam<sup>2</sup>

<sup>1</sup>Center of Excellence in Membrane Science and Technology, Polymer Science Program, Division of Physical Science, Faculty of Science, Prince of Songkla University, Hat-Yai, Songkhla 90110, THAILAND

<sup>2</sup>Membrane Research Laboratory, Department of Chemical Engineering, National Institute of Technology, Tiruchirappalli, Tiruchirappalli 620 015, INDIA

---

### ABSTRACT

The polymeric membrane composed of polyvinyl chloride (PVC) blended with polyethylene glycol (PEG) as a supporting membrane was prepared as a flat sheet aspect. The supporting membrane was prepared using the phase inversion technique and established by the casting method. The morphology of cross-section images from a scanning electron microscope (SEM) showed a finger-like and sponge-like structure after adding higher contents of PEG with an averaged molecular weight of 400 g/mol. The mechanical properties of the polymeric membrane were improved with increasing PEG molecular weight. The membrane's mechanical properties were investigated using a dynamic mechanical thermal analyzer (DMTA).

*Keywords:* PVC, PEG, membrane

---

### INTRODUCTION

The membrane technology has been progressing over the last few decades, and it is also fascinating for various implementations such as gas separation, wastewater treatment, water purification, etc. Due to their advantageous qualities such as simplicity of processability, strong chemical and heat resistance, superior mechanical properties, cost-effectiveness, and ease of fabrication. On the other hand, they always suffer from a "trade-off" between the two main critical criteria: permeability, and selectivity, limiting their gas separation uses. The notion of polymer blend or mixed matrix membrane (MMM) was introduced to circumvent the polymer membranes' "trade-off" limits. The two polymers were blended to form a polymer blend or inorganic/organic additives in solid, liquid, or mixing; both solid and liquid forms are preferred for incorporation into the polymer matrix to form a polymer blend or a mixed matrix membrane. This combination can improve both components' separation performances [1, 2].

Polyvinyl chloride (PVC) is a commercial thermoplastic with rigid and stiff behaviors. It may be significantly adjusted for flexibility by adding a plasticizer [3]. Furthermore, PVC is likely to be manufactured as a dense and supporting membrane. Therefore, PVC was chosen to build a flat sheet membrane because of its outstanding physicochemical and mechanical qualities, cheap cost, low mass transfer resistance, and PVC recycling due to its thermoplastic properties. Polyethylene glycol (PEG) consists of the formula of HO-(CH<sub>2</sub>-CH<sub>2</sub>-O)<sub>n</sub>-H, which has many proper properties such as uncharged hydrophilic groups and very high mobility. It can be selected to blend into the PVC matrix as pore former behavior. Chakrabarty et al. (2008) determined the influence of the molecular weight of PEG on the porosity of polysulfone (PSf), and they can conclude that the increase of molecular weight of PEG had affected the increment of the number of pores and pores area per unit surface area (porosity). This research would like to study the morphological structure, wettability, mechanical and thermal properties of PVC membranes blended with the various PEG using phase inversion to prepare the flat sheet membranes.

### MATERIALS AND METHODS

This research used the non-solvent induces phase separation (NIPS) technique to prepare flat sheet membranes and studied the diffusion exchange between solvent and non-solvent in the coagulant bath. [4, 5]. The flat sheet membrane was fabricated from casting solutions containing PVC, PEG, and DMF. PVC was supplied by Thai Plastic and Chemical Co., Ltd by varying K-values 580 and 610. DMF (99.8% grade) was bought from Ajax Finechem Pty Ltd. and used as a solvent; PEG 400 and 4000 Dalton were bought from Honam Petrochemical, Co., Ltd., by varying concentration of PEG from 1.0 to 15.0 wt% and used as pore former. The mixed solution between PVC and PEG solution was homogenized by using a hot plate magnetic

stirrer of VS-130SH from Vision Scientific Co., Ltd; these solutions were heated at a temperature 60 °C for approximately 4 hours to ensure that the polymer could be dissolved entirely as a homogeneous solution. Then, the dope solution was poured on a glass plate and cast with glass rod. The cast membranes were suddenly immersed into a coagulant containing a deionized water bath for 24 hours. Ensure a complete solvent and non-solvent exchange and remove residue solvent from the casting membranes.

---

#### Article history:

Received: 10 March 2022

Accepted: 7 June 2022

Published: 14 June 2022

---

#### E-mail addresses:

wirach.t@psu.ac.th (W. Taweepreda)

\*Corresponding Author

RESULTS AND DISCUSSION

Scanning Electron Microscopy

The microstructure of PVC flat sheet membranes obtained from SEM images revealed the morphological variation depends on PVC concentration and PEG content, as illustrated in Fig. 2 and 3. In Fig. 2, the dominant structures of PVC-610 with lower concentration (10 wt%) had lower number and size of macro-voids at the bottom than the higher PVC ratio as well as 10 wt% PVC had a higher thickness of finger-like pores at the top surface layer. Due to the low content of PVC, the major solvent lean phase of DMF increased the phase separation by more quickly in liquid-liquid demixing during the immersion into coagulation bath. This caused to longer finger-like structure of PVC-610 at 10 wt%. On the other hand, the higher PVC content could be created many small droplets during slow precipitation of solution, these droplets agglomerated to form larger droplets that transform shape cavities into macro-voids structures.

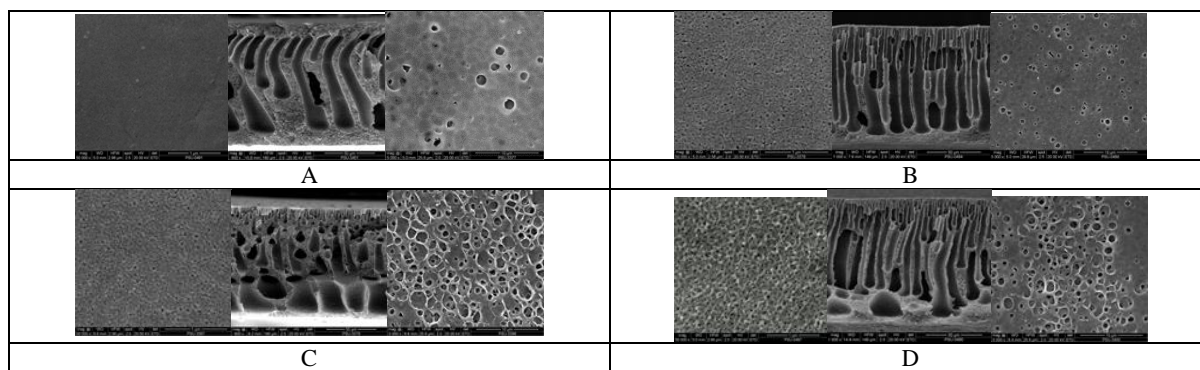


Fig. 1 : SEM images of (A) PVC580-PEG-400 5wt%, (B) PVC580- PEG-400 10wt%, (D) PVC580-PEG-4000 5wt% and (E) PVC580-PEG-4000 10wt%

TABLE 1 : Contact angle results of flat sheet membranes

Membrane	Contact angle (°)
PVC-580-Pure (16 wt%)	88.28 ± 1.22
PVC-580-G400 (5%)	87.62 ± 1.32
PVC-580-G400 (10%)	85.34 ± 2.21
PVC-580-G400 (15%)	80.76 ± 3.26
PVC-610-Pure (10 wt%)	91.23 ± 3.17
PVC-610-Pure (12 wt%)	89.83 ± 1.78
PVC-610-Pure (14 wt%)	89.46 ± 2.15
PVC-610-Pure (16 wt%)	89.36 ± 2.08

CONCLUSIONS

This study showed that the blending PVC-PEG membranes were successfully prepared by casting method, the optimized condition is the moderate concentration of PVC-580 and PVC-610 was mixed solvent in DMF. The blended PEG with PVC membranes should show finger-like substructures and dense skin layers. The higher molecular weight of PEG affected to high porous structure, more hydrophilicity, as well as decreased thermal stability, while the high molecular weight of PVC promoted the high viscosity casting solution resulting in the difficulty of solvent and non-solvent exchanging during membrane formation.

ACKNOWLEDGEMENTS

The authors were grateful for the financial support from the National Science and Technology Development Agency (NSTDA) and the supporting from Labthink Instruments Co. Limited, regarding the testing membrane for gas permeation. Besides, this work was supported by the Higher Education Research Promotion and National Research University Project of Thailand, Office of the Higher Education Commission. Finally, our team research would like to thank the Graduate School and Faculty of Science, Prince of Songkla University for supporting budgets and locations during this research.

**REFERENCES**

- [1] I. Khalilnejad, A. Kargari, and H. Sanaeepur, "Preparation and characterization of (Pebax 1657+ silica nanoparticle)/PVC mixed matrix composite membrane for CO<sub>2</sub>/N<sub>2</sub> separation," *Chemical Papers*, vol. 71, pp. 803-818, 2017.
- [2] E. Kianfar, M. Salimi, F. Kianfar, M. Kianfar, and S. A. H. Razavikia, "CO<sub>2</sub>/N<sub>2</sub> separation using polyvinyl chloride iso-phthalic acid/aluminium nitrate nanocomposite membrane," *Macromolecular Research*, vol. 27, pp. 83-89, 2019.
- [3] M. M. Jamel, P. Khoshnoud, S. Gunashekar, and N. Abu-Zahra, "Effect of e-glass fibers and phlogopite mica on the mechanical properties and dimensional stability of rigid PVC foams," *Polymer-Plastics Technology and Engineering*, vol. 54, pp. 1560-1570, 2015.
- [4] J. Garcia-Ivars, M.-I. Alcaina-Miranda, M.-I. Iborra-Clar, J.-A. Mendoza-Roca, and L. Pastor-Alcañiz, "Enhancement in hydrophilicity of different polymer phase-inversion ultrafiltration membranes by introducing PEG/Al<sub>2</sub>O<sub>3</sub> nanoparticles," *Separation and Purification Technology*, vol. 128, pp. 45-57, 2014.
- [5] G. R. Guillen, Y. Pan, M. Li, and E. M. Hoek, "Preparation and characterization of membranes formed by nonsolvent induced phase separation: a review," *Industrial & Engineering Chemistry Research*, vol. 50, pp. 3798-3817, 2011.

## **DEVELOPMENT OF 3D PRINTED HUMAN BRAIN MODELS USING THERMOPLASTIC POLYURETHANE/RUBBER BLENDS FOR ANATOMY TEACHING PROMOTING KINAESTHETIC LEARNING PURPOSES**

S. H. A. Hisham<sup>1</sup>, I. F. Ismail<sup>1</sup>, S. A. Shamsuddin<sup>1</sup>, S. N. H. Hadie<sup>1</sup>, Z. Mohd Ismail<sup>1</sup>, F. Kasim<sup>1</sup>, N.A. Sapiai<sup>2</sup>, N. A. Mat Zin<sup>2</sup>, and K. I. Ku Marsilla<sup>2\*</sup>

<sup>1</sup> School of Medical Sciences, Health Campus, Universiti Sains Malaysia 16150 Kubang Kerian, Kota Bharu, Malaysia

<sup>2</sup> School of Materials and Mineral Resources Engineering, Engineering Campus, Universiti Sains Malaysia 14300 Nibong Tebal, Malaysia

---

### **ABSTRACT**

Kinaesthetic appreciation of anatomy models serves to activate a concrete sensory experience that enhances 3D visuospatial mental mapping of anatomical structures. However, most commercially available plastic anatomy models are costly and do not provide similar tactile sensation as the actual organ or structures. Polymeric materials have been used widely in additive manufacturing to produce human brain model, however none of the model resembles the accurate feeling. The aim of this study is to produce 3D printed anatomical models using customized soft 3D printing filament from TPU and two types of rubber, which are ethylene propylene diene monomer (EPDM) and styrene butadiene rubber (SBR) compounds. Actual human brain MRI scans is used to formed 3D-printed anatomy models. The MRI image obtained was in DICOM format, exported into 3D slicer software for specific brain parts extraction (whole brain, brain ventricles, circle of Willis, and dural venous sinuses) and conversion into STL format for 3D-printing. For material processing, the blending of TPU/EPDM and TPU/SBR were successfully fabricated using an internal mixer (Haake) and extruded into filament using single screw extruder with aid of filament winder. The human brain model was then printed using 3D Printer (Ender 3). It was found that all TPU blends were able to be printed into brain anatomy models but the properties of the materials were greatly affected by rubber types and compositions of the added fillers. Addition of more than 30% of the fillers gave difficulties in processing, probably due to inconsistent viscosity that led to phase separation.

*Keywords:* 3D printing, thermoplastic polymer, TPU/rubber blends, brain models.

---

### **INTRODUCTION**

Teaching in the anatomy department has used a variety of teaching aids. The human specimens require a high cost of maintenance and purchasing, need specific facilities for storage, and provide ineffective recognition of vascular structures [1][2], whereas the imaging modalities and software's main issue is that they do not provide tactile feedback [3]. While the plastic anatomy models are widely available, however, most plastic anatomy models are rigid. Therefore, this study wants to produce soft anatomy models that provide similar consistency with the actual organ using 3D printing technology as the kinaesthetic feedback allows learning intensification by enhancing spatial awareness and longer retention of knowledge [4]. Medical students with poor anatomical knowledge when practicing medicine can lead to medical litigations due to anatomical errors [5]. 3D printing has been used widely in manufacturing organ structures for pre-surgical simulations, prostheses, and even for teaching [6]. 3D printing process enables the construction of various customized models, allows the formation of multiple identical models, and cheaper than the commercially available anatomy plastic models [7]. 3D printing applied the rapid prototyping process of additive manufacturing which enables the construction of objects by depositing materials layer by layer [8]. The process of forming a 3D object is feasible with the use of 3D printers. Choosing the right 3D printers depends on the technique used to print the object. Among various techniques to render 3D printed objects, namely Fused Filament Fabrication (FFF), Stereolithography (SLA), Selective laser sintering (SLS), material jetting, or binder jetting, FFF has been mainly used to 3D print polymeric materials. The FFF technique is by layering down melted filament (semi-liquid) in a 2D horizontal manner via a heated nozzle on a heated build plate. Temperature settings to melt filament should considerably be slightly higher than the melting temperature of the material. The build-up layers formed thus assembled the object into 3D form. This process makes the printed product anisotropic. Post-processing methods such as oven heating, painting, and chemical processing may be required to make the layers more coherent [9]. This makes objects made from the FFF method have modest mechanical properties if compared to other methods of plastic manufacturing such as thermoforming, extrusion,

or injection moulding [10]. Thus, the mechanical stability of the fabricated filament must be tested with regard to its tension and compression properties. The important indicators that are accountable for the mechanical properties of the printed object include the material composition and processing, and the printing parameters (temperature, speed, and layer height) [11]. As for the material, TPU is a linear segmented copolymer that demonstrates similar properties to conventional rubbers at room temperature and melting properties like thermoplastic polymer at higher temperatures. Thus, TPU exhibits flexible properties making it a preferred

---

#### *Article history:*

Received: 10 March 2022

Accepted: 7 June 2022

Published: 14 June 2022

---

#### *E-mail addresses:*

ku\_marsilla@usm.my (K. I. Ku Marsilla)

\*Corresponding Author

material when the elastic object is desired. TPU is made up of two segments, the hard segments are for cross-linking, and the soft segments are for flexibility. The ability of TPU to form irreversible cross-linking would benefit the need to create long-lasting prototypes [12]. Additionally, adding rubber fillers to TPU could reduce its hardness of TPU [13]. 3D printing using TPU filament should be set above 195°C as it was shown to yield the highest printing stability [14].



Fig.1: Flexible 3D printed brain model

## MATERIALS AND METHODS

### Materials

Thermoplastic urethane (TPU) filament 85 (Shore A) and 95 (Shore A) with a diameter of 1.75mm were purchased from ROBOTEDU ENTERPRISE. Ethylene propylene diene monomer (EPDM), Vistalon™ 2504N was purchased from ExxonMobil Chemical Asia Pacific. Styrene-butadiene rubber (SBR) 1502 was obtained from Bayer (M) Ltd.

### Sample preparations

The TPU filament 95 (Shore A) was pelletized into small pellets of 2mm length using a filament shredder. EPDM and SBR were cut into cubes of 0.5x0.5cm size using a rubber cutter and scissors. The TPU pellets were pre-dried in the oven with a temperature of 40°C for 24 Hours. The EPDM and SBR rubber were kept in airtight plastic bags to reduce exposure to humidity.

### Preparation TPU: EPDM (75:25) TPU: SBR (75:25) blends

TPU: EPDM 75:25 and TPU: SBR 75:25 blends were combined in Haake internal mixer on two separate occasions using the same parameters of temperature at 160°C, rotation speed 50rpm, for 12 minutes. TPU 95 (Shore A) was inserted into the internal mixer first, after 7 minutes, rubbers (EPDM, SBR) were added to mix with TPU for 5 minutes until uniform blends are formed. Post internal mixing, TPU: EPDM and TPU: SBR were cooled under room temperature for 2 minutes, and then inserted into airtight plastic bags separately. The blended polymers were then minced into smaller pieces using a rubber cutter and grinder.

### Filament Extrusion

A single screw extruder was used to extrude TPU: EPDM and TPU: SBR filaments. Before extrusion, the TPU: EPDM and TPU: SBR blends were dried in the oven at using a temperature of 40°C for a duration of 24 Hours. The temperature for TPU: EPDM and TPU: SBR was 180/190/190/185°C. Post-extrusion, each TPU: EPDM and TPU: SBR filament passes through a cooling water bath before winding into a spool by a winder. The rotator speed of the winder was 4-8rpm. The TPU: EPDM and TPU: SBR filaments were then air-dried at room temperature before they were kept in an airtight plastic bag.

### 3D printing of tensile properties samples

TPU filament 85 (Shore A) and filament 95 (Shore A), TPU: EPDM, and TPU: SBR samples were printed using 3D printer (Ender 6s, nozzle size 0.4mm). The dumbbell image was drawn using Solidwork Software following standard ASTM 638 type 5. Temperatures used to print TPU filament 85 (Shore A), TPU filament 95 (Shore A), TPU: EPDM, and TPU: SBR samples were 230/80°C, 230/80°C, 225/80°C, and 225/80°C respectively. Infill density was set to 100%, print speed 50rpm, layer height 0.2mm.

### Characterizations

#### Tensile properties

Tensile tests were performed on 3D printed ASTM638 Type 5 dumbbell-shaped specimens. The dimension for the specimen is 9.53mm in length, 3.18mm in width, and 3mm in thickness. The tests were conducted at room temperature using the Instron-3366 universal testing system. The crosshead speed was set to 50mm/min with a load level of 0.2kN. Tensile strength, elongation at break, and Young's moduli were recorded in TABLE 1. Five samples were used to obtain the average tensile strength and modulus for each material.

TABLE 1: Tensile properties of 3D printed TPU 85A, TPU 95A, TPU: EPDM and TPU:SBR blends

Tensile properties	TPU 85A	TPU 95A	TPU: EPDM	TPU: SBR
Average Young modulus, E (MPa)	22.52	51.47	73.84	36.83
Average Tensile strength (MPa)	19.62	16.56	10.40	8.05
Average Elongation at break (%)	720.00	466.16	356.82	323.62

### *Methods*

#### *Obtaining image*

An MRI image of the head of an actual human was obtained from the radiology department, Hospital Universiti Sains Malaysia. MRI image was used because it can show better contrast of soft tissue. The MRI study used was in the format DICOM (Digital Imaging and Communications in Medicine).

#### *Segmentation of MRI image*

The regions of interest were segmented using 3D Slicer software, on open software. Different parts of the brain structures require different MRI sequences. The segment editor was then used to select the regions of interest using the threshold tool. The island tool was used to remove an unwanted region of interest, and the smoothing tool was used to smoothen the outer surface. The segmented brain structures were then exported as STL format and inserted into Autodesk Meshmixer software. The Autodesk Meshmixer software was used to close up any holes in the object, make structures hollow (blood vessels, ventricles), smoothen the surface, and remove any unwanted mesh.

#### *3D printing of anatomical structures models*

STL format images of the segmented brain structures were opened in Creality Slicer 4.8.2 3D software. The brain structures were printed using Ender 3 3D printer (nozzle diameter 0.4mm) in G-code format. Brain structures printed were the whole brain, ventricle, Circle of Willis, and dural venous sinuses. Since the models are non-manifold and blood vessel models have overhanging structures, support was required, and raft type build plate adhesion was set prior to the printing process to prevent dislodging of printed models during the printing process. Post-processing using filament cutter and sandpaper was required to remove the support and round off the models' surfaces. The 3D printer parameters were extruder temperature 230°C, build plate temperature 90°C, print speed 20rpm, infill density 0%, layer height 0.2mm.

## **RESULTS AND DISCUSSIONS**

### *Tensile properties*

The recorded material tensile strength and elongation at break from highest to lowest TPU 85A, TPU 95A, TPU: EPDM, and TPU: SBR. SBR and EPDM generally have lower tensile strength than TPU. One study shows that TPU: EPDM versus TPU: SBR blends revealed that TPU: EPDM has a higher tensile strength which corresponds to the tensile strength of unfilled EPDM vs unfilled SBR [15][16]. TPU can become softer by incorporating EPDM fillers because the diene monomers of EPDM have higher cross-linking flexibility than TPU. However, the result shows TPU: EPDM 75:25 is the stiffest, as represented by the highest value of Young's modulus. This is because EPDM blends can produce better tensile strength until 10% EPDM maximally as the soft and hard segments microphase separation of TPU is stronger. EPDM ratio that exceeds 10%, however, results in lower tensile strength of TPU: EPDM blend as EPDM is no longer compatible with TPU. This has been discussed in previous studies which illustrate the morphological changes in the network of cross-linking between EPDM and the soft segment of TPU. The studies revealed a thicker network and wider mesh size, and when 30% EPDM is used, phase separation ensued [17][18]. Meanwhile, Young's modulus of TPU: SBR is evident to be lower than TPU 95A, but higher than TPU 85A, which means that TPU: SBR is more elastic than TPU 95A but stiffer than TPU 85A. Elongation at the break for 25% SBR value of 323.62 is comparable with another study with elongation at break ranging between 280-340% [18]. Fillers, such as carbon black, silica, and calcium carbonate may need to be added to SBR to improve its physical properties [20].

## **CONCLUSIONS**

A higher load will be required to break TPU 85A and elastically deform TPU: EPDM. TPU: EPDM shows the least flexible properties, whereas TPU 85A has the best tensile strength and highest elasticity. Finally, 3D printed models of brain structures displaying ventricles, arteries, and veins of the brain were successfully manufactured using TPU 85A. All the printed structures can be separated from one another. The consistencies of the brain models to touch feel softer than the conventional plastic brain models.

## **ACKNOWLEDGEMENTS**

This study is supported by Universiti Sains Malaysia under grant number :304/PPSP/6315504. The authors would like to thank the School of Materials and Mineral Resources Engineering, for their help and support to complete this research with access to facilities and laboratory equipment.



REFERENCES

- [1] McMenamin, P. G., Hussey, D., Chin, D., Alam, W., Quayle, M. R., Coupland, S. E., & Adams, J. W. (2021). The reproduction of human pathology specimens using three-dimensional (3D) printing technology for teaching purposes. *Medical Teacher*, 43(2), 189–197. doi:10.1080/0142159X.2020.1837357
- [2] Darras, K. E., de Bruin, A. B. H., Nicolaou, S., Dahlström, N., Persson, A., van Merriënboer, J., & Forster, B. B. (2018). Is there a superior simulator for human anatomy education? How virtual dissection can overcome the anatomic and pedagogic limitations of cadaveric dissection. *Medical Teacher*, 40(7), 752–753. doi:10.1080/0142159X.2018.1451629
- [3] Ellis, H. (2002). Medico-legal Litigation and its Links with Surgical Anatomy. *Surgery (Oxford)*, 20(8), i–ii. doi:10.1383/surg.20.8.0.14518
- [4] Hernandez, J. E., Vasan, N., Huff, S., & Melovitz-Vasan, C. (2020). Learning Styles/Preferences Among Medical Students: Kinesthetic Learner’s Multimodal Approach to Learning Anatomy. # *International Association of Medical Science Educators*. doi:10.1007/s40670-020-01049-1
- [5] Ligon, S. C., Liska, R., Stampfl, J., Gurr, M., & Mülhaupt, R. (2017). Polymers for 3D Printing and Customized Additive Manufacturing. *Chemical Reviews*. doi:10.1021/acs.chemrev.7b000746.
- [6] Mogali, S. R., Yeong, W. Y., Tan, H. K. J., Tan, G. J. S., Abrahams, P. H., Zary, N., ... Ferenczi, M. A. (2018). Evaluation by medical students of the educational value of multi-material and multi-colored three-dimensional printed models of the upper limb for anatomical education. *Anatomical Sciences Education*, 11(1), 54–64. doi:10.1002/ase.1703
- [7] Yan, Q., Dong, H., Su, J., Han, J., Song, B., Wei, Q., & Shi, Y. (2018, October 1). A Review of 3D Printing Technology for Medical Applications. *Engineering*. Elsevier Ltd. doi:10.1016/j.eng.2018.07.021
- [8] Ye, Z., Jiang, H., Nie, C., Zhao, S., Wang, T., Dun, A., & Zhai, J. (2020). The role of a 3D printed model in the teaching of human anatomy: a meta-analysis. doi:10.21203/rs.2.22724/v2
- [9] Dizon, J. R. C., Espera, A. H., Chen, Q., & Advincula, R. C. (2018). Mechanical characterization of 3D-printed polymers. *Additive Manufacturing*. doi:10.1016/j.addma.2017.12.002
- [10] Pop, M. A., Croitoru, C., Bedo, T., Geamăn, V., Radomir, I., Zaharia, S. M., & Chicoş, L. A. (2020). Influence of internal innovative architecture on the mechanical properties of 3D polymer printed parts. *Polymers*, 12(5). doi:10.3390/POLYM12051129
- [11] Mohamed, O. A., Masood, S. H., & Bhowmik, J. L. (2017). Characterization and dynamic mechanical analysis of PC-ABS material processed by fused deposition modelling: An investigation through I-optimal response surface methodology. *Measurement: Journal of the International Measurement Confederation*, 107, 128–141. doi:10.1016/j.measurement.2017.05.019
- [12] Kim, J. H., & Kim, G. H. (2017). Mechanical properties of dynamically vulcanized thermoplastic polyurethane (TPU)/polybutadiene rubber (BR) blends. *International Journal of Engineering and Technology Innovation*, 7(1), 39–47.
- [13] Kim, J. H., & Kim, G. H. (2014). Effect of rubber content on abrasion resistance and tensile properties of thermoplastic polyurethane (TPU)/rubber blends. *Macromolecular Research*, 22(5), 523–527. doi:10.1007/s13233-014-2077-y
- [14] Wang, J., Yang, B., Lin, X., Gao, L., Liu, T., Lu, Y., & Wang, R. (2020). Research of TPU materials for 3D printing aiming at non-pneumatic tires by FDM method. *Polymers*, 12(11), 1–19. doi:10.3390/polym12112492
- [15] Low, K. O., & Teo, W. C. (2012). Characteristics of SBR, Neoprene and EPDM compounds in a single-pass pendulum scratch. *Tribology International*, 54, 9–16. doi:10.1016/j.triboint.2012.05.006
- [16] Yun, J., Isayev, A. I., Kim, S. H., & Tapale, M. (2003). Comparative analysis of ultrasonically devulcanized unfilled SBR, NR, and EPDM rubbers. *Journal of Applied Polymer Science*, 88(2), 434–441
- [17] Tan, J., Ding, Y. M., He, X. T., Liu, Y., An, Y., & Yang, W. M. (2008). Abrasion resistance of thermoplastic polyurethane materials blended with ethylene-propylene-diene monomer rubber. *Journal of Applied Polymer Science*, 110(3), 1851–1857. doi:10.1002/APP.2875
- [18] Wang, X., & Luo, X. (2004). A polymer network based on thermoplastic polyurethane and ethylene-propylene-diene elastomer via melt blending: Morphology, mechanical properties, and rheology. *European Polymer Journal*, 40(10), 2391–2399. doi:10.1016/j.eurpolymj.2004.06.00
- [19] ALEXANDRESCU, L., GEORGESCU, M., Maria, S. N., & NIÈȘUICĂ, M. (2020). Biodegradable polymeric composite based on recycled polyurethane and rubber wastes: Material for green shoe manufacturing. *Revista de Pielarie Incaltaminte*, 20(3), 323.
- [20] Naebpetch, W., Junhasavasdikul, B., Saetung, A., Tulyapitak, T., & Nithi-Uthai, N. (2017). Influence of filler type and loading on cure characteristics and vulcanisate properties of SBR compounds with a novel mixed vulcanisation system. *Plastics, Rubber and Composites*, 46(3), 137–145.

## MAGNETIC CHITOSAN HYDROGEL BEADS AS ADSORBENT FOR COPPER REMOVAL FROM AQUEOUS SOLUTION

N.A. Khalil<sup>1\*</sup>, A.M.A. Huraira<sup>1</sup>, S.N.D. Janurin<sup>1</sup>, A.N.S. Fikal<sup>1</sup>, N. Ahmad<sup>2</sup>, M. Zulkifli<sup>3</sup>, M.S. Hossain<sup>4</sup>, A.N.A. Yahaya<sup>5\*</sup>

<sup>1</sup>Universiti Kuala Lumpur, Branch Campus Malaysian Institute of Chemical and BioEngineering Technology, 78000 Alor Gajah, Melaka, Malaysia.

<sup>2</sup>Student Development Section, Branch Campus Malaysian France Institute, Universiti Kuala Lumpur, 43650 Bandar Baru Bangi, Selangor, Malaysia.

<sup>3</sup>Aero Composite Cluster, Universiti Kuala Lumpur, Branch Campus Malaysian Institute of Aviation Technology, Jalan Jenderam Hulu, 43800 Dengkil, Selangor, Malaysia.

<sup>4</sup>School of Industrial Technology, Universiti Sains Malaysia, Gelugor, 11800 Penang, Malaysia.

<sup>5</sup>Green Chemistry and Sustainability Cluster, Universiti Kuala Lumpur, Malaysian Institute of Chemical and Bioengineering Technology, 78000 Alor Gajah, Melaka, Malaysia.

---

### ABSTRACT

Magnetic chitosan hydrogel beads (MCHB) were synthesized by blending chitosan and magnetite (Fe<sub>3</sub>O<sub>4</sub>) in sodium alginate solution. The MCHB is used to remove Cu (II) metal ions in an aqueous solution. The performance of MCHB to remove Cu (II) ions was evaluated by a batch adsorption experiment at different parameters such as the initial pH of the solution, contact time, and various magnetite ratios of the hydrogel beads. This study indicated that MCHB managed to remove Cu (II) ions by adsorption at pH 5 at 24 hours of contact time. The MCHB-0.5 (C:M:A ratio by weight of 1:0.5:2) shows the highest Cu (II) ions removal efficiency of 56.51%. The addition of magnetite at the minimal ratio does not hinder the removal of Cu (II) ions. The magnetite in the beads also eases the separation of the hydrogel beads from the solution by an external magnet after treatment.

*Keywords:* hydrogel beads, magnetic adsorbent, wastewater treatment, copper removal.

---

### INTRODUCTION

Adsorption is the most promising method to remove metal ions such as Cu (II) ions due to its low-cost process and ease of operation. Many adsorbents have been utilized in the past, including activated carbon, silica, and biomass [1] (Nitsae et al., 2016). Theoretically, the adsorption relies on the interaction between the adsorbents' functional groups and the metal ions, which influence the effectiveness, capability, selectivity, and reusability.

Chitosan (C) is a natural adsorbent with the presence of the amino (–NH<sub>2</sub>) and hydroxyl (–OH) groups which are suitable for the adsorption of metal ions [2], [3]. Chitosan has good adsorption capability, however poor acid resistance, low stability, and low volume density [2], [4]. Alginate (A) is a polysaccharide biopolymer, which shows a high affinity to metal ions and has a tendency to swell in water [2]. Chitosan and alginate can be blended to form chitosan-alginate hydrogel beads by electrostatic interaction between the amino group of chitosan and carboxyl group of alginate. The alginate's ability to swell in water will transport the metal ions by diffusion to react with the functional group of chitosan encapsulated in the beads. On top of that, Magnetite, Fe<sub>3</sub>O<sub>4</sub>, (M) can also be blended together to form the hydrogel beads for easier separation from the solution using an external magnet [5].

The present study explores the performance of the magnetic chitosan hydrogel beads (MCHB) to remove Cu (II) ions from an aqueous solution. Batch adsorption experiments were conducted and its parameters such as the initial pH of the solution, contact time, and the ratio of C:M:A were evaluated.

### MATERIALS AND METHODS

#### *Materials*

Chitosan (Biobasic), sodium alginate (R&M Chemicals, chemically pure), magnetite nanopowder (Fe<sub>3</sub>O<sub>4</sub>) with 50-100 nm particle size (Sigma-Aldrich, 97% trace metal basis) were used in this study.

---

#### *Article history:*

Received: 10 March 2022

Accepted: 7 June 2022

Published: 14 June 2022

---

#### *E-mail addresses:*

nafifah.khalil@s.unikl.edu.my (N.A.Khalil)

naim@unikl.edu.my (A.N.Ahmad Yahaya)

\*Corresponding Author

#### *Preparation of MCHB*

MCHB were prepared as shown in TABLE 1 by varying the weight of magnetite based on different ratio with CHB-O as control sample. Desired weight of sodium alginate was mixed with 200mL of ultrapure water. The alginate solution was stirred using a mechanical stirrer for 1 hour at room temperature. Then, the desired weight of magnetite was added into the alginate solution and stirred. Finally, chitosan was added to the solution and stirred until the mixture was mixed well. The final solution was poured into a burette and dropped

into 100mL of 2% calcium chloride solution (CaCl<sub>2</sub>) to form the MCHB. The MCHB was then cured for 24 hours in the CaCl<sub>2</sub> solution (Germanos et al., 2017). CHB-0 was prepared using similar procedure without addition of magnetite. After 24 hours, the beads were rinsed using ultrapure water for three times to ensure no excess CaCl<sub>2</sub>. The beads were stored in ultrapure water until further experiment (H. Zhang et al., 2019a).

TABLE 1: Formation of Chitosan hydrogel beads based on ratio of Chitosan: Magnetite: Sodium alginate (C:M:A)

Type	Chitosan	Magnetite	Sodium alginate
CHB-0	1	0	2
MCHB-0.5	1	0.5	2
MCHB-1.0	1	1	2

*Preparation of solution*

*1000 ppm Cu (II) Sulphate.*

0.1g of copper sulphate pentahydrate powder (CuSO<sub>4</sub>.5H<sub>2</sub>O) was mixed with 1L deionized water to prepare 1000ppm of Cu (II) ions stock solution. The stock solution was diluted to obtained standard Cu (II) ions solution of desired concentration.

*0.1 M of Sodium hydroxide.*

0.4 g of sodium hydroxide pellets were weighed, dissolved in deionized water, and stirred using a magnetic stirrer. The solution was poured into a volumetric flask of 100 mL. Deionized water was filled until the calibration mark was reached, and the flask was well shaken.

*0.1 M of hydrochloride acid.*

0.8 mL of 37% hydrochloric acid was transferred into a 100 mL volumetric flask using a pipette. Deionized water was filled until the calibration mark was reached, and the flask was well shaken.

*Batch adsorption experiments*

The adsorption studies of the MCHB were in a series of batch experiments, conducted in duplication. The adsorption study was conducted on parameters such as the initial pH of solution, contact time and at various ratio of magnetite (Fe<sub>3</sub>O<sub>4</sub>) for the removal of Cu (II) ions by MCHB.

Generally, 100mL of Cu (II) ions stock solution was poured into conical flasks and the pH was adjusted to pH 5. The MCHB with different Fe<sub>3</sub>O<sub>4</sub> ratio (CHB-0, MCHB-0.5, MCHB-1.0) were placed on a clean paper to remove access water. Then, 10 beads with each ratio were weight and added to the Cu (II) ions solution. The beads were placed inside an incubator shaker (CSI100, Protech) at room temperature and at a speed of 150 rpm. Sampling was done by extracting the solution (approximately 5 mL) by using a pipette at 0 mins, 10 mins, 20 mins, 30 mins, 40 mins, 1 hr, 2 hrs, 4 hrs, 24 hrs, and 48 hrs. The samples were filtered and analyzed by AAS to determine the concentration of Cu (II) ions.

The effect of the pH on the adsorption of the chitosan hydrogel beads was determined by varying the pH (pH 3, 5, 6, 8 and 11) of 100 ppm of Cu (II) solution. Then, 10 beads with each ratio were weight and added to the Cu (II) ions solution and placed inside an incubator shaker at room temperature and a speed of 150 rpm. The samples were taken by extracting the solution at 24 hours. The samples were filtered and analyzed by Atomic Absorption Spectroscopy, AAS (Perkin Elmer) to determine the concentration of Cu (III).

*Cu (II) ions removal efficiency of MCHB.*

The removal efficiency of Cu (II) ions of MCHB were calculated according to Eq. 1 [4], [6] as presented in Eq 1 and Eq 2.

$$\text{Removal} = \left( \frac{C_0 - C_t}{C_0} \right) \times 100\% \quad \text{Eq. 1}$$

Where, C<sub>0</sub> is the initial concentration of Cu (II) ions [mg/L] and C<sub>t</sub> is concentration of copper (II) ions after adsorption at certain time [mg/L].

**RESULTS AND DISCUSSION**

*Effect of initial pH of solution on the removal of Cu (II) ions*

The Cu (II) ions removal was studied under different pH ranges 3 to 11. The analysis reveals at higher pH 7 and above, the removal of Cu from the solution via precipitation as Cu(OH)<sub>2</sub> resulted from reaction between CuSO<sub>4</sub> and NaOH. [2], [7]. The removal of Cu (II) ions via adsorption by MCHB only happened at pH below pH 6 which is due to the electrostatics attraction between the cationized chitosan active sites on the MCHB (such as amino and hydroxyl groups) and the predominant Cu (II) ions [6], [8]. Therefore, the removal of Cu (II) ions via adsorption of MCHB surfaces in this work only being studied at <pH7.

Fig. 1 shows the removal trend of Cu (II) by MCHB at varying pH (pH 3, pH 5 and pH 6). The trend shows Cu (II) ions removal by both MCHB-0.5 and CHB-0 increased when the initial pH of solution increased from pH3 to pH 5. Low removal performance at pH 3 is due to the existence of H<sup>+</sup> ions (due to acid addition for pH adjustment), competing with Cu (II) ions for the adsorption on the active site of MCHB [9]. As the initial pH increased, less H<sup>+</sup> ions were added, hence increased the adsorption of Cu (II) ions on the MCHB. By increasing the pH also, the electrostatic interaction between the active site on the MCHB (-COOH- in alginate, -NH<sub>2</sub>- and -OH- in chitosan) become stronger, hence, higher adsorption performance lead to

higher Cu (II) ion removal [9]. Beyond pH5, the removal efficiency of Cu (II) ion by MCHB decreased. As a conclusion, the best pH for removal of Cu (II) ions via adsorption of the MCHB occurred at pH 5.

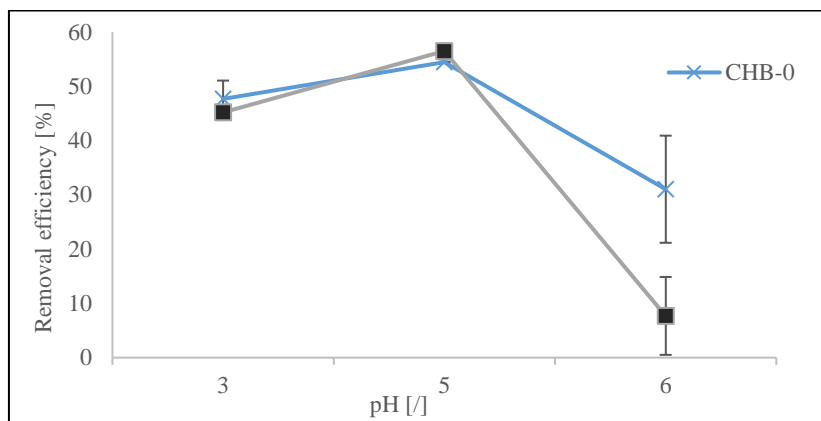


Fig. 1: Removal efficiency of Cu (II) ion by MCHB at different pH.

*Effect of contact time on the removal of Cu (II) ions by MCHB*

Fig. 2 shows the removal of Cu (II) ions by MCHB at pH for varying contact time. Rapid adsorption was observed shown by significant increase in Cu (II) ions removal efficiency from 0 to 5 hours, as the Cu (II) was easily attached to the unoccupied adsorption site of the MCHB surface. The removal increased further in between 5 to 24 hours. The removal rate was nearly consistent starting beyond 24 hours for all types of MCHB, indicated that most of the adsorption sites were practically saturated with the Cu (II) ions [10]. Based on these results, the adsorption of Cu (II) ions by MCHB has reach equilibrium at 24 hours with the highest Cu (II) ion removal ranging between 54 to 57% for all MCHB.

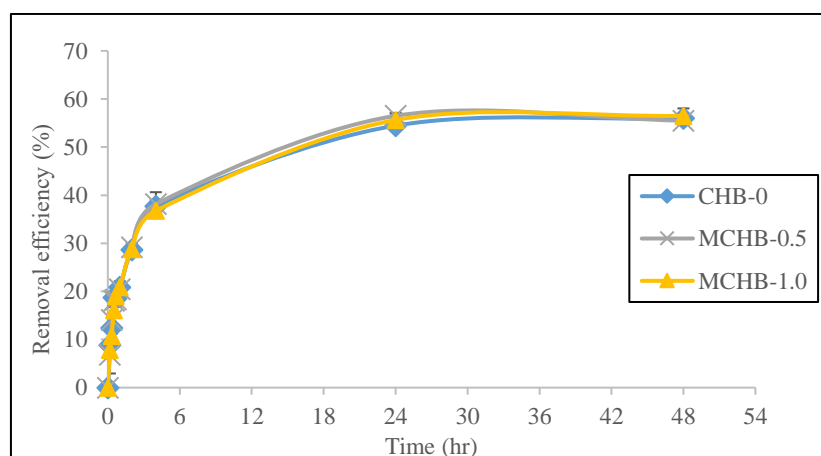


Fig. 2: Removal efficiency of Cu (II) ion by MCHB for various contact time and pH5

*Effect of Magnetite ratio on the removal of Cu (II) ions by MCHB*

Fig. 3 shows the Cu (II) ions removal efficiency of MCHB at different magnetite ratio with CHB-0 as control sample.

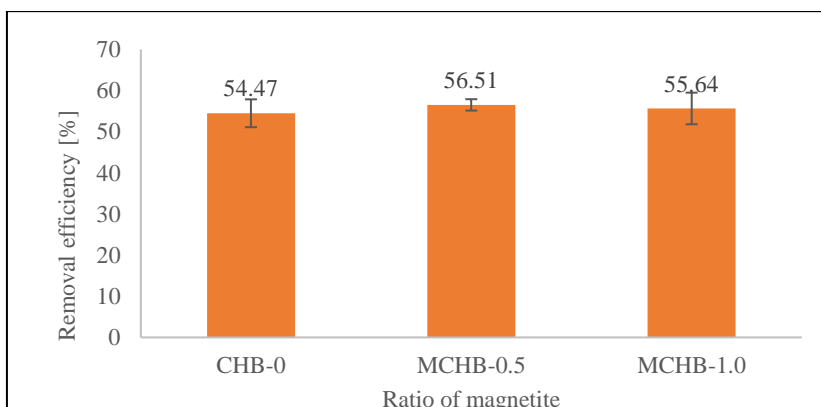


Fig. 3: Adsorption capacity Cu (II) ion by MCHB with different magnetite ratio

The addition of magnetite in the chitosan hydrogel beads of MCHB-0.5 managed to remove 56.51 % of Cu (II) ion compared to CHB-0 (54.41%). Further addition of magnetite reduced the removal efficiency of Cu (II) ions to 55.64%. The reduction in removal performance may be associated with factors such as the competitive effect of magnetite on active sites in the hydrogel

network, an increase in cross-linking points in the polymer hydrogel network and a decrease in the water diffusion rate [11]. Therefore, the minimum amount of magnetite should be added in the formation of the MCHB, just enough to induce the ability for separation of the beads from the solution by a magnet.

## CONCLUSIONS

The magnetic chitosan hydrogel beads (MCHB) were successfully synthesized and used as adsorbent for Cu (II) ions removal from aqueous solution. The performance of MCHB in removing Cu (II) ions by adsorption were studied at varying initial pH of solution, contact time and ratio of magnetite in MCHB. This study indicated that MCHB managed to remove Cu (II) ions by adsorption at pH 5 at 24 hours of contact time. The MCHB-0.5 (C:M:A ratio by weight of 1:0.5:2) shows the highest Cu (II) ions removal efficiency of 56.51%.

## ACKNOWLEDGEMENTS

This work was supported by the thank Ministry of Higher Education (MoHE), Malaysia under Fundamental Research Grant Scheme (FRGS/1/2018/STG07/UNIKL/03/1). The authors would also like to acknowledge Universiti Kuala Lumpur for providing support under UniKL Excellent Research Grant Scheme (UniKL/CoRI/UER20016).

## REFERENCES

- [1] M. Nitsae, A. Madjid, L. Hakim, and A. Sabarudin, "Preparation of chitosan beads using tripolyphosphate and ethylene glycol diglycidyl ether as crosslinker for Cr(VI) adsorption," *Chem. Chem. Technol.*, vol. 10, no. 1, pp. 105–114, 2016, doi: 10.23939/chcht10.01.105.
- [2] W. S. W. Ngah and S. Fatinathan, "Adsorption of Cu(II) ions in aqueous solution using chitosan beads, chitosan-GLA beads and chitosan-alginate beads," *Chem. Eng. J.*, vol. 143, no. 1–3, pp. 62–72, 2008, doi: 10.1016/j.cej.2007.12.006.
- [3] Y. Lin, H. Chen, K. Lin, B. Chen, and C. Chiou, "Application of magnetic particles modified with amino groups to adsorb copper ions in aqueous solution," *J. Environ. Sci.*, vol. 23, no. 1, pp. 44–50, 2011, doi: 10.1016/S1001-0742(10)60371-3.
- [4] H. C. Tao, S. Li, L. J. Zhang, Y. Z. Chen, and L. P. Deng, "Magnetic chitosan/sodium alginate gel bead as a novel composite adsorbent for Cu(II) removal from aqueous solution," *Environ. Geochem. Health*, vol. 41, no. 1, pp. 297–308, 2019, doi: 10.1007/s10653-018-0137-5.
- [5] H. Zhang, A. M. Omer, Z. Hu, L. Y. Yang, C. Ji, and X. kun Ouyang, "Fabrication of magnetic bentonite/carboxymethyl chitosan/sodium alginate hydrogel beads for Cu (II)adsorption," *Int. J. Biol. Macromol.*, vol. 135, pp. 490–500, 2019, doi: 10.1016/j.ijbiomac.2019.05.185.
- [6] N. A. Khalil *et al.*, "Microcrystalline cellulose (MCC) as an adsorbent in copper removal from aqueous solution," *IOP Conf. Ser. Mater. Sci. Eng.*, vol. 1195, no. 1, p. 012022, 2021, doi: 10.1088/1757-899x/1195/1/012022.
- [7] Q. Huang *et al.*, "Preparation of polyethylene polyamine@tannic acid encapsulated MgAl-layered double hydroxide for the efficient removal of copper (II) ions from aqueous solution," *J. Taiwan Inst. Chem. Eng.*, vol. 82, pp. 92–101, 2018, doi: 10.1016/j.jtice.2017.10.019.
- [8] M. B. Kasiri, "Application of chitosan derivatives as promising adsorbents for treatment of textile wastewater," in *The Impact and Prospects of Green Chemistry for Textile Technology*, Elsevier Ltd., 2018, pp. 417–469.
- [9] A. S. A. Rahman *et al.*, "Effect of magnetite on alginate-based hydrogel beads composite bio-sorbent for copper removal," in *IOP Conference Series: Materials Science and Engineering*, Oct. 2021, vol. 1195, no. 1, p. 012052, doi: 10.1088/1757-899X/1195/1/012052.
- [10] A. M. Khalid *et al.*, "Isolation and characterization of magnetic oil palm empty fruits bunch cellulose nanofiber composite as a bio-sorbent for Cu(II) and Cr(VI) removal," *Polymers (Basel)*, vol. 13, no. 1, pp. 1–22, 2021, doi: 10.3390/polym13010112.
- [11] A. T. Paulino, L. A. Belfiore, L. T. Kubota, E. C. Muniz, V. C. Almeida, and E. B. Tambourgi, "Effect of magnetite on the adsorption behavior of Pb(II), Cd(II), and Cu(II) in chitosan-based hydrogels," *Desalination*, vol. 275, no. 1–3, pp. 187–196, 2011, doi: 10.1016/j.desal.2011.02.056.

## **EFFECT OF PARAMETERS MANIPULATION ON CELLULOSE EXTRACTION PROCESS USING ECO-FRIENDLY SOLVENT AND PRODUCTION OF CELLULOSE TRANSPARENT FILM FROM OIL PALM FROND**

A. F. Lajulliadi<sup>1</sup>, N. A. Khalil<sup>1</sup>, A. N. A. Yahaya<sup>1</sup>, M. Zulkifli<sup>2\*</sup>

<sup>1</sup>Universiti Kuala Lumpur, Branch Campus Malaysian Institute of Chemical and Bioengineering Technology, 78000 Alor Gajah, Melaka, Malaysia

<sup>2</sup>Green Chemistry and Sustainability Cluster, Universiti Kuala Lumpur, Branch Campus Malaysian Institute of Chemical and Bioengineering

---

### **ABSTRACT**

The purpose of this study is to optimize the cellulose extraction method from oil palm frond using three different methods. The first method involves the suspension of OPF in mixture of formic acid and hydrogen peroxide. Second method using basic, NaOH and acidic, H<sub>2</sub>O<sub>2</sub> suspension of OPF in three cycle operation and lastly, the third method is suspension of OPF in a mixture of NaOH and H<sub>2</sub>O<sub>2</sub> at 70°C assisted with mechanical stirring. The optimal method is dictated by the FTIR result focusing on the lignin peak intensity at 1656 cm<sup>-1</sup>. The result revealed that method 2 is the best extraction method supported by the lowest intensity of lignin peak. In term of yield of cellulose, method 3 has the highest value which is 93.61% followed by method 2, 74.06% and method 1, 69.61%.

*Keywords:* cellulose, lignin, extraction, eco-friendly reagent

---

### **INTRODUCTION**

The British administration introduced ornamental plants from Nigeria's Oil River Protectorate to Malaysia in the 1870s. Tennamaran Estate produced the first palm oil in Selangor in 1917. Palm oil, or *Elaeis guineensis*, has become one of Malaysia's most important economic drivers, surpassing Indonesia as the world's second biggest producer. In 2018, agriculture contributed 7.3% of Malaysia's GDP, with oil palm accounting for 37.9% [1]. Cellulose is a linear strip-molded glucose polymer. The anomeric C1 carbon embraces the -arrangement, and the solitary glucose units are linked by glycosidic connections between C1 and C4. Each glucose unit rotates about 180° relative to its neighbors, forming two hydrogen bonds. Cellulose's unaltered C1-carbon and C4-hydroxyl groups form the polymer's reducing and nonreducing ends. A nucleophilic replacement reaction transports a glucose unit from UDP-glucose to the polymer's C4-hydroxyl group. The acceptor hydroxyl is deprotonated by an overall base [2].

Cellulose polymers may reach 15,000 glucose units [3]. Because cellulose includes both core hydroxyl bunches that point radially away from the pyranose ring's essence and hub hydrogen particles that point in the opposite direction, it possesses both hydrophilic and hydrophobic properties. Once the amphipathic macromolecule self-relates, it becomes insoluble in water. Many organisms have used van der Waals interactions between glucopyranose rings to collect cellulose polymers into supramolecular structures [4].

Although certain aquatic species may possess lignin or "lignin-like" components, lignin is found in all terrestrial plants as a natural polymer. Lignin molecules develop by cross coupling between a monolignol radical and the previously generated dimeric or oligomeric lignol radicals, commencing with dimerization of two monolignol radicals. Lignins are phenylpropanoid-based plant polymers. They have the highest concentration of wood methoxyl. The disadvantages of lignin in cellulose-based products making them easily oxidized, affecting the durability, soluble in alkaline and bisulfite solutions, and easily condensed with phenols or thiols [5].

### **MATERIALS AND METHODS**

---

#### *Article history:*

Received: 10 March 2022

Accepted: 7 June 2022

Published: 14 June 2022

---

#### *E-mail addresses:*

afiqhri.lajulliadi@s.unikl.edu.my (A. F. Lajulliadi)

nafifah.khalil@s.unikl.edu.my (N.A.Khalil)

naim@unikl.edu.my (A.N.Ahmad Yahaya)

\*Corresponding Author

#### *Materials*

Fresh Oil Palm Frond (OPFs) were collected from private palm oil plantation at Senggarang, Batu Pahat, Johor (1.75195° N, 103.05258° E). The chemical used were sodium hydroxide (NaOH), hydrogen peroxide (H<sub>2</sub>O<sub>2</sub>) and formic acid (CH<sub>2</sub>O<sub>2</sub>) to assists in physical treatment, an autoclave was used. All chemical used were in analytical grade.

#### *Method*

##### *Oil Palm Frond Pre-treatment*

##### *Method 1*

1000 g of 500 µm OPF were soaked with distilled water for 30 min and washed several times until the water observed become clear. The purpose of washing is to remove the dirt

and other impurities from raw materials. The fiber was further dried at 50°C until constant weight was obtained after 3 days. The 30g of OPF were dewaxed with 300ml of 70% ethanol using Soxhlet extractor for 3 hours and dried for overnight. 50g of the dewaxed fibers were suspended in 10% NaOH and autoclaved for one hours at 121°C and 1.5 atm. The mixture of supernatant and fibers were separated and washed until clear water was observed. 10g of treated fiber were suspended in 10% H<sub>2</sub>O<sub>2</sub> and placed into incubator shaker for 1 hour at room temperature for bleaching treatment. The bleached fibers were washed with distilled water and dried at 70°C overnight.

*Method 2 and 3*

Raw OPF were grinded and washed with distilled water until the water become clear. Raw OPF were then sieved to obtain 500 µm OPF and it was oven dried at 70°C until the mass become plateau.

*Cellulose extraction*

*Method 1*

15 g pre-treated fibres were soaked in a 1:1 solution of 20% formic acid and 10% H<sub>2</sub>O<sub>2</sub>. The soaked fibre was delignified at 85°C for 90 minutes. The delignified cellulose was washed with 10% formic acid and then rinsed with distilled water to pH 7. The cellulose was then dried in conventional oven overnight at 70°C. The α-cellulose content was calculated by Mohtar et al, [6] proposed method.

*Method 2*

Dried OPF were treated with three cycles of basic and acidic treatment according to Mohd Rasli et al [7]. 5g treated fibre was stirred in 4% NaOH for 2 hours at 80°C. The fibre was then filtered and treated in 30% H<sub>2</sub>O<sub>2</sub> at 60°C. Following the cycle, the fibres were filtered and dried in a normal oven at 70°C overnight. This fraction was collected and the yield percentage (% wt) was calculated. The α-cellulose content was calculated by Mohtar et al, [6] proposed method.

*Method 3*

15 g of dried OPF were suspended in mixture of 300 ml of 4% NaOH and 30 ml of 30% (w/v) H<sub>2</sub>O<sub>2</sub>. The mixture heated at 70°C and mechanically stirred at 4000 rpm for 1 hour. Fibre cleaned using distilled water until pH ~ 7 and oven dried for 24 hours at 70°C. The α-cellulose content was calculated by Mohtar et al, [6] proposed method.

*Characterization*

*Fourier-transform infra-red spectroscopy (FTIR)*

The Perkin Elmer Spectrum 400 FT-IR/FT-NIR recognized the functional group of raw OPF, processed OPF, cellulose removed, and clear thin film. The substance was homogenized by mixing it with KBr 100:1. Analyzed at 0.02 cm<sup>-1</sup> for wavelengths 400-4000 cm<sup>-1</sup>.

**RESULTS AND DISCUSSION**

*Yield of cellulose*

TABLE 1 shows the cellulose percentage of yield extracted from OPF. Method 3 shows the highest percentage of yield at 93.61% followed by method 2 at 74.06% and method 1 at 69.61%. Even though method 3 holds the highest yield compared to other method as the mass of lignin itself affect the final weight of the extracted cellulose [8]. The lignin content in method 3 and 1 considered as high as shown in the FTIR result where the intensity of lignin at 1658 cm<sup>-1</sup> is stronger compared to method 2. This result supported by the observation of extracted cellulose from each method in Fig. 1, whereas the product from method 3 and 1 displayed darker colour compared to product from method 2 indicating the presence of lignin in the cellulose [9].

TABLE 1: Yield percentage of cellulose from OPF

Method	Initial weight, g	Final weight, g	Yield, % (w/w)
1	15.00	10.47	69.61
2	15.05	11.14	74.06
3	15.02	14.08	93.61

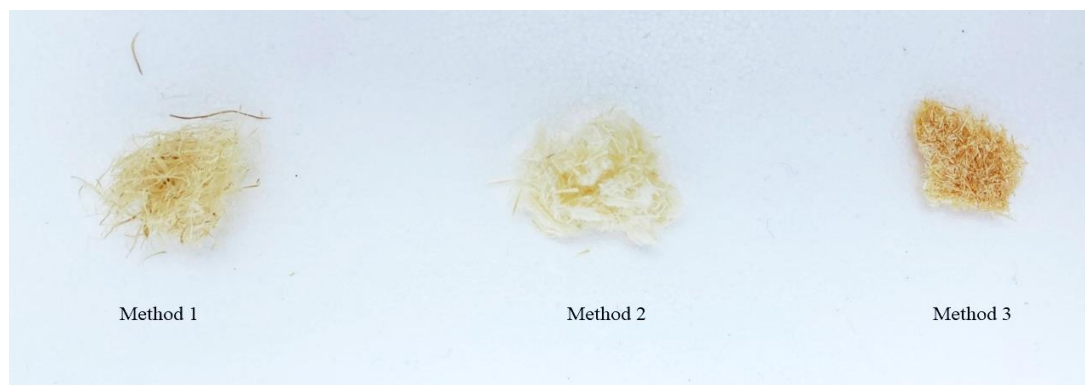


Fig. 1: Observation of yield from each method

**FTIR**

Fig. 2 indicates the FTIR result for extracted cellulose from OPF from different method. The characteristic peak of cellulose at  $3391.23\text{ cm}^{-1}$  correspond to hydroxyl group (-OH) [10]. Method 3 reveal the highest intensity compared to other method. Then, peak at  $1656\text{ cm}^{-1}$  is attributed to characteristic peak of lignin. Method 2 has the lowest intensity showing that the removal of lignin in method 2 is better compared to other method. This is due to the higher usage of  $\text{H}_2\text{O}_2$  acting as lignin removal agent [11]. Lastly at peak  $1162.44\text{ cm}^{-1}$  denoted as C-O-C pyranose [10].

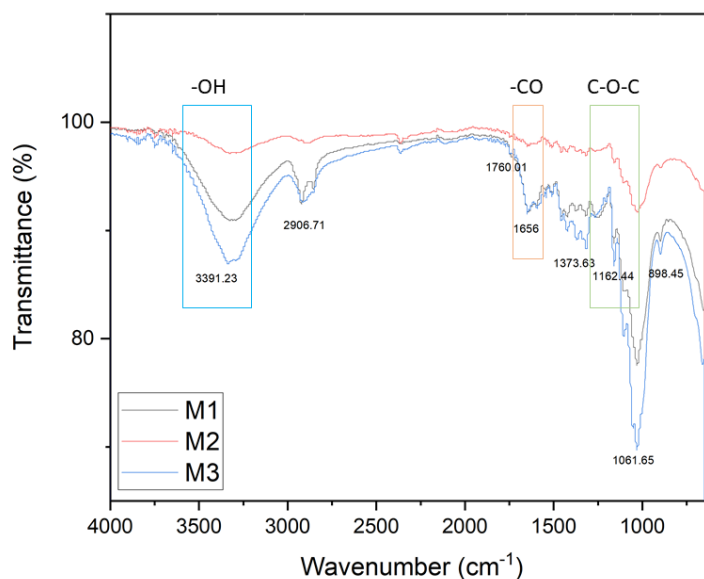


Fig. 2: FTIR result of OPF for each method

**ACKNOWLEDGMENT**

The authors would like to thank Universiti Kuala Lumpur Malaysia Institute of Chemical and Bioengineering Technology (MICET) for the opportunity and support given throughout the duration of this study under Short Term Research Grant (STRG) (UniKL/CoRI/str19036) and Dana Penyelidikan & Inovasi MARA (DPIM 2021).

**REFERENCES**

- [1] Ghulam Kadir, Ahmad Parveez. (2020). Oil palm economic performance in malaysia and R&D progress in 2019. *Journal of Oil Palm Research*. 32. 10.21894/jopr.2020.0032.
- [2] Morgan, J., McNamara, J., Fischer, M. et al. Observing cellulose biosynthesis and membrane translocation in crystallo. *Nature* 531, 329–334 (2016). <https://doi.org/10.1038/nature16966>
- [3] Somerville, C. (n.d.). Cellulose synthesis in higher plants. *Annual Reviews*. Retrieved May 11, 2022, from <https://www.annualreviews.org/doi/full/10.1146/annurev.cellbio.22.022206.160206>
- [4] Conformational features of crystal-surface cellulose from higher plants ... (n.d.). Retrieved May 10, 2022, from [https://www.researchgate.net/publication/11312357\\_Conformational\\_features\\_of\\_crystal-surface\\_cellulose\\_from\\_higher\\_plants](https://www.researchgate.net/publication/11312357_Conformational_features_of_crystal-surface_cellulose_from_higher_plants)
- [5] Lu, F., & Ralph, J. (2010, March 17). Lignin. *Cereal Straw as a Resource for Sustainable Biomaterials and Biofuels*. Retrieved June 8, 2022, from <https://www.sciencedirect.com/science/article/pii/B9780444532343000067>
- [6] Mohtar SS, Tengku Malim Busu TN, Md Noor AM, Shaari N, Mat H. An ionic liquid treatment and fractionation of cellulose, hemicellulose and lignin from oil palm empty fruit bunch. *Carbohydr Polym*. 2017 Jun 15;166:291-299. doi: 10.1016/j.carbpol.2017.02.102. Epub 2017 Feb 27. PMID: 28385235.
- [7] Extraction and characterization of cellulose from agricultural residue - oil palm fronds. (2017). *Malaysian Journal of Analytical Science*, 21(5). <https://doi.org/10.17576/mjas-2017-2105-08>
- [8] Donaldson, L., Nanayakkara, B., & Harrington, J. (2016, September 6). Wood growth and development. *Encyclopedia of Applied Plant Sciences (Second Edition)*. Retrieved June 8, 2022, from <https://www.sciencedirect.com/science/article/pii/B9780123948076001143>
- [9] Lightness and lignin content in flax fibers treated with laccase at ... (n.d.). Retrieved June 8, 2022, from [https://www.researchgate.net/figure/Lightness-and-Lignin-Content-in-Flax-Fibers-Treated-with-Laccase-at-Different\\_tbl4\\_26460111](https://www.researchgate.net/figure/Lightness-and-Lignin-Content-in-Flax-Fibers-Treated-with-Laccase-at-Different_tbl4_26460111)
- [10] Izzaha1, N. S., Yahaya2, A. N. A., Zuhudi3, N. Z. M., Khalil1, N. A., & Zulkifli1, M. (2021, October 1). *IOPscience*. IOP Conference Series: Materials Science and Engineering. Retrieved June 8, 2022, from <https://iopscience.iop.org/article/10.1088/1757-899X/1195/1/012062/meta>
- [11] Zeronian, S. H., & Inglesby, M. K. (n.d.). Bleaching of cellulose by hydrogen peroxide - cellulose. *SpringerLink*. Retrieved June 8, 2022, from <https://link.springer.com/article/10.1007/BF00811817>



## **INTERFACIAL SHEAR PROPERTIES OF TREATED KENAF/POLYPROPYLENE WITH SILANE PVA/ UREA**

N. I. S. Anuar\*<sup>1</sup>, S. Zakaria<sup>2</sup>, Q. Zuo<sup>3</sup>, C. Wang<sup>3</sup>

<sup>1</sup>*Fibre and Biocomposite Centre, Malaysian Timber Industry Board, 42700, Banting, Selangor, Malaysia*

<sup>2</sup>*Bioresources and Biorefinery Laboratory, Faculty of Science and Technology, Universiti Kebangsaan Malaysia, 43600 UKM Bangi, Selangor, Malaysia*

<sup>3</sup>*School of Textile Science and Engineering, Tiangong University, Tianjin, China, 300387*

---

### **ABSTRACT**

Kenaf fibres demonstrate enormous potential in fibre reinforced composites with excellent performance and environmental benefits. Apart of fibres strength, interfacial bonding strength between fibres reinforcement and matrix also contributes to the mechanical performance of composites. In this work, kenaf fibers were modified by PVA, Silane, Urea and combination of PVA/silane, PVA/urea and silane/urea as methods to improve the interfacial bonding between kenaf and PP. The effects of the treatments on the interfacial shear properties (IFSS) between kenaf fibres and PP matrix were systematically evaluated. In addition, the effect of treatment on the tensile strength and the surface friction coefficient of kenaf fiber were also revealed. The results indicated that combination of urea/silane treatment of kenaf fibres produced the highest interfacial shear strength between kenaf fibre and PP at 9.91 MPa. The urea treatment resulted to the highest kenaf fibre tensile strength at 362.3 MPa. These results suggested that the chemical treatment used in this study effective in improving the interfacial strength of kenaf and PP which subsequently benefit to the mechanical properties of kenaf/PP nonwoven composite.

*Keywords:* tensile, interfacial strength, bonding.

---

### **INTRODUCTION**

Interfacial interaction or bonding of fibre with matrix have a vital role in the mechanical properties of composites. The fibre-matrix interface is regulated by the degree of binding that occurs between the two components [1]. A good degree of bonding is required on the interface to achieve optimum reinforcement, mainly because it is responsible for transferring stress between matrix and reinforcement fibres.

The most serious drawback of natural fibres as fibre reinforcement is their hydrophilic nature, which causes the weak interfacial bonding between fibre and matrix in polymer composites. Various physical impurities and the presence of hydroxyl groups on the fibre surface create difficulties to be used as enforcement materials. Chemical treatment of cellulose fibre is one of the method that can be used to enhance the interfacial bonding between natural fibre and polymer matrix. Fibre treatment can enhance the interfacial bonding either by cleaning the fibre surface, chemically modifying the fibre surface, reducing the moisture absorption process, or increasing the roughness on the fibre surface [2]. The most reported fibre treatment methods for surface modification of natural fibres are acetylation, salinization, mercerization, peroxide, benzoylation, graft copolymerization, and bacterial cellulose treatment [3].

Silane is a coupling agent that is commonly used to increase the degree of cross-linking between two interfaces region, so as to enhance the bonding properties of the finished composites [4]. Urea is an organic compound with chemical formula CO(NH<sub>2</sub>)<sub>2</sub>, is also known as carbamide. Urea is an amide group with two -NH<sub>2</sub> groups joined by a carbonyl functional group. Urea was used in composites as an additive to increase plasticity in wood-plastic composites, so as to ease the blending between natural fibre and polymer [5]. The PVA is a colourless and odourless water-soluble polymer widely used in the plastic packaging industry [6]. The PVA has carboxyl and hydroxyl groups to form a hydrogen bond with natural fibres.

Asumani (2013) [7] treated kenaf with NaOH and silane by soaking method to improve the interfacial bonding between kenaf and polymer matrix. Ishikawa et al. (2014) [8] reported that PVA thin film was formed on the natural fibre surface to improve the adhesion between natural fibres and epoxy matrix. Similarly, Kim et al. (2011) [9] found that the PVA treatment on jute composites enhanced the interfacial adhesion and the bending properties of jute composites. Zaman et al. (2010) [10] asserted that urea, serving as an additive, can generate favourable conditions for the bonding between cellulose and PP.

In this study, kenaf fibres were treated by silane, PVA and urea by spraying method. The effect of the chemical treatment on the interfacial bonding between kenaf and PP matrix were studied by Interfacial Shear Strength (IFSS). It is important to highlight that the chemical used as the treatment are common in industry and the spraying method introduced in this study is also a practical way in nonwoven composite manufacturing process.

---

#### *Article history:*

Received: 10 March 2022

Accepted: 7 June 2022

Published: 14 June 2022

---

#### *E-mail addresses:*

intansaffinaz@gmail.com (N. I. S. Anuar)

\*Corresponding Author

## MATERIALS AND METHODS

### Materials

Kenaf (*Hibiscus cannabinus*) bast fibres were supplied by National Kenaf and Tobacco Board, Malaysia, in ribbon form with a ribbon length of 2 to 3 m. The kenaf ribbons were cut to 60 mm. PP fibres were purchased from Hualong Chemical Fibre Co. Ltd, De Zhou, Shandong, China. The length, diameter and melting point of the PP fibres were 65 mm, 10 denier and 165 °C, respectively. Silane three aminopropyltriethoxysilane KH550, PVA and urea was purchased from Zhejiang Feidian Chemical Co Ltd.

### Methods

The 5wt% of Silane, PVA, Urea, Silane/PVA, Silane/Urea, PVA/Urea were diluted into 15% distilled water from the weight of the mixture of the natural fibers and PP fibers. The solution of reagent was sprayed on the fibers.

The single fibre pull out test was conducted in order to analyse the interfacial shear strength (IFSS) between fibre and matrix. The PP fibres were heated and melted by using a heating plate. A single fibre was fixed on a designed paper properly and single drop of polymer was attached on the fibre and left for cooling. By using a 5 kN Universal Testing Machine (Massachusetts, USA), tests were conducted with a fixed cross-head displacement speed rate at 1 mm/min. Six replicates for each kenaf sample of both treated and untreated fibres were tested. The interfacial shear strength was estimated as referred to Zhang et al. (2009) [11].

The friction coefficient of the kenaf fibres was measured by using the Y151 Friction Coefficient Testing Instrument Changzhou DePu Textile Technology Co., Ltd. (Changzhou, China) in accordance to China National Bureau of Standard, (1983). The speed of friction roller was 30 r.p.m, and 500 mg fibre clip was adopted. A total of 20 samples were tested and the average of the friction coefficient was recorded. The test was performed at  $20\pm 1$  °C and  $65\pm 2\%$  relative humidity setting.

Tensile tests of the fibres were performed using Electronic Single Fibre Strength Tester Shimadzu GX1000 20N Load Cell (Tokyo, Japan) in adherence to ASTM D 3822-01 test methods. The test was performed at  $20\pm 1$  °C and  $65\pm 2\%$  relative humidity setting. The tests were conducted with 20 replicates. The gauge length and the cross-head speed were set at 20 mm and 2 mm/min, respectively.

## RESULTS AND DISCUSSION

### Effect of treatment on interfacial shear strength between kenaf and PP

Fig 1 displays the interfacial shear strength (IFSS) test of treated and untreated kenaf using the microdroplet test method. The test was run to assess the effect of treatment on the interfacial bonding strength between kenaf fibre and PP matrix. The different outcomes in IFSS between treated and untreated kenaf fibre had been influenced by several factors, including chemical composition on the fibre surface and the fibre surface roughness [12].

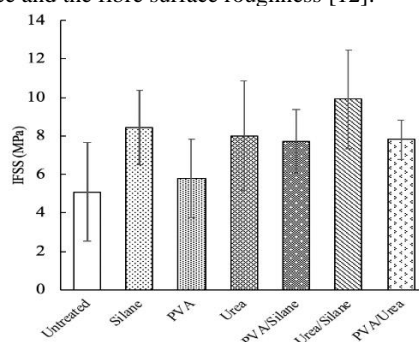


Fig. 1: Interfacial shear strength of untreated and treated KPNC

The most significant IFSS improvement was noted in urea/silane treated fibres, perhaps due to elimination of lignin and hemicellulose by silane. Removal of these compounds created voids in the fibres, which helped to make an anchor between matrix and fibres. The coupling agent penetrated the fibres and deposited in the interfibrillar regions. This effect enhanced the interfacial shear strength of between kenaf fibre and PP matrix. A similar finding on the effect of treatment on IFSS was also reported elsewhere. Merotte et al. (2018) [12] assessed the effect of adding maleic anhydride as a coupling agent on hemp and flax PP nonwoven composites. It revealed that the application of coupling agent MAPP promoted the A/B interaction between fibre and matrix, thus increasing the IFSS. They added that the elimination of some amounts of lignin and hemicellulose from the flax and hemp fibre surfaces influenced the IFSS result due to the interaction with cellulose via hydrogen bonds and with PP via van der Waals forces. Asim et al. (2016) [13] found that silane treated hemp fibres improved most significantly in IFSS value.

### Effect of treatment on coefficient friction of kenaf fibres

In Fig 2, the surface friction coefficient of all treated kenaf fibres was higher than those untreated, except for PVA that was lower than that untreated. Treatment of kenaf fibre with silane, urea, and the combinations had roughened the surface of kenaf fibre. On the contrary, treatment with PVA had turned the kenaf surface smoother, which decreased the friction coefficient value to 0.139. The PVA treatment on kenaf fibre coated the fibre surface and covered the piths, thus making the kenaf fibre surface even and smooth. Among the treated kenaf fibres, kenaf treated with silane displayed the highest friction coefficient at 0.162. Silane treatment had roughened the kenaf fibre surface by covering the fibre surface with small silane particles.

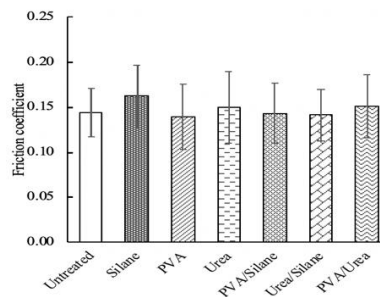


Fig. 2: Coefficient of friction of untreated and treated kenaf fibres

#### Effect treatment on tensile strength of kenaf fibres

Fig 3 shows the tensile strength of treated kenaf fibres was significantly higher than untreated. The highest tensile strength was obtained for kenaf fibre treated with urea at 362.3 MPa, which is 58.9% higher. The combination of urea/silane treatment also produced high kenaf tensile strength at 312.4 MPa, which is 37% higher than that untreated. Urea treatment increased the crystallinity of cellulose, which increased the tensile strength [14]. This study postulated that silane treatments of fibres increased the tensile strength of kenaf fibres by cementing both lignin and hemicelluloses with cellulose, thus yielding a stronger kenaf fibre bundle.

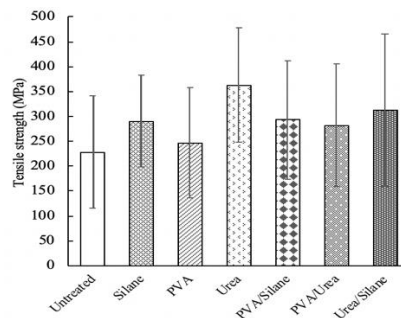


Fig. 3: Tensile strength of untreated and treated kenaf fibres

## CONCLUSIONS

Fibre treatment with silane, PVA and urea have improved the interfacial shear strength between kenaf and PP. The combination of urea/silane emerged as the best combination treatment for interfacial bonding, while urea was the most effective treatment to improve fibre strength. The improvement of interfacial bonding and tensile strength of the kenaf fibre has benefit to the mechanical properties of composite from kenaf and PP.

## ACKNOWLEDGEMENTS

The authors would like to thank Universiti Kebangsaan Malaysia for financial support via research project grants DIP 2016-004 and MRUN-2015-003 as well as Malaysian Timber Industry Board for the financial support provided and those who were involved in this study.

## REFERENCES

- [1] K.L Pickering, M.G Efendy, and T. M Le, "A review of recent developments in natural fibre composites and their mechanical performance," *Composites : Part A* 83: 98–112. 2016.
- [2] Kabir, M.M., Wang, H., Lau, K.T. & Cardona, F. 2012. Chemical treatments on plant- based natural fibre reinforced polymer composites: an overview. *Composites Part B: Engineering* 43(7): 2883–2892.
- [3] Kalia, S., Thakur, K., Celli, A., Kiechel, M. A. & Schauer, C. L. 2013. Surface modification of plant fibers using environment friendly methods for their application in polymer composites, textile industry and antimicrobial activities: A review. *Journal of Environmental Chemical Engineering* 1(3): 97–112.
- [4] Takemura, K., Miyamoto, S. & Katogi, H. 2012. Effect of surface treatment on creep property of jute fiber reinforced green composite under environmental temperature. *Key Engineering Materials* 525–526: 53–56.
- [5] Husain, M.M., Khan, Mubarak A., Idriss Ali, K.M. & Moynul Hasan, A.J.M. 1995. Wood plastic composite at different urea concentrations. *Radiation Physic and Chemistry* 45(4): 623–627.
- [6] Abdullah, Z. W., Dong, Y., Davies, I. J. & Barbhuiya, S. 2017. PVA, PVA blends and their nanocomposites for biodegradable packaging application. *Polymer-Plastic Technology and Engineering* 56(12): 1307–1344.
- [7] Asumani, O.M.L., Reid, R.G. & Paskaramoorthy, R. 2012. The effects of alkali-silane treatment on the tensile and flexural properties of short fibre non-woven kenaf reinforced polypropylene composites. *Composites Part A: Applied Science and Manufacturing* 43(9): 1431–1440.
- [8] Ishikawa, H., Takagi, H., Nakagaito, A. N., Yasuzawa, M., Genta, H. & Saito, H. 2014. Effect of surface treatments on the mechanical properties of natural fiber textile composites made by VaRTM method. *Composite Interfaces* 21(4): 329–336.
- [9] Kim, H.J., Miyamoto, S., Takada, Y. & Takemura, K. 2011. Effect of surface modification on flexural properties of jute fiber green composites. *ICCM International Conferences on Composite Materials* 6300: 2–6

## ***The International Symposium on Polymeric Materials 2022***

- [10] Zaman, H. U., Khan, M. A., Khan, R. A., Arifur Rahman, M., Das, L. R. & Al-Mamun, M. A. 2010. Role of potassium permanganate and urea on the improvement of the mechanical properties of jute polypropylene composites. *Fibers and Polymers* 11(3): 455–463.
- [11] Zhang, F. H., Wang, R.G., He, X.D., Wang, C. & Ren, L.N. 2009. Interfacial shearing strength and reinforcing mechanisms of an epoxy composite reinforced using a carbon nanotube/carbon fiber hybrid. *Journal of Materials Science* 44: 3574– 3577. <https://doi.org/10.1007/s10853-009-3484-x>
- [12] Merotte, J., Le Duigou, A., Kervoelen, A., Bourmaud, A., Behlouli, K. & Sire, O. 2018 Flax and hemp nonwoven composites: the contribution of interfacial bonding to improving tensile properties. *Polymer Testing* 66: 303–311.
- [13] Asim, M., Jawaid, M., Abdan, K. & Ishak, M. R. 2016. Effect of alkali and silane treatments on mechanical and fibre-matrix bond strength of kenaf and pineapple leaf fibres. *Journal of Bionic Engineering* 13(3): 426–435.
- [14] Omenna, E. & Oduwaye, O. 2017. Effect of variation in urea concentration used in retting, on the chemical and mechanical properties of kenaf fibres. *Journal of Experimental Agriculture International* 16(4): 1–11.

## **INFLUENCE OF AMMONIUM POLYPHOSPHATE (APP) AND SODIUM HYDROXIDE (NaOH) SURFACE TREATMENTS ON KENAF FIBRES THERMAL PROPERTIES**

W. N. W. Jusoh<sup>1</sup>, S.A.S. Abdullah<sup>2</sup>, A. H. A. Hamzah<sup>2</sup>, R. Z. Abidin<sup>2</sup>, T. T. Harun<sup>2</sup>, Nurafiqah N.K.<sup>2</sup>, Z. Sahwee<sup>3</sup>, S. Ahmad<sup>3</sup>, N. L. M. Kamal<sup>3</sup>, S. A. Hamid<sup>3</sup>, N. Norhashim<sup>3</sup>

<sup>1</sup>Universiti Kuala Lumpur, Malaysian Institute of Aviation Technology, Jalan Jenderam Hulu, Dengkil, Selangor, Malaysia.

<sup>2</sup>Aerospace Section, Universiti Kuala Lumpur, Malaysian Institute of Aviation Technology, Jalan Jenderam Hulu, 43900 Dengkil, Selangor, Malaysia

<sup>3</sup>Avionic Section, Universiti Kuala Lumpur, Malaysian Institute of Aviation Technology, Jalan Jenderam Hulu, 43900 Dengkil, Selangor, Malaysia

---

### **ABSTRACT**

Kenaf fibres have the potential to become reinforcements in the various bio-composite application. This paper aims to examine the influence of Ammonium Polyphosphate (APP), Sodium Hydroxide 6 % concentration (NaOH 6%), and a mixture of both as surface treatments to improve the thermal resistance of the fibres. The thermal properties of the fibres were analyzed using Thermogravimetric Analysis (TGA). Results from TGA showed that APP treated fibres displayed the highest degradation resistance with the least weight loss of 45 %, compared to other non-treated and treated fibres. Based on these findings, APP treatments work effectively in providing thermal stability in the kenaf fibres. *Keywords:* Tensile, Interfacial Strength, Bonding,

*Keywords:* kenaf fibres, natural fibres, flammability, sodium hydroxide, ammonium polyphosphate

---

### **INTRODUCTION**

The Malaysian government has strategized a plan to develop kenaf as a substitute crop for tobacco in accordance with the World Health Organization (WHO) Framework Convention on Tobacco Control (FCTC) Article 17, which supports an alternative source of a sustainable economy to tobacco farming labourers and growers. It was reported that the global market for kenaf is expected to expand to US\$342.2 billion by 2025 as the replacement for plastic and polystyrene, which will directly contribute to the development of the eco-fibres based industry [1-2]. Kenaf is natural fibres classified as bast fibres, being collected from the bast surrounding the stem [3]. Natural fibres are made up of celluloses, hemicellulose, lignin, wax, and pectin which are highly flammable and susceptible to thermal disintegration when exposed to fire or high-intensity heat sources [4].

In this study, APP was being used as the fire retardant additive and surface treatment to the fibres. Sodium Hydroxide (NaOH), a alkaline treatment also reduces the moisture absorption of the fibres by decreasing the number of hemicelluloses to almost half and a 9-12 % reduction of lignin content [5-6]. This study was conducted to determine the effect of pre-treatments using APP, NaOH with 6 % concentration and a combination of NaOH/APP on untreated kenaf fibres' to analyse the thermal properties by observing the weight decomposition upon heating.

### **MATERIALS AND METHODS**

#### *Fibres Preparation*

The kenaf fibres are acquired from Dynamic Agrofarm Sdn. Bhd. is an enzyme retting extraction grade, harvested four months before the experiment was conducted. The surface treatment process of fibres involved soaking the fibres in three different pre-treatment solutions, which are 6% NaOH, APP and a mixture of both. The samples and the corresponding pre-treatment solutions are tabulated as indicated in TABLE 1. Analytical grade NaOH pellets from Merck Malaysia were diluted with distilled water to prepare the 6% NaOH solution using a magnetic stirrer. Kenaf fibres weighing 200 g were soaked into the solution for 1 hour. The fibres were then washed under running water until a neutral pH is achieved to ensure complete removal of the NaOH solution. The washed fibres were then placed in a dry oven at 50 °C for 24 hours to remove excess moisture.

---

#### *Article history:*

Received: 10 March 2022

Accepted: 7 June 2022

Published: 14 June 2022

---

#### *E-mail addresses:*

wannursheila@unikl.edu.my (W. N. W. Jusoh)

\*Corresponding Author

TABLE 1. Pre-treatment solutions

Sample	Pre-Treatment Solutions
Sample 1	Untreated fibres (No pre-treatment)
Sample 2	NaOH 6%
Sample 3	APP
Sample 4	NaOH/APP

To develop the fibres' fire retardancy properties, APP flame-retardant liquid from Environgraf, United Kingdom was used. The APP acts by reducing the access to oxygen and produces char to halt the propagation of fire [8]. Similar to the previous process, the fibres were soaked in APP for 1 hour and then placed in a drying oven at 50 °C for 24 hours. For the next sample of NaOH/APP, the kenaf fibres were treated with 6 % NaOH for 1 hour and then were further soaked with APP for another hour. After all treatments were completed, the treated fibres were then stored in an airtight plastic bag to prevent any contamination and oxidation of the fibres before tests and experiments took place.

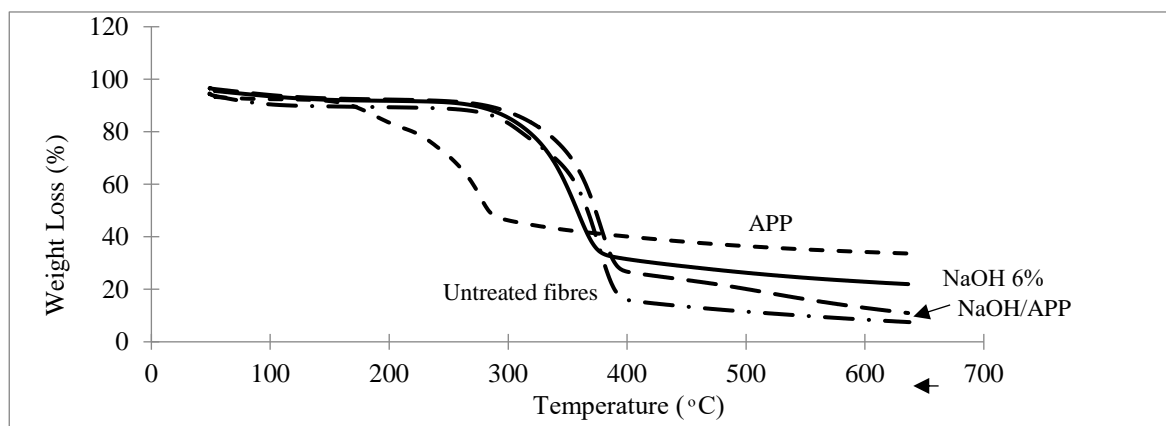
*Thermogravimetric Analysis (TGA)*

Thermogravimetric analysis (TGA) has been proven as one of the most reliable and fast methods to find the thermal stability of materials [9-10]. The TGA was conducted using Perkin Elmer Model 8000 machine where the specimen weight changes were measured as the temperature increased [11-12]. The test was conducted in a controlled nitrogen gas atmosphere at 20 ml/min with a heating rate of 10 °C/min.

**RESULT AND DISCUSSION**

*TGA Results*

The thermal stability of the samples was investigated by observing the weight loss percentage with increasing of the temperature (Fig. 1). The initial pyrolysis process was approximately occurred at around 100 °C for all samples due to evaporation and removal of moisture. For the current study, the TGA test was conducted until the maximum temperature of



650 °C.

Fig. 1: TGA profiles of the samples under the heating rate of 10 °C/min.

The sample treated with APP started to lose weight earlier than the other samples. It showed a comparatively stable condition until the temperature hits approximately 150 °C. The sample continues to degrade significantly and lost about 45% of its weight before constantly degrading until the temperature reaches 650 °C. The untreated kenaf, NaOH 6% and NaOH/APP showed similar pyrolysis profiles where no prominent weight reduction was observed until 300 °C, before starting to drop up to 60 % weight loss. At around 380 °C to 600 °C, NaOH 6% and the untreated sample became stabilised with the final residue of 22.9 % and 8.5 % respectively. As reported by Yang et al 2007, at around 400 °C, most of the cellulose had been degraded and the residuals were quite small about 6.5 % [13]. As for the NaOH/APP sample, it started to become thermally unstable once the temperature reached 290 °C and lost around 90 % of its total weight. Initial thermal stability is characterised by comparing the temperature at 15 % weight loss, referred to as T<sub>15%</sub>. The T<sub>15%</sub> for untreated kenaf is 292.8 °C as compared to 301.3 °C for kenaf treated with NaOH 6 %, while APP decomposed earlier at 192.8 °C. The sample of NaOH/APP showed the highest T<sub>15%</sub> temperature, which is 313.3 °C. This indicates that NaOH/APP possess the highest thermal stability T<sub>15%</sub> compared to other samples due to the removal of biopolymers (hemicellulose and lignin).

**CONCLUSION**

Based on the result, APP treatments give a positive influence on the kenaf fiber weight decomposition. It is found, more char residues found in APP samples compared to other surface treatments. The combination of NaOH and APP also effectively delayed the pyrolysis reaction until around 300°C.

**REFERENCE**

- [1] Bernama (2019, December 4). *Growing demand for Kenaf*. Retrieved from <https://www.bernama.com/en/news.php?id=1796068>.
- [2] Mohd Hadi Alber Basri, Arifin Abdu, Nasima Junejo, Hazandy Abdul Hamid & Khalil Ahmed (2014). *Journey of kenaf in Malaysia: A Review*. Academic Journals 9(11) 458-470. <https://doi.org/10.5897/SRE12.471>
- [3] Ouarhim Wafa, Zari Nadia, Bouhfid Rachid, E. K. Q. A. (2019). *Mechanical Performance of Natural Fibres-based Thermosetting Composites*. In Mechanical and Physical Testing of Biocomposites, Fibres-reinforced Composites and Hybrid Composites. Woodhead Publishing, 43 – 60. <https://doi.org/10.1177/0731684414559864>
- [4] Lee, C. H., Salit, M. S., & Hassan, M. R. (2014). *A Review of the Flammability Factors of Kenaf and Allied Fibres Reinforced Polymer Composites*, Advances in Material Science and Engineering, Vol 2014, 8 pages. <https://doi.org/10.1155/2014/514036>
- [5] Shukor, F., Hassan, A., Islam, S., Mokhtar, M., & Hasan, M. (2013). *Effect of Ammonium Polyphosphate on Flame Retardancy, Thermal Stability and Mechanical Properties of Alkali Treated Kenaf Fibres Filled PLA Biocomposites*. Journal of Material & Design, 54, 425-429. <https://doi.org/10.1016/j.matdes.2013.07.095>
- [6] Hanieh Kargarzadeh, Ishak Ahmad, Ibrahim Abdullah, Alain Dufresne, Siti Yasmine Zainudin and Rasha M. Sheltami (2012). *Effects of hydrolysis conditions on the morphology, crystallinity, and thermal stability of cellulose nanocrystals extracted from kenaf bast fibres*. Cellulose 19, 855-866. <https://doi.org/10.1007/s10570-012-9684-6>
- [7] Azwa, Z. N., Yousif, B. F., Manalo, A. C., & Karunasena, W. (2013). *A review on the degradability of polymeric composites based on natural fibres*. Materials and Design, 47, 424–442. <https://doi.org/10.1016/j.matdes.2012.11.025>
- [8] Koncar, V. (2019). *Smart textiles for monitoring and measurement applications*. The Textile Institute Book Series, pp 1-151. <https://doi.org/10.1016/B978-0-08-102308-2.00001-2>
- [9] Gupta, R., Kumar, V., Goyal, P. K., & Kumar, S. (2010). *Thermogravimetric Analysis of Heat Treated CR-39 Polymer*. Journal of Chemical and Pharmaceutical Research, 2(4), 629–634.
- [10] Ebnesajjad, S. (2014). *Chapter 4- Surface and Material Characterization Techniques*. Surface Treatment of Materials for Adhesive Bonding (Second Edition). 39-75. <https://doi.org/10.1016/B978-0-323-26435-8.00004-6>
- [11] N. Amir, F. A. and P. S. M. M.-Y. (2011). *Study on the Fibres Reinforced Epoxy-based Intumescent Coating Formulations and their Char Characteristics*. Journal of Applied Sciences. <http://doi.org/10.3923/jas.2011.1678.1687>
- [12] Yang, H., Yan, R., Chen, H., Lee, D. H., & Zheng, C. (2007). *Characteristics of hemicellulose, cellulose and lignin pyrolysis*. Fuel, 86, 1781–1788. <https://doi.org/10.1016/j.fuel.2006.12.013>

## **EFFECT OF WOVEN FABRIC GEOMETRICAL PARAMETERS ON THE PERMEABILITY BEHAVIOUR OF WOVEN FLAX FABRICS**

W. M. I. W. Zaludin<sup>1</sup>, N. Z. M. Zuhudi<sup>1\*</sup>, K. D. M. Aris<sup>1</sup>

<sup>1</sup>*Aero Composite Cluster, Universiti Kuala Lumpur Malaysian Institute of Aviation Technology (UNIKL MIAT), Lot 2891, Jalan Jenderam Hulu, 43800 Dengkil, Selangor, Malaysia.*

---

### **ABSTRACT**

In the fabrication process of composite materials, there are various factors that could affect its permeability behavior. Permeability behavior can be defined as the ability of fluid to flow through a porous medium during fabrication process. It is one of the important factors in order to ensure better and optimized composite materials manufactured. This study investigates the effect of woven fabric geometrical parameters on the permeability behavior of woven fabric reinforced composite. In studying the effects of woven fabric geometrical parameters, flax fabric was used for geometrical image analysis. Then the composite models were designed using TexGen software to identify the permeability behavior with different yarn width and yarn spacing respectively. These models were then simulated using Ansys CFX in the flow analysis to determine the permeability values. In the image analysis, most of the average values of the measurements were observed to be consistent throughout the areas of measurement. It was found that the geometrical parameters did affect the permeability behavior.

*Keywords:* permeability behavior, modeling approach, woven fabric, image analysis, flow analysis.

---

### **INTRODUCTION**

Permeability behavior is defined as measurement of fluid flow through a porous medium in composite materials. Most of the permeability studies by various researchers were carried out using the conventional physical experiment. However, with the introduction of modeling approach of permeability prediction, the workload and time consumption could be cut significantly while producing reliable results [1]. This method allows researchers to explore various parameters and variables that could affect permeability behavior of composite materials during fabrication process.

There are several researches the studies factors that affecting permeability behavior of composites materials during fabrication process. As an example, fabric geometrical factors are one of the common variables being investigated. The variance of fabric geometrical factors such as yarn width [2], yarn diameter [2], fiber volume fraction [3], and fabric shear angle [4] are some of the examples of parameters that could affect permeability behavior of fabricated composite. However, it is found out that previous research regarding the effect of fabric geometrical factors toward permeability behavior are quite outdated and it is hardly found any recent researches within this scope.

This paper aim is to get an outline as a preliminary work in order to study the effect of woven fabric geometrical parameters toward permeability behavior. This paper studied the effect of yarn width, yarn spacing, and fabric thickness toward the permeability behavior during composite fabrication process. A sample of dry flax fabric was used for geometrical image analysis in order to measure the yarn widths, yarn spacing, and yarn thicknesses. The image analysis was performed with the aid of optical microscope. The findings from image analysis were then used to identify permeability behavior of the fabric, in which the flow analysis was conducted in the determination of the permeability values.

### **MATERIALS AND METHODS**

#### *Materials*

A 2×2 twill weave flax fabric from EcoTechnilin was used throughout this study. The fabric has 1.27 g/cm<sup>3</sup> fibre density with the average thickness of 0.225 mm. The fabric is cut into 30 cm × 30 cm for geometrical textile image analysis. A Dinolite Premier AM4113 Digital Microscope, with the scope range of 20× - 200×, from Dpro Vision was used for the geometrical measurement.

---

#### *Article history:*

Received: 10 March 2022

Accepted: 7 June 2022

Published: 14 June 2022

---

#### *E-mail addresses:*

izzat.zaludin06@s.unikl.edu.my (W.M.I Zaludin)

zuhairah@unikl.edu.my\* (N.Z.M. Zuhudi)

kdahri@unikl.edu.my (K.D.M. Aris)

\*Corresponding Author

#### *Methods*

There were three main stages conducted during this investigation. The first one was geometrical image analysis, where flax fabrics were measured at ten different sections by using digital microscope as shown in Fig. 1. The second stage was the geometrical modeling design stage using TexGen software by using the obtained values and measurement from geometrical image analysis in the earlier stage. Then, the flow analysis was conducted to simulate the permeability value of the models using Ansys CFX Version 19.1.



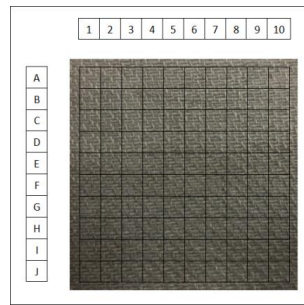


Fig. 2: The sections for geometrical image analysis on woven flax fabric

## RESULTS AND DISCUSSION

### Geometrical image analysis of yarn width

The fabric thickness was kept as a constant at value of 0.300 mm for the whole fabric. Yarn width was measured and the data was recorded as shown in TABLE 1. It was found that the measured average yarn widths were slightly different in warp and weft direction. The measurement of yarn widths in weft direction was slightly less compared to the warp direction. Besides that, the measured yarn width in weft direction for all of the sections had slight variations, while the measured yarn width in warp direction had much more consistent values.

### Geometrical image analysis of yarn spacing

The measurements of yarn spacing were also performed at all of the sections. The measured yarn spacing was divided into two groups which were in warp and weft direction between the yarns. Yarn spacing was measured as shown in and the data recorded are presented in TABLE 2. Interestingly, the average measured yarn spacing for the fabric at all sections were irregular. When been compared between both directions for the yarn spacing measurement, it can be concluded that the average value of yarn spacing in warp direction were observed to be consistent. This is probably due to the improper fabric handling that causing the fabric to shift and stretched out during fabrication process.

### Geometrical image analysis of fabric thickness

Fabric thickness of the fabric was measured at all of the sections of fabric as shown in Fig. 1. To increase the accuracy of the findings, the fabric thicknesses were measured three times at each of the sections. The results were conveyed in TABLE 3. It can be concluded that the fabric thickness were consistent throughout all of the sections, indicating that the fabric were having consistent yarn thickness. If there is any external pressure applied, the measured thickness may be varied and these could affect permeability behavior of the composite. This could become an interesting topic to be discussed for future investigation.

TABLE 2: The average yarn width measurement in weft and warp direction

Scope Position	A	B	C	D	E	F	G	H	I	J
Average Yarn Width (Weft), mm	0.358 ± 0.06	0.371 ± 0.04	0.397 ± 0.06	0.327 ± 0.06	0.376 ± 0.04	0.415 ± 0.07	0.395 ± 0.08	0.439 ± 0.08	0.351 ± 0.05	0.411 ± 0.11
Average Yarn Width (Warp), mm	0.448 ± 0.08	0.410 ± 0.08	0.443 ± 0.06	0.471 ± 0.09	0.411 ± 0.10	0.462 ± 0.09	0.441 ± 0.08	0.443 ± 0.08	0.434 ± 0.09	0.444 ± 0.08

TABLE 3: The average yarn spacing measurement in weft and warp direction

Scope Position	A	B	C	D	E	F	G	H	I	J
Average Yarn Spacing (Weft), mm	0.503 ± 0.07	0.460 ± 0.04	0.495 ± 0.09	0.527 ± 0.05	0.510 ± 0.08	0.525 ± 0.09	0.569 ± 0.11	0.537 ± 0.07	0.510 ± 0.07	0.520 ± 0.10
Average Yarn Spacing (Warp), mm	0.606 ± 0.06	0.638 ± 0.05	0.686 ± 0.12	0.648 ± 0.08	0.720 ± 0.13	0.625 ± 0.15	0.691 ± 0.08	0.631 ± 0.09	0.660 ± 0.08	0.651 ± 0.09

TABLE 4: The average yarn thickness measurement

Measurement	1	2	3
Average Thickness, mm	0.556 ± 0.05	0.553 ± 0.03	0.559 ± 0.04

### Permeability

It was found that the permeability value of the models increases as the yarn spacing increases. This may be due to the large gaps and voids presences as the yarn spacing increases, thus affecting the permeability value. Meanwhile, for the models with different yarn width, permeability value slightly decreases as the yarn width increases. However, all of the models were considerably large in values when compared to previous researches and this require further investigation in order to achieve the valid values for permeability studies [5]. These values will be further studied in the future research of the flow analysis, as this study focused on the determination of the effects of the geometrical and identify the patterns with regards to the yarn width, thickness and yarn spacing.

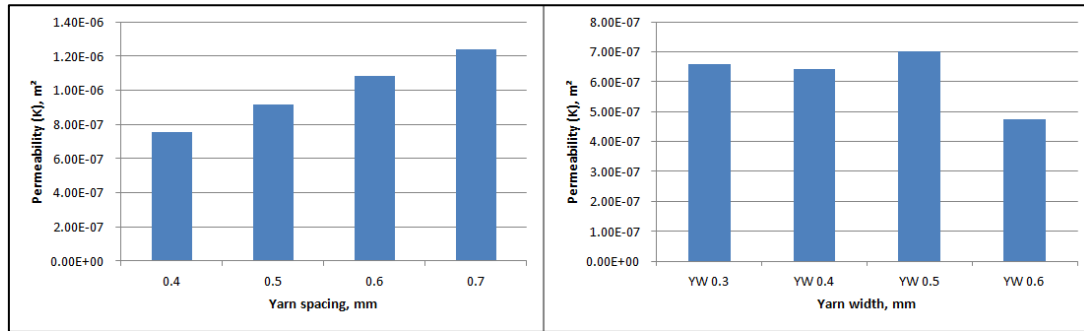


Fig. 3: The permeability values of models; models with different yarn spacing (left), models with different yarn width (right)

## CONCLUSION

The effect of geometrical parameters was observed in the study with regard to the permeability behavior of woven fabric. The experimental fabric image analysis and in-plane permeability modeling setups for this investigation were designed and compared. The fabric image analysis was conducted in order to get the average dimension of the fabric yarns. The effect of different yarn spacing toward permeability behavior of woven fabric composite was investigated by using modeling approach. The measured yarn widths were concluded for the use in the flow analysis. However, for yarn spacing measurements, the values in warp were almost constant at all sections compared to the values in weft direction. The effect of different yarn spacing and yarn width toward permeability behavior of woven fabric composite was successfully investigated by using the flow analysis approach.

## REFERENCE

- [1] Z. M. Huang, S. Y. Lee, H. M. Kim, J. R. Youn, and Y. S. Song, "Permeability analysis of non-crimp fabrics for resin transfer molding," *Polym. Polym. Compos.*, vol. 27, no. 7, pp. 429–439, 2019.
- [2] R. Umer, S. Bickerton, and A. Fernyhough, "The effect of yarn length and diameter on permeability and compaction response of flax fibre mats," *Compos. Part A Appl. Sci. Manuf.*, vol. 42, no. 7, pp. 723–732, 2011.
- [3] X. Zeng, L. P. Brown, A. Endruweit, M. Matveev, and A. C. Long, "Geometrical modelling of 3D woven reinforcements for polymer composites: Prediction of fabric permeability and composite mechanical properties," *Compos. Part A Appl. Sci. Manuf.*, vol. 56, pp. 150–160, 2014.
- [4] S. Aranda, D. C. Berg, M. Dickert, M. Drechsel, and G. Ziegmann, "Influence of shear on the permeability tensor and compaction behaviour of a non-crimp fabric," *Compos. Part B Eng.*, vol. 65, pp. 158–163, 2014.
- [5] E. E. Swery, R. Meier, S. V. Lomov, K. Drechsler, and P. Kelly, "Predicting permeability based on flow simulations and textile modelling techniques: Comparison with experimental values and verification of FlowTex solver using Ansys CFX," *J. Compos. Mater.*, vol. 50, no. 5, pp. 601–615, 2016.

## CONVERGENCE OF FINITE ELEMENT MODEL FOR TRANSIENT THERMAL SIMULATION OF COMPOSITE LAMINATE

E. E. S. M. Noor<sup>1,2\*</sup>, N. Z. M. Zuhudi<sup>1,2</sup>, A. N. A. Yahaya<sup>3</sup>, M. Zukifli<sup>3</sup>

<sup>1</sup>*Aero Composite Cluster, Universiti Kuala Lumpur Malaysian Institute of Aviation Technology (UNIKL MIAT), Lot 2891, Jalan Jenderam Hulu, 43800 Dengkil, Selangor, Malaysia.*

<sup>2</sup>*Universiti Kuala Lumpur Malaysian Institute of Chemical and Bioengineering Technology (UNIKL MICET), 78000 Alor Gajah, Melaka, Malaysia.*

<sup>3</sup>*Green Chemistry and Sustainable Cluster, Universiti Kuala Lumpur Malaysian Institute of Chemical and Bioengineering Technology, (UNIKL MICET), 78000, Alor Gajah, Melaka, Malaysia.*

---

### ABSTRACT

The main principle behind Finite Element Method (FEM) is to divide the body sample into elements. To produce trustworthy results with FEM, a suitable mesh form and size must be employed. Since the mesh size has a great influence towards to number of element and nodes, this paper discussed the transient thermal analysis result for curing process of carbon fiber using different mesh sizes specifically to study on the result of temperature and total heat flux. During the modelling of the simulation, different sizes of mesh were selected based on previous literatures. As for the material, a Hexcel AS4-8552 composite laminate was used for the simulation process. The overall process of the simulation was carried out using Ansys Workbench R2 2020. The results were further utilized to explore an optimum mesh size to be applied in the next phase of the study.

*Keywords:* Finite Element Method (FEM), transient, thermal simulation, composite, laminate

---

### INTRODUCTION

Finite element method (FEM) is a computer simulation approach for handling engineering issues such as stress analysis, heat transfer etc [1]. The idea behind FEM is to divide the body into finite elements to obtain an approximate solution [2]. TMesh convergence establishes the number of elements that are necessary in a model to ensure that the size of the mesh is appropriate for a study. At the same time, transient thermal analysis is an analysis of how a system respond under a fixed or varying conditions over time. The combination of FEM in thermal analysis has provided a bigger room for studies to be conducted. For example, Nithesh *et al.*, [4] carried out an investigation of mesh convergence test for two-dimensional disk rim of high-pressure turbine. Therefore, this paper presents the influence of the mesh sizes towards the result produced via a transient thermal analysis, mainly on the heat flux and temperature distribution using Ansys Workbench R2 2020 for all the simulation process.

### MATERIALS AND METHODS

#### *Pre-processing*

Hexcel AS4-8552 is a unidirectional prepreg with a strong epoxy and it is commonly utilised in aircraft constructions [5]. This material was selected to be used for this study. In the present research, the presented solid model was a square shaped plate with a dimension of 200 mm x 200 mm and a thickness of 1.6 mm. Quadrilateral dominant shape was used for the meshing and the mesh sizes that will be carried out in this study consisting of four different sizes starting from 10 mm, 15 mm, 20 mm, and finally 25 mm. The different mesh sizes can be observed from Fig. 1.

---

#### *Article history:*

Received: 10 March 2022

Accepted: 7 June 2022

Published: 14 June 2022

---

#### *E-mail addresses:*

ezriq.mohd19@s.unikl.edu.my (E. E. S. M. Noor)

zuhairah@unikl.edu.my\* (N.Z.M. Zuhudi)

kdahri@unikl.edu.my (A. N. A. Yahaya)

muzafar@unikl.edu.my (M. Zukifli)

\*Corresponding Author

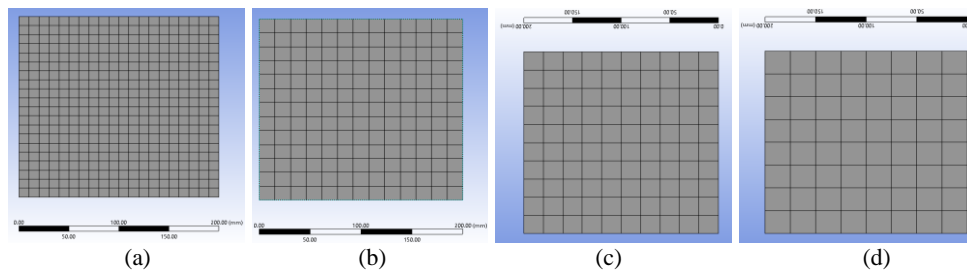


Fig. 1: Mesh sizes of (a) 10 mm, (b) 15 mm, (c) 20 mm, (d) 25 mm, respectively

The size of mesh plays a big role in displaying the accuracy of the result which will be validated later [3]. In the present paper, density of 15080 kg/m<sup>3</sup> and specific heat of 1300 J kg<sup>-1</sup> C<sup>-1</sup> of Hexcel AS4-8552 were introduced. The mechanical properties of the Hexcel AS4 material provided by the manufacturer are mentioned in TABLE 1.

TABLE 1: Material properties of Hexcel AS4-8552 [6]

Material Property		Value
i. X-Direction	<b>Coefficient of Thermal Expansion</b>	$1 \times 10^{-20}/^{\circ}\text{C}$
ii. Y/Z-Direction		
i. X-Direction	<b>Young's Modulus</b>	135 GPa
ii. Y/Z-Direction		
i. X-Direction	<b>Orthotropic Thermal Conductivity</b>	5.5 W/(m°C)
ii. Y-Direction		
iii. Z-Direction		

The mesh sizes are ranging from four different sizes which are 25 mm, 20 mm, 15 mm, and 10 mm. Since the number of elements and nodes are different in accordance with the size of mesh, TABLE 2 summarizes the value of elements and nodes for each mesh size chosen for this study.

TABLE 2: Mesh sizes

Element Size	Nodes	Elements
25 mm	81	64
20 mm	121	100
15 mm	196	169
10 mm	441	400

The fabric was set to be 0.0002mm thick. Six plies of this fabric were stacked with a layup of 4 plies layup of layup of (0/45/90/0/45/90) making the total thickness of 1.6 mm [7].

### Processing

The curing process in the present work uses a double-hold cure cycle in which the temperature rose from 22 °C to 120 °C and was maintained for 1800 seconds in the first hold. Then, it rose to 180 °C with a dwell of 1800 seconds for the second hold and in the last step, it cooled down to the normal temperature [8]. The ambient temperature for this scenario was set at 22°C. Convection condition was given to a composite plate as a thermal input load. Hence, heat convection was applied on all of the surfaces of the model except the bottom part since there is no heat applied at the bottom part. A convection coefficient of 25 W/mm<sup>2</sup> was applied. To simulate the curing process by hot bonded, the bottom surface of the model was exposed to heat flux with a magnitude of 1000 W/mm<sup>2</sup>. A total time of 10800 seconds was introduced, and it was divided into three-time steps. The first-time step in the beginning of the heating starting from 0 second until 3600 second. The second-time step starts from the 3600 seconds until 7200 seconds. Finally, the third-time step is the cooling phase starting at 7200 seconds until it reaches ambient temperature.

### Post-processing

The goal for the present study is to find out how the does the mesh size along with the number of node and element affect the result particularly on the temperature distribution and total heat flux produced during a curing process of composite laminate via transient thermal analysis. In the paper, four different mesh sizes were selected prior to carry out the simulation using a 200 x 200 mm composite laminate. During the analysis, a convection condition was introduced simulating the curing process of carbon fiber. The results obtained consisting of eight different outputs. Then, the outputs were transferred into a graph for it to be analysed. The results obtained are important as it will assist in the next stage of the author's work with regards to the study of heat transfer analysis for the aircraft bonded assemble structure repair.

## RESULTS AND DISCUSSION

An optimization stage of the simulation works is critical for aerodynamic shape optimization. It also gives a significant effect on the simulation responses as reported by R. Secco *et al.*, [9]. In the present paper, the effects of the mesh size, node and element numbers were investigated with regards to the temperature distribution and heat flux in the transient thermal analysis.

The optimization work was conducted as it influences the results in the next stage of the author's work with regards to the study of heat transfer analysis for the aircraft bonded assemble structure repair. This is mainly related for example, with the use of the hot bonder as the curing tools in the aircraft structure repair process, in ensuring a uniform distribution of heat flux and good quality of repair.

*The effect of mesh size on temperature distributions*

The simulation for all different mesh sizes were simulated using the same composite laminate. Fig. 3 shows that the mesh with bigger size indicates slightly higher temperature at the beginning of the process which is between 1800 second to 1900 second. While the mesh with smaller size shows slightly lower in temperature at the same period. However, when there is a slight temperature increase at the plateau stage, the smaller mesh size to first shows increments in temperature compared to other mesh sizes while the bigger mesh size increase in temperature about 200 seconds later than the smallest mesh size. This trend is slightly similar with a study conducted by Cano-Pleite *et al.*, [10] few mesh sizes were introduced in the numerical simulations and it was discovered that by increasing the mesh size used in the solid components which is 0.75 mm was sufficiently fine to reach mesh independent results.

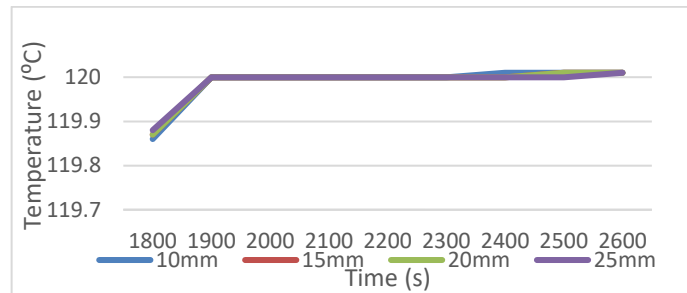


Fig. 3: Temperature difference for different mesh sizes

*The effects of mesh size on the heat flux*

Fig. 4 shows the result of the total heat flux produced by four different mesh sizes ranging from 10 mm to 25 mm. As the result, the most obvious difference can be observed during the 1800 second where the bigger the mesh size i.e. 25 mm, the lower the heat flux produced compared to the other mesh size. However, after a few seconds later, there is a huge dipping heading towards 0 W/mm<sup>2</sup> then it started to gradually increase by time. The increment for all of the mesh sizes is almost the same and there is no significance difference between those sizes. The importance of selection mesh selection for the study of heat flux was simulated by Zhang *et al.*, [11]. In their study, a significantly smaller mesh size was applied in order to achieve a higher spatial resolution which was essential for analysing the heat flux distribution via Computational Fluid Dynamics (CFD) simulation.

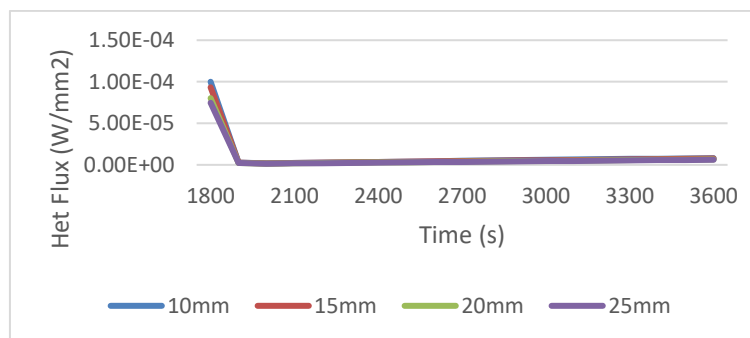


Fig. 4: Heat flux difference for different mesh sizes

**CONCLUSIONS**

In conclusion, it is critical for researchers to determine the correct mesh size in order to perform thermal analysis via finite element method. Most of this study was performed to determine the best mesh size together with the number of elements and nodes for finite element analysis via transient thermal analysis. However, this only applicable to a flat composite structure. For a more complex composite structure, it is a must to carry out the mesh selection process before proceeding with the analysis work. It is recommended for future work to perform mesh selection process on different aircraft composite structures as it might help in the future research of aircraft composite repair works.

**REFERENCES**

[1] K. Srinivas, "Verifications and Validations in Finite Element Analysis (FEA)," 2020, [Online]. Available: <http://www.advanses.com>.  
[2] J. N. Reddy, *Introduction to the finite element method*. McGraw-Hill Education, 2019.  
[3] H. Patil and P. V. Jeyakarthykeyan, "Mesh convergence study and estimation of discretization error of hub in clutch disc with integration of ANSYS," *IOP Conf. Ser. Mater. Sci. Eng.*, vol. 402, no. 1, 2018, doi: 10.1088/1757-899X/402/1/012065.

- [4] I. Publication, "ELEMENT METHOD ON HIGH PRESSURE GAS TURBINE DISK RIM USING ENERGY NORM :"
- [5] S. R. Karnati, "A mixed-mode (I-II) fracture criterion for AS4/8552 carbon/epoxy composite laminate." North Carolina Agricultural and Technical State University, 2014.
- [6] Hexcel Composites, "Product data HexPly 8552," *Hexcel*, vol. 1, no. 1, pp. 1–6, 2000, [Online]. Available: [http://www.hexcel.com/Resources/DataSheets/Prepreg-Data-Sheets/8552\\_us.pdf](http://www.hexcel.com/Resources/DataSheets/Prepreg-Data-Sheets/8552_us.pdf).
- [7] C. Bellini, L. Sorrentino, W. Polini, and A. Corrado, "Spring-in analysis of CFRP thin laminates: numerical and experimental results," *Compos. Struct.*, vol. 173, pp. 17–24, 2017, doi: 10.1016/j.compstruct.2017.03.105.
- [8] N. Kumbhare, R. Moheimani, and H. Dalir, "Analysis of composite structures in curing process for shape deformations and shear stress: Basis for advanced optimization," *J. Compos. Sci.*, vol. 5, no. 2, 2021, doi: 10.3390/jcs5020063.
- [9] N. R. Secco, G. K. W. Kenway, P. He, C. Mader, and J. R. R. A. Martins, "Efficient mesh generation and deformation for aerodynamic shape optimization," *AIAA J.*, vol. 59, no. 4, pp. 1151–1168, 2021, doi: 10.2514/1.J059491.
- [10] E. Cano-Pleite, M. Fernández-Torrijos, D. Santana, and A. Acosta-Iborra, "Heat generation depth and temperature distribution in solar receiver tubes subjected to induction," *Appl. Therm. Eng.*, vol. 204, 2022, doi: 10.1016/j.applthermaleng.2021.117902.
- [11] S. Zhang *et al.*, "Numerical analysis and analytical modeling of the spatial distribution of heat flux during friction stir welding," *J. Manuf. Process.*, vol. 33, no. May, pp. 245–255, 2018, doi: 10.1016/j.jmapro.2018.05.021.

## RECYCLING OF THE BAMBOO FIBRE COMPOSITES AND THEIR HYBRIDS

N.Z.M. Zuhudi<sup>1\*</sup>, K. Jayaraman<sup>2</sup>, R. J. T. Lin<sup>2</sup>

<sup>1</sup>*Aerocomposite Cluster, Universiti Kuala Lumpur Malaysian Institute of Aviation Technology, 43800 Dengkil, Selangor, Malaysia*

<sup>2</sup>*Center for Advanced Composite Materials, Department of Mechanical Engineering, The University of Auckland, New Zealand*

---

### ABSTRACT

The demand for composites is experiencing rapid growth in both synthetics and natural fibre-based materials. As this trend increases, it is clear that the waste management will become a crucial issue in various industries. The difficulty recycling challenge is due to their heterogeneity properties. In this study, the composite performances after recycling were investigated using the mechanical recycling as reprocessing method. Mechanical recycling provides an effective method where the original materials are broken down into granules, which then can be use as raw material for moulding process. The produced recyclates are aimed as the moulding or compounding materials as the reuse applications. The introduction of the bamboo fibres in the hybrid composites system is desirable to increase the usage of natural fibres for environmental reason. The aim of this study is also to evaluate the potential of the bamboo-glass hybrid composite recyclates as the second reuse materials, in which the decrease observed in their properties after recycling can be compensated for by the hybridisation with the presence of glass fibres.

*Keywords:* recycling, reuse, bamboo fibres, hybrids.

---

### INTRODUCTION

Many different recycling techniques have been studied for the last decade focusing on these three main methods as reported by Oliveux et al [1], which involves mainly on the mechanical process by grinding, pyrolysis and solvolysis. PP based composites have been given special attention among polymer composites because of their recyclability [2]. Although PP cannot be categorised as a biodegradable polymer, it has been used widely in various applications in green composites. Many investigations have been performed on the potential recyclability of PP based NFRCs. Many authors have reported a deteriorating trend in mechanical properties after recycling compared to the original polymers [3]. In Europe, the waste materials generated by glass fibre reinforced polymer (GFRP) are usually sent to landfills due to the difficulty in recycling them [4]. Glass fibres are widely used in composites both in thermoset or thermoplastic matrices. Although a lot of studies have been carried out on the bamboo-PP composites [5], [6], very little research has been done with the recycling of bamboo-glass hybrid composites. It is desirable to re-use the materials after recycling. Mechanical recycling provides an effective method where the original material is broken down into granules, which then can be used as raw material for moulding purposes. The aim was to evaluate the functional properties of the composites in terms of their recyclability. The decrease in their properties can be compensated for by the hybridisation with the presence of glass fibres. This study clearly identifies a potential solution by identifying performance and developing a cost-effective end use-application for the recyclates based on the natural fibres and their hybrids, thus contributing to a more sustainable fibre-reinforced polymer composites.

### MATERIALS AND METHODS

#### *Materials*

The raw materials used to fabricate the BPP composites in this work were polypropylene and woven bamboo fabric. The matrix used was polypropylene (PP) random copolymer, Moplen RP241G, manufactured by Lyondell Basell Industries and supplied by Field International Ltd., Auckland, New Zealand. The PP sheets have a nominal thickness of 0.38 and 0.58 mm. 100% bamboo fabric twill- woven was obtained from Xinchang Textiles Co.Ltd., Guangzhou, China. The bamboo fabrics with a width of 1500 mm and weight of 220 gsm were used, having specification of 20\*20 tex and 108\*58 per square inch for yarn count and density, respectively. The glass pre-preg supplied by Plytron ICI Ltd. UK with nominal glass volume fraction and density of 35% and 1480 kg/m<sup>3</sup>. The nominal thickness and sheet width are 0.47 mm and 240 mm, respectively.

#### *Methods*

The compression moulding process was used in this research to produce composite laminates. The closed mould was heated until the required temperature of 185°C was reached. The ply stack that had been dried earlier was placed in the mould cavity for preheating, and the loaded mould was continuously heated for about five minutes without pressure to allow the polypropylene to start melting and percolating through the fibres. At this point, the consolidation pressure of 0.80 MPa was applied and held steady for five minutes. During this impregnation stage, pressure was applied to force the molten polymer into the fabrics while removing the excess air and volatiles. During the cooling period, the pressure applied was maintained until the temperature of the mould cavity dropped

---

#### *Article history:*

Received: 10 March 2022

Accepted: 7 June 2022

Published: 14 June 2022

#### *E-mail addresses:*

zuhairah@unik.edu.my (N.Z.M. Zuhudi)

kjayaraman@auckland.uni.ac (K. Jayaraman)

rtj.lin@auckland.uni.ac (R.T.J. Lin)

\*Corresponding Author

down to 40°C or lower when the laminate could be removed from the mould. The bamboo polypropylene (BPP) composites and their bamboo-glass polypropylene (BGPP) hybrid composites were fabricated in the range of about 55-65% fibre weight fraction, all in warp direction. The hybrid composites were fabricated with about 30% of bamboo and 20% of glass fibre weight fraction. The composites were investigated in terms of the economics of reprocessing and reuse. A step by step process and the materials produced in the steps are shown in Fig 1. The composite sheets were cut into small pieces and then granulated using an SG granulator model SG-2427H-CE with mesh spacing of 5 mm diameter. Then, the granulated materials were put into a dryer for at least 24 hours, and extruded in a LABTECH (a LHFS1-271822 type) twin screw extruder at 13 rpm. The temperature settings were kept between 180°C and 200°C during the extrusion process of the materials. The material sample was poured into the hopper, where it was continuously mixed by a rotating blade and fed continuously into the extruder. The compounded material then passed through a two port die producing two strands which were passed through a water bath, partially dried by an exhaust and then pelletised. The compounded materials were pelletised using the LABTECH strand pelletizer (a LZ-120 type) and then dried under vacuum at 60°C for 48 hours. Finally, the pellets were injection moulded to produce specimens using a BOY 50A injection moulding machine with a capacity of 50 tonnes. Temperature profile was kept between 175°C and 195°C. The die temperature was kept constant by cooling with water conditioned to 23°C, and the injection pressure was maintained at 100 bar. The specimens were analysed in terms of density, melting and crystallisation temperature. The specimens were tested in tensile, flexure and Charpy impact testing according to ASTM 3039, ASTM 790-10, and ASTM D6110, respectively. For the measurement of the fibre length of the composites after recycling, the fibre was extracted from the composites using the Soxhlet extraction method. An optical microscope was used to obtain images of the extracted fibres. The images captured from the microscopy were then analysed using “Image J” software to provide an estimation of the length and variation in the length of the fibres.

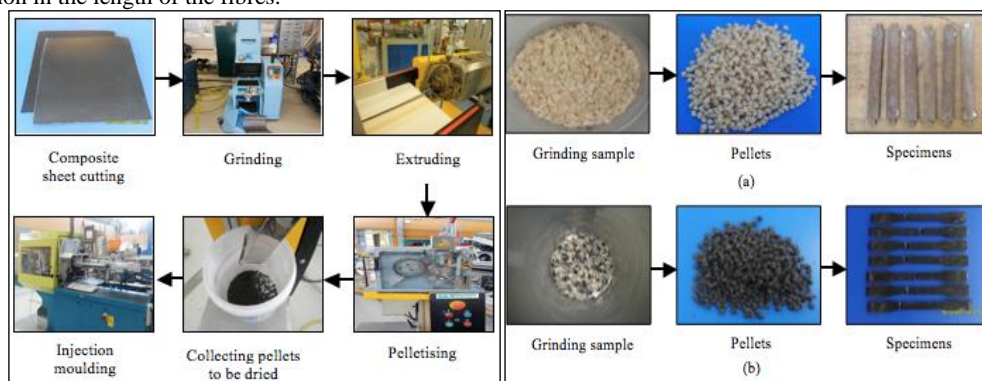


Fig. 1: Recycling process of the composites (left) and the product of each recycling step (right)

## RESULTS AND DISCUSSION

### Mechanical Properties after Recycling

TABLE 1 compares the mechanical properties of PP, the composites and their recycled composites. It is shown that the tensile strength and modulus of the BPP decrease 52% and 25% after recycling. A decrease of 78% in the impact strength of the BPP composites was also observed after recycling. However, no significant reduction was found in the flexural properties of the BPP composites after recycling. The results for the recycled BPP composites were found to be higher than the neat PP in all mechanical properties tested in this study. A decrease was observed in the mechanical properties the hybrid composites after recycling. Tensile strength and modulus of the hybrid composites reduced to 67% and 74% respectively after recycling. A significant decrease occurred in the flexural properties of the recycled hybrid composites, where the strength and modulus decreased by 71% and 58% respectively after recycling. A similar pattern was observed in the impact properties of the recycled hybrid composites. A reduction about 84% compared to the hybrid composites before recycling. The tensile and flexural properties in the recycled hybrid composites were higher than that of the neat PP. Interestingly, a slight reduction was observed in the impact properties of the recycled hybrid composite as compared to the neat PP. The reduction in the mechanical properties of BPP composites after recycling was mainly because of the degradation of bamboo fibres after several recycling stages. The decrease in mechanical properties can be compensated for by the presence of glass fibres which in agreement as reported in the literature [6,7].

TABLE 1: Mechanical properties of PP and the composites

Samples	Tensile strength (MPa)	Tensile modulus (GPa)	Flexural strength (MPa)	Flexural modulus (GPa)	Impact strength(J/m)
PP	21.7 ±0.09	1.0 ±0.04	24.5 ±2.4	1.0 ±0.04	204.1 ±8.2
BPP composites	71 ±1.25	2.1 ±0.01	70 ±0.8	2.7 ±0.03	531 ±94.3
Recycled BPP composite	34 ±1.57	1.6 ±0.02	64.5 ±4.8	2.6 ±0.03	112.5 ±5.2
Hybrid composite	136 ±7.02	6.9 ±0.94	312 ±24.7	11.8 ±1.15	1199 ±86.9
Recycled hybrid composite	45.3 ±7.02	1.8 ±0.17	90.5 ±1.67	4.98 ±0.08	194.5 ±10.6

### Fibres Length Analysis after Recycling

There were 423 bamboo yarns and 132 glass fibres observed in the analysis. The average length of the bamboo yarns is 0.724 mm, with the highest percentage of yarns between 0.5-1.0 mm. There is little difference in the percentages of yarn fragments in the range of 0.1-0.5 mm and 1.0-1.5 mm in length. The percentages of the two ranges of yarn length are 34.3% and 24.1% respectively. There is no difference in the percentages of yarn fragments in the range of 1.5-2.0 mm and 2.0-5.0 mm. The



average of glass fibres length was 0.327 mm with the 77.3% of fibre length in the range of 0.5-1.0 mm. There is a large difference in the fibre length with the range of 0.5-1.0 mm (21.9%) compared to the fibre length with the range of 0.1-0.5 mm. Almost no glass fibre longer than 1 mm. A reduction in the length after recycling was observed because of mechanical recycling processes such as extrusion, pelletizing and injection moulding. The length of fibre was reduced to below 5 mm, which was expected as a screen of 5 mm diameter was used during pelletising. The length was further dropped after extrusion. This decrease in the fibre length was likely due largely to the fibre breakage during the extrusion processes, where high shear stresses were exerted on the fibres during mixing in the extruder. There is a mixture of bamboo yarns and fibres due to separation of the bamboo fabric. For glass fibres, the average fibre length is shorter than that of the average bamboo yarn length. This may be because the bamboo fibres in the staple have been twisted into yarns, making them more difficult to separate than glass fibres. There was a fibre breakage induced by grinding and subsequent processing during recycling.

#### *Thermal Properties after Recycling*

The changes of the melting temperature and crystallinity after recycling of the BPP and hybrid composites are shown in the DSC data in TABLE 2. For the BPP composites, it can be seen that there was no difference in the melting and crystallisation temperatures of the composites after recycling. However, the recycling process did affect the crystallinity of the composite. The crystallinity of the recycled composites was 41% lower than that of the BPP composites. For the hybrid composites, the melting temperature of the hybrid composites was slightly higher than that after recycling. However, the recycling did not influence the crystallisation temperature. The crystallinity of the hybrid composites was 38% lower after recycling. The recycling process did affect the crystallinity of the composite. The decrease in the crystallinity of the recycled composites was observed because of the presence of fibres inhibiting crystallisation around the fibre and making it lose its ability to create nucleation sites for the polymer, which decrease trans-crystallisation.

TABLE 2: DSC results of PP and the composites

Sample	Melting temperature (°C) $T_m$	Crystallisation temperature (°C) $T_c$	Enthalpy of fusion (J/g) $\Delta H$	Crystallinity (%)
PP	149.80	110.49	45.39	21.93
BPP	155.67	112.54	24.97	24.13
BPP recycled	154.47	111.09	14.70	14.20
30B:20G	155.14	111.82	27.35	29.36
30B:20G recycled	158.31	111.20	16.86	18.10

## CONCLUSIONS

The effect of hybridisation on recycled products was examined. A decrease was observed in the mechanical properties of the hybrid composites after recycling. The severity of the drop was reduced by the presence of glass fibres. The changes in the fibre architecture induced this significant reduction in the mechanical properties after recycling. The reduction in the fibre length and degradation in the bamboo fibre and PP due to mechanical recycling also contributed to these reductions in properties. A decrease was also observed in the crystallinity of the recycled composites compared to the original composites. The drop in crystallinity of the hybrid composites after recycling was reduced by hybridisation. The use of glass fibres in the hybrid composites preserved the mechanical properties of the composites. The value of recycled materials can be enhanced if they can be used in a way to exploit some of their unique properties.

## ACKNOWLEDGEMENTS

This research was supported by the Universiti Kuala Lumpur Malaysia Institute of Aviation Technology (UniKL MIAT). Thanks also go to the staff at the Center for Advanced Composite Material (CACM), The University of Auckland.

## REFERENCES

- [1] G. Oliveux, L. O. Dandy, and G. A. Leeke, "Current status of recycling of fibre reinforced polymers: Review of technologies, reuse and resulting properties," *Prog. Mater. Sci.*, vol. 72, pp. 61–99, 2015, doi: <https://doi.org/10.1016/j.pmatsci.2015.01.004>.
- [2] N. Vidakis *et al.*, "Sustainable Additive Manufacturing: Mechanical Response of Polypropylene over Multiple Recycling Processes," *Sustainability*, vol. 13, no. 1. 2021, doi: 10.3390/su13010159.
- [3] A. Bourmaud and C. Baley, "Investigations on the recycling of hemp and sisal fibre reinforced polypropylene composites," *Polym. Degrad. Stab.*, vol. 92, pp. 1034–1045, Jun. 2007, doi: 10.1016/j.polymdegradstab.2007.02.018.
- [4] A. C. Meira Castro *et al.*, "Sustainable waste recycling solution for the glass fibre reinforced polymer composite materials industry," *Constr. Build. Mater.*, vol. 45, pp. 87–94, 2013, doi: <https://doi.org/10.1016/j.conbuildmat.2013.03.092>.
- [5] A. Muhammad, M. R. Rahman, S. Hamdan, and K. Sanaullah, "Recent developments in bamboo fiber-based composites: a review," *Polym. Bull.*, vol. 76, no. 5, pp. 2655–2682, 2019, doi: 10.1007/s00289-018-2493-9.
- [6] A. M. Radzi *et al.*, "Bamboo-Fiber-Reinforced Thermoset and Thermoplastic Polymer Composites: A Review of Properties, Fabrication, and Potential Applications," *Polymers*, vol. 14, no. 7. 2022, doi: 10.3390/polym14071387.

## UV-SHIELDING BIODEGRADABLE FILMS BASED ON CARBOXYMETHYL CELLULOSE FILLED WITH HENNA EXTRACTS

N. Danmatam<sup>1,3</sup> and D. Pattavarakorn<sup>1,2\*</sup>

<sup>1</sup>Department of Industrial Chemistry, Faculty of Science, Chiang Mai University, 50200, Chiang Mai, Thailand

<sup>2</sup>Center of Excellence in Materials Science and Technology, Faculty of Science, Chiang Mai University, Muang, Chiang Mai, 50200, Thailand

<sup>3</sup>Graduate School, Chiang Mai University, 50200, Chiang Mai, Thailand

---

### ABSTRACT

UV-shielding biodegradable films based on carboxymethyl cellulose (CMC) have been prepared using henna extracts from henna powder as the UV blocker additive. The influence of variation in henna extracts content from 0-10v% on the mechanical, thermal, and optical properties, moisture content, and water vapour permeability of the prepared CMC films has been studied. The results showed that the total phenolic compounds content of henna extracts was  $0.1803 \pm 0.0097$  g/15 g dry weight of henna powder. The addition of henna extracts to CMC increased moisture content of the films but decreased the water vapor permeability. The henna extracts addition also gave films having reduced tensile strength compared to film produced from neat CMC. From optical properties testing, it was found that colour of the henna extracts filled CMC films tended to be darker; L\* and %transmittance decreased with the increase of henna extracts content. Moreover, the addition of henna extracts significantly improved the UV-shielding ability of the CMC films. In particular, the CMC film with 10%v henna extracts showed 100% shielding ability against UVC (100-280 nm) and UVB (280-315 nm) and 99.90% shielding ability against UVA (315-400 nm).

*Keywords:* UV-Shielding, biodegradable films, carboxymethyl cellulose, henna extracts, polyphenol.

---

### INTRODUCTION

Plastic packaging has become an important consideration in encapsulating products for many industries and their customers. The packaging must have the following important properties: it must protect products giving acceptable shelf life and it must allow the product to be clearly visible to attract consumers, hence enhancing the marketing success and value of products. Plastic packaging is widely used and is ranked as having the highest economic growth rate in the group of materials used for packaging. Nevertheless, increasing population growth combined with economic, social, cultural and technological developments have resulted in ever increasing demand for plastic packaging that has given rise to considerable plastic waste problems that have a serious impact on the environment. Plastic wastes take long time to decompose and effective plastic waste disposal systems are still restricted in many areas of the world causing very damaging accumulations of plastic wastes. Bioplastics based on cellulose are termed "cellulosic bioplastics" and are produced from natural cellulosic materials such as wheat gluten, rice flour, beets or are produced from agricultural wastes such as rice straw, papaya peel, durian peel, coconut shell. Because such raw materials are available in large quantities at low cost and are sustainable through replanting the cellulosic bioplastics are receiving increasing attention. Moreover, cellulosic bioplastics are biodegradable, eco-friendly and can help to reduce the environmental pollution associated with the disposal of plastics

Ultraviolet (UV) radiation is electromagnetic emission from the sun having wavelengths in the range of 100–400 nm with frequencies of 1015-1217 Hz. UV radiation consists of 3 types; UVA has wavelength around 320-400 nm and energy around 3.10-3.94 electron volts, UVB has wavelength around 280-320 nm and energy around 3.94-4.43 electron volts and UVC has wavelength around 200-280 nm and energy around 4.43-12.4 electron volts. UV rays are classified as radiation that is harmful to organic compounds especially to UV-sensitive products such as food and medicine [1].

Toward potential use as environmentally friendly bio-plastic packaging, this report examines the preparation of UV-shielding CMC films filled with henna extracts containing phenolic compounds as the UV protective filler. The CMC films filled with varied additions of henna extracts were fabricated via a solution casting method in which glutaraldehyde and glycerol are used as crosslinking agent and plasticizer, respectively. The effects of henna extracts content on the chemical, thermal and mechanical properties, and on the UV-shielding capability of the prepared CMC films have been studied.

### MATERIALS AND METHODS

#### *Materials and reagents*

Carboxymethyl cellulose sodium salt (CMC) and Gallic acid monohydrate were purchased from ACRÖS Organic (New Jersey, USA). Henna powder was purchased from Henna Industries Pvt. Ltd. (Haryana, India). Glycerol was purchased from Qchemical Co., Ltd. (QRëC, New Zealand). Glutaraldehyde was purchased from LOBA CHEMIE Pvt. Ltd (Mumbai, India). Follin-Ciocalteu phenol reagent was purchased from Merck KGaA (Darmstadt, Germany). Sodium

---

#### *Article history:*

Received: 10 March 2022

Accepted: 7 June 2022

Published: 14 June 2022

---

#### *E-mail addresses:*

datchanee.p@cmu.ac.th (D. Pattavarakorn)

nanticha\_d@cmu.ac.th (N. Danmatam)

\*Corresponding Author

Carbonate Anhydrous was purchased from APS Finechem (New South Wales, Australia). All reagents used were analytical grade.

Preparation of henna extracts

Henna extracts were extracted from henna powder using the Soxhlet extraction method. 15 g of henna powder was added into 200 mL distilled water and then extracted for 6 hr. The solid impurities were vacuum filtered from the extracts.

Preparation of CMC and CMC/H films

CMC Films were prepared by solution casting method. CMC (2 %w/v) was mixed with glycerol (30%w/w), glutaraldehyde (2%%w/w) and henna extracts (0, 2, 4, 6, 8 and 10% v/v). Then CMC/H solution were then dried at 80°C for 24 hr.

Characterization methods

The total phenolics content was expressed in term of milligrams of gallic acid monohydrate equivalents per gram of aqueous henna extracts. The color of each film specimen was determined using a spectrophotometer (Konica Minolta, CM-700d, Japan). Moisture content was calculated with equation (1). The ASTM E96-00<sup>E1</sup> (2002) standard method was used for water vapor permeability measurements on the film. The water vapor permeability rate (WVPR) and water vapor permeability (WVP) were calculated with equation (2) and (3), respectively. The thermal stability of the films was tested by TGA using a Simultaneous Thermal Analyzer (Rikagu TG-DTA8120, Rikaru Corporation, Inc.). The tensile properties of the films were determined using a Lloyd universal testing machine (model LRX) according to ASTM D882-02 in a pull-with-yield mode. A UV-VIS Spectrophotometer SPECORD PLUS (Analytik-jena Far East, Thailand) was used for examination of the transparency and UV-shielding capability of the films. The biodegradability of the neat CMC and CMC/H films in the soil was obtained according to equation (4).

$$\text{Moisture content} = [(m_1 - m_2) / m_2] \times 100 \quad (1)$$

$$\text{WVPR (g/m}^2 \cdot \text{day)} = (G/T) / A = \text{slope} / A \quad (2)$$

$$\text{WVP (g} \cdot \text{m} \cdot \text{day} \cdot \text{mmHg/m}^2) = (\text{WVPR} \times l) / \Delta P \quad (3)$$

$$\% \text{ Biodegradation} = (W_1 - W_2) / W_1 \times 100 \quad (4)$$

Where  $m_1$  (g) was initial weight of the specimen,  $m_2$  (g) was the weight of specimen after oven drying, G/T is the weight change rate per time, A is the surface area of sample ( $\text{m}^2$ ), l is film thickness (m),  $\Delta P$  is pressure difference,  $W_1$  is the initial dry weight of the samples (g) and  $W_2$  is the dry residual weight of the samples after biodegradation in soil (g).

RESULTS AND DISCUSSION

Total phenolic compound

The total phenolic compound of aqueous henna extracts was found to be  $1803 \pm 0.0097$  g/15 g dry weight.

Appearance and optical properties

As presented in Fig. 1 both CMC and CMC/H films prepared by solution casting method were apparently transparent and homogeneous. The addition of henna extracts into the CMC matrix resulted in yellowish to yellowish-brown colors for the CMC/H films. Color and transmittance parameters of the CMC and CMC/H films are reported in TABLE 1. Addition of henna extracts can decrease the transparency of the films. The  $a^*$ ,  $b^*$  and h parameters of film showed that the CMC/H films are in the shade of dark-red-brown color.

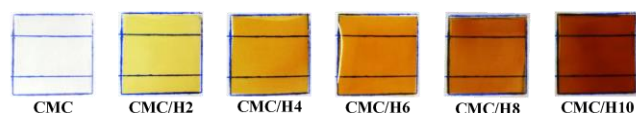


Fig. 1: The photograph images of CMC and CMC/H films.

TABLE 1: Color properties, transmittance and UV protection properties of CMC and CMC/H films

Sample	Color properties					Transmittance (%)	%UV-shielding capability		
	L*(D65)	a*(D65)	b*(D65)	C*(D65)	h(D65)		UVC	UVB	UVA
CMC	91.83 ± 0.03	0.09 ± 0.01	-2.35 ± 0.02	2.35 ± 0.01	272.28 ± 0.25	93.28 ± 0.01	99.89 ± 0.03	81.49 ± 0.08	44.68 ± 0.04
CMC/H2	81.21 ± 0.88	1.35 ± 0.49	34.49 ± 2.86	34.51 ± 2.87	87.79 ± 0.66	86.57 ± 0.00	99.89 ± 0.09	99.91 ± 0.01	97.59 ± 0.04
CMC/H4	72.91 ± 1.11	8.05 ± 1.06	48.77 ± 2.75	49.43 ± 2.88	80.65 ± 0.70	76.54 ± 0.00	100.05 ± 0.10	99.98 ± 0.01	99.89 ± 0.02
CMC/H6	67.32 ± 0.51	13.05 ± 0.73	50.09 ± 2.47	51.76 ± 2.41	75.38 ± 1.00	74.68 ± 0.00	99.94 ± 0.04	99.98 ± 0.01	100.00 ± 0.03
CMC/H8	58.94 ± 3.80	19.03 ± 3.51	47.72 ± 2.85	51.48 ± 2.04	68.20 ± 4.46	73.00 ± 0.01	99.97 ± 0.04	99.98 ± 0.03	99.96 ± 0.03
CMC/H10	56.19 ± 3.17	20.62 ± 1.68	43.16 ± 3.86	47.91 ± 2.70	64.31 ± 3.93	64.14 ± 0.00	100.00 ± 0.09	99.99 ± 0.02	99.96 ± 0.02

Moisture content

From TABLE 2, moisture content of CMC film was lower than CMC/H films. The moisture contents the CMC/H films decreased slightly with increasing henna extracts since the interaction between CMC and the henna extracts forms hydrogen

bonds that can limit the -OH group availability. However, there are still sufficient OH groups in the extracts to interact with moisture thus leading to the higher moisture contents of the CMC/H films compared to CMC.

*Water vapor permeability*

It is the most important property in food packaging applications to control the moisture transfer between food and the surrounding atmosphere. From TABLE 2, WVP of the CMC/H specimens was lower than that of neat CMC but appears to be independent of the amount of henna extracts addition possibly because of the formation of a coherent network of H-bonding between -OH groups of the CMC matrix and -OH groups of the henna extracts.

*Mechanical properties*

From TABLE 2, the addition of henna extracts resulted in decreased tensile properties of the CMC/H films. This may be because the phenolic compounds in henna extracts act as lubricant between CMC chains[2]. However, further increases of the extracts content from 4% to 10% v/v led to increasing tensile strengths. This effect may be caused by molecular interactions between the extracts and CMC molecular chains such as hydrogen bond formation between hydroxyl groups of CMC polymer chain and the hydroxyl groups of henna extracts (e.g., hydroxyl groups in Kaempferol 3-glyceride, Caffeic acid and Gallic acid[3]), these interactions having a greater effect on strength with increasing addition of henna extracts above 2% v/v.

TABLE 2: Moisture content, water vapor permeability and thickness of CMC and CMC/H films.

Sample	Physical properties			Mechanical properties		Thermal properties			Biodegradability
	Moisture content	WVP (x10 <sup>-5</sup> )	Thickness (mm)	Tensile strength (MPa)	Elongation at break (%)	T <sub>onset</sub> (°C)	T <sub>50</sub> (°C)	T <sub>max</sub> (°C)	Percent weight loss
CMC	17.20 ± 0.34	5.58 ± 8.41	0.10 ± 0.01	37.74 ± 5.40	7.16 ± 3.94	95	270	283	72.81 ± 5.57
CMC/H2	21.08 ± 0.76	3.68 ± 1.25	0.09 ± 0.02	24.96 ± 2.68	6.47 ± 2.75	111	270	283	45.22 ± 19.28
CMC/H4	20.78 ± 0.56	2.15 ± 3.72	0.10 ± 0.01	30.25 ± 3.82	5.93 ± 3.23	83	269	283	33.64 ± 6.40
CMC/H6	19.55 ± 0.78	4.56 ± 3.32	0.11 ± 0.01	32.03 ± 5.35	5.13 ± 2.68	90	267	281	49.10 ± 22.60
CMC/H8	19.49 ± 0.27	3.07 ± 2.18	0.11 ± 0.02	32.68 ± 1.37	5.58 ± 2.32	91	267	282	39.12 ± 6.48
CMC/H10	19.10 ± 0.38	2.08 ± 1.36	0.12 ± 0.01	34.19 ± 1.53	5.41 ± 1.90	107	269	279	36.63 ± 8.68

*Thermal stability*

From TGA and DTG curves, the initial decomposition temperature at 10% weight loss (T<sub>onset</sub>), decomposing temperature at 50% weight loss (T<sub>50</sub>) and temperature of maximum rate of degradation (T<sub>max</sub>) for CMC and CMC/H films are summarized in TABLE 2. The addition of henna extracts did not seem to affect the thermal properties of the films since the T<sub>50</sub> and T<sub>max</sub> values of neat CMC and CMC/H films were not significantly different.

*UV-shielding capability*

The UV-shielding or UV protection ability is an importance indicator of the suitability of packaging materials for UV sensitive products. The CMC film showed near complete transmission of UVB, UVA and visible regions wavelengths. As summarized in TABLE 1. the differences between the-shielding capability against UVA UVB of the neat CMC and CMC/H films revealed that the addition of henna extracts into CMC considerable improved the UV protection of the CMC film.

*Biodegradation ability*

TABLE 2 shows that the neat CMC film exhibited the highest %weight loss (72.81% ± 5.57), demonstrating the highest biodegradability. This behaviour is related to the chemical structure of the hydroxyl groups in CMC polymer chains. Glycosidic bonds are easily fractured in nature by bacteria and fungi in soil that are activated by moisture and heat. The biodegradation ability decreased as the addition amount of henna extracts was increased.

**CONCLUSIONS**

UV-shielding biodegradable film has been successfully prepared by using additions of polyphenol-containing henna extractives to CMC matrices. The water vapour permeability and mechanical properties of CMC film was found to be reduced by the addition of henna extracts. The differences in UV light transmittance between CMC film and the CMC/H films revealed that the addition of henna extracts can improve the UV protection ability of the CMC film and hence has potential for use as UV blocked biodegradable packaging material.

**ACKNOWLEDGEMENTS**

This research work was partially supported by the Center of Excellence in Materials Science and Technology, Faculty of Science, Chiang Mai University and the Graduate School, Chiang Mai University.

**REFERENCES**

[1] W. K. Tobiska *et al.*, "The SOLAR2000 empirical solar irradiance model and forecast tool," *Journal of Atmospheric and Solar-Terrestrial Physics*, vol. 62, pp. 1233-1250, 09/01 2000, doi: 10.1016/S1364-6826(00)00070-5.

[2] M. Narayanan, S. Loganathan, R. B. Valapa, S. Thomas, and T. O. Varghese, "UV protective poly(lactic acid)/rosin films for sustainable packaging," *International Journal of Biological Macromolecules*, vol. 99, pp. 37-45, 2017/06/01/2017, doi: https://doi.org/10.1016/j.ijbiomac.2017.01.152.

[3] K. Dhaouadi *et al.*, "Commercial Lawsonia inermis L. dried leaves and processed powder: Phytochemical composition, antioxidant, antibacterial, and allelopathic activities," *Industrial Crops and Products*, vol. 77, pp. 544-552, 12/01 2015, doi: 10.1016/j.indcrop.2015.09.037.

## WATER ABSORPTION BEHAVIOUR OF BAMBOO-GLASS HYBRID POLYPROPYLENE COMPOSITES

N.Z.M. Zuhudi<sup>1\*</sup>, K. Jayaraman<sup>2</sup>, R. J.T. Lin.<sup>2</sup>

<sup>1</sup>*Aerocomposite Cluster, Universiti Kuala Lumpur Malaysian Institute of Aviation Technology, 43800 Dengkil, Selangor, Malaysia*

<sup>2</sup>*Center for Advanced Composite Materials, Department of Mechanical Engineering, The University of Auckland, New Zealand*

---

### ABSTRACT

The poor resistance towards water absorption is considered as a major weakness of natural fibre reinforced composites (NFRCS). The hydrophilic nature of bamboo fibre means that these composites are susceptible to considerable water absorption which may lead to degradation of their mechanical properties. The effect of the hybridisation is approached with the study of immersion in water at different temperatures, 23°C and 60°C, for a period of 1680 hours. The process of absorption was observed to demonstrate the kinetics and mechanism proposed by Fick's theory. The diffusion coefficients increase with the increase in immersion temperature for the composites in this study. A decreasing trend of diffusion coefficient is observed as the bamboo content decreases. The presence of outer layers of glass effectively decelerates water diffusion into the bamboo polypropylene (BPP) composites. These results indicate that, by replacing several layers of glass with bamboo fabric in glass-polypropylene composites, a hybrid concept is feasible for developing an excellent and economical light-weight composite.

*Keywords:* water absorption, diffusion coefficients, hybridisation, bamboo-glass, degradation.

---

### INTRODUCTION

Bamboo as an alternative material because of their advantages over the synthetics [1], [2]. In a bamboo fabric composite, diffusion is the major mechanism for moisture penetration. The bamboo fabric will be the main channel allowing water transport in the composites. The hydrophilic nature of bamboo fabric means that these composites are susceptible to considerable water absorption which may lead to degradation of their mechanical properties [3], [4]. Introducing hybrid concept may preserve this problem [5]. These hybrid composites are expected to have superior resistance to water and temperature due to their glass content. Moisture absorption is considered in terms of three different types of diffusion behaviour i.e. Fickian or Non-Fickian diffusion. The three cases of diffusion can be theoretically described by the shape of the sorption curve [6]. The value of  $n$  differs in each of the three cases. For Fickian diffusion, case I,  $n = 0.5$ , while for Case II,  $n = 1$  and for Case III (anomalous diffusion),  $n$  is an intermediate value ( $0.5 < n < 1$ ). The value of  $k$  is a characteristic of the sample which indicates the interaction of moisture between the material and water. The values of  $k$  and  $n$  were determined by linear regression analysis. The diffusion coefficient is the most important parameter of Fick's model, as this shows the ability of the water molecules to penetrate inside the composite laminate. The water absorption into the composite is investigated by applying Fick's second law of diffusion [7].

### MATERIALS AND METHODS

#### *Materials*

The raw materials used to fabricate the BPP composites in this work were polypropylene and woven bamboo fabric. The matrix used was polypropylene (PP) random copolymer, Moplen RP241G, manufactured by Lyondell Basell Industries and supplied by Field International Ltd., Auckland, New Zealand. The PP sheets have a nominal thickness of 0.38 and 0.58 mm. 100% bamboo fabric twill- woven was obtained from Xinchang Textiles Co.Ltd., Guangzhou, China. The bamboo fabrics with a width of 1500 mm and weight of 220 gsm were used, having specification of 20\*20 tex and 108\*58 per square inch for yarn count and density, respectively. The glass pre-preg supplied by Plytron ICI Ltd. UK with nominal glass volume fraction and density of 35% and 1480 kg/m<sup>3</sup>. The nominal thickness and sheet width are 0.47 mm and 240 mm, respectively.

#### *Methods*

The compression moulding process was used in this research to produce composite laminates. The bamboo polypropylene (BPP) composites and their bamboo-glass polypropylene (BGPP) hybrid composites were fabricated in the range of about 55-65% fibre weight fraction, all in warp direction. The hybrid composites were fabricated with about 30% of bamboo and 20% of glass fibre weight fraction. The water absorption study was carried out according to ASTM 570-98. This standard specifies a 2 or 24 hours immersion test, depending on the absorption rate of the material in distilled water at  $23 \pm 1^\circ\text{C}$ . The specimens were removed at 2 hourly intervals during the immersion, for the first 6 hours. Readings were also taken after 24, 48 hours and then every 10 days up to 70 days. The immersion study was also performed at  $60 \pm 1^\circ\text{C}$  to investigate the effect of higher temperature.

---

#### *Article history:*

Received: 10 March 2022

Accepted: 7 June 2022

Published: 14 June 2022

---

#### *E-mail addresses:*

zuhairah@unik.edu.my (N.Z.M. Zuhudi)

kjayaraman@auckland.uni.ac (K. Jayaraman)

rtj.lin@auckland.uni.ac (R.T.J. Lin)

\*Corresponding Author

RESULTS AND DISCUSSION

Effect of hybridisation on water absorption

The amount of water absorbed was obtained by the weight gained by the samples after immersion. Fig. 1 shows the percentages of water absorbed plotted against time for all the samples at 23°C and 60°C respectively after 1680 hours of immersion in water. The same behaviour was observed at both temperatures; the samples absorbed water very rapidly until saturation, where water content stabilized. It is concluded that the water absorption behaviour of all the composites followed the so-called Fickian behaviour. The water absorption of BPP composites at 23°C after 1680 hours is 14.6%. As anticipated, absorption was quite rapid initially, reaching almost 13.01% after about 720 hours. Further immersion increased the weight about 1.59% more after 1680 hours of immersion. The absorption rate was significantly higher in the first 30 days (comprising 89% of the total absorption). The BPP composites had nearly reached saturation after 1680 hours. For the 30B:20G, 20B:35G and 10B:45G hybrid composites, as anticipated water absorption at 23°C was quite rapid initially, reaching almost 10.56%, 7.30%, and 2.81% respectively after 720 hours. Water absorption almost reached saturation by 1200 hours. It can be seen that hybridisation between these two reinforcements increased the water resistance over that of the BPP composites.

Effect of temperature on water absorption

The water absorption increases with increasing immersion temperature for all of the composites. Saturation was reached after 336 hours and remained constant until 1680 hours for both temperatures. The water absorption of BPP composites at 60°C after 1680 hours was 16.5%. As anticipated the water absorption was quite rapid initially, reaching almost 12.64% after 168 hours of immersion. Further immersion until 720 hours, only increased it to 15.68%. After 1680 hours, a near-saturation level of 16.50% was reached. Absorption rate was significantly higher at 60°C, with 80% of the total absorption in the first 14 days. The BPP composites had nearly reached equilibrium after 720 hours of immersion. For immersion of 30B:20G, 20B:35G and 10B:45G hybrid composites at 60°C, the water absorption was also quite fast initially, reaching almost 10.91%, 7.94%, and 3.26% for each composite respectively after only about 168 hours. A very slight further increase was observed at 336 hours, and saturation had been almost reached after 720 hours. The final water contents were 12.28%, 9.93% and 4.52% respectively. The composites approached equilibrium faster at 60°C than at 23°C.

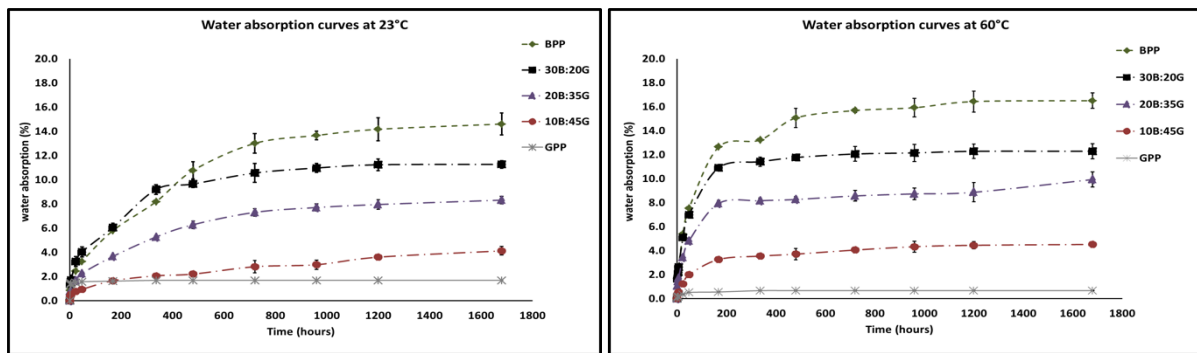


Fig. 1: Water absorption curves for composites immersed at the two temperatures

Diffusion case parameters

The parameters  $n$  and  $k$  obtained from the fitting as described earlier are shown for all the composite samples in Fig. 2. It can be seen that the  $n$  values of all the composites approached 0.5, which shows they approach Fickian behaviour. This behaviour is in agreement with the water absorption behaviour curve presented earlier. The  $n$  values at the higher temperature were found to be higher for all of the composites except for 20B:35G. For instance, the  $n$  value of BPP at 60°C was 0.4795, which was higher than that at 23°C. A similar pattern was observed for 30B:20G and 10B:45G and GPP composites. However, for the 20B:35G composite there was no significant difference in the  $n$  values observed. Interestingly, the  $n$  and  $k$  values for the hybrid composites immersed at 60°C show an increasing trend when bamboo fabric content was reduced, but this behaviour did not hold for the 23°C tests, which showed a drop in both  $n$  and  $k$  for the 10B:45G composite. A large difference in the  $n$  value for the GPP composites was found between the two temperatures. The  $k$  values represent the interaction between the materials and the water. No pattern in  $k$  values was observed for any of the composites. The  $k$  values for BPP composites were the highest among all except the 10B:45G composites.

The diffusion coefficients

The moisture diffusion coefficient were determined. The diffusion coefficients increase with the increase in immersion temperature for all of the composites. There was a 142% increase in the coefficients of samples immersed at 60°C ( $7.054 \times 10^{-9} \text{ m}^2 \cdot \text{s}^{-1}$ ) compared to those at 23°C ( $2.915 \times 10^{-9} \text{ m}^2 \cdot \text{s}^{-1}$ ) for BPP composites. For the effect of hybridisation, the diffusion coefficient of 30B:20G hybrid composites at 60°C, was 60% higher than that at 23°C. A similar pattern was found for 20B:35G, 10B:45G, and GPP composites, which showed higher diffusion coefficients, with increases of 122%, 186%, and 246% compared to the values at 23°C. The temperatures influenced the diffusion coefficients. There is a clear increasing trend of diffusion coefficients with the increase in bamboo content. A large difference in the diffusion coefficients between those two temperatures was found in this study.

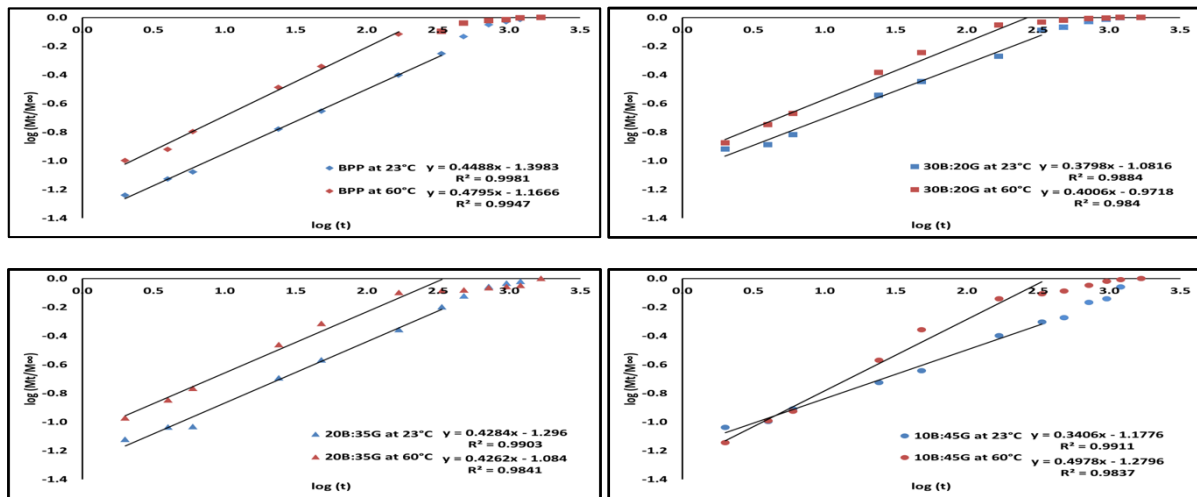


Fig. 2: The diffusion case parameters for the composites at different temperatures

TABLE 2: The diffusion coefficients at different temperatures

Samples	Diffusion coefficients ( $m^2.s^{-1}$ ) at 23°C	Diffusion coefficients ( $m^2.s^{-1}$ ) at 60°C
BPP	$2.915 \times 10^{-9}$	$7.054 \times 10^{-9}$
30B:20G	$2.116 \times 10^{-9}$	$3.452 \times 10^{-9}$
20B:35G	$1.482 \times 10^{-9}$	$3.302 \times 10^{-9}$
10B:45G	$1.056 \times 10^{-9}$	$3.023 \times 10^{-9}$
GPP	$0.353 \times 10^{-9}$	$1.223 \times 10^{-9}$

## CONCLUSION

An understanding of durability in terms of factors such as moisture and temperature over time is important. Fickian behaviour is displayed by the composites in the current study; the water absorption rate of the composite is proportional to the square root of time and gradually approaches equilibrium. The  $n$  values being not exactly 0.5 may be explained by fibre swelling, fibre-matrix interface weakening, micro-cracking, or other water absorption mechanisms active in the composites. Higher values of  $n$  and  $k$  were found in the composites with the highest amount of bamboo content. These values tend to be less for the hybrid composites. The diffusion coefficients increase with the increase in immersion temperature for the composites in this study. Hybridisation improved the water resistance of the BPP composites, effectively acting as a barrier to slow down the penetration of the water. This reduction in absorption and the improved properties obtained demonstrate promise for these hybrid materials in future applications.

## ACKNOWLEDGEMENTS

This research was supported by the Universiti Kuala Lumpur Malaysia Institute of Aviation Technology (UniKL MIAT). Thanks also go to the staff at the Center for Advanced Composite Material (CACM), The University of Auckland.

## REFERENCES

- [1] A. M. Radzi *et al.*, “Bamboo-Fiber-Reinforced Thermoset and Thermoplastic Polymer Composites: A Review of Properties, Fabrication, and Potential Applications,” *Polymers*, vol. 14, no. 7. 2022, doi: 10.3390/polym14071387.
- [2] A. Muhammad, M. R. Rahman, S. Hamdan, and K. Sanaullah, “Recent developments in bamboo fiber-based composites: a review,” *Polym. Bull.*, vol. 76, no. 5, pp. 2655–2682, 2019, doi: 10.1007/s00289-018-2493-9.
- [3] D. Chandramohan, B. Murali, P. Vasantha-Srinivasan, and S. Dinesh Kumar, “Mechanical, moisture absorption, and abrasion resistance properties of bamboo–jute–glass fiber composites,” *J. Bio-and Tribo-Corrosion*, vol. 5, no. 3, pp. 1–8, 2019.
- [4] M. Ramesh, L. RajeshKumar, and V. Bhuvaneshwari, “Bamboo fiber reinforced composites,” in *Bamboo Fiber Composites*, Springer, 2021, pp. 1–13.
- [5] B. K. Venkatesha, R. Saravanan, and A. B. K., “Materials Today : Proceedings Effect of moisture absorption on woven bamboo / glass fiber reinforced epoxy hybrid composites,” *Mater. Today Proc.*, no. xxxx, 2020, doi: 10.1016/j.matpr.2020.10.421.
- [6] H. M. Akil, C. Santulli, F. Sarasini, J. Tirillò, and T. Valente, “Environmental effects on the mechanical behaviour of pultruded jute/glass fibre-reinforced polyester hybrid composites,” *Compos. Sci. Technol.*, vol. 94, pp. 62–70, 2014.
- [7] S. Panthapulakkal and M. Sain, “Studies on the water absorption properties of short hemp–glass fiber hybrid polypropylene composites,” *J. Compos. Mater.*, vol. 41, no. 15, pp. 1871–1883, 2007.

## **A REVIEW: RMS – RAPID MOTION SCANNER TECHNIQUE ON MEASURING MATERIAL VELOCITY AND THICKNESS OF FLAX FIBER PREPREG**

S. N. Fatin<sup>1</sup>, K. D. M. Aris<sup>1,\*</sup>, M. N. Ismail<sup>1</sup>

<sup>1</sup>*Advanced Composite Research Cluster, Universiti Kuala Lumpur Campus Malaysian Institute of Aviation Technology, 43900 Dengkil, Selangor, Malaysia*

---

### **ABSTRACT**

The interest in using sustainable materials has been a part of the Sustainable Development Goals (SDG) by the United Nations. The use of engineered bio fiber has the potential to replace the usage of synthetic fibers. However, the diversification of the application is limitless. The intended paper investigates the detection of impurities of cured pre-impregnated biocomposite by using C-scan ultrasound. The flax fibre reinforced plastic (FFRP) composites were fabricated and cured with heat-assisted curing. The panels were inspected to obtain the correct value of sound velocity in detecting thickness by using RMS 2 Ultrasonic Corrosion Mapping. As the result, the test obtained a reference value of sound velocity to detect the thickness of flax.

*Keywords:* Composite material, density, Natural Fiber Composite (NFC), non-destructive testing, sustainable engineering.

---

### **INTRODUCTION**

Over the past decades, there are an increasing interest and demand in engineering fields, such as aerospace, automotive, manufacturing, and sports industry in utilizing sustainable, eco-friendly, and biodegradable materials to replace synthetic composite structures [1]. Flax fibers are one of the NFC that are strongly preferred in replacing current synthetic fibers in conventional polymer composites and it has a low density and great strength and stiffness. [2]. Duflou et al studied the mechanical strength between flax fiber and fiberglass, results show that flax fiber can be a great choice for fiberglass replacement.

In this research, dry layup flax-prepreg samples are tested with the ultrasonic method. The rapid motion scanner (RMS) technique is being selected because of its High-Speed, and High-Accuracy capabilities. As the objective of this study is to further investigate the ability of the RMS technique to accurately test and detect the velocity required and design thickness of dry layup flax-prepreg specimen.

### **MATERIALS AND METHODS**

#### *Flax-preg T-UD 110*

Flax-preg T-UD is a range of pre-impregnated materials based on epoxy resin and the 100% unidirectional flax fibers reinforcement developed by EcoTechnilin/ Lineo.[3] Flax-preg T-UD is widely used in sports, transportation, and wind energy due to its mechanical and acoustic properties, dampening properties, lightweight and exhibit behaviour of aramid (source: technical data sheet of Flax-preg T-UD 110, EcoThecnilin 2021).

#### *RMS-Rapid Motion Scanner Technique*

RMS 2 is advanced non-destructive equipment that is a high-speed, high-accuracy remote-access ultrasonic system. It is widely used in tanks, pipelines, pressure vessels, and other critical equipment for thickness mapping. [3] [4] The scanning head is a high-performance system controller that can be customized to suit inspection requirements and designed to maximize scanning rates on large surface areas. It is embedded with high torque stepper motors and powerful magnetic drive wheels to ensure the scanner remains fixed to the inspection surface, especially the circumferential area. RMS 2 comes with its own advanced data acquisition and analysis software.

#### *Fabrication Process*

In this research flax specimens for testing are fabricated by using a dry layup method by using temperature assisted curing with a vacuum bagging process by using the hot bonder ANITA Hot Bonder produced by GMI Aerospace. [5], [6] and [7].

Vacuum pressure is kept at 22 in Hg thought out the curing with cycle curing referred from the Flax prepreg Material datasheet. The curing temperature is set at 1300C. The dimension of the laminate is 300mm X 300mm. The arrangement of the bagging sequence is shown in Fig. 1.

---

#### *Article history:*

Received: 10 March 2022

Accepted: 7 June 2022

Published: 14 June 2022

---

#### *E-mail addresses:*

sfathinadlina@unikl.edu.my (S. N. Fatin)

khdahri@unikl.edu.my (K. D. M. Aris)

najib.ismail@unikl.edu.my (M. N. Ismail)

\*Corresponding Author



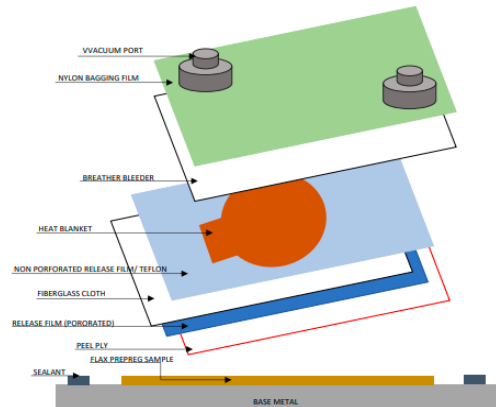


Fig. 1: Layup sequence utilizing hot bonder [4]

## RESULTS AND DISCUSSION

SEM results show the cross-sectional view from the cured flax prep. The imperfection is seen as void and porosity presence on the cured laminate. It is assumed inherit during the debulking process whereby the air trap is trapped and locked in the place. However, the sizing is small and does not lead to delamination. A further investigation of the fiber resulted from the existence of hairiness in the fabric is a yarn type. Therefore, it created an additional interference-fit or interlock between the reinforcing fibers thus increasing the strength of the laminate.

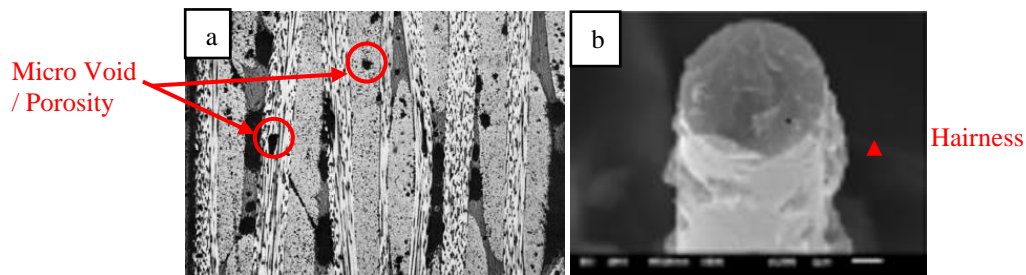


Fig. 2: The cross-sectional view via scanning electron microscopic (SEM) of (a) flax-prep containing micro void/porosity and (b) sign of hairiness on the flax fiber

Contact inspection was conducted on two types of material flax-prep and carbon-prepreg to obtain the correct value of sound velocity and evaluate the thickness of both samples. The thickness retrieved for both cured laminates were 3mm and 4 mm respectively. The results of the C-Scan mapping obtain the value of sound velocity 3.17(31700mm/s) that can be used as a future reference to inspect any type of specimen using the same tested material in this study by using RMS2 from Eddyfi Technologies. The machine utilizes a spot check method by having a continuous flow of water serves to couple the ultrasonic waves from the transducer to the specimen. During scanning mode, water is the primary medium to provide low attenuation and consistent coupling from the transducer to the specimen. Fig. 3 shows the results in the 2D C-Scan display for both carbon-prepreg and flax-prep specimens. Display colour code blue indicates that ultrasound can detect thickness range 3.5mm up to 4.5mm, yellow thickness range from 3.0mm to 3.5mm, and red indicates thickness range below 3.0mm. In Fig. 3(a) the ultrasound can penetrate and the scanning results show that all scanning areas (45mm x 100mm) with variable thicknesses were recorded. As for Fig. 3(b) inconsistent readings were recorded as no thickness was detected in the white colour. Further assessment using SEM in Fig. 2 shows the detailed cross-sectional of the area. The transducer was unable to capture the return ultrasound signal due to micro void/porosity and the hairiness of the fiber. This is one of the reasons the ultrasound becomes scattered and the low signal produced and not being captured by the transducer.

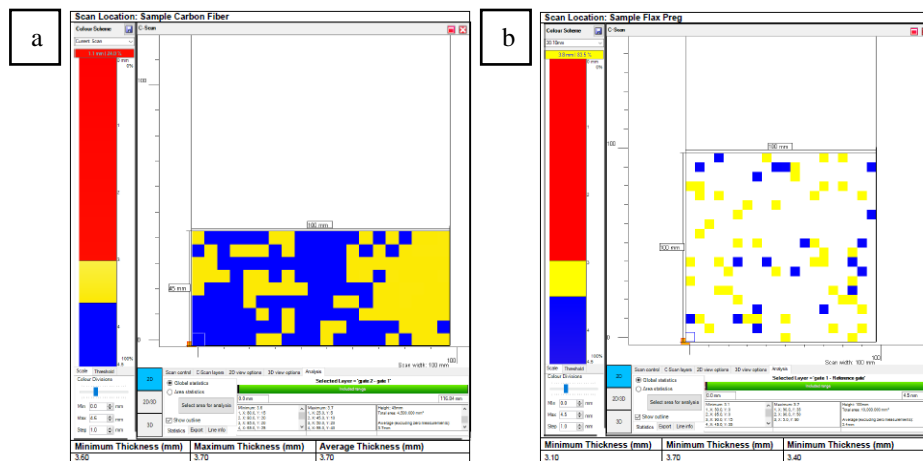


Fig. 3: (a) 2D C-scan of carbon-prepreg specimen and (b) 2D C-scan of Flax-prepreg specimen

## CONCLUSIONS

Based on the C-scan mapping data, it shows that the RMS 2 can detect both synthetic material and NFC thickness. However, thickness on flax-prepreg specimen only parts of the sample area can be detected. The probability of error in detecting the thickness of the flax-prepreg sample is:

- a) Flax fiber categorize as hydrophilic, it has a higher the to absorb moisture. The wetting of the fiber contributes to weak interfacial adhesion, this causes an error in detecting the flax thickness.
- b) During the hand layup process of the sample, the high probability of the sample not being properly cured and contributing to poor adhesion causes an air trap or air bubble between the layers. These affect the scanning process and error in the sound velocity of the probe.
- c) Based on the results of the research, the curing process can be replaced by using an autoclave curing process as autoclave has the advantages of decreasing the void formation and improving the quality of the surface and interfacial adhesion [4]

## REFERENCES

- [1] K. Senthilkumar, I. Siva, N. Rajini, J. T. W. Jappes, and S. Siengchin, *Mechanical characteristics of tri-layer eco-friendly polymer composites for interior parts of aerospace application*, no. November. 2018.
- [2] L. Yan, N. Chouw, and K. Jayaraman, "Flax fibre and its composites - A review," *Compos. Part B Eng.*, vol. 56, pp. 296–317, 2014, doi: 10.1016/j.compositesb.2013.08.014.
- [3] *Technical Data Sheet Of Flax-Preg T-UD 110*, EcoThecnilin 2021 "RMS 2 Ultrasonic Corrosion Mapping."
- [4] Mohd Aris, K. D., Mustapha F., Sapuan S. M., Majid D. L., *A Structural Health Monitoring of a Pitch Catch Active Sensing of PZT Sensor on Normal, Damage and Repair Aircraft Spoiler*. Key Engineering Materials Vols 471-472 (2011) pp 1124~1129
- [5] Mohd Yusoff Mohd Haris, Khairul Dahri Mohd Aris, Muzafar Zulkifli, Tajul Adli Abdul Razak, Nurul Zuhairah Mahmud Zuhudi, *Vacuum Infusion Simulation for Radome Manufacturing using Woven Flax Fibre and Glass Fibre*, *Journal of Advanced Research in Fluid Mechanics and Thermal Sciences*, Vol. 88, Issue 3 (2021), pg. 49-56
- [6] S. A. S. Abdullah, N. Z. M. Zuhudi, K. D. Mohd Aris, M. N. Roslan, M. D. Isa, *Influence of Yarn Parameters on Cotton/Kenaf Blended Yarn Characteristics*, *Journal Of Mechanical Engineering And Sciences (2020)*, Vol 14, Issue 4, 7622-7628
- [7] Zuhudi, N.M., Jayaraman, K., Lin, R.T.J., Aris, K.D.M., *Recycling of the Natural Fibre Composites and Their Hybrids: A Preliminary Study*, *Test Engineering and Management*, Vol. 83 (2020), 7767–7776.

## **POLYMERIC MATERIALS USED FOR IMMOBILIZATION OF MICROALGAE FOR THE BIOREMEDIATION OF PALM OIL MILL EFFLUENT**

M.E. Azni<sup>1</sup>, M. Suhaini<sup>1</sup>, R. Noorain<sup>1</sup>, S.H.S. Mariam<sup>1</sup>, M.N. Azra<sup>2</sup>, Y.Y. Yeong<sup>2</sup>, M. Rozyanti<sup>1\*</sup>

<sup>1</sup>*Malaysia Institute of Chemical & Bioengineering Technology, Universiti Kuala Lumpur, Lot 1988 Kawasan Perindustrian Bandar Vendor, Taboh Naning, 78000, Alor Gajah, Melaka, Malaysia.*

<sup>2</sup>*Institute of Marine Biotechnology, Universiti Malaysia Terengganu, 21030, Kuala Nerus, Terengganu, Malaysia.*

---

### **ABSTRACT**

The immobilization of microalgae on polymeric material such as polyurethane foam (PUF) media carrier has shown distinct advantages over non-immobilized technique with significant pollutant degradation efficiencies. However, the effect of PUF volume and pore size on the microalgae performance to remove organics and ammonium has not been extensively investigated. In this study, a down flow hanging sponge (DHS) reactor packed with PUF carrier for the immobilization of microalgae was utilized in treating the palm oil mill effluent. The result of chemical oxygen demand (COD) degradation indicates that the smaller the pore sizes (0.56 mm) and the higher PUF volume (38 %) will increase the DHS reactor total performance. In addition, the study also found that the growth of microalgae also has a great influence by different of PUF pore size and volume.

*Keywords:* PUF carrier, microalgae immobilization, palm oil mill effluent, pollutant removal.

---

### **INTRODUCTION**

High strength wastewater is characterized as wastewater with high concentration of Chemical Oxygen Demand (COD) and Biochemical Oxygen Demand (BOD), Total Suspended Solid (TSS) and nitrogen than typical domestic wastewater. It can pose a great threat to our surface water supply if not treated properly. Palm oil mill effluent (POME) is the perfect example of high strength wastewater. POME is produced throughout the processing of oil palm and uses a lot of water. The raw POME has high COD, BOD and nitrogen content which before discharging it to the water channel, a proper treatment should be done to minimize its impact to the environment [1].

DHS system is a relatively new technique for the treatment of wastewater. The DHS reactor's fundamental concept is to use a polyurethane foam (PUF) sponge material as a media for attaching and growing various viable microorganisms that remove pollutants from wastewater [2]. Microorganisms such as microalgae that grow by consuming organic compounds in a way reduce it from the wastewater [3]. Another advantage is the microalgae can be extracted and converted into other valuable products [4]. Other than that, sponges as a porous polymeric material have become commonly used in many industries such as chemical, energy, bioengineering purposes. It is relatively easy to find and very cost effective [5]. The microalgae that can be immobilized in the sponges also reduce the carbon dioxide (CO<sub>2</sub>) in the wastewater [6].

The microalgae immobilization performance in DHS system depends on the physical properties of the PUF such as its volume, porosity, pore size and ability to absorb and retain water. Higher volume and porosity permits substrate to pass through, allowing for perfect compatibility between the sponge's media and the growth conditions of the microalgae [7]. The sponge pore size on the other hand will allow the wastewater to easily pass through the sponges thus maximize the pollutant removal by the microalgae [8]. Furthermore, because the microalgae thrive in a thoroughly wetted environment, the ability of a media to absorb water is a crucial consideration when choosing a material for an attached microalgae growth system [9]. This study investigates the effect of PUF volume and pore size to the DHS performance in reducing pollutants from POME.

---

#### *Article history:*

Received: 10 March 2022

Accepted: 7 June 2022

Published: 14 June 2022

---

#### *E-mail addresses:*

edyazuan@unikl.edu.my (M.E. Azni)

suhainim@unikl.edu.my (M. Suhaini)

sitinoorain@unikl.edu.my (R. Noorain)

sharifahmariam@unikl.edu.my (S.H.S. Mariam)

azramn@umt.edu.my (M.N. Azra)

yeong@umt.edu.my (Y.Y. Yeong)

rozyanti@unikl.edu.my\* (M. Rozyanti)

\*Corresponding Author

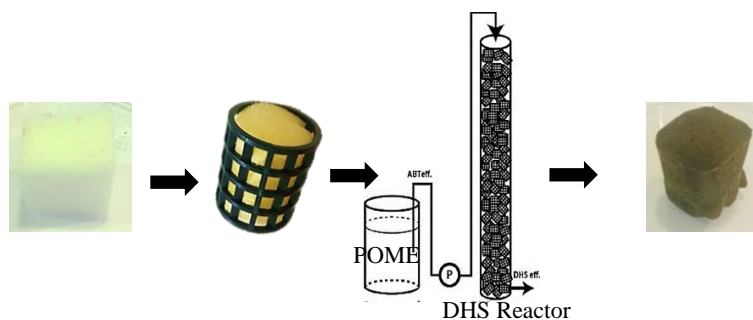


Fig. 1: The physical appearance of Polyurethane foam before and after used in downflow hanging sponges (DHS) reactor

**MATERIALS AND METHODS**

*Wastewater Characteristics*

The high strength wastewater used in this study were the Palm Oil Mill Effluent (POME) collected from circulation pond from BELL Kilang Sawit Linggi, Negeri Sembilan. The POME was deposited in high-density Polyethylene (HDPE) container and filtered using stainless steel sieve with the size of 500µm to remove suspended materials before storing at 4 °C.

*DHS Reactor Operation*

The reactor was operated in 75 cm in height cylindrical tube with inner diameter of 4 cm. 18 sponges were tied in series to become 1 string as shown in Fig 1. POME was pump to the top of the reactor and let to flow downward via gravity flowing onto each of the sponges. The reactor was operated for 42 days in stable and steady-state operating conditions. The sponge to reactor volume was set starting from 38.0% then reduce into 25.5%, and 12.7% by taking out 10 sponges from the DHS system. Then, COD analysis has been carried out using spectrophotometer model DR 900 and Hach standard reagent every 24 hours.

*Materials*

For this study, polyurethanes foam with 3 pore size has been used. The sponges have been cut into constant volume of 80 cm<sup>3</sup> each. PUF1, PUF2 and PUF3 were unused sponges and PUF16, PUF2+ and PUF3+ were the sponges collected from the DHS reactor after 42 days as illustrated in Fig. 3.

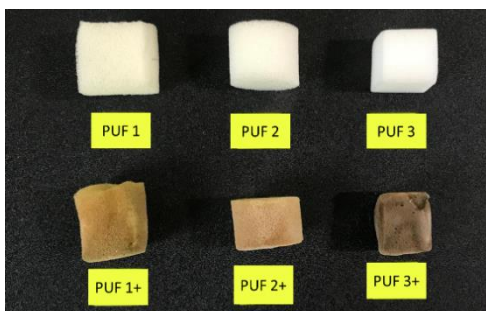


Fig. 2: Polyurethane Foam (PUF)

*Pore size and porosity*

SEM images were used to determine the average pore size (APS) and porosity (Po) of the PUF. The SEM experiments were carries out at Universiti Malaysia Terengganu (UMT) and photographed using JEOL JSM-6360LA.

**RESULTS AND DISCUSSION**

*COD removal*

The POME COD removal performances were evaluated throughout the 42 days of DHS operations. Fig. 3 presented the results of the DHS reactor’s performance when operating with 3 types of sponges volume. It is clearly shown that, by reducing the sponge to reactor volume will reduce the DHS reactor performance significantly. The DHS performance indicate that the reduction of sponge to reactor volume from 38.0% to 25.5% has decrease the COD removal from 55 ± 9% to 44 ± 8%. With further volume reduction to 12.7% produced the lowest performance of 27 ± 6%. This result clearly concluded that larger sponge to reactor volume will give better COD removal result as more wastewaters can pass through the system in particular certain time.

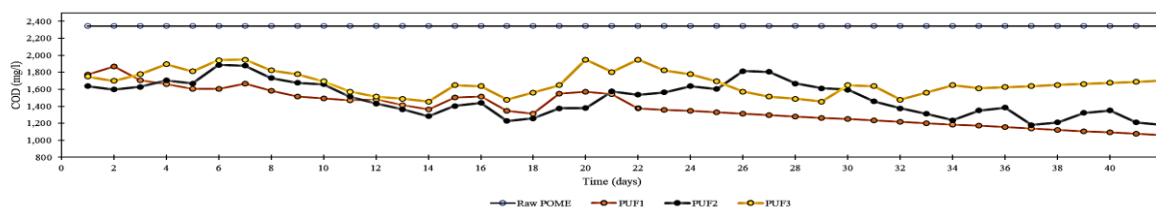


Fig. 3: DHS’s POME COD removal performance for 3 types of PUF

Pore size

The SEM images of the PUF's are shown in Fig. 4. The pore has irregular shape and varies from the 3 types of sponges. PUF1 has the largest average pore size of 774  $\mu\text{m}$  with porosity of 98% followed by PUF2 and PUF 3 of 97 and 96% respectively. Larger pore size does improve the immobilization of microalgae by permitting it to attached deeper inside the sponges. It also can be seen that, sponges with the smaller pore size tend to capture more sludges. This will help in reducing TSS content from the DHS effluent by entrapment and/or adsorption, followed by decomposition.

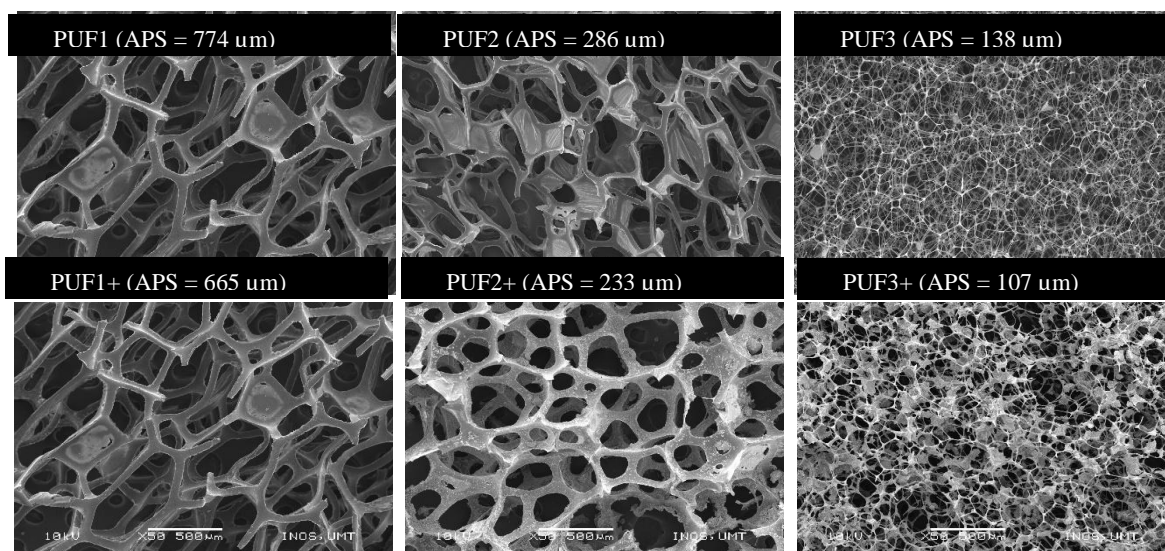


Fig. 4: Scanning electron microscope image and its pore size PUF before and after used in DHS reactor

CONCLUSIONS

Increasing the sponges to reactor volume significantly improves the DHS performance in removing COD. However, smaller pore size does give advantage in reducing the sludges from the wastewater. Different reactor configuration effect differently to the overall performance of the system. This show that proper design and operating conditions need to be carefully study in constructing treatment techniques for POME wastewater treatment. Nevertheless, this study has proved that DHS reactor system immobilize with microalgae can be used for the treatment of high strength wastewater. However, further investigations are still needed to improve the overall performance of this system.

ACKNOWLEDGEMENTS

We would like to thank Southeast Asian Regional Centre for Tropical Biology (SEAMEO-BIOTROP) for grant no 404/DIPARES/III/2021, Universiti Kuala Lumpur for Short Term Research Grant (STR19039), and Ministry of Higher Education under the Fundamental Research Grant Scheme (FRGS) FRGS/1/2020/TK0/UNIKL/02/9 for funding this project.

REFERENCES

- [1] N. A. Osman, F. A. Ujang, A. M. Roslan, M. F. Ibrahim, and M. A. Hassan, "The effect of Palm Oil Mill Effluent Final Discharge on the Characteristics of Pennisetum purpureum," *Sci. Rep.*, vol. 10, no. 1, pp. 1–10, 2020, doi: 10.1038/s41598-020-62815-0.
- [2] A. Nurmiyanto and A. Ohashi, "Downflow Hanging Sponge (DHS) Reactor for Wastewater Treatment - A Short Review," *MATEC Web Conf.*, vol. 280, p. 05004, 2019, doi: 10.1051/mateconf/201928005004.
- [3] P. Bhuyar, F. Farez, M. H. Ab. Rahim, G. P. Maniam, and N. Govindan, "Removal of nitrogen and phosphorus from agro-industrial wastewater by using microalgae collected from coastal region of peninsular Malaysia," *African J. Biol. Sci.*, vol. 3, no. 1, pp. 58–66, 2021, doi: 10.33472/afjbs.3.1.2021.58-66.
- [4] N. Rapi, C. Jane, M. E. Azni, S. M. S. Hitam, R. Mohamad, and R. Noorain, "Biological treatment of palm oil mill effluent by using a downflow hanging sponge reactor," *IOP Conf. Ser. Earth Environ. Sci.*, vol. 922, no. 1, 2021, doi: 10.1088/1755-1315/922/1/012049.
- [5] V. K. Tyagi *et al.*, "Future perspectives of energy saving down-flow hanging sponge (DHS) technology for wastewater valorization—a review," *Rev. Environ. Sci. Biotechnol.*, vol. 20, no. 2, pp. 389–418, 2021, doi: 10.1007/s11157-021-09573-1.
- [6] R. Prasad *et al.*, "Role of microalgae in global co2 sequestration: Physiological mechanism, recent development, challenges, and future prospective," *Sustainability*, vol. 13, no. 23, 2021, doi: 10.3390/su132313061.
- [7] Y. Shen *et al.*, "Enhancing cadmium bioremediation by a complex of water-hyacinth derived pellets immobilized with *Chlorella sp.*," *Bioresour. Technol.*, vol. 257, pp. 157–163, 2018, doi: 10.1016/j.biortech.2018.02.060.
- [8] M. J. Khan *et al.*, "Diatom microalgae as smart nanocontainers for biosensing wastewater pollutants: recent trends and innovations," *Bioengineered*, vol. 12, no. 2, pp. 9531–9549, 2021, doi: 10.1080/21655979.2021.1996748.
- [9] V. D. Tsavatopoulou and I. D. Manariotis, "The effect of surface properties on the formation of *Scenedesmus rubescens* biofilm," *Algal Res.*, vol. 52, no. September, p. 102095, 2020, doi: 10.1016/j.algal.2020.102095.

## VARIATION AND KINETICS OF POLY(3-HYDROXYBUTYRATE) DEPOLYMERIZATION BEHAVIOR IN STEAM-ASSISTED HYDROLYSIS

E. N. Othman<sup>1\*</sup>, H. Ariffin<sup>2</sup>, N. Haruo<sup>3</sup>, A. Yoshito<sup>3</sup>, M. Ahmad<sup>4</sup>, M. Z. W. Yunus<sup>5</sup>, M. A. Hassan<sup>2</sup>

<sup>1</sup>Universiti Kuala Lumpur, Malaysian Institute of Chemical and Bioengineering Technology, Taboh Naning Vendor City, 78000, Alor Gajah, Melaka, Malaysia

<sup>2</sup>Department of Bioprocess Technology, Faculty of Biotechnology and Biomolecular Sciences, Universiti Putra Malaysia, 43400 UPM Serdang, Selangor, Malaysia

<sup>3</sup>Graduate School of Life Science and Systems Engineering, Kyushu Institute of Technology, 2-4 Hibikino, Wakamatsu, Kitakyushu, Fukuoka 808-0196, Japan Malaysia

<sup>4</sup>Faculty of Science, Universiti Putra Malaysia, 43400 UPM Serdang, Selangor, Malaysia

<sup>5</sup>Chemistry Department, National Defence University of Malaysia, Sungai Besi Camp, 57000, Kuala Lumpur, Malaysia

---

### ABSTRACT

The behavior of poly[(R)-3-hydroxybutyrate] (PHB) depolymerization in steam-assisted hydrolysis within a temperature range of 110 – 160 °C was investigated. Two distinct depolymerization mechanisms occurred within narrow temperature range. <sup>1</sup>H-NMR analysis of PHB samples treated between 110 – 150 °C suggested that the original chemical structure of PHB was remained and the occurrence of random chain scission at the ester bond through hydrolysis. Nevertheless, at 160 °C, β-elimination was found occurring to form crotonyl groups at chain ends, suggesting mixed-depolymerization mechanisms at elevated temperatures in the melt accompanied by rapid PHB molecular weight (MW) reduction at 160 °C. The resulting  $E_a$  and  $k$  values of PHB depolymerization was recorded as 102 kJ/mol and  $2.0 - 40 \times 10^{-5} \text{ s}^{-1}$  with high  $R^2$  value. It was proposed that the elevated hydrolysis temperature accelerate the scission reaction of the neighbouring ester group faster than the original scission of ester groups resulted in the acceleration of β-elimination and increased of the depolymerization rate. In the melt fractions, β-elimination scission occurred preferentially and thus, producing crotonyl chain ends. This finding shall provide new insight on the steam-hydrolysis of PHB. Correlation of hydrolyzed products characteristics and reaction kinetics provided clearer reaction occurring in the steam-assisted hydrolysis.

*Keywords:* poly[(R)-3-hydroxybutyrate] (PHB), steam-assisted hydrolysis, β-elimination scission, chemical recycling

---

### INTRODUCTION

Polyhydroxyalkanoates (PHA) is the most promising aliphatic polyester which can be degraded biologically with unique characteristics of thermoplastic. The potential of PHA application is very much influenced by its molecular weight [1] and terminal functionality [2]. PHA in nature has high molecular weight, up to 2000 kDa. There have been many studies reported on the application and degradation of polyhydroxyalkanoates (PHA) due to its biodegradability and biocompatibility. The constituent of PHA, polyhydroxybutyrate (PHB) is depolymerized into a compound which is biocompatible to human as the compound is a natural constituent of blood, making the PHB suitable for biomedical applications, exhibits some insecticidal, antimicrobial and antiviral activities [3]. Several approaches have been investigated in the degradation of PHA, using thermal (also known as pyrolysis), enzymatic degradation, alcoholysis, photolysis, irradiation and microwave-assisted degradation [4]. Degradation products and their characteristics are very much dependent on the degradation method used.

Environmental and experimental conditions were reflected to have a great extent of influence on the degradation mechanism and kinetics. Despite the predominant effect of experimental set up, the thermochemical properties of the materials undergo degradation may influence the process. The use of steam for PHB hydrolysis is an interesting and practical approach as it is easy to control the hydrolysis conditions. Moreover, the non-involvement of solvent and harsh chemicals makes the process safe, more environmental friendly and easy product recovery. Despite of its interesting characteristics, there is still lack of information made available on the physical and chemical characteristics of degraded PHA from steam treatment, especially for low temperature range (below melting point). To date, steam hydrolysis of biopolyester at a low temperature range was only reported for poly-L-lactic acid (PLLA) [5]. In this study, degradation behavior and kinetics of PHB in steam-assisted degradation was investigated. PHB was degraded at temperatures below its melting temperature, *i.e.* 110 – 160°C and characterized for molecular weight, thermal properties and crystallinity. Molecular weight reduction during the steam hydrolysis is also discussed in order to suggest the ability to control PHB degradation via steam-assisted degradation with detail degradation behavior and kinetics.

### MATERIALS AND METHODS

---

#### Article history:

Received: 10 March 2022

Accepted: 7 June 2022

Published: 14 June 2022

---

#### E-mail addresses:

elmynahida@unikl.edu.my (E.N. Othman)

\*Corresponding Author

#### Materials

PHB natural origin powder with weight-average molecular weight ( $M_w$ ) of 390 kDa based on polystyrene standards (purchased from Sigma–Aldrich) and used as received. All other chemicals *i.e.* chloroform and deuterated-chloroform were of the highest purity commercially available and were used without further purification unless otherwise stated.

Methods

Preparation of PHB disk and degradation. PHB disks of  $400 \pm 50 \mu\text{m}$  in thickness were prepared by using pressurized vacuum molding machine set at 7 MPa for 1 minute. Approximately  $60 \pm 5 \text{ mg}$  of PHB powder was vacuum compressed at room temperature to form a disk of  $1.3 \times 0.40 \text{ cm}$  in diameter and thickness, respectively. Prepared disks were then kept in an airtight glass vial prior to use. Steam-assisted degradation of PHB disks were performed in a 100 mL miniclave (Buchi) made of SUS 316 filled with 50 mL of distilled water without submersion. The disks were hydrolyzed at the prescribed temperatures; A: 110 °C; B: 120 °C; C: 130 °C; D: 140 °C; E: 150 °C and F: 160 °C for 10 – 210 min. Internal temperature of the miniclave was thermostated within  $\pm 0.3^\circ\text{C}$ .

Characterization techniques

Degraded PHB disks weight loss % were calculated. The quantity of crotonic acid were monitored using High performance liquid chromatography (HPLC) (Shimadzu LC-10) equipped with a SPD-10A UV/VIS detector and an acid analysis column (Bio-rad Laboratories, Aminex HPX-87H ion exclusion column,  $300 \times 7.8 \text{ mm}$ ). Determination of chemical structures of original and hydrolyzed PHB films was carried out using a 500-MHz JEOL JNM-ECP500 FT NMR. All samples were dissolved in deuterated-chloroform ( $\text{CDCl}_3$ ) and analyzed. The chemical shifts were reported as  $\delta$  values (ppm) relative to internal tetramethylsilane (TMS) unless otherwise noted. Size exclusion chromatography (SEC) on a TOSOH HLC-8120 GPC was used to measure molecular weight of the PHB disk samples. It was equipped with refractive index (RI) and ultraviolet (UV) detectors. Low polydispersity polystyrene standards with  $M_n$  in a range of  $5.0 \times 10^2$  to  $1.11 \times 10^6$  from TOSOH Corporation were used for calibration. Thermal properties: glass transition temperature ( $T_g$ ), melting temperature ( $T_m$ ) and percentage of crystallinity ( $X_c$ ) were determined by differential scanning calorimeter (DSC) using Mettler Toledo instruments DSC 823E in a 3-step mode at 1st and 2nd-heating rate of  $10^\circ\text{C}/\text{min}$  and cooling rate of  $-20^\circ\text{C}/\text{min}$  under nitrogen flow of 20 mL/min. The selected temperature range was 25 -  $220^\circ\text{C}$  and the sample weight was in the range of 5.5 – 6.5 mg.

Evaluation of kinetic parameters, ( $k_{Mw}$ ) and activation energy ( $E_a$ )

Accurate determination of  $k_{Mw}$  and  $E_a$  values were made without any weight loss and the  $M_w$  was calculated within homogeneous random degradation before critical point. The slope of  $\ln M_w$  and  $\ln M_n$  had the similar slope pattern as compared to the theoretical plots [5].

RESULTS AND DISCUSSION

Morphological observation of steam-degraded PHB disks

The size and weight of PHB disks before and after hydrolysis were monitored. It was observed that the appearance of PHB disks treated at 110 – 150 °C remained unchanged and minimal weight loss (0.7 – 2.4 %) indicating the volatilization of low MW PHB fractions during steam-assisted degradation. On the other hand, a marked weight loss of 39.8 % was recorded when the PHB was treated at 160 °C (data not shown). Additionally, it was observed that the PHB disk was deformed when treated at 160 °C, unlike the other PHB disks treated at lower temperature which were still intact after treatment.

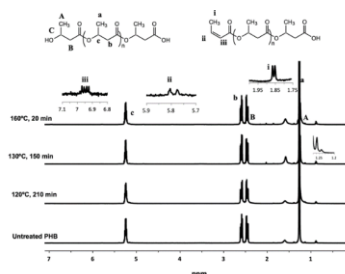
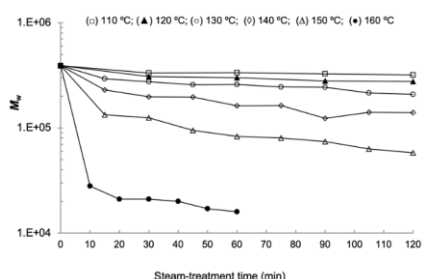


Fig. 1:  $M_w$  changes of PHB hydrolyzed at different reaction temperatures and steam-treatment time Fig. 2:  $^1\text{H}$  NMR spectra of original and steam hydrolyzed PHB

Molecular weight (MW) reduction

SEC analysis of hydrolyzed PHB disks showed that MW reduction was varied in the range of 15 – 96 % when treated at different temperature (Fig. 1). Overall, the MW reduction increased with the increase in reaction temperature. Relationship between MW changes and steam-treatment time at different reaction temperatures are plotted in Fig 2. Abrupt MW reduction was observed for PHB hydrolyzed at 160°C, whereby the MW value was drastically reduced by about 93% within the first 10 min of steam-treatment. The slope of the plot at 160°C is steeper than other plots, indicating that higher rate of degradation occurred at this temperature.

Chemical structure of hydrolyzed PHB by  $^1\text{H}$  NMR

Fig. 2 shows  $^1\text{H}$  NMR spectra of original and steam-degraded PHB at various treatment conditions. Original PHB spectrum consists of three types of proton in 3-HB unit with large and clear signals labeled as a ( $\delta = 1.27 \text{ ppm}$ ), b ( $\delta = 2.4 - 2.6 \text{ ppm}$ ) and c ( $\delta = 5.25 \text{ ppm}$ ) for methyl, methylene and methine groups, respectively (19). These main peaks were not significantly altered after steam-assisted degradation. However, minor signal at  $\delta = 1.23 \text{ ppm}$  was clearly detected when the PHB was degraded at 120 °C onwards. This peak was assigned to methyl group protons adjacent to hydroxyl end group, i.e.  $\text{HO-CH}(\underline{\text{CH}_3})$ . Interestingly, this was accompanied by additional of three proton signals in the  $^1\text{H}$  NMR spectrum (magnified and labelled as i, ii and iii in Fig 3), indicating that new chemical structure was produced during PHB degradation at this temperature. Three new signals at  $\delta = 1.85, 5.80$  and  $6.95 \text{ ppm}$  were observed and identified as methyl ( $\underline{\text{CH}_3}\text{-CH=CH-}$ ) and methine peaks ( $\text{CH}_3\text{-CH}=\underline{\text{CH}}\text{-}$  and  $\text{CH}_3\text{-CH}=\underline{\text{CH}}\text{-}$ ) of crotonyl terminus [6, 7]. Detailed analysis on the  $^1\text{H}$  NMR signals of

methyl group protons in chain-end units was conducted and listed in TABLE 1. It was observed that the intensity of methyl signal of hydroxyl terminus became higher as the PHB molecular weight reduced. However when the PHB was treated at 160 °C for 20 min, the intensity of the signal reduced even though the molecular weight value was almost similar with the PHB treated at 150°C for 150 min. The reduction in HO-CH(CH<sub>3</sub>) intensity which was accompanied by the appearance of crotonyl chain end signals, suggesting that mixed-degradation mechanisms occurred at 160°C to produce PHB with crotonyl terminus.

TABLE 1: Characterization of untreated and hydrolyzed PHB by GPC and <sup>1</sup>H NMR

Hydrolysis condition	M <sub>w</sub> (kDa)	<sup>1</sup> H NMR analysis (mol %)	
		Hydroxyl end	Crotonyl end
Untreated	390 ± 2.0	ND	ND
110°C, 210 min	290 ± 6.5	ND	ND
120°C, 210 min	245 ± 5.5	Shoulder peak	ND
130°C, 150 min	195 ± 7.5	16.7	ND
140°C, 150 min	140 ± 24.5	24.2	ND
150°C, 150 min	25 ± 2.0	29.6	ND
*160°C, 20 min	20 ± 1.0	16.5	0.8

ND – not detected \* Melt samples

The hydrolysis rate constant,  $k_{Mw}$  values were in the range of  $1.95 - 40.0 \times 10^{-5} s^{-1}$  for 110 – 150°C while  $E_a$  was recorded at 102 kJ/mol. On the other hand at 160 °C,  $k_{Mw}$  value was almost four times higher ( $150 \times 10^{-5} s^{-1}$ ) compared to the one at 150°C, and higher  $E_a$  at 116 kJ/mol was recorded for degradation at 110-160°C. The difference in  $E_a$  and  $k_{Mw}$  values at these two temperature ranges can be contributed by the physical and chemical structure changes in the steam-degraded samples. As being discussed earlier, at temperatures below 150°C, degradation solely occurred through hydrolysis while at above 150°C, additional mechanism *i.e.* β-chain scission took place. It is interesting to note that β-chain scission occurred in steam-assisted degradation, and the occurrence was temperature dependent. Generally, β-chain scission proceeds when a pseudo-six-membered transition structure is formed, which is normally induced by the molten state of the PHB. After steam treatment at 160°C, PHB disk was found deformed, indicated that the sample was melted during the reaction. This explains why β-chain scission occurred when the PHB was exposed to steam temperature of 160°C.

## CONCLUSIONS

Degradation behavior of PHB during the course of steam hydrolysis at temperatures below its melting temperature was clarified in this study. At temperature range of 110 – 150°C, the degradation occurred merely by random chain scission at the ester linkage, which suggested hydrolysis as the exclusive degradation mechanism. However, at 160°C, the degradation behavior changed as shown by the mixed degradation products. PHB treated by steam at 160°C generated low molecular weight PHB fractions with crotonyl chain ends as minor products, which indicated that chain scission by β-elimination occurred as an additional mechanism. Unexpected β-elimination scission of PHB during the course of steam degradation can be explained by the formation of transient six-membered ring, which occurs preferentially at molten state. Molecular weight reduction during the hydrolysis caused the lowering in melting point of lower molecular weight polymer chains, and hence provided favorable condition for the occurrence of the transient six-membered ring. Overall, the finding from this study provides new insight on the degradation behavior of PHB during steam hydrolysis. Kinetic study is currently in progress in order to further clarify the mechanisms involved in PHB steam degradation.

## ACKNOWLEDGEMENTS

The authors gratefully acknowledge Kyushu Institute of Technology (Kyutech) and Universiti Putra Malaysia for analytical supports and travel grants. The authors also would like to thank Mr Tanoe Shota, Mr Takaaki Maeda, Mr Kohtarō Watanabe, Mrs Rusnani Amirudin, Miss Shareena Safiai and Mr Mohd Naquib Mohammad from Kyutech, Universiti Putra Malaysia and Universiti Kuala Lumpur MICET for the helps during samples preparation and analysis. The authors also would like to acknowledge Universiti Kuala Lumpur for the provision of scholarship to the first author

## REFERENCES

- [1] Laycock B, Halley P, Pratt S, Werker A, Lant P. "The chemomechanical properties of microbial polyhydroxyalkanoates," *Prog Polym Sci*, vol. 38, pp. 536 - 583, 2013.
- [2] Špitalský Z, Lacík I, Lathová E, Janigová I, Chodák I. "Controlled degradation of polyhydroxybutyrate via alcoholysis with ethylene glycol or glycerol," *Polym Degrad Stab*, vol. 4, pp. 856 - 861, 2006.
- [3] Iwata T, Doi Y, Nakayama S, Sasatsuki H, Teramachi S. "Structure and enzymatic degradation of poly(3-hydroxybutyrate) copolymer single crystals with an extracellular PHB depolymerase from *Alcaligenes faecalis* T1," *Int J Biol Macromol*, vol 25, pp. 169 - 176. 1999.
- [4] Ariffin H, Nishida H, Shirai Y, Ali M. "Highly selective transformation of poly [(R) -3-hydroxybutyric acid ] into trans-crotonic acid by catalytic thermal degradation," *Polym Degrad Stab*, vol. 95, pp. 1375 - 1381, 2010.
- [5] Mohd-adnan A, Nishida H, Shirai Y. "Evaluation of kinetics parameters for poly ( L-lactic acid ) hydrolysis under high-pressure steam," *Polym Degrad Stab*. vol. 93, pp. 1053 – 1058, 2008.
- [6] Tokiwa Y, Ugwu CU. "Biotechnological production of (R)-3-hydroxybutyric acid monomer," *J Biotechnol*. vol. 132, pp. 264 – 272, 2007.
- [7] Ariffin H; Nishida H; Mohd Ali H; Shirai Y. "Chemical recycling of polyhydroxyalkanoates as a method towards sustainable development," *Biotechnol J*. vol. 5, pp. 484 – 492, 2010.



## NANOFILLER-CONTENT RUBBER COMPOSITES

A. S. Norfarhana<sup>1,2</sup>, R.A. Ilyas<sup>1,3\*</sup>, N. Ngadi<sup>1</sup>, A.H. Nordin<sup>1</sup>, Nur Hafizah Ab Hamid<sup>1</sup>

<sup>1</sup>*School of Chemical and Energy Engineering, Faculty of Engineering, Universiti Teknologi Malaysia, 81310 UTM Skudai, Johor, Malaysia*

<sup>2</sup>*Department of Petrochemical Engineering, Politeknik Tun Syed Nasir Syed Ismail, Pagoh Education Hub, 84600 Pagoh Muar Johor, Malaysia*

<sup>3</sup>*Centre for Advanced Composite Materials (CACM), Universiti Teknologi Malaysia (UTM), Johor Bahru 81310, Johor, Malaysia*

---

### ABSTRACT

The revolution of nanotechnology has introduced several innovative nanofiller-content materials that shows potential in polymer composites. Nanofillers such as silica, clay, carbon, natural fibers, nanocellulose, and others have been used to enhance the properties of polymers for various applications. The development of nanofiller-content rubber composites is a turning point in polymer research for many applications of industries. This review focuses on the recent advances in nanofiller-content nanocomposites and the techniques used to fabricate them on the successive property enhancements. The practical value of reinforcing nanofiller in rubber nanocomposites is extensively studied in terms of filler dispersion, processing, and mechanical properties of filled rubber compounds.

*Keywords:* nanofiller, rubber, nanocomposites, polymer matrix, preparation, mechanical properties.

---

### INTRODUCTION

Polymer composites have piqued researchers' interest for more than half a century, owing to the increasing demands for materials with unique properties [1]. To date, rubber-based polymer, known as elastomers, is commonly used for its high tensile strength, elasticity, flexibility, crack resistance, and ability to act as a flame retardant [2]. There are many applications for rubber composites that are directly related to human life, including car and aircraft tires, sports goods, glues, belts, footwear hose, gasket applications, and so on [3]. Due to its versatility and application volume, the elastomer is one of the most important used polymer composites. However, the low modulus and strength of natural rubber limit its applications. The mechanical properties of this group of materials have been improved significantly to expand their strengths and applications. The addition of reinforcing filler from various sources, as well as the aggregate size/aspect ratio, enhances their mechanical and thermal properties, crystallinity, and low cost [4]–[6]. To date, nanoscale fillers have received increased attention in both academia and industry for the success of rubber reinforcement due to their increased specific surface area compared to conventional fillers [7]. The most frequently used fillers in the rubber industry are carbon materials (carbon black (CB), carbon fiber (CF), carbon nanotubes (CNTs), graphite, graphene), inorganic particles (nanoclays, silica, calcium carbonate, talc, zinc oxide, titanium oxide) and biofillers (cellulose, husk, wood, coir) [4]. If well disseminated in the host medium, nanofillers are predicted to provide a high interface area with the polymeric medium, allowing for polymer-filler interactions [8]. This paper reviews the recent advances in nanofiller-content nanocomposites and the techniques used to fabricate them on the successive property enhancements, including the practical value of reinforcing nanofiller in rubber nanocomposites in terms of filler dispersion, processing, and mechanical properties of filled rubber compounds.

#### *Nanofillers-content rubber composites*

Nanofillers have gained a broad interest as reinforcing agents for elastomeric materials due to their large interfacial area with the polymeric medium, allowing for polymer-filler interactions [1], [8], [9]. There are two types of nanofillers used in the rubber industry, inorganic and organic nanofiller (Fig. 1). Silica and carbon black are the most commonly used filler in commercialised rubber products [6]. Silica (SiO<sub>2</sub>) is a spherical particle naturally which can be found in sand, quartz, quartzite, perlite, and Tripoli. Silica nanoparticles such as fumed silica, precipitated silica, and ground silica is commonly used in the rubber industry to enhance abrasion resistance and wet grip while lowering rolling resistance [10]. Nonetheless, silica with hydroxyl groups forms bundles between particles due to hydrogen bonding, which will result in poor dispersion and poor adhesion of polymer fillers [4]. In this regard, significant methods such as hybrid nanofillers are required. D'Arienzo et al.

[10] synthesized a novel hybrid nanofiller, silica nanoparticles @ polyhedral oligomeric silsesquioxane (SiO<sub>2</sub>@POSS) blending with SBR nanocomposites. The results found that the hybrid filler increases the material's tensile and air permeability properties. Meanwhile, carbon black is the foremost common material used to enhance filled rubber composites. But the use of carbon black as a prevalent filler to enhance the rubber strength is a main challenge from the environmental perspective [3]. Therefore, biobased filler is the most suitable alternative to replace the conventional filler.

Rubber composites reinforced with varieties of biofillers such as lignocellulosic fibers and nanocellulose have been the attention of researchers for many decades as a way to replace

---

#### *Article history:*

Received: 10 March 2022

Accepted: 7 June 2022

Published: 14 June 2022

---

#### *E-mail addresses:*

farahfarhana.as@gmail.com (A. S. Norfarhana)

ahmadilyasrushedan@yahoo.com (R.A. Ilyas)

norzita@utm.my (N. Ngadi)

abuhassannordin@gmail.com (A.H. Nordin)

nurhafizah.abhamid@utm.my (Nur Hafizah Ab Hamid)

\*Corresponding Author

non-renewable carbon black [11]. Fig. 1b shows the advantages of natural fiber-based rubber composites. Dominic et al. [12] synthesized chitin nanowhiskers from shrimp shell waste as a green filler in acrylonitrile-butadiene rubber and investigated the processing and performance properties of polymer composites. The results found that adding chitin nanowhiskers increased nanocomposites' tensile strength and tear strength by 116% and 54%, respectively. This is because the chitin nanowhiskers were dispersed out in the matrix in the right way. In addition, increased concentrations of chitin nanowhiskers significantly improved the thermal stability of nanocomposites. Although the addition of biofillers to the rubber matrix is a potential approach to the production of renewable and sustainable rubber, the hydrophilicity and surface features of the resultant rubber nanocomposites have a significant influence on their dispersion and interface qualities. In order to achieve better distribution and interfacial properties with the rubber matrix, it is common to employ biofillers with appropriate fabrication techniques [13].

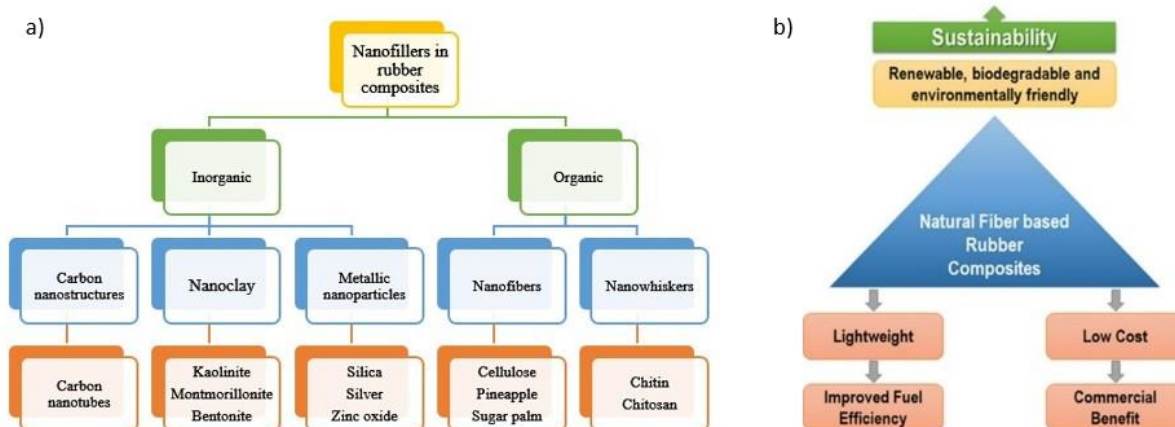


Fig. 1: a) Classification of nanofillers in rubber composites and b) the advantages of natural fiber-based rubber composites.

*Fabrication techniques of nanofiller-content rubber composites*

The dispersion of nanofiller in a polymer matrix can be controlled through a variety of fabrication techniques. TABLE 1 shows the various sources of nanofiller and fabrication methods that affect the properties of rubber nanocomposites. The most effective way to obtain nanofiller polymer composites for commercial applications is melt blending [2]. The procedure is completely solvent-free and environmentally friendly. Fillers were evenly distributed and mechanical reinforcement was achieved by melting a diene elastomer matrix with tailored nanocellulose powders with both a high specific surface area and an altered interface, as reported by Fumagalli et al. [14]. Another technique for rubber processing is two-roll mill which are effective dispersive mixer with the assistance of the operator. Azizli et al. [2] study the hybrid rubber nanocomposite blends based on (80/20) XNBR/EPDM containing different nanofiller compatibilizers by a two-roll mill technique. Dominic et al. [12] fabricated chitin nanowhiskers (CHNW) from shrimp shells in acrylonitrile butadiene rubber (NBR) matrix composites utilizing two-roll mills.

TABLE 1: Various sources of nanofiller, fabrication techniques and properties for rubber nanocomposites

Rubber polymer	Nanofiller sources	Fabrication techniques	Properties	Ref.
NR	Pineapple leaf CNC	Sulfur vulcanization (S-vul) and Electron beam vulcanization (EB)	<ul style="list-style-type: none"> <li>The sulfur-vulcanized composites had better mechanical properties chemical resistant than the irradiated composites. The CNCs/NR composite was best distributed at 2.5 parts per hundred (phr) resulted highest tensile strength compared to all loadings</li> </ul>	[15]
XNBR/EPDM	Cloisite Carbon black (CB) Nanosilica	Two-roll mill	<ul style="list-style-type: none"> <li>Incorporating fillers enhanced the modulus, tensile strength, hardness, fatigue strength, and elongation at break of composites</li> <li>The nanofillers enhanced thermal stability of composites and act as reinforcing impact and cure accelerators</li> </ul>	[2]
ENR	Tunicate CNC	Latex mixing	<ul style="list-style-type: none"> <li>The healing rate, tensile strength, and tensile modulus were greatly enhanced by the addition of nanofillers.</li> <li>The nanocomposites' better self-healing ability is due to the synergistic effect of molecular interdiffusion through slightly cross-linked rubber and enhanced hydrogen bonding supramolecular network between rubber and filler</li> </ul>	[16]

SBR	Hardwood pulp MFC & Cotton linter CNC	Melt blending	<ul style="list-style-type: none"> <li>• These nanofillers were efficiently dispersed into the hydrophobic matrix up to a volume fraction of 20%.</li> <li>• Covalently bonding nanocellulose to the rubber matrix resulted in an increase in strain stiffness.</li> </ul>	[14]
-----	--	---------------	--	------

\*NR=Natural rubber, CNC=cellulose nanocrystal, XNBR/EPDM=Carboxylated nitrile rubber/ Ethylene propylene diene monomer rubber, ENR=Epoxidized natural rubber, MFC=Microfibrillated cellulose

## CONCLUSIONS

Rubber composites exhibit elastic, flexible, ductile and rigid behaviors that are usually used in various applications such as tires, gloves, hoses, conveyor belts, toys, footwear, foam mattress, and so on. Rubber has always been compounded with fillers to meet the property requirements of a specific application. Recently, nanofillers have been added to rubbers to make them stronger, change their electrical or thermal conductivity, and make them easier to work with.

## ACKNOWLEDGEMENTS

The authors would like to thank Universiti Teknologi Malaysia and the Ministry of Education, Malaysia for their financial support. The authors would like express gratitude for the financial support received from the Universiti Teknologi Malaysia, project “The impact of Malaysian bamboos' chemical and fibre characteristics on their pulp and paper properties, grant number PY/2022/02318— Q.J130000.3851.21H99”. The research has been carried out under the program Research Excellence Consortium (JPT (BPKI) 1000/016/018/25 (57)) provided by the Ministry of Higher Education Malaysia (MOHE).

## REFERENCES

- [1] J. George and H. Ishida, “A review on the very high nanofiller-content nanocomposites: Their preparation methods and properties with high aspect ratio fillers,” *Prog. Polym. Sci.*, vol. 86, pp. 1–39, 2018, doi: 10.1016/j.progpolymsci.2018.07.006.
- [2] M. J. Azizli, M. Mokhtary, H. A. Khonakdar, and V. Goodarzi, “Hybrid Rubber Nanocomposites Based on XNBR/EPDM: Select the Best Dispersion Type from Different Nanofillers in the Presence of a Compatibilizer,” *J. Inorg. Organomet. Polym. Mater.*, vol. 30, no. 7, pp. 2533–2550, 2020, doi: 10.1007/s10904-020-01502-z.
- [3] K. Roy, S. C. Debnath, and P. Potiyaraj, “A critical review on the utilization of various reinforcement modifiers in filled rubber composites,” *J. Elastomers Plast.*, vol. 52, no. 2, pp. 167–193, 2020, doi: 10.1177/0095244319835869.
- [4] K. Song, *Micro- and nano-fillers used in the rubber industry*. Elsevier Ltd, 2017.
- [5] M. Mariano, N. El Kissi, and A. Dufresne, “Cellulose nanocrystal reinforced oxidized natural rubber nanocomposites,” *Carbohydr. Polym.*, vol. 137, pp. 174–183, 2016, doi: 10.1016/j.carbpol.2015.10.027.
- [6] N. Anizah, M. Aini, N. Othman, M. H. Hussin, and K. Sahakaro, “Hydroxymethylation-Modified Lignin and Its,” *Processes*, vol. 7, p. 315, 2019.
- [7] K. Sahakaro, *Mechanism of reinforcement using nanofillers in rubber nanocomposites*. Elsevier Ltd, 2017.
- [8] L. Bokobza, “Natural rubber nanocomposites: A review,” *Nanomaterials*, vol. 9, no. 1, 2019, doi: 10.3390/nano9010012.
- [9] A. S. Norfarhana, R. A. Ilyas, and N. Ngadi, “A review of nanocellulose adsorptive membrane as multifunctional wastewater treatment,” *Carbohydr. Polym.*, vol. 291, p. 119563, Sep. 2022, doi: 10.1016/j.carbpol.2022.119563.
- [10] M. D’Arienzo *et al.*, “Hybrid SiO<sub>2</sub>@POSS nanofiller: A promising reinforcing system for rubber nanocomposites,” *Mater. Chem. Front.*, vol. 1, pp. 1441–1452, 2017, doi: 10.1039/c7qm00045f.
- [11] Y. Zhou, M. Fan, L. Chen, and J. Zhuang, *Lignocellulosic fibre mediated rubber composites: An overview*, vol. 76. Elsevier Ltd, 2015.
- [12] D. C.D.M. *et al.*, “Chitin nanowhiskers from shrimp shell waste as green filler in acrylonitrile-butadiene rubber: Processing and performance properties,” *Carbohydr. Polym.*, vol. 245, p. 116505, 2020, doi: 10.1016/j.carbpol.2020.116505.
- [13] N. M. F. Hakimi *et al.*, “Surface modified nanocellulose and its reinforcement in natural rubber matrix nanocomposites: A review,” *Polymers (Basel)*, vol. 13, no. 19, pp. 1–24, 2021, doi: 10.3390/polym13193241.
- [14] M. Fumagalli *et al.*, “Rubber materials from elastomers and nanocellulose powders: Filler dispersion and mechanical reinforcement,” *Soft Matter*, vol. 14, no. 14, pp. 2638–2648, 2018, doi: 10.1039/c8sm00210j.
- [15] W. Chawalitsakunchai *et al.*, “Properties of natural rubber reinforced with nano cellulose from pineapple leaf agricultural waste,” *Mater. Today Commun.*, vol. 28, no. January, p. 102594, 2021, doi: 10.1016/j.mtcomm.2021.102594.
- [16] L. Cao, D. Yuan, C. Xu, and Y. Chen, “Biobased, self-healable, high strength rubber with tunicate cellulose nanocrystals,” *Nanoscale*, vol. 9, no. 40, pp. 15696–15706, 2017, doi: 10.1039/c7nr05011a.

## INFLUENCE OF FILAMENT FABRICATION PARAMETER ON TENSILE PROPERTIES OF 3D PRINTING PLA FILAMENT

S. Hamat<sup>1,2,\*</sup>, M.R. Ishak<sup>2,3,4</sup>, S.M. Sapuan<sup>4,5</sup>, N. Yidris<sup>2</sup>

<sup>1</sup>Faculty of Mechanical Technology Engineering, Universiti Malaysia Perlis, 02600 Ulu Pauh, Perlis Malaysia

<sup>2</sup>Department of Aerospace Engineering, Faculty of Engineering, Universiti Putra Malaysia, 43400 UPM Serdang Selangor, Malaysia

<sup>3</sup>Aerospace Malaysia Research Centre (AMRC), Universiti Putra Malaysia, Serdang 43400, Selangor, Malaysia

<sup>4</sup>Laboratory of Biocomposite Technology, Institute of Tropical Forestry and Forest Products (INTROP), Universiti Putra Malaysia, Serdang 43400, Selangor, Malaysia

<sup>5</sup>Advanced Engineering Materials and Composites Research Centre (AEMC), Department of Mechanical and Manufacturing Engineering, Universiti Putra Malaysia, Serdang 43400, Selangor, Malaysia

---

### ABSTRACT

As known Polylactic acid (PLA) is a popular and widely used thermoplastic material used in fused filament fabrication (FDM) due to its biodegradability and biocompatibility. The aim of this paper is to study the effect of extrusion parameters on the quality of the 3D printing filament. The study began by extruding a 3D850D grade PLA pellet from Ingeo Natureworks into a single filament extruder machine with an extrusion temperature range of 170 °C to 190 °C and a screw rate of 2rpm to 6rpm. The 90° raster angle of line infill pattern with 100% infill density was used for the 3D printing specimens. Taguchi method was implemented to design the experiment. Mechanical test standards such as ASTM D638 were used for tensile testing to analyze the strength quality of the extruded PLA filament.

*Keywords:* polymer composite, biodegradable filament, polylactic acid, 3D printing, tensile test

---

### INTRODUCTION

3D printing refers to rapid prototyping (RP) or additive manufacturing (AM), which is a process of depositing materials layer by layer to create artifacts from a 3D model created by using CAD software and the G-codes are then transferred into a 3D printer for fabrication [1]. Since the filament is the main element for efficient 3D printing applications, hence the creation of appropriate filaments has piqued the interest of both industry and academics. The filament used in the 3D printing is made of thermoplastic polymers such as Polylactic acid (PLA), Acrylonitrile-butadiene-styrene (ABS), Polycarbonate (PC), and Polyamide (PA)[2]. Polylactic acid (PLA) as a biodegradable material is becoming a famous topic in the polymetric field as the awakening of economic preservation senses has arisen. Fernandez-Vicente et al. studied the influence of the infill parameters for 3D printing on the tensile properties of the product, and they concluded that using 100% infill density and the rectilinear pattern shows the higher tensile strength among the parameter used[3]. Then, to improve the tensile strength of the 3D printing specimen, the Taguchi method as one of the Design of Experiment (DOE) analysis techniques [4,5] will be implemented using five-level factors in this research.

### MATERIALS AND METHODS

#### *Materials*

3D850 grade PLA (purchased from Ingeo Natureworks) pellets for 3D printing monofilament fabrication were used in this study.

#### *Methods*

The 3D850 grade PLA pellets were dried at 80°C for 8 hours in the oven to remove moisture from the pellets. The pellets are then will be fed into the tabletop single screw machine with an interval of extrusion temperature of 25°C and an interval extrusion speed of 1 rpm to fabricated into filaments. The temperature used for the extrusion is 165°C,170°C,175°C,180°C, and 185°C. Then, the extrusion speed used is 2rpm, 3rpm, 4rpm, 5rpm and 6rpm were implemented as Fig. 1 shows the example of extruded filament shape in different parameters. The effect of filament extrusion parameters such as extrusion speed and temperature on the diameter and tensile properties of the PLA filament was investigated. The diameter of the

filament was measured using the vernier caliper every 1 meter during extrusion. Five specimens were designed using CATIA software and printed using a Qidi X-Max 3D printer from each combination of the extruding parameters according to ASTM D638 specimen design [6].

---

#### *Article history:*

Received: 10 March 2022

Accepted: 7 June 2022

Published: 14 June 2022

---

#### *E-mail addresses:*

\*sanusi@unimap.edu.my (S. Hamat)

mohdridzwan@upm.edu.my (M.R.Ishak)

sapuan@upm.edu.my (S. M. Sapuan)

nyidris@upm.edu.my (N. Yidris)

\*Corresponding Author

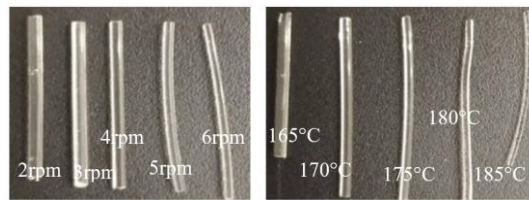


Fig.1 Fabricated filament shape at different speeds and temperature

TABLE 1:3D Printing parameters

Parameter	Value
Extruder temperature(°C)	210
Bed temperature(°C)	60
Printing speed(mm/s)	60
Nozzle diameter(mm)	0.4
Infill pattern	Line
Infill density (%)	100

TABLE 2: Filament fabrication factor considering the level

Extrusion factors	Levels					Unit
	1	2	3	4	5	
Extrusion temperature)	165	170	175	180	185	°C
Extrusion speed (rpm)	2	3	4	5	6	rpm

The infill pattern chosen for the specimens is a line pattern of 90° raster angle with an infill density of 100% to achieve the ultimate strength of the specimens and constant printing parameters, as a list in TABLE 1. The tensile testing was performed using the Universal Testing Machine (UTM) with 10kN pulling force and with a pulling speed of 1mm/min until the testing specimen broke. The ultimate tensile strength was calculated based on the basic stress formula. As a reference, the commercial 3D printing filament is  $1.75 \pm 0.05\text{mm}$ [10] and 26.4MPa for ultimate tensile strength [7]. The filament fabrication factor considering the level is shown in TABLE 2 above. Since only two factors and five levels for each parameter were studied so the Taguchi method with two factors and five levels in the equation of  $N = 5^2$ , hence an orthogonal array of  $L_{25}(5^2)$  was used which mean total of 25-runs will be done for the test parameters.

## RESULTS AND DISCUSSION

### Effect of extrusion temperature and screw speed on Ultimate Tensile Strength of PLA filament

The ultimate tensile strength of the filaments is essential in their applicability. A brittle filament will break during the printing process and affect the printing process's continuation. As seen in TABLE 3, the ultimate tensile strength recorded at 175 °C and 180°C is with the lowest stress produced of 24.35 MPa and the highest stress recorded is about 27.85 MPa, which is within the tolerance of the commercial 3D printing filament, around 26.4MPa. The results obtained for 165°C and 170°C are slightly lower than the commercial ultimate tensile strength as a result. It was recorded between 21.63MPa to 25.24MPa. In contrast, 185°C recorded the lowest ultimate tensile strength among the five extruding temperatures used, as it recorded below 20.5MPa. Plasticization of the filament may occur due to thermal degradation as the maximum melting point for 3D850 PLA is over 180°C[8]. Hence this may affect the mechanical properties of the PLA filament, the Young Modulus and the yield strength at 175°C were determined via the plotted stress-strain graph shown in Fig. 2 below. The Young modulus represents the material's modulus of elasticity and is represented by the relationship between the tensile stress and the tensile strain in the linear elastic region. As can be seen in TABLE 4 below, at an extrusion temperature of 175°C, the highest yield strength recorded is at 5rpm with 27.63 MPa yield stress. The lowest yield strength was recorded at 6rpm with a yield strength of 23.59 MPa. The fracture region and its stress-strain graph for each specimen at 175 °C under different extrusion speeds are shown in TABLE 7 below.

TABLE 3: Ultimate tensile stress under different extrusion temperatures and extrusion speed

Speed\Temperature	165°C	170°C	175°C	180°C	185°C
2 rpm	21.63 MPa	22.55MPa	25.58 MPa	24.35 MPa	18.59MPa
3 rpm	22.56MPa	22.76MPa	25.87 MPa	24.68 MPa	19.73 MPa
4 rpm	23.65MPa	24.23MPa	26.67 MPa	26.25 MPa	19.89 MPa
5 rpm	24.59MPa	25.24MPa	27.85MPa	27.11 MPa	20.56 MPa
6 rpm	22.73MPa	24.94MPa	25.97 MPa	25.65MPa	19.35 MPa

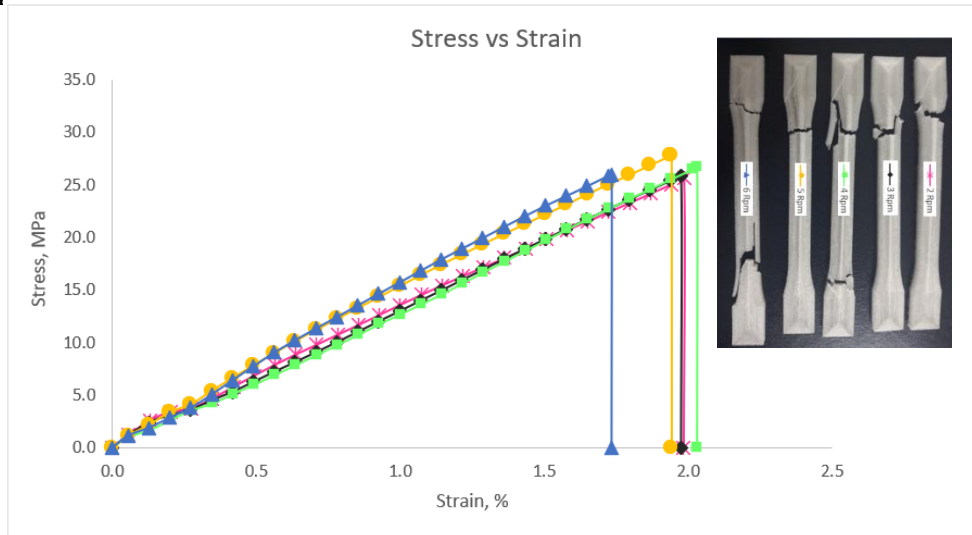


Fig. 2: Stress-strain graph at an extrusion temperature of 175 °C

TABLE 4: Mechanical tensile properties of filament under extrusion temperature of 175°C

Speed	Ultimate tensile strength	Yield stress	Young modulus
2 rpm	25.58 MPa	25.16 MPa	0.0130 GPa
3 rpm	25.87 MPa	25.70 MPa	0.0131 GPa
4 rpm	26.67 MPa	25.81 MPa	0.0133 GPa
5 rpm	27.85MPa	27.63 MPa	0.0143 GPa
6 rpm	25.97 MPa	23.59 MPa	0.0153 GPa

*Effect of extrusion temperature and screw speed on Diameter of PLA filament*

The diameter of the filament obtained from the extruding was recorded in TABLE 5 below. As the extrusion speed remained constant, the diameter of the filament extruded decreased with the extrusion temperature increasing. For example, at an extrusion speed of 4rpm, the diameter of the filament decreases from 1.94mm to 1.62mm with increasing temperature. When the extrusion temperature is constant, the diameter of the filament was observed to increase with the extrusion speed, as at an extrusion temperature of 175°C, the diameter of the filament increases from 1.71mm to 1.79mm. This may be due to the volume of PLA accumulated at the die increases; hence larger diameter filament will be produced. The diameter of filament decreases with the increasing temperature may be due to when the temperature increases will reduce the viscosity of the PLA and result in an increasing the melting rate of the plastic; hence slimmer filament will be produced with speed stayed constants. The result was proven in previous Fig. 1 above.

TABLE 5: Diameter of filament under different extrusion temperatures and extrusion speed.

Speed\Temperature	165°C	170°C	175°C	180°C	185°C
2 rpm	1.85mm	1.78 mm	1.71 mm	1.68 mm	1.48 mm
3 rpm	1.89 mm	1.80 mm	1.72 mm	1.70 mm	1.58 mm
4 rpm	1.94 mm	1.82 mm	1.75 mm	1.75 mm	1.62 mm
5 rpm	1.96 mm	1.88 mm	1.77 mm	1.76 mm	1.63 mm
6 rpm	1.97 mm	1.92 mm	1.79 mm	1.80 mm	1.66 mm

**CONCLUSIONS**

PLA is a biodegradable thermoplastic and is one of the most common filament materials used in the 3D printing industry. The effect of process parameters such as extrusion temperature and screw speed on the tensile properties of the PLA filament produced via the FFF method was studied. The optimum parameter for ultimate tensile strength was obtained at an extrusion temperature of 175 °C to 180°C and screw speed of 2-5 rpm as the filament extruded meets the required diameter of commercial 3D printing filament. The compression and flexural validation experiment remain a future work to study the effect of design parameters on the quality of the PLA filament.

**ACKNOWLEDGEMENTS**

The authors would like to thank the Faculty of Mechanical Engineering Technology, Universiti Malaysia Perlis (UniMAP), for the laboratories and research facilities. This research was supported and funded by Fundamental Research Grants Scheme (FRGS) under a grant number of FRGS/1/2019/TK03/UNIMAP/03/5 from the Ministry of Higher Education Malaysia.

**REFERENCES**

- [1] X. Wang, M. Jiang, Z. Zhou, J. Gou, and D. Hui, "3D printing of polymer matrix composites: A review and prospective," *Compos. Part B Eng.*, vol. 110, pp. 442–458, 2017, doi: 10.1016/j.compositesb.2016.11.034.
- [2] J. M. Pearce, "Digital Commons @ Michigan Tech Mechanical Properties of Components Fabricated with Open-Source 3-D Printers Under Realistic Environmental Conditions," vol. 246, pp. 242–246, 2014.
- [3] M. Fernandez-Vicente, W. Calle, S. Ferrandiz, and A. Conejero, "Effect of Infill Parameters on Tensile Mechanical Behavior in Desktop 3D Printing," *3D Print. Addit. Manuf.*, vol. 3, no. 3, pp. 183–192, 2016, doi: 10.1089/3dp.2015.0036.
- [4] S. M. Karazi, M. Moradi, and K. Y. Benyounis, *Statistical and Numerical Approaches for Modeling and Optimizing Laser Micromachining Process-Review*. Elsevier Ltd., 2019.
- [5] M. J. Cimbala, "Taguchi Orthogonal Arrays," *Instrumentation, Meas. Stat.*, no. September, pp. 4–6, 2014, [Online]. Available: [https://www.mne.psu.edu/me345/Lectures/Taguchi\\_orthogonal\\_arrays.pdf](https://www.mne.psu.edu/me345/Lectures/Taguchi_orthogonal_arrays.pdf).
- [6] American Society for Testing and Materials, "ASTM D638-14, Standard Practice for Preparation of Metallographic Specimens," *ASTM Int.*, vol. 82, no. C, pp. 1–15, 2016, doi: 10.1520/D0638-14.1.
- [7] C. M. Dc, "Technical data sheet," vol. 41, no. 0, pp. 2–4, 2014.
- [8] M. Applications and P. Information, "Ingeo Biopolymer 3D850 Technical Data Sheet 3D Printing Monofilament – High Heat Grade," pp. 1–5.

## EXPERIMENTAL ANALYSIS OF COMPRESSION PROPERTIES IN 3D PRINTING PLA FILAMENT

S. Hamat<sup>1,2,\*</sup>, M.R. Ishak<sup>2,3,4</sup>, S.M. Sapuan<sup>4,5</sup>, N. Yidris<sup>2</sup>

<sup>1</sup>Faculty of Mechanical Technology Engineering, Universiti Malaysia Perlis, 02600 Ulu Pauh, Perlis Malaysia

<sup>2</sup>Department of Aerospace Engineering, Faculty of Engineering, Universiti Putra Malaysia, 43400 UPM Serdang Selangor, Malaysia

<sup>3</sup>Aerospace Malaysia Research Centre (AMRC), Universiti Putra Malaysia, Serdang 43400, Selangor, Malaysia

<sup>4</sup>Laboratory of Biocomposite Technology, Institute of Tropical Forestry and Forest Products (INTROP), Universiti Putra Malaysia, Serdang 43400, Selangor, Malaysia

<sup>5</sup>Advanced Engineering Materials and Composites Research Centre (AEMC), Department of Mechanical and Manufacturing Engineering, Universiti Putra Malaysia, Serdang 43400, Selangor, Malaysia

---

### ABSTRACT

Despite its biodegradability and biocompatibility, Polylactic acid (PLA) is the most popular thermoplastic material used in fused filament fabrication (FFF). This research aims to investigate the impact of extrusion settings on 3D printing filament quality. Extruding 3D850D grade PLA pellets from Ingeo Natureworks into a single filament extruder machine with an extrusion temperature range of 170 °C to 190 °C and a screw rate of 2rpm to 6rpm was the first step in the experiment. The 3D printing specimens were created using a 90° raster angle line infill pattern with a density of 100% infill. For the investigation, the Taguchi method was implemented. Compression testing was conducted using compression mechanical test standards ASTM D695.

*Keywords:* polymer composite, biodegradable filament, polylactic acid, 3D printing, compression test

---

### INTRODUCTION

Rapid prototyping (RP) or additive manufacturing (AM) is a process of depositing materials layer by layer to construct a product[1]. The model is created in CAD software, and the control codes are generated by slicing software layer by layer. Finally, the printer may print the components based on control codes. TABLE 1 shows the 3D printing parameters that were employed in this study. Because the filament is the primary component of efficient 3D printing applications, the development of suitable filaments has aroused the interest of both industry and academia. The thermoplastic polymers used in 3D printing filament include Polylactic acid (PLA), Acrylonitrile-butadiene-styrene (ABS), Polycarbonate (PC), and Polyamide (PA)[2]. As economic preservation instincts awaken, polylactic acid (PLA) as a biodegradable material is becoming a popular issue in the polymetric realm. Brischetto et al. studied the compressive behavior of the FDM PLA model using ASTM D695[3], while Amza et al. and Farah et al. investigated the PLA mechanical characteristics and their application in the medical field and found the strength improvement in terms of compressive strength in 3d printed medical part [4]. Then, to improve the compressive strength of the 3D printing specimen in this research, the Taguchi method as one of the Design of Experiment (DOE) analysis techniques [4,5] will be implemented using five-level factors.

### MATERIALS AND METHODS

#### *Materials*

3D850 grade PLA (purchased from Ingeo Natureworks) pellets for 3D printing monofilament fabrication were used in this study.

#### *Methods*

The 3D850 grade PLA pellets were dried in the oven at 80°C for 8 hours to removed moisture from the pellets. The pellets will then be fed into a desktop single screw machine with an extrusion temperature interval of 25°C and an extrusion speed interval of 1rpm to be blended into filaments. Temperatures utilized for extrusion are 165°C, 170°C, 175°C, 180°C, and 185°C. Extrusion speeds of 2rpm, 3rpm, 4rpm, 5rpm, and 6rpm are employed as Fig. 1 shows the example of extruded filament shape in different parameters. The thickness and compression properties of the PLA filament were examined regarding filament

extrusion parameters such as extrusion speed and temperature. During extrusion, the diameter of the filament was measured with a caliper every 1 meter. The cuboid shape specimen was printed using a Qidi X-Max 3D printer according to the dimension in standard ASTM D695. The infill pattern chosen for the specimens is a line pattern of 90° raster angle with an infill density of 100% to achieve the ultimate strength of the specimens.

---

#### *Article history:*

Received: 10 March 2022

Accepted: 7 June 2022

Published: 14 June 2022

---

#### *E-mail addresses:*

sanusi@unimap.edu.my (S. Hamat)

mohdridzwan@upm.edu.my (M.R.Ishak)

sapuan@upm.edu.my (S. M. Sapuan)

nyidris@upm.edu.my (N. Yidris)

\*Corresponding Author



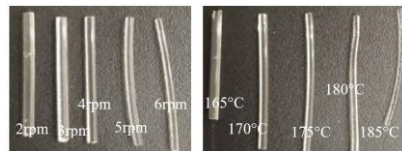


Fig.1 Fabricated filament shape at different speeds and temperatures

The compression testing was performed using the Universal Testing Machine (UTM) with 10kN compression force and with a pulling speed of 5mm/min until the testing specimen broke. The ultimate tensile strength was calculated based on the basic stress formula. The filament fabrication factor considering the level is shown in TABLE 2 below. Since only two factors with five levels for each parameter were studied, the Taguchi method with two factors and five levels in the equation of  $N = 5^2$  is applied. Hence an orthogonal array of  $L_{25}(5^2)$  was used, which means a total of 25-runs will be done for the test. As a reference, the commercial 3D printing filament is  $1.75 \pm 0.05\text{mm}$ [9] and 26.4MPa for ultimate tensile strength[7].

TABLE 2: Filament fabrication factor considering the level

Extrusion factors	Levels					Unit
	1	2	3	4	5	
Extrusion temperature)	165	170	175	180	185	°C
Extrusion speed (rpm)	2	3	4	5	6	rpm

## RESULTS AND DISCUSSION

### Effect of extrusion temperature and screw speed on Ultimate Tensile Strength of PLA filament

The filament's ultimate tensile strength is critical to its applicability as brittle filament will break throughout the printing process and will cause incomplete printing. As shown in TABLE 3, the ultimate tensile strength measured at 175°C and 180°C has minimum stress of 24.56 MPa and maximum stress of 27.99 MPa, which is within the tolerance of commercial 3D printing filament, which is around 26.4MPa. The findings obtained at 165°C and 170°C are slightly lower than the commercial ultimate tensile strength, ranging from 21.73MPa to 25.34MPa. While 185°C had the lowest ultimate tensile strength of the five extruding temperatures tested, it was less than 20.66MPa. Due to the maximum melting temperature of 3D850 PLA being over 180°C, plasticization of the filament may occur due to heat deterioration which may cause alteration in the mechanical properties of the PLA filament [8], as Fig. 2 shows the deformation of specimen in different temperature during the compression test. Fig. 3 show the stress-strain curve under 175°C with different extrusion speed. As can be seen in TABLE 4 below, at an extrusion temperature of 175°C, the highest yield strength recorded is at 4rpm with 5.01 MPa yield stress. The lowest yield strength was recorded at 6rpm with a yield strength of 0.15 MPa.

TABLE 3: Ultimate tensile strength under different extrusion temperatures and extrusion speed

Speed\Temperature	165°C	170°C	175°C	180°C	185°C
2 rpm	22.63 MPa	22.68MPa	25.38 MPa	24.56 MPa	18.69MPa
3 rpm	22.89MPa	22.81MPa	25.77 MPa	24.78 MPa	19.83 MPa
4 rpm	23.65MPa	24.26MPa	26.63 MPa	26.28 MPa	19.99 MPa
5 rpm	24.32MPa	25.34MPa	27.99MPa	27.21 MPa	20.66 MPa
6 rpm	21.73MPa	24.92MPa	25.88 MPa	25.75MPa	19.45 MPa



Fig. 2: Compression Specimen (a) before the test (b) after the test

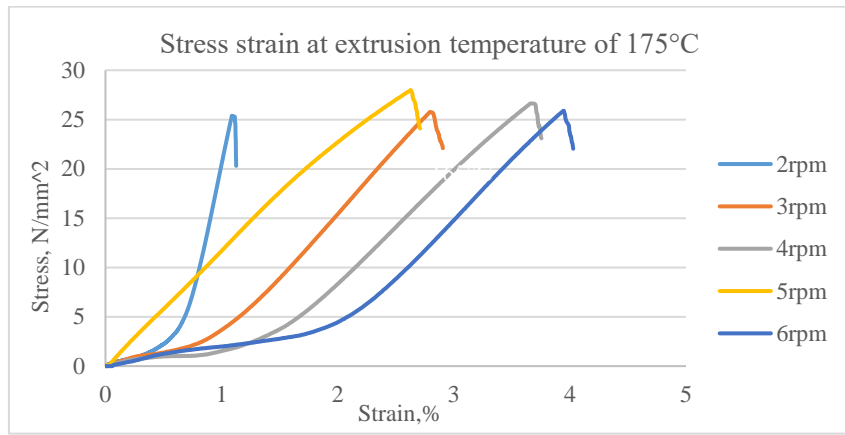


Fig. 3: Stress-strain graph at 175°C

TABLE 4: Mechanical strength of filament at an extrusion temperature of 175°C

Speed	Ultimate tensile strength	Yield stress	Young modulus
2 rpm	25.38 MPa	1.91 MPa	0.0042 GPa
3 rpm	25.77 MPa	4.27 MPa	0.0040 GPa
4 rpm	26.63 MPa	5.01 MPa	0.0030 GPa
5 rpm	27.99 MPa	1.28 MPa	0.0108 GPa
6 rpm	25.88 MPa	0.15 MPa	0.0015 GPa

*Effect of extrusion temperature and screw speed on Diameter of PLA filament*

The diameter of the filament formed during extrusion is shown in TABLE 5 below. As the extrusion speed stayed constant, the diameter of the extruded filament shrank as the extrusion temperature rose. For example, at 4rpm extrusion speed, the diameter of the filament reduces from 1.93mm to 1.64mm as the temperature rises. When the extrusion temperature is constant, the diameter of the filament grows with the extrusion speed, as at 175°C, the diameter of the filament increases from 1.70mm to 1.79mm. This could be because the volume of PLA collected at the die grows, resulting in a greater diameter filament. The diameter of the filament lowers with rising temperature, maybe because increasing the temperature reduces the viscosity of the PLA and so increases the melting rate of the plastic, resulting in a slimmer filament with constant speed. The outcome is seen in Fig 1 previously.

TABLE 5: Diameter of filament under different extrusion temperatures and extrusion speed.

Speed\Temperature	165°C	170°C	175°C	180°C	185°C
2 rpm	1.84mm	1.76 mm	1.70 mm	1.68 mm	1.48 mm
3 rpm	1.88 mm	1.79 mm	1.73 mm	1.70 mm	1.58 mm
4 rpm	1.93 mm	1.81 mm	1.75 mm	1.75 mm	1.64 mm
5 rpm	1.95 mm	1.86 mm	1.77 mm	1.76 mm	1.65 mm
6 rpm	1.96 mm	1.93 mm	1.79 mm	1.80 mm	1.66 mm

**CONCLUSIONS**

PLA is a biodegradable thermoplastic that is widely used in the 3D printing industry as filament material. The effect of process parameters like extrusion temperature and screw speed on the compression behavior of PLA filament generated using the FFF method was investigated. As the filament extruded fulfills the specified diameter of the commercial 3D printing filament, the optimal parameter for ultimate tensile strength was determined at an extrusion temperature of 175 °C to 180 °C and screw speed of 2-5 rpm. The tensile and flexural validation experiments will be studied further in the future to learn more about the effect of design parameters on the quality of the PLA filament.

**ACKNOWLEDGEMENTS**

The authors would like to express their gratitude to the Faculty of Mechanical Engineering Technology at Universiti Malaysia Perlis (UniMAP) for providing laboratories and research facilities. The Malaysian Ministry of Higher Education supported and sponsored this research under the Fundamental Research Grants Scheme (FRGS) with grant number FRGS/1/2019/TK03/UNIMAP/03/5.

**REFERENCES**

[1] X. Wang, M. Jiang, Z. Zhou, J. Gou, and D. Hui, “3D printing of polymer matrix composites: A review and prospective,” *Compos. Part B Eng.*, vol. 110, pp. 442–458, 2017, doi: 10.1016/j.compositesb.2016.11.034.

[2] J. M. Pearce, “Digital Commons @ Michigan Tech Mechanical Properties of Components Fabricated with Open-Source 3-D Printers Under Realistic Environmental Conditions,” vol. 246, pp. 242–246, 2014.

## ***The International Symposium on Polymeric Materials 2022***

- [3] S. Brischetto and R. Torre, “Tensile and Compressive Behavior in the Experimental Tests for PLA Specimens Produced via Fused Deposition Modelling Technique,” 2020, doi: 10.3390/jcs4030140.
- [4] S. Farah, D. G. Anderson, and R. Langer, “Physical and mechanical properties of PLA , and their functions in widespread applications — A comprehensive review ☆,” *Adv. Drug Deliv. Rev.*, vol. 107, pp. 367–392, 2016, doi: 10.1016/j.addr.2016.06.012.
- [5] S. M. Karazi, M. Moradi, and K. Y. Benyounis, *Statistical and Numerical Approaches for Modeling and Optimizing Laser Micromachining Process-Review*. Elsevier Ltd., 2019.
- [6] M. J. Cimbala, “Taguchi Orthogonal Arrays,” *Instrumentation, Meas. Stat.*, no. September, pp. 4–6, 2014, [Online]. Available: [https://www.mne.psu.edu/me345/Lectures/Taguchi\\_orthogonal\\_arrays.pdf](https://www.mne.psu.edu/me345/Lectures/Taguchi_orthogonal_arrays.pdf).
- [7] Z. Raheem, “Designation : D695 – 15 Standard Test Method for Compressive Properties of Rigid Plastics 1 Standard Test Method for Compressive Properties of Rigid Plastics 1,” no. July, 2019, doi: 10.1520/D0695-15.
- [8] C. M. Dc, “Technical data sheet,” vol. 41, no. 0, pp. 2–4, 2014.

## **EFFECT OF FILAMENT FABRICATION PARAMETER ON FLEXURAL PROPERTIES OF 3D PRINTING PLA FILAMENT**

S. Hamat<sup>1,2,\*</sup>, M.R. Ishak<sup>2,3,4</sup>, S.M. Sapuan<sup>4,5</sup>, N. Yidris<sup>2</sup>

<sup>1</sup>*Faculty of Mechanical Technology Engineering, Universiti Malaysia Perlis, 02600 Ulu Pauh, Perlis Malaysia*

<sup>2</sup>*Department of Aerospace Engineering, Faculty of Engineering, Universiti Putra Malaysia, 43400 UPM Serdang Selangor, Malaysia*

<sup>3</sup>*Aerospace Malaysia Research Centre (AMRC), Universiti Putra Malaysia, Serdang 43400, Selangor, Malaysia*

<sup>4</sup>*Laboratory of Biocomposite Technology, Institute of Tropical Forestry and Forest Products (INTROP), Universiti Putra Malaysia, Serdang 43400, Selangor, Malaysia*

<sup>5</sup>*Advanced Engineering Materials and Composites Research Centre (AEMC), Department of Mechanical and Manufacturing Engineering, Universiti Putra Malaysia, Serdang 43400, Selangor, Malaysia*

---

### **ABSTRACT**

Polylactic acid (PLA) is a popular thermoplastic material used in fused deposition modeling (FDM) for its biodegradability and biocompatibility. The purpose of this research is to investigate the impact of extrusion settings on the flexural behavior of 3D printing PLA filament. By extruding 3D850D grade PLA pellets from Ingeo Natureworks with an extrusion temperature range of 170 °C to 190 °C and a screw rate of 2rpm to 6rpm, the quality of the produced filament was studied. For the 3D printed specimen, a 90° raster angle of line infill pattern with 100% infill density was employed. The experiment was designed using the Taguchi technique. Finally, flexural testing was performed by using mechanical test standards of ASTM D790 to study the effect of extrusion parameters on 3D printing specimens.

*Keywords:* polymer composite, biodegradable filament, polylactic acid, 3D printing, flexural test, FFF

---

### **INTRODUCTION**

3D printing refers to rapid prototyping (RP) or additive manufacturing (AM), which is a process of depositing materials layer by layer to create artifacts from a 3D model created by using CAD software and the G-codes are then transferred into a 3D printer for fabrication [1]. Since the filament is the main element for efficient 3D printing applications, hence the creation of appropriate filaments has piqued the interest of both industry and academics. As the awaking of economic preservation senses has developed nowadays, polylactic acid (PLA) as a biodegradable substance is becoming a popular issue in the polymetric field [2]. For example, Christiyan et al. and Rodriguez et al., in their recent studies, have concluded that the flexural properties of PLA components produced under various 3D printing conditions and parameters such as orientation, layer thickness and printing speed would influence the flexural properties of the 3D printed parts[3,4]. Then, to improve the flexural strength of the 3D printing specimen, the Taguchi method as one of the Design of Experiment (DOE) analysis techniques [5] will be implemented using five-level factors in this research.

### **MATERIALS AND METHODS**

#### *Materials*

3D850 grade PLA (purchased from Ingeo Natureworks) pellets for 3D printing monofilament fabrication were used in this study.

#### *Methods*

To eliminate moisture from the 3D850 quality PLA pellets, they were oven-dried for 8 hours at 80°C [6]. The pellets will then be put into a desktop single screw machine where they will be extruded into filaments at a temperature of 25°C and a speed of 1rpm. The temperature of the single screw extruder will be set as follows. 165°C, 170°C, 175°C, 180°C, and 185°C are the temperatures utilized for extrusion. Next, 2rpm, 3rpm, 4rpm, 5rpm, and 6rpm of extrusion speeds were employed. The impact of filament extrusion parameters such as extrusion speed and temperature on the diameter and tensile characteristics of PLA filament was studied. During extrusion, the diameter of the filament was measured with a vernier caliper every 1 meter as Fig. 1 shows the example of extruded filament shape in different parameters. From each combination of extruding parameters, five

specimens were created using CATIA software and manufactured using a Qidi X-Max 3D printer according to the ASTM D790 for the flexural testing of rigid plastic. Then, the infill pattern of a line with a 90° raster angle and a density of 100% was used to obtain the specimens' maximal strength.

---

#### *Article history:*

Received: 10 March 2022

Accepted: 7 June 2022

Published: 14 June 2022

---

#### *E-mail addresses:*

sanusi@unimap.edu.my (S. Hamat)

mohdridzwan@upm.edu.my (M.R.Ishak)

sapuan@upm.edu.my (S. M. Sapuan)

nyidris@upm.edu.my (N. Yidris)

\*Corresponding Author

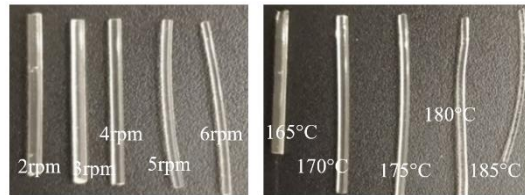


Fig.1 : Fabricated filament shape at different speeds and temperature

Next, the Universal Testing Machine (UTM) was used to do flexural testing with a 10kN drawing force and a 5mm/min pulling speed until the testing specimen broke. The gauge length used for the flexural test is 50 mm, as shown in Fig. 2. Then, the ultimate tensile strength was calculated based on the basic stress formula. As a reference, the commercial 3D printing filament is  $1.75 \pm 0.05\text{mm}$  [7] and 26.4MPa for ultimate tensile strength [8]. The filament fabrication factor considering the level is shown in TABLE 1 below. Since only two factors and five levels for each parameter were studied, the Taguchi method with two factors and five levels in the equation of  $N = 5^2$  is applied. Hence an orthogonal array of  $L_{25}(5^2)$  which mean the total of 25-runs will be done for the test parameters.



Fig. 2: Setting of specimens with 50mm gauge length

TABLE 1: Filament fabrication factor considering the level

Extrusion factors	Levels					Unit
	1	2	3	4	5	
Extrusion temperature)	165	170	175	180	185	°C
Extrusion speed (rpm)	2	3	4	5	6	rpm

## RESULTS AND DISCUSSION

### Effect of extrusion temperature and screw speed on Ultimate Tensile Strength of PLA filament

The printing process will be disrupted if a fragile filament breaks during the printing process; hence the filament must be able to within high stress or force. As shown in TABLE 2, the ultimate tensile strength measured at 175°C and 180°C has the lowest stress of 24.55 MPa and maximum stress of 27.18 MPa, both of which are within the 26.4MPa tolerance of commercial 3D printing filament. The findings for 165°C and 170°C were marginally lower than the commercial ultimate tensile strength, with values ranging from 21.55 MPa to 25.54 MPa. At a temperature of 185°C, it has shown the lowest ultimate tensile strength of the five extruding temperatures tested, with a value of less than 20.06 MPa. Because the maximum melting temperature of 3D850 PLA is over 180°C, plasticization of the filament may occur owing to heat deterioration. As a result, the PLA filament's mechanical characteristics may be affected [9]. Fig. 5 shows the young modulus and the yield stress identified from the plotted stress-strain graph with an extrusion temperature of 175°C. As shown in TABLE 3 below, at an extrusion temperature of 175°C, the highest yield strength recorded is at 5rpm with 27.12 MPa yield stress. The lowest yield strength was recorded at 2 rpm with a yield strength of 4.25 MPa.

TABLE 2: Ultimate tensile strength under different extrusion temperatures and extrusion speed

Speed\Temperature	165°C	170°C	175°C	180°C	185°C
2 rpm	21.55 MPa	22.78 MPa	25.03 MPa	24.85 MPa	19.03 MPa
3 rpm	21.89 MPa	22.79 MPa	25.65 MPa	24.55 MPa	19.53 MPa
4 rpm	22.33 MPa	24.63 MPa	26.38 MPa	26.73 MPa	19.89 MPa
5 rpm	24.48 MPa	25.54 MPa	27.12 MPa	27.18 MPa	20.06 MPa
6 rpm	22.63 MPa	23.94 MPa	25.45 MPa	25.75 MPa	19.55 MPa

TABLE 3: Mechanical strength of specimen at an extrusion temperature of 175°C

Speed	Ultimate tensile strength	Yield stress	Young modulus
2 rpm	25.03 MPa	4.25 MPa	0.026 GPa
3 rpm	25.65 MPa	12.34 MPa	0.023 GPa
4 rpm	26.38 MPa	18.1 MPa	0.024 GPa
5 rpm	27.12 MPa	8.56 MPa	0.021 GPa
6 rpm	25.45 MPa	9.47 MPa	0.020 GPa

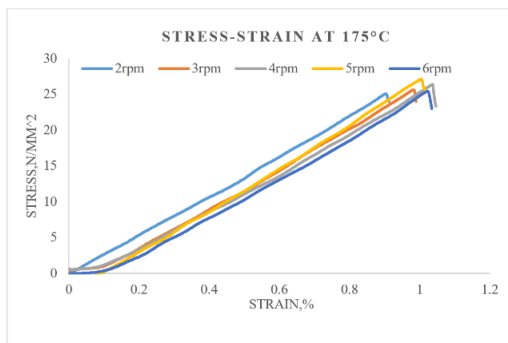


Fig. 3: Stress-strain graph at an extrusion temperature of 175°C

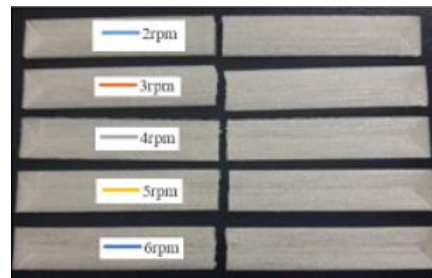


Fig. 4: Specimen break location

*Effect of extrusion temperature and screw speed on Diameter of PLA filament*

TABLE 4 below shows the diameter of the filament developed during extrusion. The diameter of the filament produced reduced as the extrusion temperature increased while the extrusion speed remained constant. With increasing temperature, the diameter of the filament reduces from 1.94mm to 1.62mm at a 4rpm extrusion speed. When the extrusion temperature is constant, the diameter of the filament grows with the extrusion speed, as shown by the diameter of the filament increasing from 1.71mm to 1.79mm at an extrusion temperature of 175°C. This could be because the amount of PLA deposited at the die grows, producing a greater diameter filament. The diameter of the filament drops as the temperature rises, possibly because the increased temperature reduces the viscosity of the PLA, increasing the melting rate of the plastic, resulting in thinner strands being created at constant speeds. Fig. 1 previously illustrate the findings.

TABLE 4: Diameter of filament under different extrusion temperatures and extrusion speed.

Speed\Temperature	165°C	170°C	175°C	180°C	185°C
2 rpm	1.85mm	1.78 mm	1.71 mm	1.68 mm	1.48 mm
3 rpm	1.89 mm	1.80 mm	1.72 mm	1.70 mm	1.58 mm
4 rpm	1.94 mm	1.82 mm	1.75 mm	1.75 mm	1.62 mm
5 rpm	1.96 mm	1.88 mm	1.77 mm	1.76 mm	1.63 mm
6 rpm	1.97 mm	1.92 mm	1.79 mm	1.80 mm	1.66 mm

**CONCLUSIONS**

PLA is a renewable polymer, one of the most widely used filament materials in 3D printing. The influence of process variables like extrusion temperature and screw speed on the flexural characteristics of PLA filament made using the FFF technique was investigated. When the filament extruded fulfills the specified diameter of the commercial 3D printing filament, the optimal parameter for ultimate tensile strength was reached at an extrusion temperature of 175°C to 180°C and a screw speed of 2-5 rpm. The compression and tensile validation experiments will be carried out in the future to learn more about the impact of design parameters on PLA filament quality.

**ACKNOWLEDGEMENTS**

The authors would like to thank the Faculty of Mechanical Engineering Technology, Universiti Malaysia Perlis (UniMAP), for the laboratories and research facilities. This research was supported and funded by Fundamental Research Grants Scheme (FRGS) under a grant number of FRGS/1/2019/TK03/UNIMAP/03/5 from the Ministry of Higher Education Malaysia.

**REFERENCES**

- [1] X. Wang, M. Jiang, Z. Zhou, J. Gou, and D. Hui, “3D printing of polymer matrix composites: A review and prospective,” *Compos. Part B Eng.*, vol. 110, pp. 442–458, 2017, doi: 10.1016/j.compositesb.2016.11.034.
- [2] J. M. Pearce, “Digital Commons @ Michigan Tech Mechanical Properties of Components Fabricated with Open-Source 3-D Printers Under Realistic Environmental Conditions,” vol. 246, pp. 242–246, 2014.
- [3] K. G. Jaya Christiyana, U. Chandrasekhar, and K. Venkateswarlu, “Flexural Properties of PLA Components Under Various Test Condition Manufactured by 3D Printer,” *J. Inst. Eng. Ser. C*, vol. 99, no. 3, pp. 363–367, 2018, doi: 10.1007/s40032-016-0344-8.
- [4] J. A. Travieso-Rodríguez, R. Jerez-Mesa, J. Llumà, O. Traver-Ramos, G. Gomez-Gras, and J. J. Roa Rovira, “Mechanical Properties of 3D-Printing Poly(lactic Acid) Parts subjected to Bending Stress and Fatigue Testing,” *Materials (Basel)*, vol. 12, no. 23, p. 3859, 2019, doi: 10.3390/ma12233859.
- [5] A. Alaswad, K. Y. Benyounis, and A. G. Olabi, *Optimization Techniques in Material Processing*. Elsevier Ltd., 2016.
- [6] M. J. Cimbalá, “Taguchi Orthogonal Arrays,” *Instrumentation, Meas. Stat.*, no. September, pp. 4–6, 2014, [Online]. Available: [https://www.mne.psu.edu/me345/Lectures/Taguchi\\_orthogonal\\_arrays.pdf](https://www.mne.psu.edu/me345/Lectures/Taguchi_orthogonal_arrays.pdf).
- [7] S. R. Subramaniam *et al.*, “Preliminary investigations of poly(lactic acid) (PLA) properties,” *AIP Conf. Proc.*, vol. 2059, no. January, 2019, doi: 10.1063/1.5085981.
- [8] C. M. De, “Technical data sheet,” vol. 41, no. 0, pp. 2–4, 2014.
- [9] M. Applications and P. Information, “Ingeo Biopolymer 3D850 Technical Data Sheet 3D Printing Monofilament – High Heat Grade,” pp. 1–5.

**NORMALIZATION OF IMPACT ENERGY BY DIFFERENT LAYER  
ARRANGEMENT FOR KENAF-GLASS HYBRID COMPOSITE LAMINATES**

S. Yunus<sup>1</sup>, Z. Salleh<sup>2\*</sup>, N. R. N. M. Masdek<sup>2</sup>, A. Jumahat<sup>2</sup>, S. Kushairi<sup>2</sup>, F. A. Ghazali<sup>3</sup>, Z. Halim<sup>4</sup>

<sup>1</sup>Foundation, Pre-University & General Studies Department, German Malaysian Institute (GMI) 43000 Kajang, Selangor, Malaysia

<sup>2</sup>School of Mechanical Engineering, College of Engineering, Universiti Teknologi Mara (UiTM) 40450 Shah Alam, Selangor, Malaysia

<sup>3</sup>Mechanical & Fabrication, Universiti Kuala Lumpur Kampus Cawangan Malaysia France Institute (MFI), 43650 Bandar Baru Bangi, Selangor, Malaysia

<sup>4</sup>Department of Manufacturing and Materials, Kulliyah of Engineering, International Islamic University Malaysia (IIUM), Gombak, 53100 Kuala Lumpur, Malaysia

---

**ABSTRACT**

An increase of interest to mesh up two or more fillers in the matrix is increasing. The main objective is to improve the performance of single filler reinforced matrix with other fillers that have higher strength as compared to the initial fibre. Thus, in this study, kenaf fibre plies have been hybridised with woven glass fibre mats in order to improve its post impact tensile properties. These hybrid composite materials were fabricated by hand lay-up and cold press techniques. Two different systems were fabricated based on specific fibre layer arrangements of kenaf-glass fibre reinforced polymer (KGFRP) hybrid composites. The results revealed that the woven glass fibre at the outer layer arrangement produced better strength than having kenaf fibre at the outer layer as shown in Normalized Stress curve. This arrangement helps to sustain more impact, as a consequence, exhibit more resistance to crack growth.

*Keywords:* kenaf fibre, kenaf-glass fibre reinforced polymer hybrid composites, post impact tensile, normalized stress curve

---

**CONDUCTIVITY AUGMENTATION OF POLYANILINE (PANI)-PEDOT: PSS  
HYBRID INDUCED COTTON FABRIC**

M. S. Parvez<sup>1,2</sup>, M. M. Rahman<sup>1\*</sup>

<sup>1</sup>*Advanced Materials Research Group, Department of Mechanical Engineering, College of Engineering, Universiti Malaysia Pahang, Lebuhraya Tun Razak, 26300 Gambang, Kuantan, Pahang, Malaysia*

<sup>2</sup>*Department of Textile Engineering, Khulna University of Engineering & Technology (KUET), Bangladesh*

---

**ABSTRACT**

With the advent of cutting-edge technological progress, soft electronics has emerged as the next-generation niche sector for formulating flexible and wearable electronic devices. Integration of conductive polymer like Polyaniline (PANI) is one of the potent ways of intriguing interactive functionality into a conventional textile material. PANi is acting as a protagonist since it inherently harnesses the optical properties of metals or semiconductors by generating a network of conducting layers. However, the rigid-brittle form of PANi, degree of conductivity, and specific choice of solvents sometimes limit its applications. Incorporating promising polymer hybridization can open a whole new frontier using PANi. This study aims to adopt a facile hybridization technique with intrinsic conducting polymer, Poly(3,4-ethylenedioxythiophene) polystyrene sulfonate (PEDOT:PSS) and PANi to enhance the conductivity of Cotton fabric. It is found that PANI-PEDOT:PSS hybrid material can be successfully incorporated over cotton fabric via in-situ polymerization of polyaniline and can augment the surface conductivity by multiple folds. Probe conductivity test, FTIR, FE-SEM, followed by EDX were performed to validate the results. The developed fabric may further expand its purposes towards sensing, joule-heating and electromagnetic shielding applications.

*Keywords:* polyaniline, PANi, PEDOT:PSS, hybridization, wearable electronics

---



## **ACKNOWLEDGEMENTS**

Advanced Engineering Materials and Composites Research Centre (AEMC), Department of Mechanical and Manufacturing Engineering, Faculty of Engineering, Universiti Putra Malaysia, Malaysia

Plastics & Rubber Institute Malaysia (PRIM), Malaysia

Universiti Kuala Lumpur, Malaysian Institute of Chemical and Bio-Engineering Technology (UniKL MICET), Malaysia

Dr. Mohammad Jawaid



**UPM**  
UNIVERSITI PUTRA MALAYSIA  
BERILMU BERBAKTI



**UniKL**  
UNIVERSITI  
KUALA LUMPUR



*Editors:*

*S. M. Sapuan  
R. A. Ilyas  
M. Y. M. Zuhri  
E. S. Zainudin  
M. Jawaid  
Z. Leman  
A. N. A. Yahaya  
M. A. Azman  
M. Zulkifli  
N. A. Khalil  
N. Z. M. Zuhudi  
C.N. Aiza Jaafar  
M. N. M. Azlin  
K. Z. Hazrati  
M. M. Harussani  
M. F. Banjar  
R. M. O Syafiq  
A. Nazrin  
A. F. Lajulliadi  
J Tarique*

ISBN 978-967-26793-0-1



9 7 8 9 6 7 2 6 7 9 3 0 1